Buoyancy Effects on Smoldering of Polyurethane Foam

by

Jose Luis Torero

B.S.(Pontificia Universidad Catolica del Peru) 1988
M.S.(University of California at Berkeley) 1991

A dissertation submitted in partial satisfaction of the

requirements for the degree of

Doctor of Philosophy

in

Engineering-Mechanical Engineering

in the

GRADUATE DIVISION

of the

UNIVERSITY of CALIFORNIA at BERKELEY

Committee in charge:

Professor Carlos Fernandez-Pello
Professor Patrick J. Pagni
Professor Robert B. Williamson

1992

The dissertation of Jose Luis Torero is approved:

A C F. Kelly 11/18/92
Chair Date

Patrick J. Pagni 11/19/92
Date

Robert B. Williamson 11/19/92
Date

University of California at Berkeley

1992

BUOYANCY EFFECTS ON SMOLDERING OF POLYURETHANE FOAM

by

Jose Luis Torero

ABSTRACT

An experimental study has been carried out to investigate the effects of buoyancy on smoldering of polyurethane foam. The experiments are conducted with a high void fraction flexible polyurethane foam as fuel and air as oxidizer, in a geometry that approximately produces a one-dimensional smolder propagation. The potential effect of buoyancy in the process is analyzed by comparing upward and downward smolder propagation through a series of normal gravity and variable gravity experiments. Both opposed and forward mixed (free and forced) flow smolder configurations are studied. In opposed smolder the oxidizer flow opposes the direction of smolder propagation, and in forward smolder both move in the same direction. Variable gravity free flow tests are also conducted in an aircraft flying a parabolic trajectories that provides low gravity periods of up to 25 sec. Measurements are performed of the smolder reaction propagation velocity and temperature as a function of the location in the sample interior, the foam and air initial temperature, the direction of propagation and the air flow velocity. This information is used in conjunction with previously developed smolder theoretical models to determine the smolder controlling mechanisms and the effect of gravity.

Three zones in the fuel sample with clearly defined smolder characteristics are identified. A zone close to the igniter where smolder is affected by the external heat, a zone at the end of the sample where smolder is affected by the environment, and

a zone at the end of the sample where smolder is affected by the environment, and a zone, in the middle of the foam, that is free from external effects. This last zone is the most characteristic of one dimensional, self-supported smolder, and the one that is studied in greater detail. In mixed flow convection buoyancy induced flows together with the forced flow are the primary mechanism of oxidizer transport to the reaction zone, while diffusion has a secondary importance. In natural convection, downward smoldering is of the opposed type while upward smoldering resembles more the forward type. For opposed flow smoldering, both natural and forced, the smolder propagation velocity is found to increase with the oxidizer mass flux reaching the reaction zone. This result confirms predictions from previously developed theoretical models that the smolder velocity is proportional to the oxygen mass flux. The experimental data is correlated in terms of a non-dimensional smolder velocity derived from these models, the results show very good agreement between theory and experiments for strong smolder. To implement the models, an analysis of the gas flow field is developed where the effect of significantly different permeabilities between char and foam is been. Extinction is observed for very low and for very high flow rates, which shows that smolder is controlled by a sensitive competition between oxygen supply and heat losses to and from the reaction zone. Under these conditions the models do not describe the experiments well.

The forward flow smolder experiments show that forward smoldering is controlled not only by the competition between oxygen supply and heat losses to and from the reaction zone but also by the competition between pyrolysis and oxidation.

For low flow velocities a regime resembling the opposed flow is observed. As the air flow velocity is increased, foam pyrolysis followed by char oxidation is the controlling smolder mechanism. For both these conditions the theoretical models describe the experiments well. Increasing the flow velocity further results in a smolder propagation velocity controlled by total fuel consumption, in downward burning. For upward burning transition to flaming is observed for very high air flow velocities. This last regime is not well predicted by the theoretical models.

The results from the experiments in variable gravity environment conducted in the KC-135A and Learjet airplanes confirm the normal gravity observations that the competition between heat losses and oxidizer transport is the major mechanism controlling smolder. The absence of convective flow in low gravity results in higher temperature in the unburnt fuel and char due to smaller heat losses to the surroundings. However, the oxidizer transport to the reaction zone also decreases and as a result the temperature at the reaction zone decreases indicating a weakening of the reaction. The presence of pyrolytic reactions in forward smolder and their capability to inhibit smoldering complicates the above described smolder mechanisms.

A.C.Fernandez-Pello

Chairman, Dissertation Committee

To my father,
he knows why

Table of Contents

NOMENCLATURE

C_p	Specific heat capacity
D	Mass Diffusivity of Oxygen in air
d_p	Pore Diameter
g	Gravitational Acceleration
Gr_K	Grashof Number
K	Permeability
L	Length
$\dot{m}''$	mass flux per unit area
P	Pressure
Q	Energy released per mass of O_2 consumed
$\dot{q}$	Heat flux
$\dot{r}'''$	reaction rate
Ra_x	Raleigh Number
Re_K	Reynolds Number
t	Time
T	Temperature
U_S	Smoldering velocity
u_b	Buoyant velocity in x direction
u_D	Velocity induced by natural draft
u_f	Forced velocity

u_g	Total average air flow velocity
v_b	Buoyant velocity in y direction
W	Width
x	x coordinate
Y	Mass fraction
y	y coordinate

Greek Symbols

α	Thermal diffusivity
β	Volume expansion coefficient at constant pressure
ν	Stoichiometric coefficients
δ	Boundary layer thickness
δ_c	Conduction characteristic length
δ_D	Diffusion characteristic length
δ_T	Thermal boundary layer thickness
λ	Thermal conductivity
μ	Dynamic viscosity
ϕ	Void fraction
ρ	Density
σ	Stephan-Boltzman constant

Subscripts

A	Air
C	Cold
CH	Char

Acknowledgements

I would like to thank my research adviser, Carlos Fernandez-Pello, for giving me the opportunity to conduct this research; but mainly, I would like to thank him for making clear to me what is good and bad in this profession. Special thanks go to Professor Antoni K. Oppenheim for caring.

This work was supported by the National Aeronautics and Space Administration under Grant N° NASA-NAG3-443. The technical input of David Urban, and the advice, friendship and hard work of Professor Michio Kitano have all been very important. The idea of comparing upward and downward experiments suggested by Mrs.Olson has to be acknowledged.

The help of the Hesse Hall technical staff has been essential to this work, my special gratitude to Scott and Wendy for their smiles. I would like to thank Corey, Drazen, Javier, Murray and Steve T. for surviving my never ending complaints. Betsy, thank you for the fights, arguments and mutual frustration, I really enjoyed all of them. Gordon and Steve B. your tolerance to my perpetual bad temper is greatly acknowledged, you are the best roommates.

Special thanks to Virgilio and Margot for all these years of company and support, your friendship has been invaluable. I would like to thank Liming whose genuine friendship and advice are very important to me. To the Von Breymann family, thank you for your friendship and encouragement. My gratitude to Carlos Montero for being there every time I needed him.

I am for ever indebted to my parents, grandparents and brothers; this work belongs to them. Shelley, thank you, for everything.

Chapter 1
INTRODUCTION AND LITERATURE REVIEW

1.1 Introduction and Description of the Problem

Smoldering combustion is defined as a self-sustaining, propagating exothermic reaction wave deriving its principal heat from heterogeneous oxidation of the fuel (direct attack of oxygen on the fuel surface) [1]. For the smolder reaction to propagate, enough heat must be transferred from the exothermic reaction to the virgin fuel ahead to bring its temperature to high enough levels to initiate the surface combustion reaction. At the same time enough oxygen must be present in the fuel porous, or transported to the reaction zone from outside, to sustain the reaction. Thus, smolder involves complex processes related to fluid flow and heat and mass transfer in a porous media, together with surface chemical reactions. The interaction between these physical and chemical processes determines the final characteristics of the smolder reaction. In addition to the thermochemical properties that are important in determining the combustion reaction characteristics, other fuel physical properties like void fraction, permeability to gas flow, and thermal properties, and external factors like insulation from the environment, buoyant flows, and the nature of the ignition source are also important factors in the smolder reaction characteristics and its propagation rate.

Smoldering, like flaming, is a combustion process which spreads through a fuel when heat released by oxidation is transferred to adjacent elements of the fuel. Heat release in smoldering is characteristically very low [2] and stable smoldering is

possible in some circumstances at air/fuel ratios a few percent of stoichiometric [1]. All this information points to a weak process with a sensitive competition between oxidizer transport to the reaction and heat transport from the reaction.

Smoldering involves the exothermic attack of heat and oxygen on condensed phase polymeric materials at a rate sufficient to overcome heat losses and thus be self-sustaining. In the absence of oxygen, the typical polymeric fuel will be endothermically degraded by heat to smaller volatile molecules, sometimes also leaving a solid residue of a variable aromatic nature referred to as a char; this char pyrolyzes much more slowly than the initial polymer [1]. Studies of polyurethane degradation in both air and nitrogen using thermogravimetric analysis [3] show that the original polyurethane is converted into char by two competing routes; the subsequent oxidation of the char provides most of the heat driving smolder.

A simple chemical mechanism that only incorporates char formation and oxidation has been proposed to explain the chemistry of smoldering for polyurethane, tobacco, cellulose and wood fibers [1,4], the reactions are as follows

$$\begin{aligned} \nu_F[\mathrm{FOAM}] + Q_p \nu_F M_F &\rightarrow \nu_{CH}[\mathrm{CHAR}] + \nu_{gp1}[\mathrm{GASPRODUCTS}] \\ \nu_{CH}[\mathrm{CHAR}] + \nu_O O_2 &\rightarrow \nu_{gp2}[\mathrm{GASPRODUCTS}] + Q \nu_O M_O \end{aligned} \qquad (1.1)$$

Since the second reaction (oxidation) is much faster than the first reaction (pyrolysis), thermal analysis [1] shows that the two step reaction mechanism can be well approximated by a one step reaction [5,6,7,8].

$$\nu_F[\mathrm{FOAM}] + \nu_O O_2 \rightarrow \nu_{CH}[\mathrm{CHAR}] + \nu_{gp}[\mathrm{GaseousProducts}] + Q \nu_O M_O \qquad (1.2)$$

Depending on the characteristics of the smoldering wave one or the other mechanism

gives an adequate description of the reaction [9].

For smoldering to occur sufficient oxidizer has to reach the reaction zone either by diffusion and/or convection. Different reaction pathways can be followed depending on the oxidizer supply, an endothermic pyrolytic path competes for the original fuel with an exothermic oxidative degradation path. Pyrolysis forms a tar that inhibits smolder, instead, oxidation generates a char which can be subject to further exothermic oxidation. The ability of a material to form an oxidizable char determines, in part, its ability to smolder in a given configuration. The char forming capacity of a material depends in varying degrees on its chemical composition, the gaseous environment (inert or oxidative), and the heating rate regime, all of which can affect the kinetics of char vs. tar formation competition [3]. In general, for polymers, the balance between the quantities of char or tar formed is sensitive to several factors [1,4,10].

For polyurethane foam the oxygen concentration strongly determines the pathway to be followed by the reaction. The depletion or exhaustion of the oxygen supply will then tend to lower the oxidation, favor the pyrolysis reaction and bring the cessation of smolder. The rate of heating also shifts the proportion of polymer degraded along the two general pathways. Char formation is favored by slow heating. High heating rates shift the oxidative process toward higher temperatures by a greater amount than they shift pyrolysis; pyrolysis to tar then dominates [3]. During char formation the structure of the fuel tends to be preserved. This, added to the small mass loss, tends to enhance the transport of oxidizer to the reaction

zone. During tar formation, the filaments that form the polyurethane foam [5] tend to contract to liquid spheres as a consequence, presumably, of surface tension forces [11]. This restricts the flow of air through the material and consequently inhibits the propagation of a smolder wave [3,5].

Smoldering ignition is induced by an external heat source, since the heat released by the oxidative reaction is small, compared to other combustion processes [2]. Heat losses are a significant element in the ignition process. Temperature as well as oxidizer availability are restrictive parameters for the successful ignition and propagation of a smolder reaction. Only a narrow range of temperatures and oxidizer supply to the reaction allow the process to follow the char formation path. Endothermic pyrolysis and smolder inhibition will result for all conditions outside the limiting ranges. Smoldering reactions initiated in the surface of the fuel need external heat supply to support the propagation until enough char is left behind to insulate the reaction. This self-insulating property of the char allows for a reaction that can proceed onwards without assistance [4]. Under certain conditions complete or almost complete char oxidation leaves the reaction exposed and, as a consequence, extinction occurs.

The heat transfer mechanisms involved in smoldering propagation are convection, conduction and radiation. Heat is being transferred from the reaction zone to the fuel and the rate at which the fuel increases its temperature to the reaction temperature determines the smoldering propagation velocity. Many fuels of interest are very porous, and consequently, conduction is a poor mode of heat

transfer [12]. Thus, radiation heat transfer is often important despite the relatively low temperatures encountered in smoldering combustion - peak temperatures are usually between 350°C and 500°C [4].

The porous material is saturated with air which migrates and carries energy through the material. In the field of fluid mechanics, the dynamics of fluid flow through a porous medium is relatively old. The conceptual centerpiece in this branch of fluid dynamics -the Darcy flow model [13]-originated in the nineteenth century in connection with the engineering of public fountains. Convective heat transfer by flow through porous media is a relatively new topic and only in the late twentieth century has extensive work been performed [14]. The influence of convection on the smolder process could be very significant [9]. Convective flow in a porous media can be induced by pressure difference, temperature gradients and density gradients, and its magnitude is strictly related to the permeability of the fuel.

One-dimensional smolder can be conceptualized as propagating in two distinct modes, forward and opposed smolder, according to the direction of the oxidizer flow relative to the direction of propagation of the reaction. Figure 1.1 shows a schematic representation of both smolder modes. In forward smolder, the reaction front moves in the same direction of the oxidizer flow. In opposed smolder, the smolder front propagates in a direction opposed to the oxidizer flow. It is important to mention that in most real smolder situations, propagation is a mixture of these two modes. Significantly different permeabilities between char and foam combined with temperatures gradients induce recirculating flows when ever an open interface is

Table 1-1
Properties

$Cp_A = 1.088$ KJ/Kg
$Cp_F = 1.700$ KJ/Kg
$D = 4.53 \times 10^{-5}$ m^2/s
$d_p = 0.05$ mm
$K_{CH} = 8.40 \times 10^{-7}$ m^2 (Natural Convection Experiments)
$K_F = 2.76 \times 10^{-9}$ m^2
$g = 9.81$ m/s^2
$L_C = 150$ mm
$W = 150$ mm
$\Delta P_{HOOD} = 65.2$ N/m^2
$n_C = 0.7550$ moles
$n_H = 2.872$ moles
$T_i = 293$ K
$T_W = 483$ K
$Y_{O,i} = 0.235$
$\alpha = 1.122 \times 10^{-5}$ m^2/s
$\beta = 1.684 \times 10^{-3}$ K^{-1}
$\lambda_{eff} = 0.047$ W/mK
$\mu = 1.50 \times 10^{-5}$ Kg/ms
$\phi_{CH} = 0.9775$
$\phi_F = 0.9750$
$\rho_C = 1.225$ Kg/m^3
$\rho_H = 0.299$ Kg/m^3
$\rho_F = 1,034.0$ Kg/m^3
$\sigma = 5.67$ W/m^{2}K^4

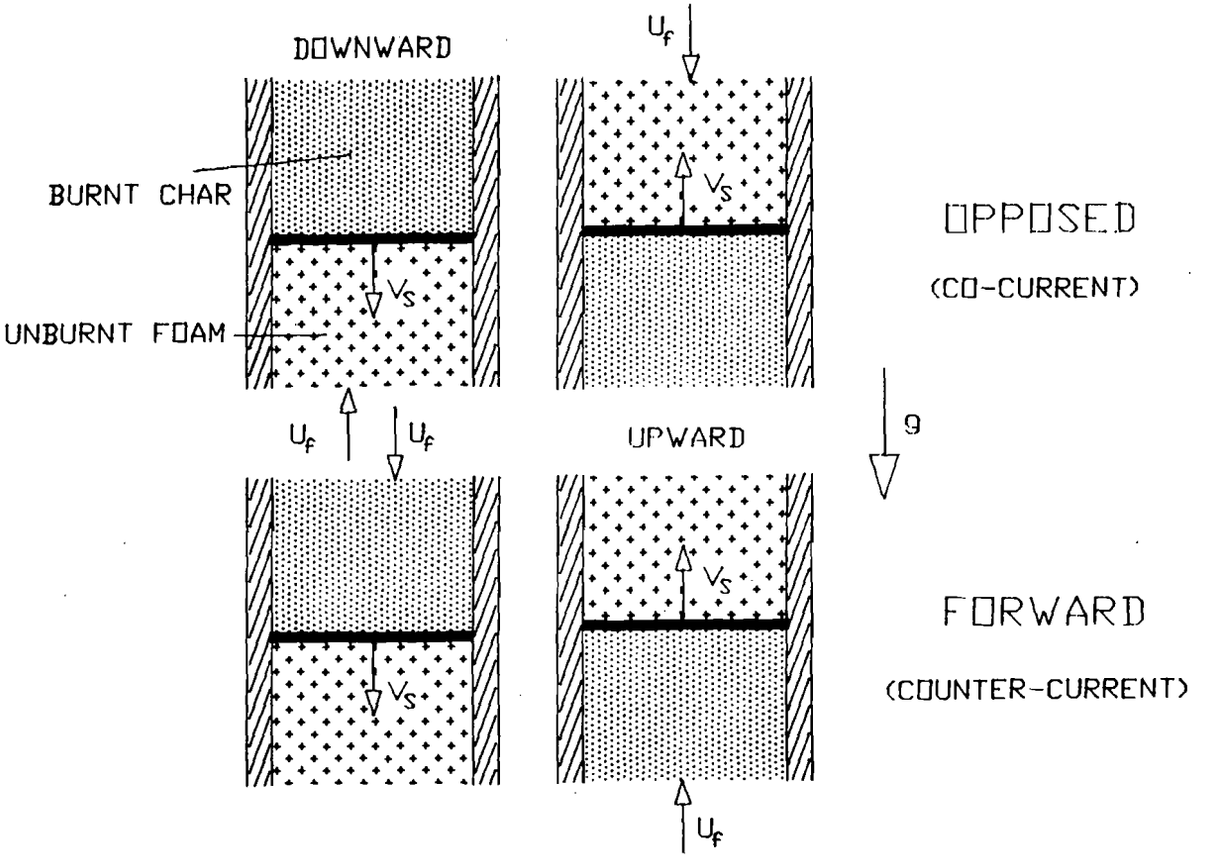

Figure 1.1 - Schematic representation of one-dimensional opposed and forward smolder. For forward smolder, The reaction and the forced flow move in the same direction. For opposed smolder, the reaction and the forced flow move in opposite directions. In downward burning, the reaction propagates in the direction of the gravitational acceleration; for upward burning, the reaction propagates opposite to the gravitational acceleration.

present. Since one of these two modes is, in general, dominant, these configurations provide a very useful framework within which to discuss smolder.

The porous combustible material used throughout this work is polyurethane foam, whose properties are shown in Table 1-1 and typical smolder characteristics are outlined in Table 1-2. This table is presented to provide a point of reference for the characteristics of this process. The values in Table 1-2 present order of magnitude approximations for opposed and forward smolder of polyurethane foam. The exact values vary with the multiple parameters of the problem. The interest in using this material is two fold; it is a common material, and its structure permits upward burning experiments without the fuel collapse problems that occur with cellulose and other loose materials.

Table 1-2
General Smolder Characteristics of Polyurethane Foam(*)

SMOLDER CHARACTERISTICS	OPPOSED CONFIGURATION	FORWARD CONFIGURATION
Maximum Temperature	400°C	450°C
Smolder Propagation Velocity	0.1 mm/sec	0.8 mm/sec
Reaction Zone Thickness	10 mm	5 mm
Heat release (per Kg of oxidizer)	5,000 KJ/Kg	5,000 KJ/Kg
Loss of Mass	10%	35%

(*) values obtained from [2,3,4,9,15]

Although smoldering is present in a variety of combustion processes, it is of particular interest in the fire safety field because of its role as a potential fire

initiation source [1,3,10,15,16,17,18,19,20]. Smoldering combustion is a weakly reacting phenomenon which can propagate slowly for long periods of time [1,10,15,17,20], and suddenly transition to flaming initiating a rapidly propagating and potentially hazardous fire. Furthermore, once established, it is difficult to detect and extinguish because it can propagate through the interior of the porous combustible material. These features of the process are the least understood and most hazardous. In addition to the possibility of transition to flaming, smoldering combustion products are, in general, toxic [21,22]. The toxicity of the post-combustion gases is of great relevance to space-based fire safety, since space systems are small, self-contained and carefully planned human environments. Therefore, there is a critical need to be able to detect and mitigate unwanted smolder. In normal gravity environments, convective transport of oxidizer to the reaction zone and heat convection from the reaction zone are important parameters. Under low gravity conditions, these transport mechanisms either have a small effect or do not exist. There are very few studies dealing with the effect of gravity on smoldering combustion [5,6,8,23], therefore, there is a need to obtain greater understanding on how smoldering will behave in a space-based environment. Experimental works and modeling attempts in the literature are covered in the following review.

1.2 Literature Review

Smolder combustion has been a subject of study for several decades, as and the smoldering behavior of number of materials has been extensively studied. Many

materials can sustain smoldering. These include carbon [24], coal [25,26], cotton [16,27], cellulosic fibers [5,6,7,8,17,23,28,29], paper [30], polyurethane foams [3,4,9,15,31], wood [12,18], cigarettes [32,33,34], thermal insulation materials [19], various dusts [20,35,36]. One characteristic that all these materials have in common is a tendency to form char upon heating in the presence of oxygen [3]. Early work in smoldering combustion was conducted by Palmer [20], since then, researchers have studied smoldering combustion in a wide variety of configurations. Opposed smoldering, also called co-current, is probably the most extensively studied, theoretically and experimentally. Relatively little attention has been given to smoldering combustion in the forward (counter-current) configuration [1,9,34]. Most of the work in this configuration has been done in the context of coal gasification in a packed bed [37,38]. The complexity of the chemistry as well as the unclear understanding of heat and mass transfer in porous media make the task of modeling smoldering combustion a very difficult one. In addition to being difficult to model smoldering is also difficult to analyze experimentally. Smolder is an extremely slow process (Table 1-1) therefore experiments could last a few hours. In addition, porous materials do not lend themselves to visual data acquisition methods, and in situ methods such as thermocouples and invasive gas sampling are the norm. These factors have resulted in a body of smolder research which has concentrated heavily on parametric experimental evaluations of specific materials, configurations or limited environmental effects (such as changes in air flow velocities, oxygen concentrations and pressure). Nevertheless, certain physical factors have emerged

as having an impact on smoldering.

1.2.1 Smolder Propagation Models

Attempt to develop predictive models of smoldering combustion have proved difficult. The most detailed model of smolder propagation presently in the literature is that of Ohlemiller [1]. In this model a few overall lumped reactions with apparent kinetic parameters describe the chemistry of the process, all the kinetic parameters are determined by thermal analysis, the accuracy of these kinetic parameters is still quite poor. The thermophysical problem is fully described but the complexity of the resulting equations precludes general solution. The one-dimensional limiting cases are explored extensively but the existence of temperature and species gradients simultaneously on the fuel-particle scale and on the reaction-wave scale do not allow a full characterization of the problem. The usefulness of the model is therefore limited to the information obtained from examining the quantitative interaction among the numerous model parameters.

Because of the difficulties involved in the modeling of smoldering, phenomenological as well as numerical approaches have been more frequent. Cohen and Luft [35] measured smolder propagation velocities through a variety of materials in a horizontal layer configuration and correlated the results with a one-dimensional balance of conductive and convective heat transfer in the bed and the assumption that the air supply is determined by a buoyancy/drag balance in the bed. No consideration is given to diffusive oxygen supply. Motivated by the geometry of

cigarettes, extensive work has been done on cylindrical rods; Kinbara et al. [30] performed experiments on vertical rods of various materials, mainly densely-packed cellulosics. The vertical rod was open to ambient atmosphere and oxidizer diffused through a natural boundary layer. The model was later refined by Sato and co-workers [39,40]. The basis of the model is a one dimensional steady state heat conduction equation. It considers only gradients in the longitudinal direction of the fuel rod and heat generation is limited by oxygen transport to the reaction zone. In a similar geometry Gugan [41] devised a mechanism to describe the observed conical shape of the reaction front; this mechanism balanced radial diffusion of oxygen from the surrounding air with oxygen consumption. A similar idea was used by Palmer [20] for upward smolder in deep dust piles. Williams briefly discussed smolder propagation as a fire-spread mechanism [42,43]. An approximate criterion for extinction is proposed; smolder will cease as soon as the kinetic rate of oxygen consumption falls below the diffusive supply rate, i.e. as soon as kinetics become the rate-limiting step in the heat release process. Dosanjh et al. [5,6,7,8] used a straight forward extension of the Zeldovich/Frank-Kamenetskii/Semenov [44,45] premixed flame analysis to obtain an expression for opposed one-dimensional smoldering velocities, an unsteady model is proposed for forward smoldering. Activation energy asymptotics are used to obtain smoldering temperatures, a qualitative assessment of the importance of buoyancy is presented.

Numerical modeling has been attempted by several authors in an effort to explain experimental results. A series of experiments on low density fibrous cellulose

cylinders smoldering horizontally in stagnant atmospheres of varying oxygen content were numerically modeled by Moussa et. al [29]. Diffusion through a natural boundary layer was used as the oxidizer transport mechanism. Baker [33], Bradbury et al. [46] and Ortiz-Molina [47] split the reaction wave in two parts for subsequent analysis. A planar interface is assumed to separate an endothermic pyrolysis zone from a char oxidation zone. This model was used for several different geometries. A more detailed study of the pyrolysis reaction is presented by Muramatsu [32] for a one-dimensional smolder reaction in a quiescent environment, the geometry is again the one of cigarettes. Steady-state conservation equations are solved numerically. Leisch [48] provided a more general one-dimensional model to describe steady-state two-dimensional smolder propagation that allowed both pyrolytic and oxidative reactions to occur simultaneously. Summerfield et al. [34] developed a one-dimensional unsteady model for cigarette burning under high constant draw (steady flow); radiation, conduction and convection are included as heat transfer mechanisms. Finally, Ohlemiller et al. [4] modeled a two step reaction mechanism for smoldering of polyurethane foams, linear finite elements were used to approximate the spatial dependency.

1.2.2 Physical Parameters Controlling Smoldering

1.2.2.1 Oxygen Mass Flux

Oxidizer mass flux has been found to be the primary controlling factor in smolder propagation [3,5,6,7,8,17,29]. Smoldering propagation velocities and

temperatures were measured by Palmer [20] for dusts and fibrous materials. It was found that smolder velocity increases with air velocity. Ortiz-Molina et al. [47] studied polyurethane foams covered with cotton cloth, suspended horizontally and allowed to smolder naturally. The oxygen concentration was decreased until extinction could be observed. These experiments were used to rank the smoldering tendencies of different foams. Experiments on a horizontal cylinder were performed by Moussa et al. [29], diffusion of oxygen occurred through a free convective boundary layer and oxygen partial pressure and concentration were varied. These experiments for cellulosic materials showed that in the region of steady smoldering (Figure 1.2 and 1.3), the measured propagation speed and the maximum temperature in the smoldering zone all depend on the oxygen partial pressure and mole fraction in the environment. The results showed that steady smoldering speed increased with oxygen mole fraction and oxygen partial pressure. A series of tests, systematically changing heat loss and oxygen supply conditions to asses the smoldering tendency of several materials was proposed by Ohlemiller and Rogers [3]. In this work Ohlemiller and Rogers conclude that oxidizer availability imposes a series of restrictive conditions for smoldering ignition. Smoldering propagation velocities are proportional to oxidizer supply. They observed that almost no oxidizer is left behind the reaction front, confirming that smoldering combustion is an oxygen limited process. Rogers and Ohlemiller [11] found, by doing experiment with polyurethane foams, that smolder velocities increased with the volume percent of oxygen in nitrogen and with the total oxygen flow (Figure 1.4 and 1.5). They also found that

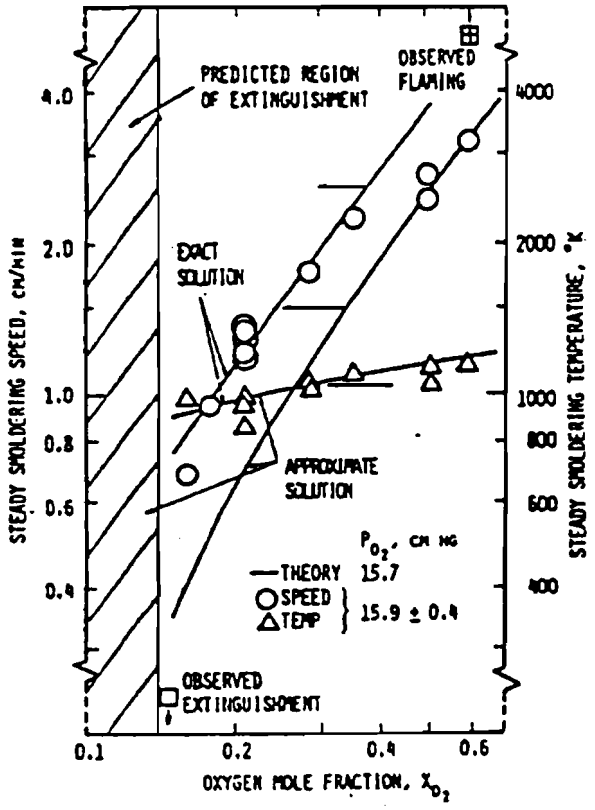

Figure 1.2 - Comparison of theory and experiment for the steady smoldering speed and corresponding temperature versus ambient oxygen mole fraction (X_{O2}). Cellulosic samples are mounted horizontally (diameter = 0.86 cm and density = 0.06 g/cm^3).(From Moussa et al.[8]).

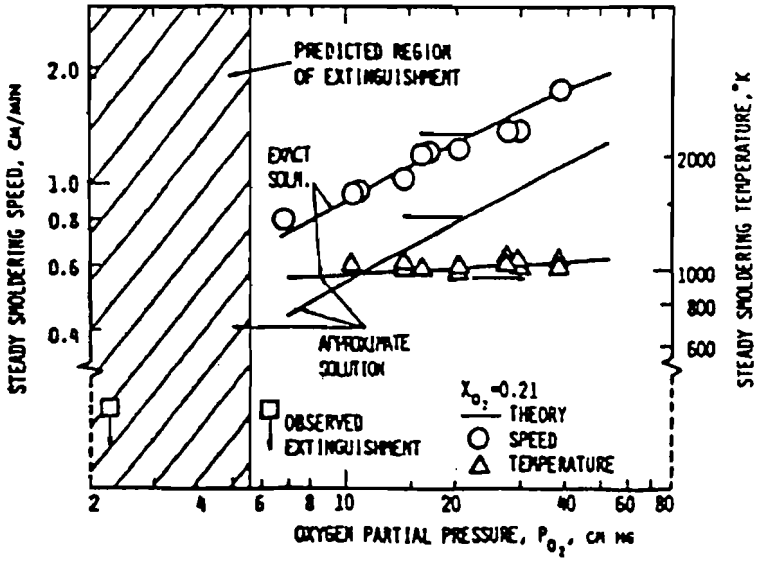

Figure 1.3 - Comparison of theory and experiment for the steady smoldering speed and corresponding temperature versus ambient oxygen partial pressure (P_{O2}). Cellulosic samples are mounted horizontally (diameter = 0.86 cm and density = 0.06 g/cm^3).(From Moussa et al.[8]).

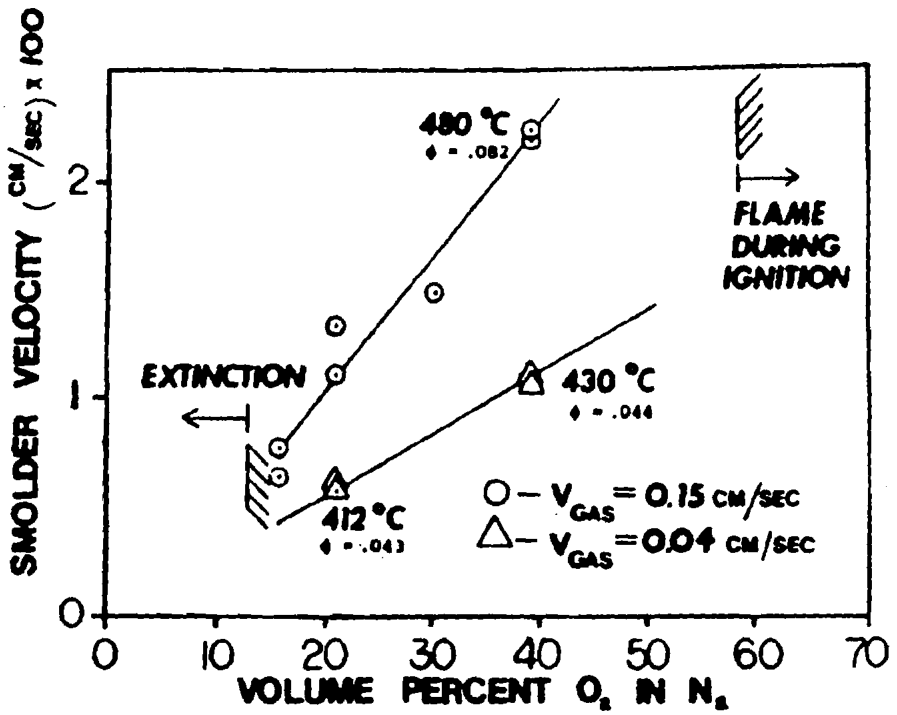

Figure 1.4 - Effect of oxygen supply (flow rate and percent O_2) on smolder velocity in a flexible polyurethane. Also note temperature and equivalence ratio (ϕ) variations; for stoichiometric burning ϕ = 2.46 g_{O2}/g_{foam}.(From Rogers and Ohlemiller [31])

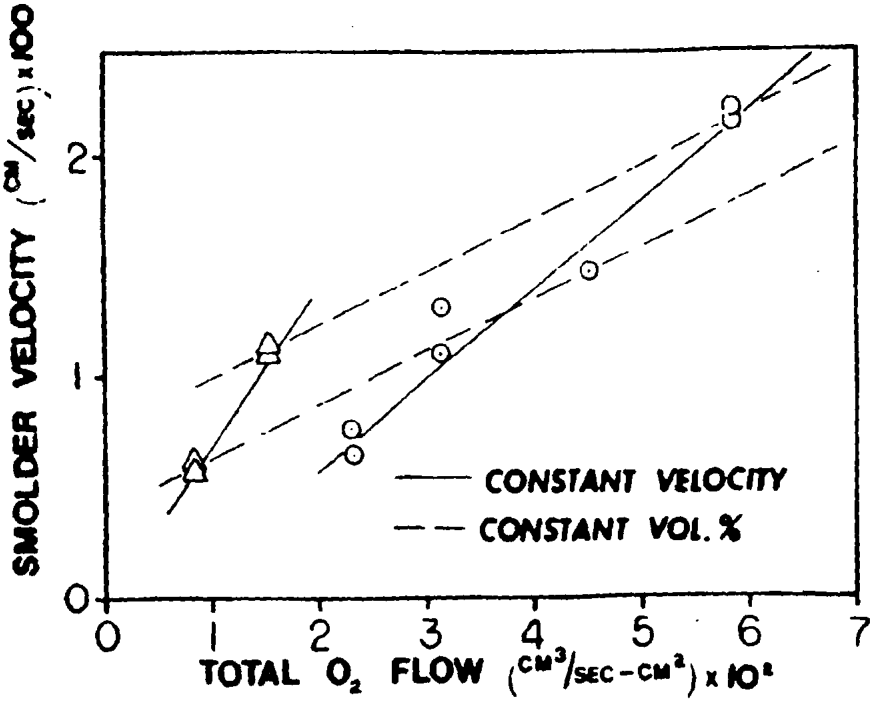

Figure 1.5 - Effect of absolute rate of O_2 supply on smolder velocity in a flexible polyurethane.(From Rogers and Ohlemiller [31])

a small increase in oxygen concentration can shift the balance from pyrolytric tar formation to oxidatively promoted char formation. These experimental results agreed quite well with the model proposed by Ohlemiller et al. [4]. The effect of air supply from buoyantly induced recirculations in the ignition interface was studied by Cantwell [49]. Results for natural convection and forced flow experiments show again that smoldering velocity increases with oxidizer supply. Cantwell explored different sources of oxidizer: flow induced by a natural draft, boundary layer recirculation flows and forced flow. These experiments tried to quantify the effect of buoyantly induced flows on smoldering combustion of polyurethane foams.

1.2.2.2 Pressure

The effect of pressure on a smolder reaction has been examined by Dosanjh et al. [6] and by Newhall et al. [23], both in the context of an attempt to examine the effect of buoyancy on smolder. Dosanjh et al. [6] present both theoretical and experimental results for downward burning opposed smolder of cellulose powder in a natural convection environment. Experiments were conducted in a large pressure vessel for pressures from 0.5 to 1.2 atm with a chimney fitted over the fuel container to enhance the natural draft and to avoid entrainment of air through the ignition interface. The smolder propagation velocity was found to be zero for ambient pressures below 0.6 atm and to increase linearly with ambient pressure increase for pressures higher than 0.6 atm. This increase is attributed to the changes in the buoyant flows induced by the pressure change. Newhall et al. [23] reported results

for the same configurations but varying both ambient pressure and the forced flow velocity. Small influence of the ambient pressure was found for mass fluxes greater than 1 g/s.m^2, as no difference could be observed for pressures ranging from 0.6 atm to 1 atm. Both Dosanjh et al. and Newhall et al. performed their experiments on cellulose with opposed smoldering.

1.2.2.3 Buoyancy

Buoyancy effects in smoldering combustion have only recently been a field of interest. Naturally induced flows through a porous sample can be of two types: natural draft, induced by a density difference between hot gases inside a duct and cold gases outside, and boundary layer flow, induced by a temperature gradient making an angle with the gravitational acceleration. Buoyantly induced flows serve as a mechanism for oxidizer and heat transport. Only the works of Summerfield and Mesina [2], Dosanjh et al. [6,7,8], Dosanjh [5] and Cantwell [49] have dealt with this parameter. Summerfield and Messina [2] presented a review of the relevant parameters in the design of a space-based experiment. An extensive review of the relevant literature is presented. Dosanjh [5,6,7,8] determined that for cellulose powder, with void fractions of approximately 0.8, diffusion of oxidizer towards the reaction zone would not be sufficient to self-sustain the reaction, therefore, in the absence of buoyantly induced flows, a forced flow would be necessary to sustain the smolder reaction. Cantwell [49] performed a series of experiments using high void fraction polyurethane foam (0.97) in the opposed configuration. The experiments

were performed in a drop tower (NASA Lewis research Center 2.2 sec. drop tower) and an airplane following a parabolic trajectory (KC-135). In the absence of buoyancy reaction temperatures dropped, pointing towards oxidizer transport as the dominant consequence of buoyancy. Experiments in the drop tower, for a reaction propagating near the ignition interface, showed a decreasing effect of buoyantly induced flows as the forced flow velocity increased.

1.2.2.4 Heat Loss

As with most flame propagation processes, smolder essentially spreads through a coupling of heat release, from exothermic reaction, and heat transfer mechanisms [1,50]. When the energy released in the fuel oxidation reaction is able to balance the energy needed to preheat the fuel and oxidizer ahead of the reaction, plus the heat losses to the environment, the reaction will propagate [5,51,52]. Heat loss effects and oxygen supply rate are tightly coupled in a smolder reaction [53]. Heat loss effects have proven difficult to quantify. The model by Ohlemiller [1] states independent conservation equations for solid and gas, in an attempt to quantify heat exchange between the phases. In general thermal equilibrium between phases has been assumed [2,4,5,6,7,8]. Sato and Sega [54] found that for very low oxidizer concentrations, gas phase heat losses overcome the heat added by the reaction leading to a decline in the reaction strength. Further evidence of convective heat transfer from the reacting solid towards the gas is given by Ohlemiller [53] where differences between forward and opposed smolder are attributed to convective heat

transfer at the tip of the reaction.

Experiments like those of Ortiz-Molina et al. [47], where a piece of polyurethane foam was covered, in some cases, by cellulosic fabric material, observed that this enhanced smoldering. The burning cellulose seems to provide energy to the foam, as well as insulation. Therefore, the model describing these experiments only balanced the heat absorbed by endothermic pyrolysis with the heat released by the exothermic oxidation reaction. Other substantial heat sinks mentioned in the literature are vaporization of water and pyrolysis [1].

1.2.3 Convection in Porous Media

Smoldering occurs in a porous media, therefore, the parameters that control flow and mass and heat transfer in porous media are of extreme relevance. Most of the theoretical work done on smoldering assumes simple flow patterns through the porous material. Moussa et al. [29] assumed diffusion of oxidizer through a natural boundary layer formed around the sample. The models by Ohlemiller and co-workers [1,4] study the diffusion problem but do not take on account the structure of the flow inside the porous media. The model of Kailasanath and Zinn [52] does not account for convection, neither does the model of Johnson et al. [51]. Summerfield et al.[34] assumed a constant forced flow through the cigarette, boundary layer considerations for the exterior flow were made. Similar procedure is followed by other authors working on a cigarette like geometry [32,39,40,54]. The work by Dosanjh et al. [5,6,7,8] is the first one to attempt to quantify the effect of

a natural draft in a duct filled with a porous material. The characteristics of the cellulosic fuel used for their analysis resulted in neglectable influence of the draft effect on the flow characteristics. The influence of buoyancy was only evident in an increase in the magnitude of the forced flow used for their analysis. Cantwell [49] used the flow analysis that is derived in later chapters of this work to explain observations of smolder characteristics near an air/fuel interface.

Extensive work analyzing flow in porous media exists in the literature. The fundamental work in this field is Darcy's empirical formulation [13], which states that a bulk velocity is proportional to the pressure gradient imposed over the porous medium. Darcy's formulation in its most general form is

$$u=-\frac{K}{\mu}\left(\frac{\partial P}{\partial x}-\rho g\right) \qquad (1.3)$$

Numerous works followed this empirical formulation, relevant to this work are the studies dealing with natural convection flow, forced flow and mixed flow in ducts filled with a porous material. The basic principles needed for the analysis of the flow characteristic in the fuel are developed in the works of Bejan [14] and Nield and Bejan [55].

The problem of natural convection flow in porous media has been studied in great detail several works relevant to this study have been published. The early work of Horton and Rogers [56] considered the problem of the convection of a fluid through a permeable medium as the result of a vertical temperature gradient, a simple criteria to predict the minimum temperature at which convection can occur

was obtained. Burns et al.[57] studied the convection problem in a vertical slot filled with porous insulation and obtained an analytical solution for the velocity profile and heat transfer to the walls when both vertical walls have different temperatures. Chan et al.[58] stated the problem of flow induced by temperature gradients in an enclosed rectangular porous medium. Numerical solutions for different aspect ratios and wall temperatures are presented. Scaling arguments are used to identify the characteristic time scales for unsteady natural convection in an enclosed porous medium, numerical solution are given for different aspect ratios and Rayleigh numbers and the convergence to known steady state solutions is verified. An extensive review on flows which arise in fluids due to the interaction of the force of gravity and density differences caused by the simultaneous diffusion of energy and of chemical species is presented by Gebhart and Pera [59]. Similarity solutions for plumes and vertical flows adjacent to surfaces are developed. A model for boundary layer convection in a porous layer is developed by Weber [60] for large temperature differences. Experiments confirm the model by means of Nusselt number calculations and temperature profiles. Other works on free convection, in ducts, induced by vertical temperature gradients are useful for the insight they provide on density inversion and the effect of the Rayleigh number [61,62].

In the presence of a forced flow the problem is that of mixed convection, and its treatment is clearly defined by the review paper by Lai et al.[63]. Few works deal with mixed convection in vertical ducts; Lai et al [64] performed a numerical study on the case where the heat source is a strip of height H on an otherwise adiabatic

wall. The other wall was isothermically cooled; aiding or opposing darcy flow was considered. Hadim and Govindarajan [65] calculated solutions for an isothermically heated vertical channel. The did not succeed in calculating temperature and velocity fields. The approach used by these works and others, in similar configurations [66,67], is not necessarily consistent, but in general they agree in considering the Rayleigh and Peclet numbers as the fundamental non-dimensional parameters describing convective flow and heat and mass transfer.

1.3 The Current Contribution

In order to study the effects of buoyancy and heat losses on one-dimensional smoldering combustion, the smolder behavior of a high void fraction polyurethane foam has been examined experimentally. Smoldering propagation velocities and temperatures are obtained at different locations in the sample and a detailed analysis of the characteristics of the reaction as a function of the distance from ignition is conducted. Three zones with clear characteristics could be identified, a first zone close to the igniter where the effect from the heat supplied by the igniter was observed. A second zone at the end of the sample was observed, the effect of the environment was clear. Finally a zone in the center of the foam, free from end effects is identified, this zone is the most characteristic of one dimensional smolder. For all the experiments the reaction front is assumed to be one-dimensional. The effect of significantly different permeabilities between char and virgin foam has been introduced in an analysis of the flow field. The results of this flow analysis has been

incorporated in different models that predict smoldering propagation in various configurations and the results correlated with the experimental data.

A series of natural convection experiments are reported in Chapter 2. Downward and upward burning experiments were conducted for different sample lengths. For downward burning the opposed configuration is dominant. Air is induced by natural draft through the duct reaching the reaction through the foam. Upward burning resembles more the forward configuration since, for this case, air is induced by natural draft through the char towards the reaction. The thermal boundary layers formed near the walls induce a flow of significant magnitude that, in the analytical solution for the flow field, is superposed on the flow induced by natural draft and the air coming with the pores. Since air flow velocities are small and void fractions are high the air contained in the foam pores represents a significant source of oxidizer to the reaction. In a frame of reference attached to the reaction, fuel and oxidizer move towards the reaction zone. The model developed by Dosanjh et al. [5,7] for forced opposed smolder is used to correlate the data. The forced flow term is given by an average velocity resulting from the previously explained analysis. For downward burning there is very good agreement with the model. For upward burning a simplified model based on the work of Johnson [51] that does not account for pyrolysis is used to correlate the data for the smoldering propagation velocities. , for upward burning, oxidation of the char and pyrolysis of the foam cause the experimental results to deviate from the model. Transition to flaming is observed only for upward burning experiments of length 300 mm.

Chapter 3 looks in detail at the opposed flow configuration, experiments were conducted for different flow velocities, sample lengths and initial temperatures in downward and upward burning configurations. Flow velocities were increased from no flow to flow velocities that resulted in extinction. Sample lengths were changed to detect any influence of the sample geometry. The initial temperature was changed for strong smolder and extinction regimes. The model of Dosanjh et al. [5,7] was used to correlate the experimental data. The air flow was obtained by superposing the forced flow, an average boundary layer flow and the air content in the pores. The experimental data correlated well except for the cases where extinction was observed. Extinction occurred for very low flow rates and for very high flow rates, which points to a sensitive competition between oxygen supply and heat losses to and from the reaction zone.

Forward smoldering is the subject of Chapter 4. Downward and upward burning experiments were conducted in this configuration for different flow rates. Smoldering velocities are correlated with the non-pyrolytic model of Johnson [51], the agreement of the model for very low flow rates is good. As the flow rate is increased, it is necessary to incorporate in the model the energy required to pyrolyze the foam. Significant evidence of pyrolysis is obtained from the temperature histories. The agreement with this corrected model is good. For high flow rates, the experimental results deviate from either model. A correlation with the model developed by Dosanjh et al. [5,8], for forward smoldering with no ash left, is attempted unsuccessfully. Transition to flaming is observed for very high flow rates

only in upward burning experiments. Significant evidence that buoyantly induced flows are of considerable importance for all ranges of forced flow is obtained from these forward smoldering experiments.

Once a clear data-base was obtained from ground-based experiments, a series of tests were performed in aircraft flying parabolic trajectories that provide periods of low gravity as well as periods of high gravity. Chapter 5 describes this series of experiment performed in the NASA KC-135 and Learjet planes. These experiments were conducted in purely natural convection. No forced flow experiments were conducted since it was assumed that a forced flow would only damp the effect of buoyant flows. The results confirmed the observations described in the previous chapters. The competition between heat losses and oxidizer transport was clearly observed. For strong smolder, oxidizer transport is the dominant mechanism. For weak smolder, heat losses will lower the reaction temperature resulting in slower reaction kinetics leading towards extinction. The presence of pyrolytic reactions in forward smolder was confirmed and their ability to inhibit smolder was observed.

A final chapter, Chapter 6, outlines the overall conclusions of this work, outlines space-based experiments in progress and suggests future paths and further space-based studies which may be directly comparable with this work.

Chapter 2
NATURAL CONVECTION SMOLDER

2.1 Introduction

An experimental study is carried out to determine the effect of buoyancy on the propagation velocity of a free convection smolder reaction through a porous combustible material. Measurements are performed of the smolder velocity through polyurethane foam as a function of the smolder reaction location in the sample, the sample size, and the direction of propagation. Upward and downward burning free convection experiments show that three different zones can be identified in the process. In downward smoldering there is an initial zone where heat transfer from the igniter results in a slightly higher smolder velocity than in the sample center. This zone is followed by another one where an approximately constant smolder velocity is observed. The length of this region increases with the foam length. Then there is a final zone that is characterized by a strong increase in the smolder velocity. For upward burning the same three zones were identified.

A theoretical analysis of the flow field induced by buoyancy inside the foam is performed. By incorporating this analysis of the flow field to the model developed by Dosanjh [5] for opposed forced smolder and correlating the experimental smoldering velocities; it can be observed that downward smoldering is a steady process controlled by the supply of oxidizer to the reaction zone. Experimental observations and correlations show instead that upward burning is an unsteady

process also controlled by the amount of oxygen reaching the reaction zone, but where the accumulation of heat in the foam, convected by the products of combustion, increases the smoldering velocity and can lead to transition to flaming. For these experiments the assumption of negligible heat losses is valid, and under this assumption smolder process is found to be able to self-sustain with no other oxygen supply than the air from the pores of the foam. This conclusion is particularly important for a space based environment where gravity and consequently buoyancy could be negligible.

2.2 Description of the Experiment and Experimental Hardware

The fuel used in the experiments is an open cell, unretarded, white polyurethane foam, with a 26.5 Kg/m3 density and 0.975 void fraction. The porous fuel is contained in a vertical parallelepiped consisting of an aluminum frame and insulation Fiberfax walls whose basic composition is alumina-silica and binders, as shown in figure 2.1. To avoid diffusion of oxidizer through the walls, the walls were covered entirely with aluminum foil.The parallelepiped dimensions are varied to determine the effect of scale on the smolder process. The wall material was selected for insulation purposes in an attempt to ensure a one dimensional smolder spread in a region of at least 50 mm in diameter from the sample centerline.

The foam ignition is accomplished with an electrically heated igniter placed in close contact with the foam. The igniter is made of a nichrome wire placed in between two, 5 mm thick, porous ceramic honeycomb plates that provide rigidity to

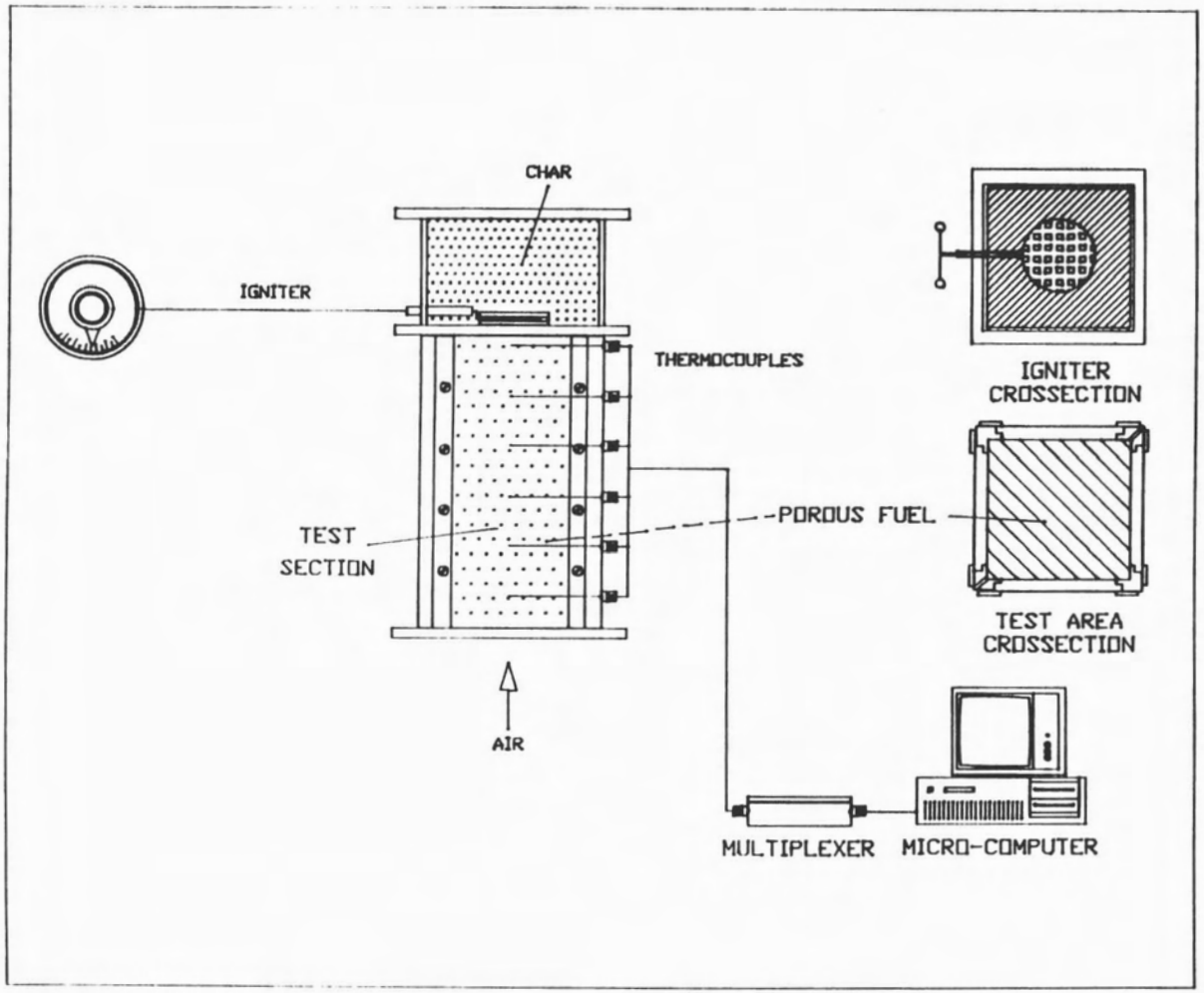

Figure 2.1 - Schematic of the experimental apparatus. Vertical and horizontal cross-sections of the test section and igniter section are presented. The nichrome wire igniter is controlled by a variable resistor, and a micro-computer stores in real time the data from the thermocouples.

the igniter and heating uniformity. To insulate the ignition zone and simulate an ongoing smolder process, a layer of char from an already smoldered foam is placed at the other side of the igniter. The foam ignition requires a supply of 1.70 KW/m^2 for approximately 900 sec., which is the approximate time required to heat up the igniter to an approximate temperature of 500°C. During the course of this work it was found that the onset of foam smoldering occurs only under very restrictive conditions of igniter type, temperature and time. Too high a temperature results in the melting or flaming of the foam, and too low in its pyrolytic decomposition. The ceramic heater, temperature and heating period used in these experiments were selected to ensure the self-supported propagation of the smolder reaction in the foam. The above observations concerning the restrictive conditions of smoldering initiation agree with those discuss by Ohlemiller and Rogers [11].

Eight Chromel-Alumel thermocouples 0.8 mm in diameter are embedded at predetermined positions in the porous fuel with their junction placed in the fuel centerline. The rate at which smolder spreads is measured from the temperature histories of the thermocouples, and it is calculated from the time lapse of reaction zone arrival to two consecutive thermocouples, and the known distance between thermocouples. The arrival of the reaction zone is characterized by a maximum in the temperature profile. However, under most experimental conditions this maximum is not sharply defined, and the location of the smolder zone is obtained by drawing tangents to the temperature curves and cutting them by a line at a temperature near to the maximum (350°C in this work). The smolder velocity is

calculated from the time lapse between two consecutive intersections. These thermocouples are also used to measure the reaction zone temperature. This temperature is used for comparative purposes, and it is not considered to be the actual smolder temperature, since it is not possible to determine weather the thermocouples are measuring the foam or air temperatures. Another important source of information in the smolder process is the species concentration near the reaction zone. Our attempts to measure them using gas chromatography have failed so far due to the clogging of the sampling lines by the tars and heavy hydrocarbons produced during the smolder of the foam.

In downward smoldering experiments the foam is ignited at the top and the smolder propagates downward, and in upward smoldering the foam is ignited at the bottom and the smolder propagates upward. Both ends of the sample are open so that buoyantly induced flow can freely circulate through the char and foam.

2.3 Experimental Results

Experiments are performed with samples of cross section 150 mm in the side and heights of 150 mm, 175 mm, 200 mm, and 300 mm (smaller samples were also tested but the results were so influenced by the end-effects that did not provide useful information). The measured smolder propagation velocities at different positions along the sample are presented in figure 2.2 for downward smolder and figure 2.3 for upward smolder, each data point represents an average for six experiments. The origin of the x-axis corresponds to the ignition plane. In

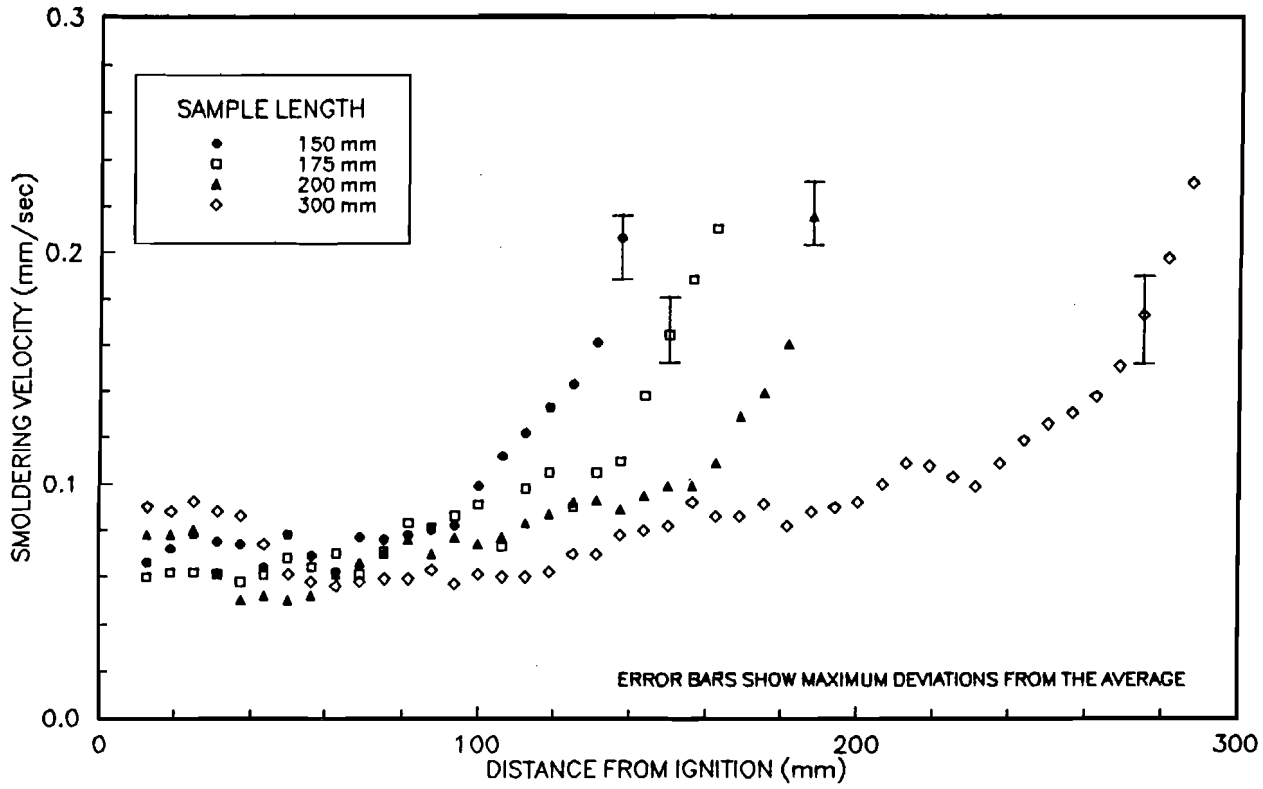

Figure 2.2 - Variation of the smolder propagation velocity as a function of the distance from ignition for downward smolder. Almost constant propagation velocities can be observed for most of the sample, a significant increase in the smolder propagation velocities occurs as the reaction reaches the end of the sample.

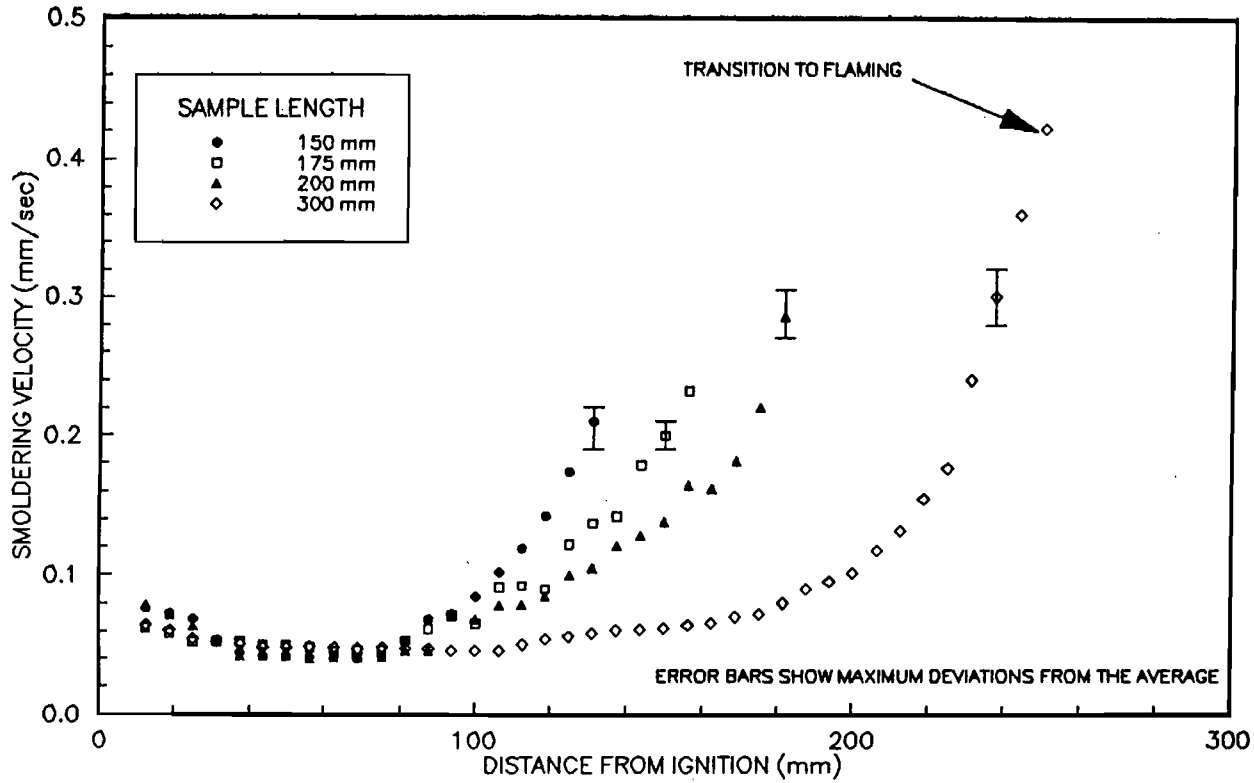

Figure 2.3 - Variation of the smolder propagation velocity as a function of the distance from ignition for upward smolder. Downward and upward burning have similar trends, but upward burning smolder velocities are significantly larger. Transition to flaming occurred for 300 mm samples.

downward burning smoldering velocities remain constant for a significant part of the sample, the length of this region increases with the foam length. Then there is a final zone approximately 50 mm deep that is characterized by a strong increase in the smolder velocity. Smoldering velocities for upward burning experiments are presented in figure 2.3. showing that in upward smoldering there is an initial zone, approximately 50 mm deep, where smoldering velocities decrease as the reaction propagates into the sample followed by a zone where smoldering velocities remains almost constant, and again a final zone where the smolder velocity increases sharply. It can be observed from comparing figures 2.2 and 2.3 that peak smoldering velocities for upward burning are significantly higher that for downward burning. Transition to flaming was observed when upward burning experiments were performed in 300 mm samples, no transition to flaming was observed for downward burning.

From the temperature histories the maximum temperatures read by each thermocouple are presented in figure 2.4 for downward burning and figure 2.5 for upward burning. It can be observed from figure 2.4 that there is an initial zone where temperatures decrease as smoldering propagates into the sample, for the rest of the sample temperatures increase slightly for thermocouples placed further away from the ignition plane. Upward burning can also be divided in two zones, figure 2.5 shows that there is an initial zone where temperatures decrease with distance from ignition, followed by a zone where temperatures increase with distance from ignition. When comparing both figures it can be observed that for both cases temperatures are in general smaller for larger samples. The initial zone can be attributed to the

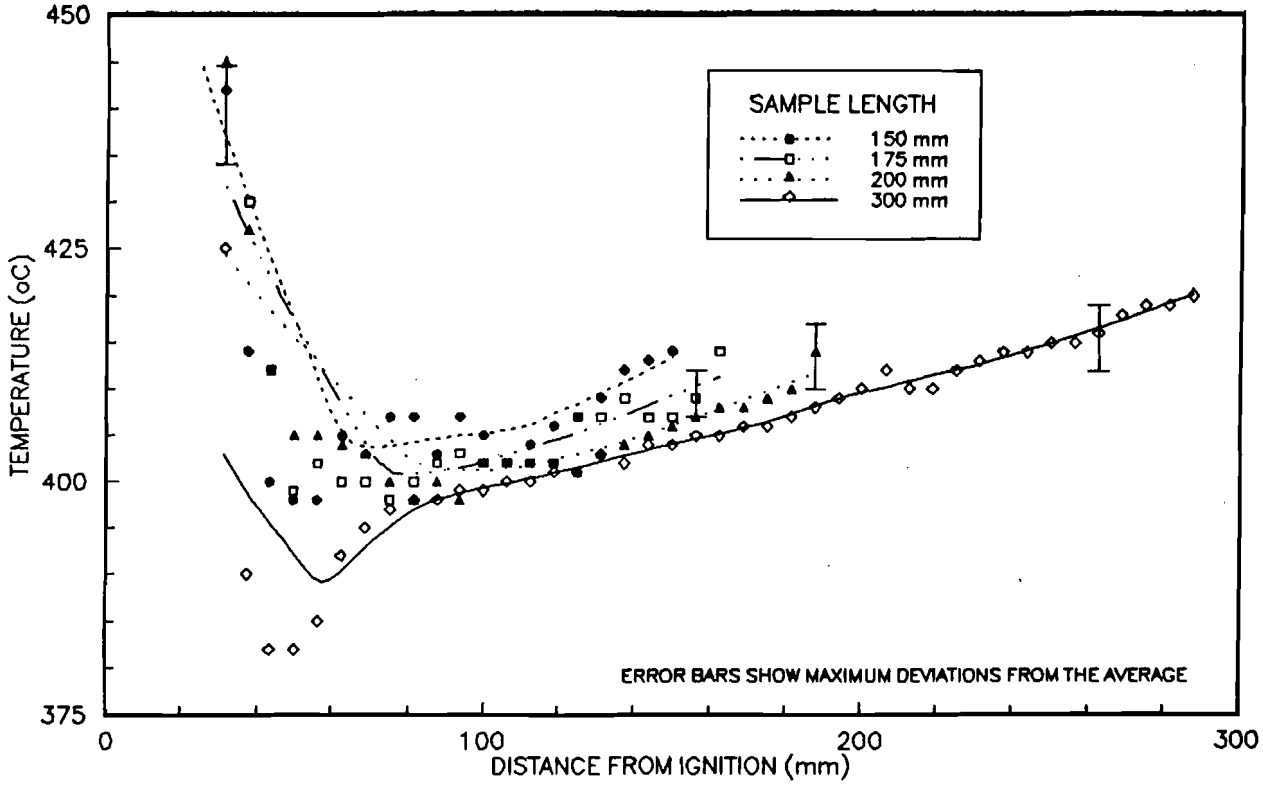

Figure 2.4 - Variation of the smolder reaction maximum temperature as a function of the distance from ignition for downward smolder. Temperatures decay in the igniter affected region. For the rest of the sample there is a small, almost linear increase in the maximum temperature. Temperatures are lower for larger samples.

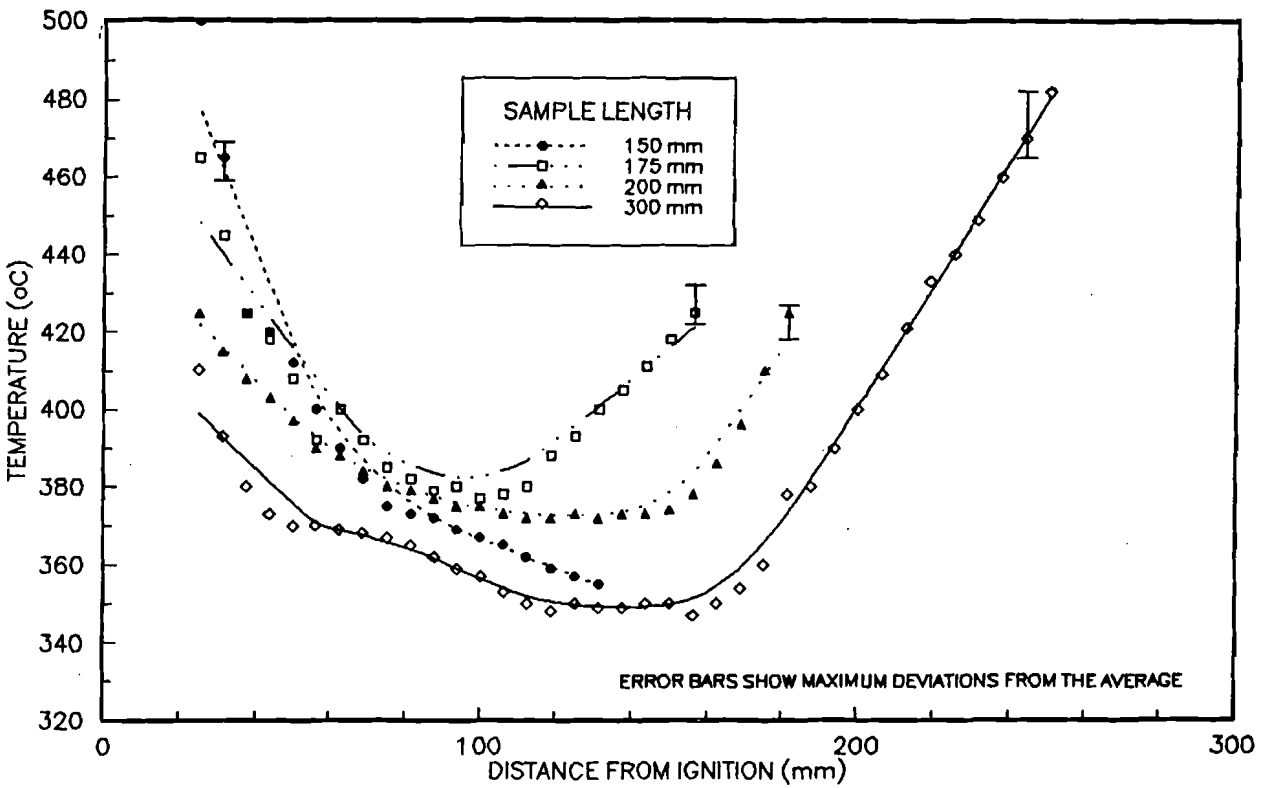

Figure 2.5 - Variation of the smolder reaction maximum temperature as a function of the distance from ignition for upward smolder. Temperatures decay as the reaction propagates into the sample, reach a minimum and then on increase, the temperature changes are much more significant for upward burning than for downward burning. Temperatures are lower for larger samples.

presence of the igniter which acts as an external source of heat for the sample. The igniter influenced zone is observed to extend into the sample deeper in upward burning that in downward burning. Upward and downward burning show a significant difference in the zone away from ignition, while downward burning temperatures remain almost constant upward burning temperatures increase significantly as the reaction moves away from the ignition plane. Maximum temperatures for upward burning drop significantly more for upward burning than for downward burning.

For both upward and downward burning, reactions occurring in the char where observed. For downward burning secondary reactions occurring after the smoldering front reached the end of the sample were observed. Smoldering will propagate almost to the end of the sample and will be immediately followed by a secondary reaction propagating upward. Figure 2.6 shows the temperature histories for eight thermocouples in a 200 mm sample burning downwards. As it can be observed from the figure, the thermocouple closest to the igniter measures temperatures higher than for other thermocouples, approximately 500°C, the next thermocouples will remain at an almost constant temperature, and only for the last two thermocouples evidence of char oxidation can be observed, the last two thermocouples are both located in the last 20 mm of the sample. Char oxidation reactions in general propagate much faster and are characterized by higher temperatures than the primary smoldering reaction. This secondary reaction will propagate upwards and increasing in strength as it gets closer to the igniter, as it can be determined from the temperature increase shown

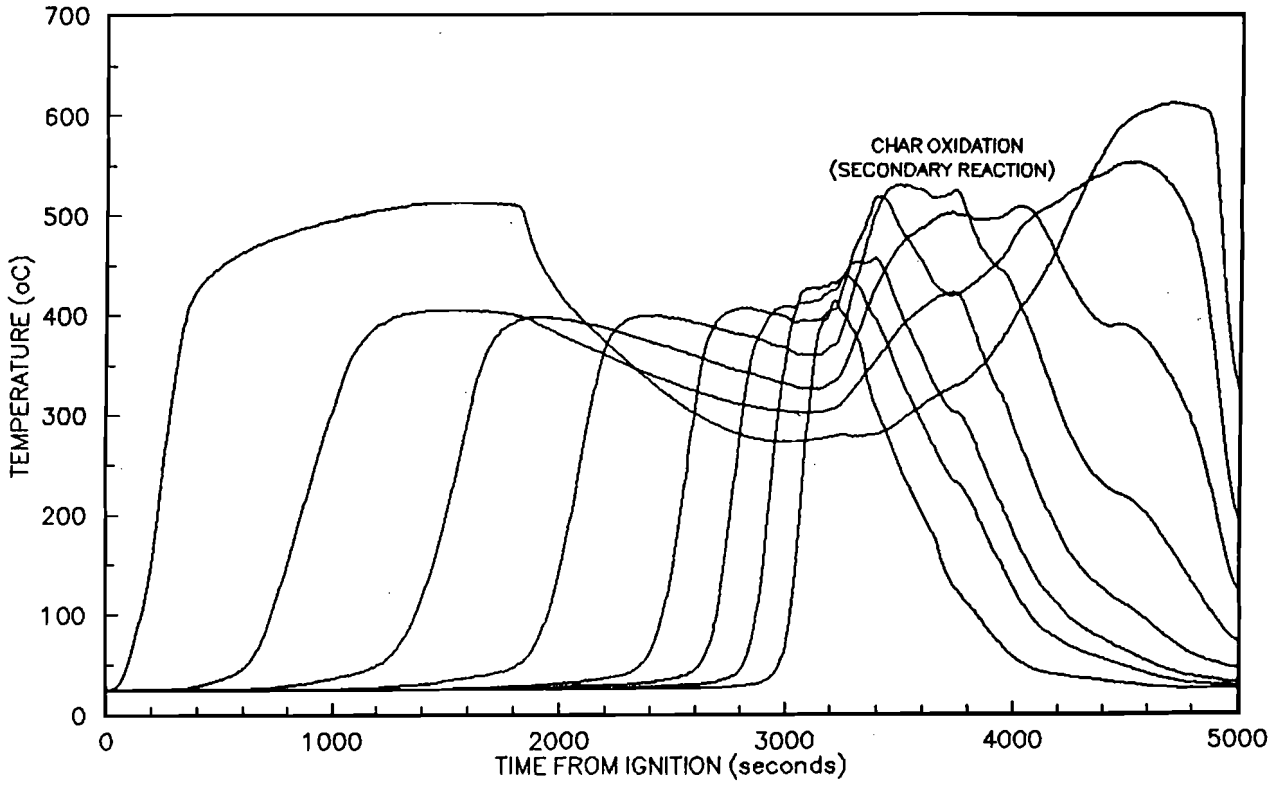

Figure 2.6 - Temperature histories for eight thermocouples, downward smoldering, 200 mm sample. Almost constant temperature smoldering reaction occurs for the first 3,000 sec. Unsteady secondary reaction occurs there after. Distance from ignition increases from left to right, the furthest to the left is the thermocouple closest to the igniter.

in figure 2.6, 3,000 sec. after ignition started. The strength of this secondary reactions increases with the length of the sample.

Temperature histories for six thermocouples placed in a 200 mm sample burning upwards are presented in figure 2.7. For upward burning buoyantly induced flows have to go through the hot char before reaching the reaction, in contrast with the downward case, explained above, where air comes through the cold foam towards the reaction zone. From figure 2.7 it can be observed that the first thermocouple undergoes a similar process as for downward burning but its temperature does not decay significantly after the reaction has moved forward, evidencing a continuous exothermic reaction in the char close to the thermocouple. This process of char oxidation has been observed earlier by Ohlemiller and co-workers [1,3,9]. Ohlemiller and Lucca [9] described a series of mechanisms of smoldering for this configuration, the results from chapter 4 confirmed experimentally for forced forward smoldering, that for flow velocities smaller than 1.5 mm/sec smoldering will propagate without condensed phase pyrolysis of the foam ahead of the reaction, for flow velocities over 1.5 mm/sec char oxidation will dominate supporting a condensed phase pyrolysis reaction in the foam, that, under appropriate conditions, could evolve to a gas phase pyrolysis reaction that could lead to transition to flaming. Pyrolysis temperatures for these experiments were approximately 320°C. The temperature histories of figure 2.7 show that for the first two thermocouples no evidence of pyrolysis can be obtained; the third thermocouple shows the first evidence of an endothermic process that is using all the energy produced by the oxidative reaction, therefore, leveling off

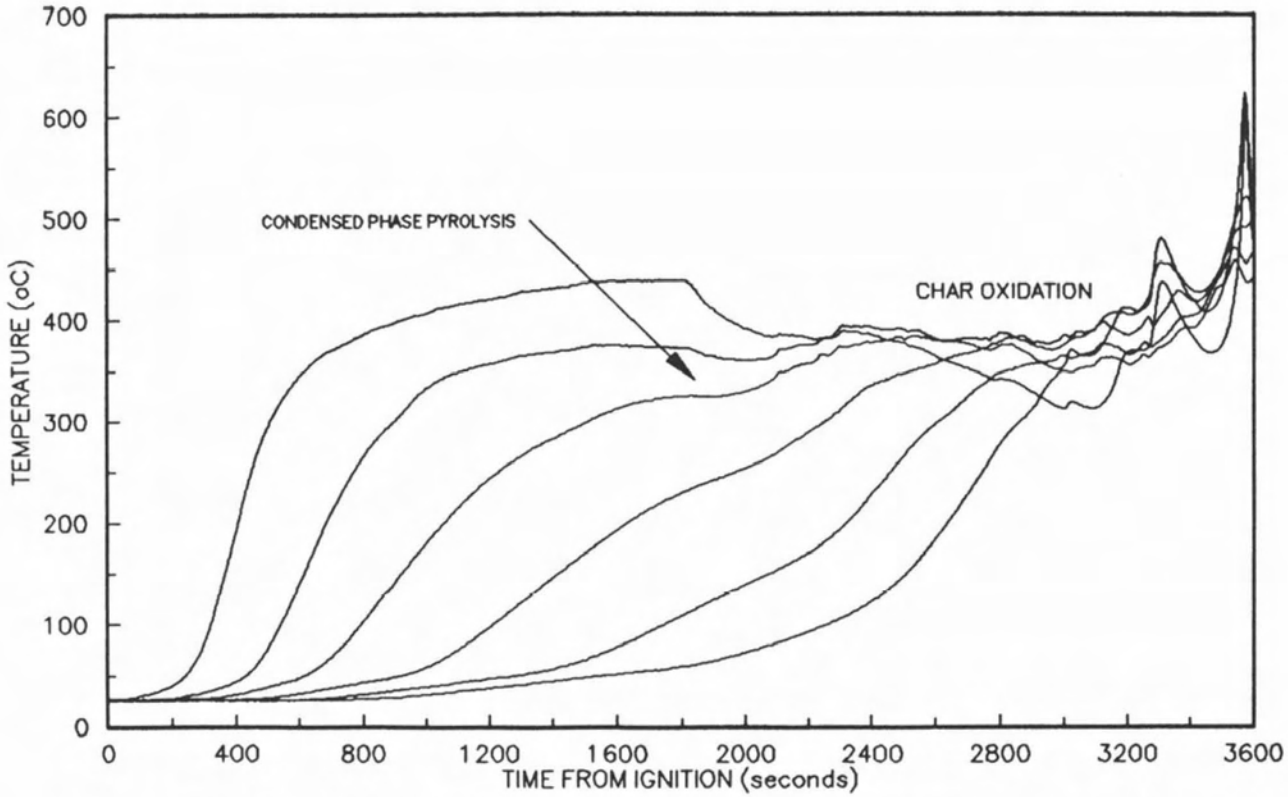

Figure 2.7 - Temperature histories for six thermocouples, upward smoldering, 200 mm sample. Distance from ignition increases from left to right, the furthest to the left is the thermocouple closest to the igniter. From left to right, the first two temperature traces show no evidence of pyrolysis. Pyrolysis is an endothermic reaction that occurs at temperatures of approximate 320°C (third temperature trace), after pyrolysis is observed unsteady char oxidation occurs (2,000 sec. after ignition).

the temperature at approximately 320°C. This region of constant temperature is immediately followed by unsteady temperature traces characteristic of char oxidation. From then on the reaction strength increases as shown by the increase in the maximum temperatures read by the thermocouples.

An important difference between upward and downward burning is the direction of convective heat transfer, for downward burning convection carries heat from the reaction into the char behind the reaction, therefore as the reaction propagates heat is being transferred to the foam by conduction and radiation only. Since both conduction and radiation are very poor modes of heat transfer, for this kind of porous material and temperatures [12], the preheated foam region is very small. So, as observed from figure 2.6, for downward burning the reaction virtually encounters fuel and oxidizer at ambient temperature. In contrast, for upward burning, convection transfers heat from the reaction to the virgin foam. The hot post-combustion gases pre-heat the foam ahead of the reaction, and, as it can be observed from figure 2.7, the reaction encounters fuel at temperatures that could be over 100°C higher than ambient, as was observed by Cantwell [49] for opposed forced flow experiments, such a change in the initial temperature can result in a significant increase in smoldering propagation velocities.

2.4 Smoldering Model

2.4.1 Discussion of the Problem

Downward burning resembles opposed forced flow smoldering and upward

burning forward forced flow smoldering. In both cases buoyantly induced flows act as the forced flow; therefore, theoretical models developed for forced flow smoldering will be used in an attempt to correlate the experimental data. The theoretical model of opposed flow developed by Dosanjh et al. [5,7] is used in this work to correlate the above reported data for downward burning. For forward smoldering no simple model can describe the process for all flow rates. For very small flow rates smoldering propagates through the virgin fuel leaving a weakly reacting char behind that does not entirely deplete the oxidizer incoming with the forced flow, and does not produce enough energy to sustain pyrolytic decomposition of the foam; as the flow rate is increased the char behind the smoldering front undergoes a stronger oxidation reaction depleting the oxidizer from the forced flow and producing enough heat to change the pathway of the reaction from smoldering to condensed phase pyrolysis [1,3,9]. This process is entirely supported by the heat incoming from the oxidation of the char. All the energy provided by the oxidation of the char is used to pyrolyse the foam, therefore a region of no temperature increase appears. The exact pyrolysis temperature is not well known, but there is extensive literature that coincide in placing it in a range between 300°C to 320°C [1,3,5,7,9].

Upward burning is a smoldering process of the forward configuration where the flow reaching the reaction is increasing as the reaction propagates into the sample, since the reaction undergoes different modes for different flow velocities no single theoretical model can predict the process for the entire flow velocity range.

The theoretical model of forward flow smolder developed by Johnson et al.[51] is used in this work to correlate the above reported data. This model is a solution for forward propagation of an exothermic reaction in the absence of pyrolysis as a heat sink. Even though this is the simplest model, the departures from the model should provide adequate insight for a better understanding of the process. To facilitate the understanding and discussion of the correlation, a brief description of the models is given here.

In downward burning, with frame of reference anchored at the reaction zone, the fuel and oxidizer enter the reaction zone in the same direction. In upward smoldering, with frame of reference anchored at the oxidation zone, the fuel and oxidizer enter the reaction zone in the opposite direction. Since smoldering is generally oxygen limited, the heat released by the smolder reaction can be expressed in terms of the mass flux of oxidizer at the reaction zone. This heat is transported by conduction and radiation downstream of the reaction zone, and sustains the propagation of the smolder front. It should be noted that the fuels of interest in smoldering combustion are very porous, and consequently conduction is a relatively poor mode of heat transfer [12]. Thus radiation heat transfer is important despite the relatively small temperatures encountered in smoldering combustion.

In the model of Dosanjh et al.[5,7] opposed smoldering is modeled as a finite rate, one-step reaction, of the form

$$\nu_F[\mathrm{FOAM}] + \nu_O O_2 \rightarrow \nu_{CH}[\mathrm{CHAR}] + \nu_{gp}[\mathrm{GaseousProducts}] + Q\nu_O M_O \qquad (2.1)$$

The stoichiometries for these reactions are obtained from Summerfield and Mesina [2].

Smoldering is assumed to be one-dimensional and steady in a frame of reference fixed to the smolder wave (figure 2.8). The gas and solid are presumed to be in local thermal equilibrium, and the solid phase is considered continuous with a constant void volume fraction. Energy transport due to concentration gradients, energy dissipated by viscosity, work done by the body forces, and the kinetic energy of the gas phase are ignored. It is assumed that the pyrolysis reaction occurs at a constant temperature [7,9]. Furthermore, since smoldering velocities are much smaller than flow velocities, flow velocities can be taken as known quantities at each location in the sample, x_S.

With the above assumptions, and neglecting heat losses to the environment, the one dimensional form of the energy conservation equation becomes

$$(\dot{m}_F'' Cp_F + \dot{m}_A'' Cp_A) \frac{dT}{dx} = (\lambda_{eff} + \lambda_{rad}) \frac{d^2T}{dx^2} + Q \frac{d\dot{m}_O''}{dx} \qquad (2.2)$$

where the mass fluxes of fuel and oxidizer entering the reaction zone are given by,

$$\dot{m}_F'' = (1-\phi)\, \rho_F U_S$$

$$\dot{m}_A'' = \rho_A u_g + \rho_A \phi U_S$$

$$\dot{m}_O'' = Y_O \dot{m}_A'' - \phi \rho_A D \frac{\partial Y_O}{\partial x}$$

for downward burning and by,

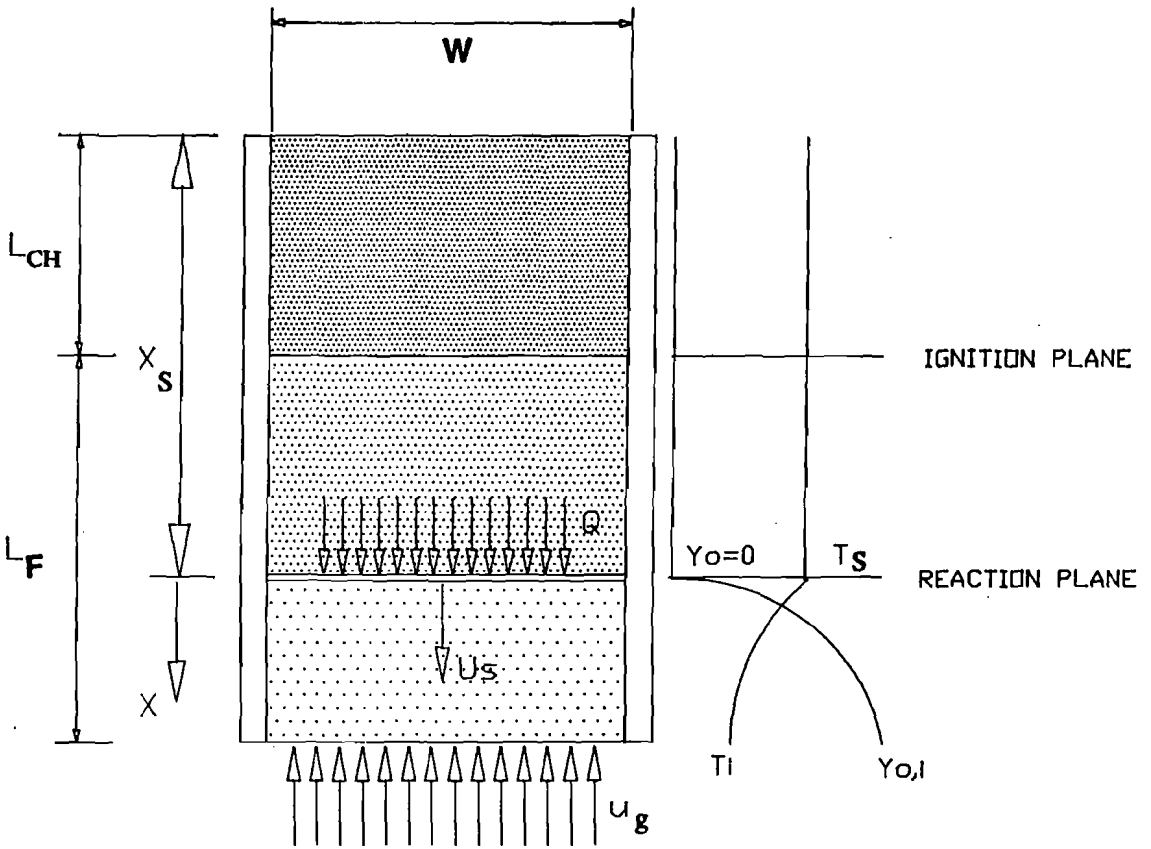

Figure 2.8 - Schematic of one-dimensional downward burning smoldering viewed in a frame of reference moving with the smolder wave.

$$\dot{m}_F'' = (1-\phi)\,\rho_F U_S$$

$$\dot{m}_A'' = \rho_A (u_g - U_S) + \rho_A \phi U_S$$

$$\dot{m}_O'' = Y_O \dot{m}_A'' - \phi \rho_A D \frac{\partial Y_O}{\partial x}$$

for upward burning.

λ_{eff} is an effective thermal conductivity of the form

$$\lambda_{eff} = \phi \lambda_A + (1-\phi)\,\lambda_F$$

Radiation is incorporated in the analysis using a diffusion approximation with an equivalent thermal conductivity given by

$$\lambda_{rad} = \frac{16 \sigma d_p T^3}{3}$$

The boundary conditions for the above equation are

$$\text{at} \quad x = x_S \qquad \frac{\partial T}{\partial x} = 0$$

$$T = T_S$$

$$\dot{m}_O'' = 0$$

$$\text{at} \quad x = x \qquad \frac{\partial T}{\partial x} = 0$$

$$T = T_i$$

$$\dot{m}_O'' = \dot{m}_{O,i}''$$

Integrating with respect to x from x_S to ∞, the following expressions are obtained for the smolder propagation velocity

$$U_S = \frac{\rho_A [Q Y_{O,i} - Cp_A (T_S - T_i)] u_g + \dot{q}_i''(x)}{\rho_F Cp_F (1-\phi)(T_S - T_i)} \qquad (2.3)$$

for downward burning and

$$U_S = \frac{\rho_A Q Y_{O,i} u_g + \dot{q}_i''(x)}{[\rho_A Cp_A \phi + \rho_F Cp_F (1-\phi)](T_S - T_i) + (1-\phi) Q \rho_A Y_{O,i}} \qquad (2.4)$$

for upward burning.

An integral solution for a semi-infinite slab with constant heat boundary condition assuming parabolic profiles [68,69] gives the following expression for the heat conducted by the igniter and the initial temperature distribution for the foam.

$$\dot{q}_i''(x) = -\frac{\dot{q}_i''(0)}{\delta_c}(x - \delta_c) \qquad \text{for} x < \delta_c$$

$$\dot{q}_i''(x) = 0 \qquad \text{for} x > \delta_c$$

$$T_i(x) = T_{0,i} + \frac{\dot{q}_i''}{\delta_c}(x - \delta_c)^2 \qquad \text{for} x < \delta_c$$

$$T_i(x) = \text{experimental} \qquad \text{for} x > \delta_c$$

the value of δ_c =52 mm is obtained assuming that the solution reaches steady state when $T_i(0) = 500°C$.

The analysis of Dosanjh et al.[5,7] also provides an expression for the smolder temperature T_S. However, the asymptotic analysis leading to that expression imposes a number of restrictive conditions that are often not applicable to the experiments. For this reason, in this work the value of the smolder reaction

temperature is obtained from the experimental data of figures 2.4 and 2.5. For upward burning experiments the initial temperature varies with time, therefore the value of the initial temperature is obtained from the temperature histories; the initial temperature is taken to be the one observed at the first inflection point in the temperature histories. The heat of combustion Q, is not well determined for smoldering combustion [1]. In this work it will be selected so that the best correlation is obtained. As it will be shown later, the resulting value for the heat of combustion agrees well with that previously reported in other works [1,2,3,5,6,7,8]. Finally, the oxidizer velocity u_g is determined by the draft induced through the duct and the possible boundary layer flows that could be established in the char. Thus, the potential generation of buoyant flows inside the char requires the treatment of the flow through the foam as a mixed flow problem, where the draft induced flow would play the role of the forced flow. This is done in the following section.

2.4.2 Analysis of the Flow Induced Through the Polyurethane Foam

All the above mentioned phenomena show that no significant explanations can be provided without analyzing the fluid dynamics of the system. A two dimensional analysis of the flows induced through the polyurethane foam will be done based on the Darcy flow model [13,14].

The problem is a combination of free flow induced by natural draft in the x direction and a boundary layer flow induced by a gradient of temperature in the y direction, between the insulation walls and the hot char (figure 2.9). Diffusion of

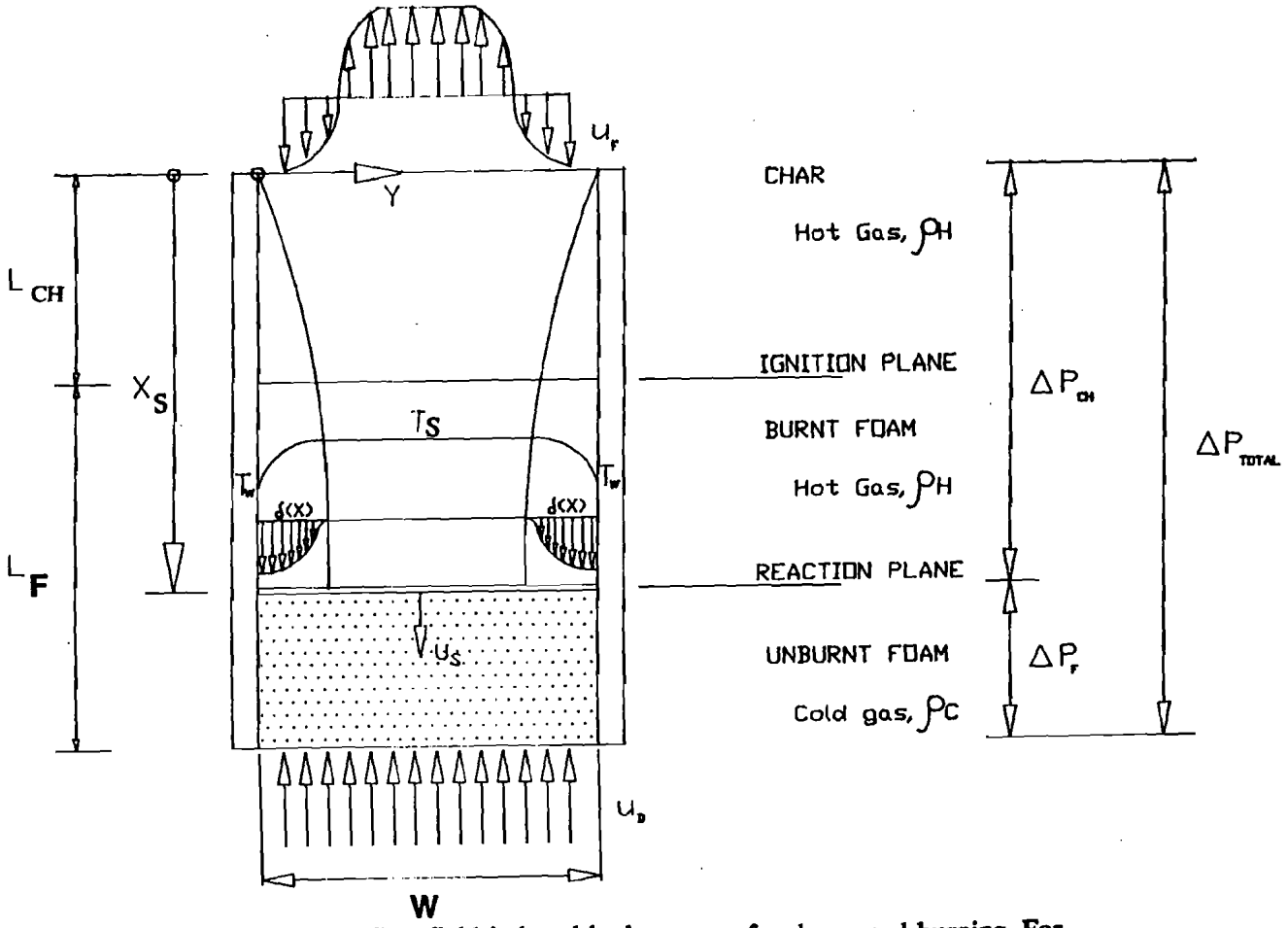

Figure 2.9 - Schematic of the flow field induced by buoyancy, for downward burning. For upward burning the diagram has to be rotated 180°, the resultant flow in the char is the same. Both in downward and upward burning recirculation flow adds to the natural draft flow in the core of the sample (aiding flow).

oxidizer to the reaction zone and the flow induced by the hood, where the experiments were performed, will be considered in the analysis. In the mathematical formulation of the problem we will assume that (i) the convective fluid and the porous medium are everywhere in thermodynamical equilibrium, (ii) there is no phase change in the solid, (iii) properties of the fluid and the porous medium are homogeneous and isotropic, and (iv) the Boussinesq approximation is invoked.

The problem is divided in four parts treated independently and the results are superposed. The following analysis is identical for both upward and downward burning, therefore only the analysis for downward burning will be presented. For downward burning air flows through the foam towards the reaction and in upward burning through the char towards the reaction. The values for all properties used are shown in table 2-1.

2.4.2.1 Natural Draft Through a Duct

The flow induced by the density difference between the hot gases and the cold air is a one dimensional problem where the equation for conservation of momentum is substituted by Darcy's empirical formulation.

$$u = -\frac{K}{\mu}\left(\frac{\partial P}{\partial x} - \rho g\right) \qquad (2.5)$$

This equation is then integrated separately in two regions, the unburnt foam and the burnt foam plus insulation char. The integration has to be done this way because char and foam have significantly different permeabilities.

Table 2-1
Properties

$Cp_A = 1.088$ KJ/Kg
$Cp_F = 1.700$ KJ/Kg
$D = 4.53 \times 10^{-5}$ m^2/s
$d_p = 0.05$ mm
$K_{CH} = 8.40 \times 10^{-7}$ (Natural Convection Experiments)
$K_F = 2.76 \times 10^{-9}$
$g = 9.81$ m/s^2
$L_C = 150$ mm
$W = 150$ mm
$\Delta P_{HOOD} = 65.2$ N/m^2
$n_C = 0.7550$ moles
$n_H = 2.872$ moles
$T_i = 293$ K
$T_W = 483$ K
$Y_{O,i} = 0.235$
$\alpha = 1.122 \times 10^{-4}$ m^2/s
$\beta = 1.684 \times 10^{-3}$ K^{-1}
$\lambda_{eff} = 0.047$ W/mK
$\mu = 1.50 \times 10^{-5}$ Kg/ms
$\phi_{CH} = 0.9775$
$\phi_F = 0.9750$
$\rho_C = 1.225$ Kg/m^3
$\rho_H = 0.299$ Kg/m^3
$\rho_F = 1{,}034.0$ Kg/m^3
$\sigma = 5.67$ W/m^{2}K^4

The results obtained are as follows:

$$\Delta P_F = -\left(\frac{\mu}{K_F} u_C - \rho_C g\right)(L_F + L_{CH} - x) \qquad (2.6)$$

$$\Delta P_{CH} = -\left(\frac{\mu}{K_{CH}} u_H - \rho_H g\right) . x \qquad (2.7)$$

from the ideal gas law and stoichiometry of the reaction [2] a relationship between u_H and u_C is established leaving equations 2.6 and 2.7 in terms only of u_C which for convenience will be called u_D.The total pressure difference between the top and bottom of the test section is

$$\Delta P_{TOTAL} = \rho_C g (L_F + L_{CH}) + \Delta P_{HOOD} \qquad (2.8)$$

the pressure difference established by the hood where the experiments were conducted is measured experimentally.

Adding equations 2.6, 2.7, equating with 2.8 and solving for u_D the following expression is obtained

$$u_D = \frac{g(\rho_H - \rho_C)x + \Delta P_{HOOD}}{\frac{\mu}{K_F}\left[(L_F + L_{CH} - x) + \left(\frac{K_F}{K_{CH}}\right)\left(\frac{\phi_F}{\phi_{CH}}\right)^{\frac{2}{3}}\left(\frac{n_H}{n_C}\right)\left(\frac{T_S}{T_i}\right)x\right]} \qquad (2.9)$$

2.4.2.2 Flow Induced by Boundary Layer

For the boundary layer flow the natural draft will be taken as a forced flow. Combined free and forced flows in porous media have not been extensively studied, the following analysis is based on the works of Bejan [14], Nield and Bejan [55], Lai et al.[63], Hadim and Govindarajan [65]. For the mixed flow problem several considerations have to be taken on account. In the char, the recirculating flow moves from top to bottom near the walls and from bottom to top near the sample centerline; therefore, for downward burning, forced and buoyantly induced flows add at the centerline (aiding flows), while for upward burning, the flows oppose at the centerline (opposing flows). A numerical study of the problem [63] showed that for aiding flows the mixed flow solution is only valid for values of the Ra/Pe smaller than 50, for values greater than 50 the solution resembles more the natural convection boundary layer solution. Instead for opposing flows the mixed flow solution gives a more accurate description of the problem for values of Ra/Pe smaller than 500. A study of the magnitude Ra/Pe using u_D as characteristic velocity and an experimentally calculated average char permeability (Table 2-1) show that the parameter Ra/Pe ranges from 0.1 to 10 for all values of x, therefore, a mixed convection solution is required.

Darcy's Law gives the following governing equations [13,14].
Continuity

$$\frac{\partial u_b}{\partial x}+\frac{\partial v_b}{\partial y}=0 \qquad (2.10)$$

Momentum

$$v_b = -\frac{K_{CH}}{\mu}\left(\frac{\partial P}{\partial y}\right)$$

$$u_b = -\frac{K_{CH}}{\mu}\left(\frac{\partial P}{\partial x} - \rho g\right) \qquad (2.11)$$

where $\rho - \rho_A = -\beta \rho_A (T - T_i)$

After invoking the Boussinesq approximation, cross differentiating the momentum equation to eliminate the pressure terms the following expression for a single momentum equation is obtained

$$\frac{\partial v_b}{\partial x} - \frac{\partial u_b}{\partial y} = \frac{\beta \rho_A g K_{CH}}{\mu}\frac{\partial T}{\partial y} \qquad (2.12)$$

The relevant boundary conditions are given by

$y=0$	$u_b = u_b(0)$
	$v_b = 0$
	$T = T_W$
$y=\delta$	$v_b = 0$
	$T = T_S$
$x=x_S$	$u_b = u_D$
	$v_b = 0$
$x=-\infty$	$u_b = u_D$
	$v_b = 0$
	$\frac{\partial T}{\partial x} = 0$

non-dimensionalizing in the following way [63,65].

$$\overline{u_b}=\frac{u_b}{u_D}$$

$$\overline{v_b}=\frac{v_B}{v} \quad \text{where} \quad v=\frac{\delta}{L_{CH}}u_D$$

$$\overline{x}=\frac{x}{L_{CH}}$$

$$\overline{y}=\frac{y}{\delta} \text{ where } \delta=\delta_T=xRa_x^{-0.5}$$

$$T=\frac{T-T_W}{T_S-T_W}$$

Natural boundary layers in porous media have a single length scale δ_T and by using this expression for the boundary layer thickness the coupling between the energy and momentum equations is avoided [14,55].

The non-dimensional equivalent of equation 2.12 is

$$\left(\frac{\delta_T}{L_{CH}}\right)^2 \frac{\partial \overline{v_b}}{\partial \overline{x}}-\frac{\partial \overline{u_b}}{\partial \overline{y}}=-\frac{Gr_K}{Re_K}\frac{\partial T}{\partial \overline{y}} \qquad (2.13)$$

where

$$\left(\frac{\delta_T}{L_{CH}}\right)^2 \ll 1$$

so equation 2.13 simplifies to

$$\frac{\partial \overline{u_b}}{\partial \overline{y}} = \frac{Gr_K}{Re_K} \frac{\partial T}{\partial \overline{y}} \qquad (2.14)$$

with the following boundary conditions

$$\overline{y}=0 \quad \begin{matrix} T=0 \\ \overline{u_b}=\overline{u_b}(0) \end{matrix}$$

$$\overline{y}=1 \quad \begin{matrix} T=1 \\ \overline{u_b}=0 \end{matrix}$$

Linear profiles for both velocity and temperature satisfy the boundary conditions, and let $\overline{u_b^*}$ be the average non-dimensional velocity in the boundary layer, therefore

$$T(\overline{y}) = \overline{y}$$

$$\overline{u_b}(\overline{y}) = -2\overline{u_b^*}(\overline{y}-1)$$

and $$\overline{u_b}(0) = 2\overline{u_b^*}$$

Substituting these expressions in equation 2.14 and averaging $\overline{u_b^*}$ over the whole sample cross-section, the following expression is obtained for the average dimensional velocity

$$u_b = \frac{2\delta}{W} \left(\frac{Gr_K}{Re_K}\right) u_D \qquad (2.15)$$

where

$$Ra_x = \frac{K_{CH} g \rho_A \beta (T_W - T_S) x}{\alpha \mu}$$

$$Re_K = \frac{\rho_A u_D K_{CH}^{0.5}}{\mu}$$

and $$Gr_K = \frac{K_{CH}^{1.5} g \rho_A^2 \beta (T_W - T_S)}{\mu^2}$$

The quotient Gr_K/Re_K is also expressed by several authors [14,55,63,65] as Ra_x/Pe

where $Pe = \frac{u_D x}{\alpha}$

2.4.2.3 Diffusion of Oxidizer into the Reaction Zone

The one point that is still to be discussed is the elimination of all diffusion terms. From the species equation will be demonstrated that the transport of oxidizer to the reaction zone is controlled by convection, therefore all the diffusion terms can be neglected. A diffusive boundary layer thickness is defined, δ_D . If this boundary layer thickness is much smaller than the problem length scale, L_{CH}, then diffusion is infinitely fast, therefore the transport of oxidizer to the reaction zone is controlled by convection.

The one dimensional diffusion problem is characterized by following equation.

$$\frac{dY_O}{dt} + (\phi U_S + u_D + u_b)\frac{dY_O}{dx} = D\frac{d^2Y_O}{dx^2} \qquad (2.16)$$

where U_S is the smoldering velocity and D is constant. This equation describes the transport of oxidizer into the reaction zone. The oxidizer concentration at the reaction zone is assumed to be zero ($Y_{O,S}=0$) and the oxidizer concentration far away from the reaction is considered to be that of air ($Y_{O,i}$). And the length region where Y_O changes is δ_D . From equation (2.16)

$$\delta_D = \frac{D}{u_D + u_b + \phi U_S}$$

substituting the appropriate parameters $\frac{\delta_D}{L_{CH}} \ll 1$ for all values of x and u_D , therefore oxidizer transport to the reaction is dominated by convection of air towards the reaction zone and the total air flow, u_g, can be expressed as

$$u_g = u_D + u_b + \phi U_S \qquad (2.17)$$

Figure 2.10 shows u_g as a function of the distance from ignition plane (x).

2.5 Discussion of the Results

2.5.1 Downward Burning

The results obtained in equation 2.17 for the oxidizer supply were incorporated to equation 2.3 to obtain a theoretical prediction for the smolder velocity as a function of the distance from ignition. These results were used to

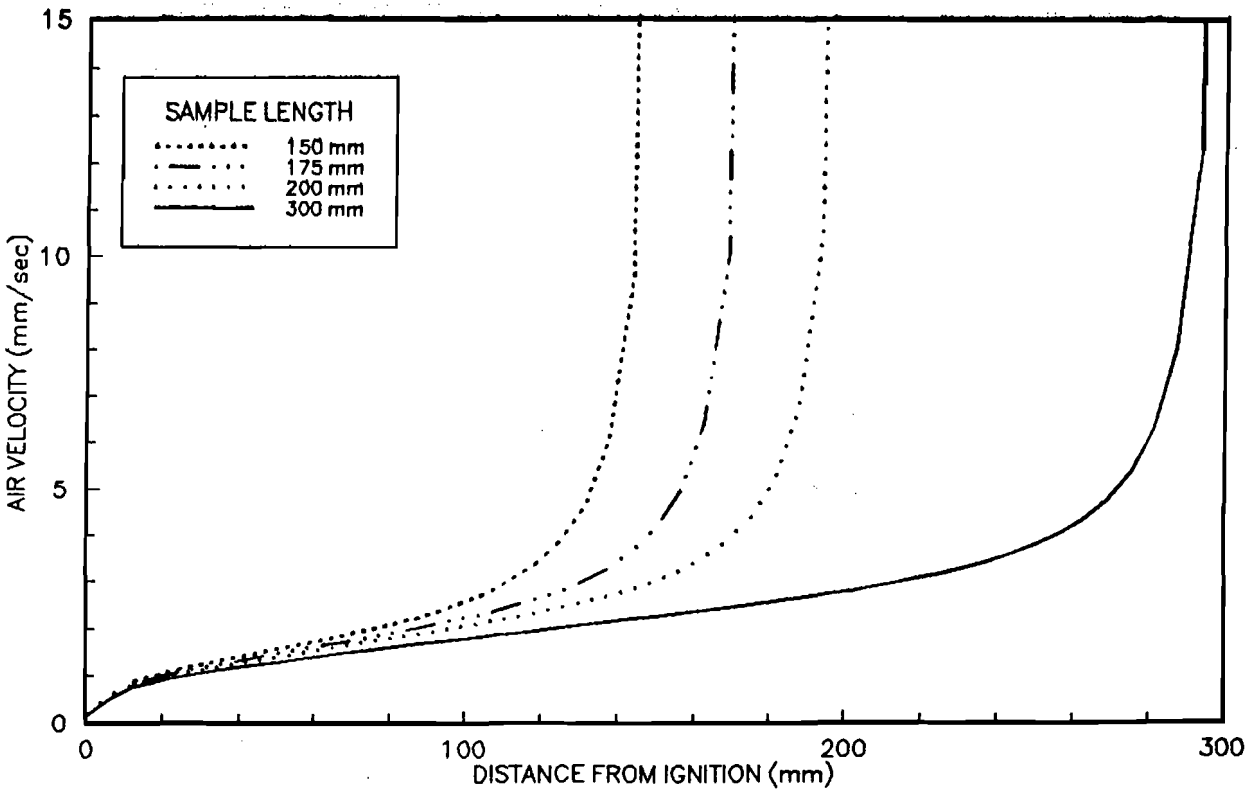

Figure 2.10 - Variation of the air flow velocity as a function of the distance from ignition. The magnitude of the air flow velocity is the same for both upward and downward smolder.

correlate the smoldering propagation velocity presented in figure 2.2. The properties used are those of Table 2.1. The results of the correlation are presented in figure 2.11. It is seen that the model predicts very well smolder velocities. This good agreement show that for these fuel and experimental conditions the simplifying assumptions used by the model are correct. The insulation provided by the fiberfax walls of the test section along with the self-insulating properties of foam and char combine to make heat losses to the environment negligible. The analysis conducted by Dosanjh [5,7] and Cantwell [49] to justify the assumption of thermal equilibrium between the phases is confirmed, since the reaction seems unaffected by the flow through the porous media. The combined effects of the flow induced by buoyancy due to horizontal temperature gradients, natural draft induced by a vertical density gradient and the air from the pores describe accurately the mechanisms of oxidizer supply to the reaction. The three flows were used independently to correlate the smoldering velocity data, obtaining smoldering velocities that were inaccurate quantitatively and qualitatively, showing that none of these effects individually describes the mechanisms of oxidizer transport to the reaction zone.

It can be observed from table 2.1 that the permeability of the char is much greater than the permeability of the foam, the value for the char permeability was obtained experimentally measuring the pressure drop through the char for different forced air flow velocities after the foam was totally burnt; the reaction was extinguished near the end of sample before the secondary reactions started. This increase in permeability is responsible for the presence of buoyantly induced

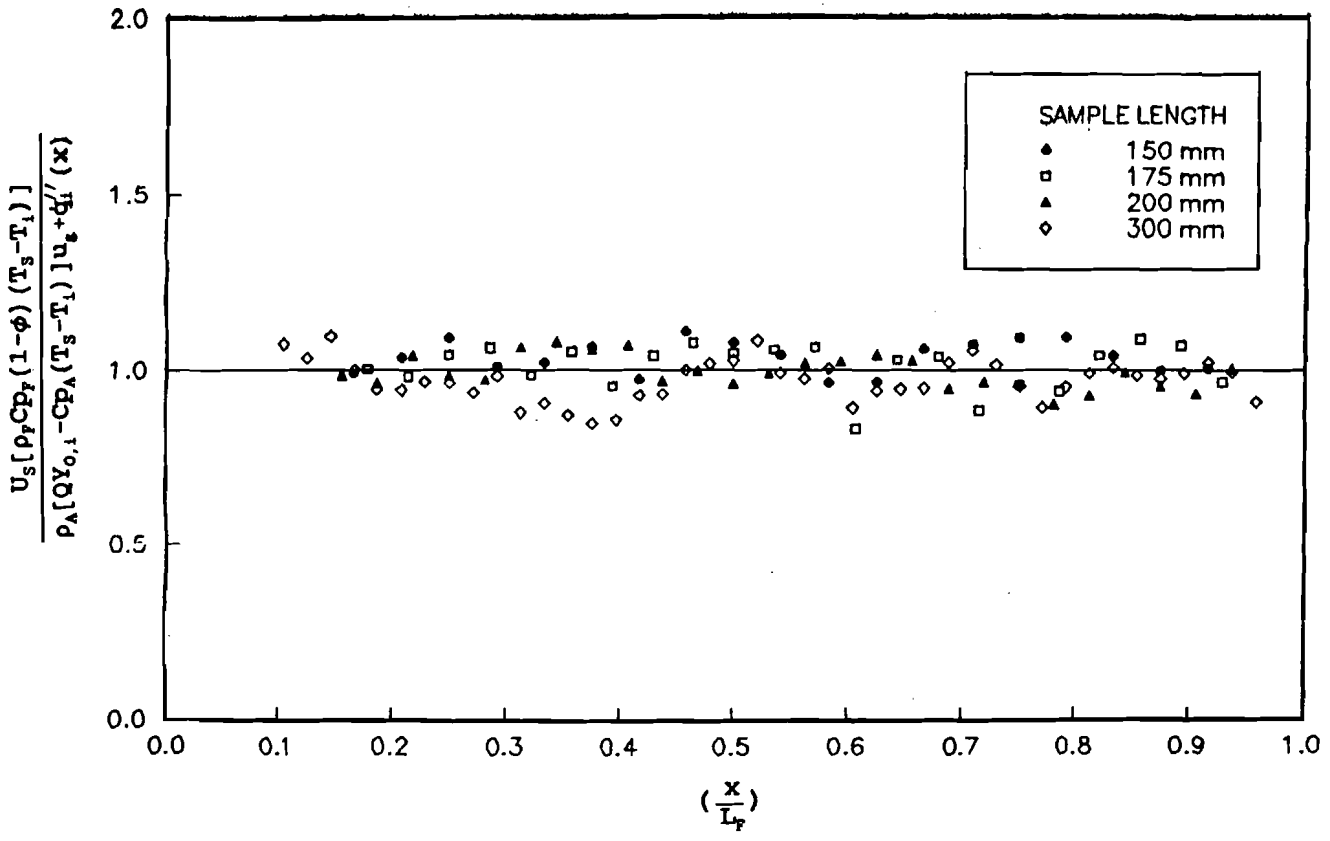

Figure 2.11 - Correlation of experimental and theoretical smoldering propagation velocities, for downward burning experiments, as a function of a non-dimensional distance from ignition.

recirculation currents inside the char, the magnitude of the boundary layer flow inside the foam is neglectable.

One of the models most severe assumptions is that of fast chemistry and total oxygen depletion in the reaction zone, this assumption is verified by the results presented above. Since smoldering is an oxygen starved process, the rate of reaction is controlled by oxygen supply to the reaction, since oxidizer supply increases as the reaction propagates into the sample, the heat generated by the reaction increases and therefore smoldering velocities increase. Under natural convection conditions in downward burning, the controlling mechanism of smolder propagation is oxidizer supply to the reaction. This confirms the results of Moussa et al.[29] and Rogers and Ohlemiller [10] presented in chapter 1 (figures 1.2, 1.3, 1.4 and 1.5).

An important phenomena that still has not been mentioned are the secondary reactions observed to occur after the smoldering front reached the end of the sample. So far the assumption that all the oxidizer incoming the reaction zone is consumed has proven to be valid, therefore smoldering leaves behind a combustible char and products of combustion. The fuel in this char is only a small percentage less than the original fuel. This fuel is a predominantly carbonaceous material of highly exothermic oxidation [1]. The surface area is enhanced with respect to the original fuel, mainly due to pores formation, its permeability is increased and, due to the high level of insulation, its temperature is almost as high as the reaction temperature. Therefore as soon as the primary reaction dies and the oxygen in the air is not entirely consumed at the reaction front, the char will smolder under the same

characteristics of upward smoldering enhanced by the fact that there is more oxygen available and that the fuel has already been preheated by the primary reaction.

2.5.2 Upward Burning

The results obtained in equation 2.17 for the oxidizer supply were incorporated to equation 2.4 to obtain a theoretical prediction for the smolder velocity as a function of the distance from ignition. These results were used to correlate the smoldering propagation velocity presented in figure 2.3. The properties used are those of Table 2.1. The results of the correlation are presented in figure 2.12. The agreement between experimental and theoretical smoldering velocities is poor, figure 2.12 shows that the experimental smoldering propagation velocities are significantly smaller than those predicted by the model, there is an initial region where experimental velocities decay with respect to theoretical values (up to x/L_F approximately 0.4) after which propagation velocities start to increase, never reaching the predicted values. Even though there is no quantitative agreement with the theory the experimental data follows the same trends for different sample lengths. There is one major exception, the data for samples 300 mm long significantly deviates from the trends followed by data from experiments for all other sample lengths, this data corresponds to experiments where transition to flaming was observed.

Upward burning represents a significantly more complicated problem than downward burning. For upward burning the oxidizer flows through the hot char before reaching the reaction zone, as it was observed from figure 1.1. The char

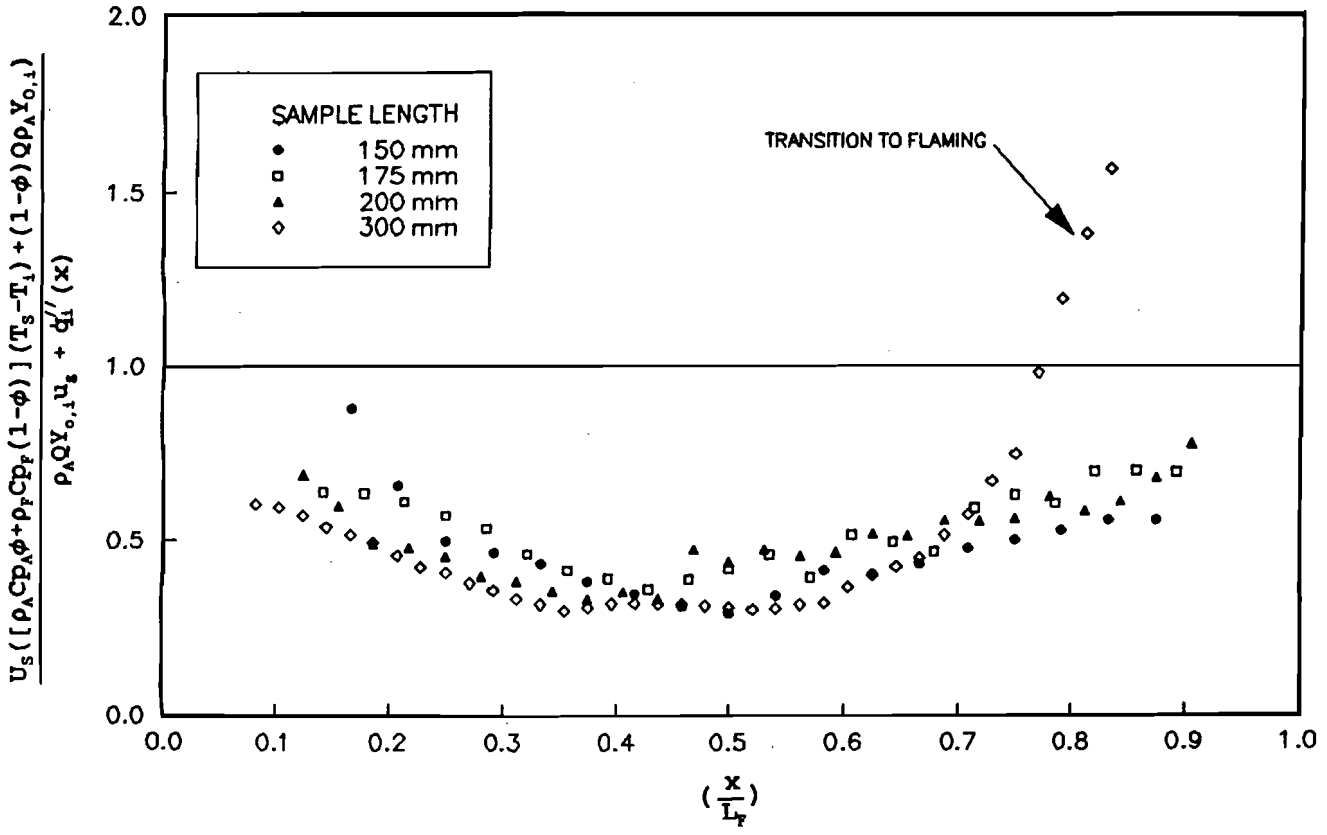

Figure 2.12 - Correlation of experimental and theoretical smoldering propagation velocities, for upward burning experiments, as a function of a non-dimensional distance from ignition. Experiments for 300 mm samples (transition to flaming) significantly deviate from the trend established by data from experiments for all other sample lengths.

behind the smoldering front is, therefore, continuously reacting reducing the oxygen content of the gases reaching the primary reaction, this has been observed by other researchers [3,4,5,7,17]. The model assumes the oxygen concentration to be that of air, thus, explaining why experimental smoldering velocities are smaller than those predicted by the model. Close to the igniter, the air flow velocities are small and therefore the char oxidation is weak. The heat generated from this oxidative reaction is unable to sustain an endothermic pyrolysis reaction of the polyurethane foam, thus, smolder continues to propagate. As the reaction propagates deeper in the sample air velocities increase, char oxidation strengthens, depleting a more significant fraction of the incoming oxidizer and therefore, the foam reaction pathway shifts more towards pyrolysis. Since pyrolysis inhibits smoldering, as explained in chapter 1, smoldering propagation velocities will decrease until direct oxidation of the foam ceases to exist (x/L_F approximately 0.4) from then on the propagation velocity, calculated from the temperature histories, is that of condensed phase pyrolysis. The oxidation reaction in the char is able to sustain a condensed phase pyrolysis reaction of the foam ahead, and its strength is again proportional to the oxidizer supply, therefore increases as the reaction moves deeper into the sample.

Dosanjh et al. [5,7] formulated a model by which a pyrolysis reaction precedes the oxidative reaction of the char, all the oxidizer is consumed when the char completely burns either to ash or gaseous products. This model could be used in trying to correlate the data from figure 2.3 but since a clear front for the char oxidation reaction can not be determined from the temperature histories the

reliability of such a correlation is doubtful.

Even though no quantitative information can be derived from this experiments the clear trends observed from figure 2.12 reaffirm the assumptions made for the analysis, oxidizer transport to the reaction zone seems to be the dominant element controlling smoldering combustion. Heat losses do not seem to be a relevant parameter for the problem and the mechanism that controls smoldering velocity is the heat transfer from the reaction zone to the unburnt fuel. Pyrolysis of the foam is not a relevant parameter for small flow velocities, but oxygen depletion in the char seems to occur for all flow rates. A more extensive study of this configuration will be presented in chapter 4.

2.5.3 Transition to Flaming

The exception to this observations is the 300 mm sample, figure 2.12 show that data for this case significantly deviates from the trends established by the data for all other sample lengths. This corresponds to the only case where transition to flaming is observed. Transition to flaming is only observed in upward burning. Downward burning is a steady process where both the heat generated and the smoldering velocity are directly proportional to the oxidizer supply to the reaction zone, all the heat generated is transferred to the fuel thus establishing the smolder velocity, temperatures are almost constant so the reaction rate can be considered to be free of temperature dependency. For upward burning there is a transient element which is the heat transferred to the foam by the products of combustion, as the length of

the sample is increased the time for the reaction to propagate through the whole sample increases therefore increasing the energy accumulated in the foam. The initial temperature of the fuel increases and, therefore, the necessary energy to heat the foam to either pyrolysis or smoldering temperature decreases; as a consequence propagation velocities increase. Upward burning is therefore a transient process which eventually will lead to gas phase pyrolysis and transition to flaming.

2.6 Conclusion

Smoldering combustion incorporates a range of parameters different to any other combustion phenomena making it in many cases more complex and hazardous. One of the complexities of this phenomena is its existence inside a porous medium, which restricts the transport of oxidizer and insulates the reaction zone.

Buoyantly induced flow provides, along with the air inside the pores of the fuel, the oxidizer for the reaction. Smoldering combustion is a oxygen starved process, therefore oxygen supply is the controlling parameter of the problem. The amount of oxygen supplied to the reaction is directly proportional to the heat released and all the heat released is transferred ahead of the reaction. Since the mechanism controlling smoldering velocity is the heat transferred to the unburnt fuel, smoldering velocity is directly proportional to oxidizer supply. By properly insulating the sample sides heat losses are eliminated as a relevant parameter for natural convection smoldering.

Downward smoldering is a steady process controlled only by the supply of

oxidizer to the reaction zone, instead upward burning is an unsteady process where accumulation of heat in the unburnt fuel results in an increase in reaction rates, and therefore smoldering velocities, which might lead to transition to flaming. The presence of a condensed phase pyrolysis reaction supported by char oxidation further complicates the problem. The energy released by the oxidation reaction is coupled with the oxidizer supply, which is transient in nature, therefore no simple model could be found to correlate properly the experimental data.

The permeability of the char is an important parameter of the problem, the increase in permeability resulting from smoldering generates makes possible the flow structure previously described; constant permeability will result in a linear increase in the flow induced by natural draft, as the reaction moves into the sample.

Chapter 3
OPPOSED FORCED FLOW SMOLDER

3.1 Introduction

An experimental study is carried out of the effect on the propagation of a smolder reaction through the interior of a porous fuel of a forced flow of oxidizer opposing the direction of smolder propagation. The potential effect of buoyancy in the process is also analyzed by conducting the experiments in the upward and downward propagation, and comparing the respective results. The experiments are conducted with a high void fraction flexible polyurethane foam as fuel and air as oxidizer, in a geometry that approximately produces a one-dimensional smolder propagation. Measurements are performed of the smolder reaction propagation velocity and temperature as a function of the location in the sample interior, the foam and air initial temperature, the direction of propagation, and the air flow velocity. For both downward and upward smoldering three zones with distinct smolder characteristics are identified along the foam sample. An initial zone near the igniter were the smolder process is influenced by heat from the igniter, an intermediate zone where smolder is free from external effects, and a third zone near the sample end that is affected by the external environment. The smolder velocity data are correlated in terms of a non-dimensional smolder velocity derived from a theoretical model of the process previously developed. The analysis of the results confirm that the smolder process is controlled by the competition between the supply of oxidizer and the loss of heat to and from the reaction zone. At low

flow velocities oxygen depletion is the dominant factor controlling the smolder process, and the smolder velocity and temperatures are small. Increasing the flow velocity strengthens the smolder reaction due to the oxygen addition resulting in increased smolder velocities and temperatures. These parameters, however, reach a maximum and as the air velocity is increased further the smolder reaction becomes weaker and eventually dies out due the convective cooling.

The experiments are conducted in the opposed smolder configuration, for both downward and upward smolder propagation. In this configuration the reaction zone and the forced oxidizer flow move in opposite directions. This type of smoldering is also referred to as co-current smoldering because if the reaction zone is considered as stationary both the fuel and oxidizer reach the reaction zone in the same direction. In the downward smoldering experiments the foam is ignited at its top and the smolder reaction propagates downwards,in the same direction as that of gravitational acceleration, and for upward smoldering in opposite directions. Therefore, when the upward and downward experiments are compared, the difference between the two can be attributed to gravity effects. The smolder parameters that are compared in this work are the propagation velocity and reaction temperature.

3.2 Description of the Experiment and Experimental Hardware

A schematic diagram of the experimental installation is shown in figure 3.1. The test section containing the porous fuel consists of a 300 mm long vertical duct

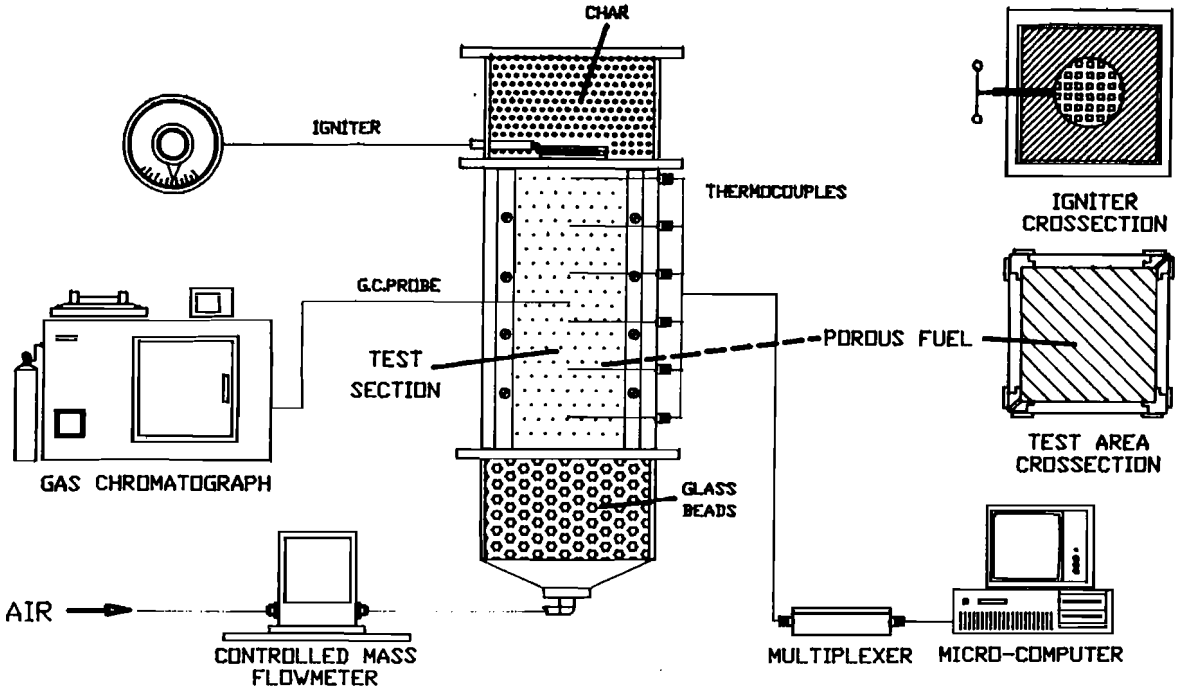

Figure 3.1 - Schematic of forced flow smoldering experimental apparatus. Vertical and horizontal cross sections of the test section and igniter section are presented. The gas chromatograph was used to sample the combustion products in the region close to the reaction, all attempts were unsuccessful due to clogging of the lines.

with a 150 mm side square cross section. The duct walls are made of insulating 10 mm thick Fiberfax sheet mounted on an aluminum frame. The exterior surface of the Fiberfax sheets are sealed with aluminum tape to prevent diffusion of air through the walls to the foam in the test section. The fuel is fitted tight to the walls in the test section to prevent preferential flow of air through the gap between the foam and the wall. For fuel lengths less than 300 mm, the fuel is positioned at the end of the test section where the igniter is located. The oxidizer gas flows into the test section through a diffuser and a 150 mm long settling section filled with glass beads that is fitted at one end of the duct. The gas flow rate is controlled and metered with a Tyland type FC280S controlled mass flow meter. Controlling the mass flow rate is important in these experiments because the pressure losses through the porous material decrease with time as the smolder reaction propagates, and conventional flow meters would not prevent the resulting increase in flow rate. The igniter and a 150 mm insulating char section are fitted at the other end of the duct. The igniter consists of a Nichrome wire sandwiched between two, 5 mm thick, porous ceramic honeycomb plates that provide rigidity to the igniter and heating uniformity. To insulate the ignition zone and simulate an ongoing smolder process, a layer of char from an already smoldered foam is placed at the other side of the igniter, such that the igniter is in contact with the virgin fuel in one side and the char in the other. Heat losses to the environment and lack of oxidizer prevent the initiation by the igniter of a forward smolder reaction in the char.

The porous combustible used in the experiments is open cell, unretarded,

white flexible polyurethane foam, with a 26.5 Kg/m^3 density and 0.975 void fraction. Most of the tests are conducted with samples 150 mm side cubes. To observe the effect on smolder of the sample length, a few tests are conducted with foam samples 150, 175, 200, and 300 mm long, and a fixed air velocity of 1.7 mm/sec. The foam sample width is selected to ensure a one dimensional smolder propagation in a region of at least 50 mm in diameter from the sample center line, and the length to permit the observation of self propagating smolder without the influence of end effects, as explained in chapter 2. Filtered, house compressed air is used as oxidizer. The foam smolder initiation (ignition) is accomplished by applying an electrical power of 1.70 KW/m^2 for approximately 900 sec, which for our igniter is the energy required to heat up the igniter ceramic plates to an approximate temperature of 500°C. During the course of this work it was found that the onset of foam smoldering occurs only under very restrictive conditions of igniter type, temperature and time. Too high a temperature results in the melting or flaming of the foam, and too low in its pyrolytic decomposition. The ceramic heater, temperature and heating period used in these experiments were selected to ensure the self-supported propagation of the smolder reaction in the foam. The above observations concerning the restrictive conditions for smolder initiation agree with those discuss by Ohlemiller and Rogers [3].

Ignition is performed without air flow to ensure a uniform ignition procedure in all the tests. Once the ignition period is completed, the igniter current is turned off and the flow of air is turned on, thus starting the forced flow smolder of the

foam. For the downward smolder experiments, the igniter and char are mounted on top of the foam sample and the air is introduced at the bottom of the test chamber. For the upward experiments the entire apparatus is simply rotated 180 degrees. A few characteristic tests in the downward configuration are conducted with the foam and air at temperatures above ambient. In these tests an in line air heater mounted at the diffuser entrance is used to heat the air and the foam to a uniform predetermined temperature prior to turning on the igniter.

The rate of smolder propagation is obtained from the temperature histories of eight Chromel-Alumel thermocouples 0.8 mm in diameter that are embedded at predetermined positions in the porous fuel with their junction placed in the fuel centerline. The smolder velocity is calculated from the time lapse of the reaction zone arrival to two consecutive thermocouples, and the known distance between the thermocouples. The location of the reaction zone is characterized by a maximum in the temperature profile. However, in many of the tests this maximum is not sharply defined, thus to reduce uncertainties the location of the smolder reaction front is defined here by the intersection of the tangent to the temperature curve at the inflexion point and a horizontal line at a temperature near to the maximum (350°C in this work). These thermocouples are also used to measure the reaction zone temperature. This temperature is used only for comparative purposes, and it is not considered to be the actual smolder temperature, since it is not possible to determine whether the thermocouples are measuring the foam or air temperature. Another important source of information in the smolder process is the species

concentrations near the reaction zone. Our attempts to measure them using gas chromatography have failed so far due to the clogging of the sampling lines by the tars and heavy hydrocarbons produced during the smolder of the foam.

3.3 Experimental Results

3.3.1 Downward Burning

The variation of the downward smolder propagation velocity through the sample length is presented in figure 3.2 for several representative opposed air flow velocities. Tests were also conducted at other flow velocities, but the results are not presented to avoid crowding of the figure. The data is the average from five tests, and the error bars describe the maximum deviations from the mean. From these data three regions with different smolder characteristics are identifiable along the foam sample. An initial zone (I) approximately 60 mm in length from the igniter where the smolder process is affected by the heat transferred from the igniter, and the smolder velocity is elevated. A second zone (II) approximately 50 mm long in the middle of the sample where the smolder process is relatively free from end effects, and the smolder velocity is approximately constant if the smolder is self sustained, or decays if smolder is at near extinction. A third zone (III) at the end of the sample where the smolder is affected by the external environment, and its velocity increases if the smolder is self sustained, or decays if at near extinction. The characteristics of the smolder reaction at each zone depend on the air flow rate. Varying the sample length does not affect the smolder characteristics in each

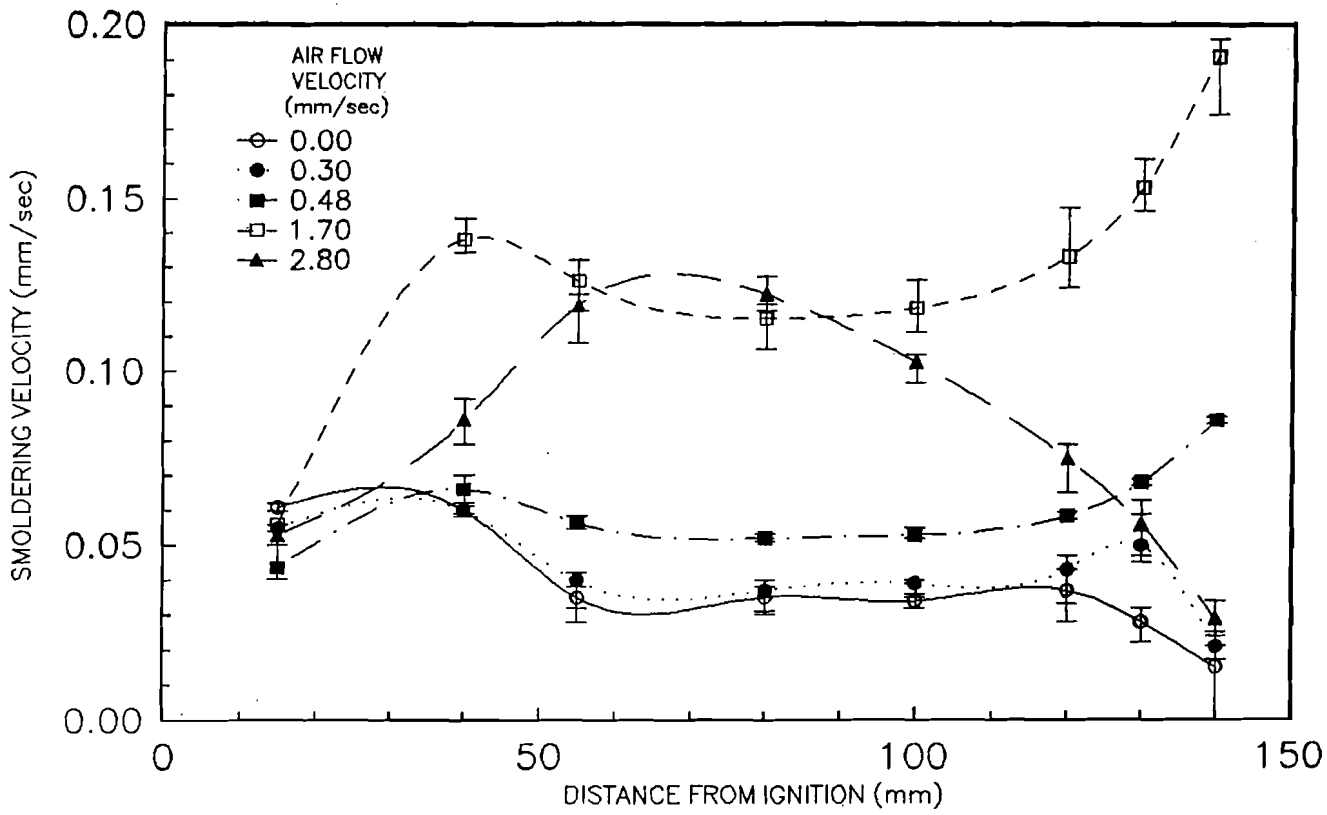

Figure 3.2 - Variation of the smolder velocity along the polyurethane foam sample for downward propagation in an opposed air flow, for several representative air flow rates. Extinction is observed for no flow and air flow velocity of 2.8 mm/sec.

region, or the extent of regions I and III. The extent of region II, however, increases as the sample length is increased. The smoldering in zone II is the most representative of a forced flow opposed smoldering, at least from the point of view of modeling, since is free from external effects. The smoldering in the other zones are also interesting, however, because they provide additional information about the process, and describe situations that may occur in practice. The smolder in zone I is representative of a situation where smoldering is supported by an external heat source. The smolder in zone III is of interest from the point of view of external ambient effects on smoldering. The measured smolder velocities are of the same order of magnitude to those reported by Ohlemiller [1], Ohlemiller and Rogers [3] and Ohlemiller et. al.[4]. However, it is difficult to compare quantitatively the actual values because the above authors report average smolder velocities rather than local velocities as it is done here.

The variation of the maximum smolder reaction zone temperature along the foam sample is presented in figure 3.3 for the same air flow velocities of figure 3.2. Although less well defined, the data also indicates the presence of the three zones described above. The temperatures in zone I are generally higher due to the igniter influence. In region II are approximately constant except under extinction conditions. In region III the temperature variation depends on the strength of the smolder reaction itself. Comparison between the results of figures 3.2 and 3.3 shows that under forced flow conditions, there is a fairly well defined correspondence between the smolder reaction temperature and the smolder velocity, with the

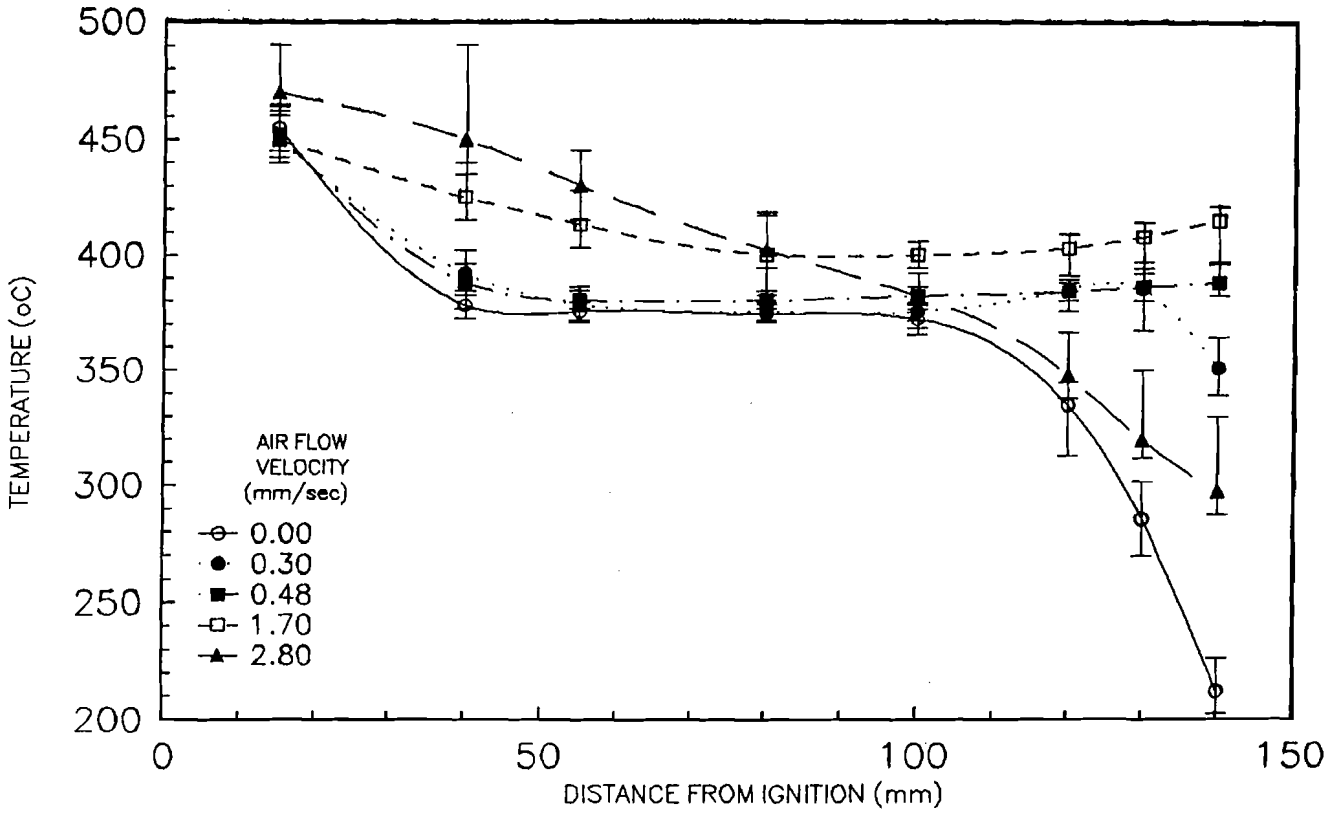

Figure 3.3 - Variation of the maximum smolder reaction temperature along the polyurethane foam sample for downward propagation in an opposed air flow, for several representative air flow rates. Extinction is observed for no flow and air flow velocity of 2.8 mm/sec.

smolder velocity being higher when the smolder temperature is higher. It is also observed that small variations in smolder reaction temperature often result in large variations on the smolder propagation velocity. These observations are in qualitative agreement with those of Moussa et al. [29], even though the fuel used in those experiments was cellulose, and they did not contemplate flow inside the foam, but diffusion of oxidizer through a natural boundary layer around the fuel sample.

The variation with the forced air flow velocity of the smolder propagation rate is presented in figure 3.4, for the three zones indicated above. The smolder velocities are obtained from the results of figure 2.2 and are averaged values of the smolder velocities at each zone. It is seen that the smolder velocity in the three zones presents a maximum at air flow rates between 1 and 3 mm/sec depending on the zone under consideration. The variation of the maximum smolder reaction temperature with the air flow rate is presented in figure 3.5, for the three zones. It is seen that the smolder temperature also presents a maximum at air velocities that approximately correspond to those of the smolder velocities, again corroborating the correspondence between the temperature of the smolder reaction and the propagation velocity.

Increasing the foam and air initial temperature results in smolder trends similar to those reported above, although for a given air velocity the smolder propagation velocity is larger at higher temperature, and the extinction conditions take place at higher air velocities. A representative example of the effect of the initial foam/air temperature on the smolder velocity is given in figure 3.6. The data

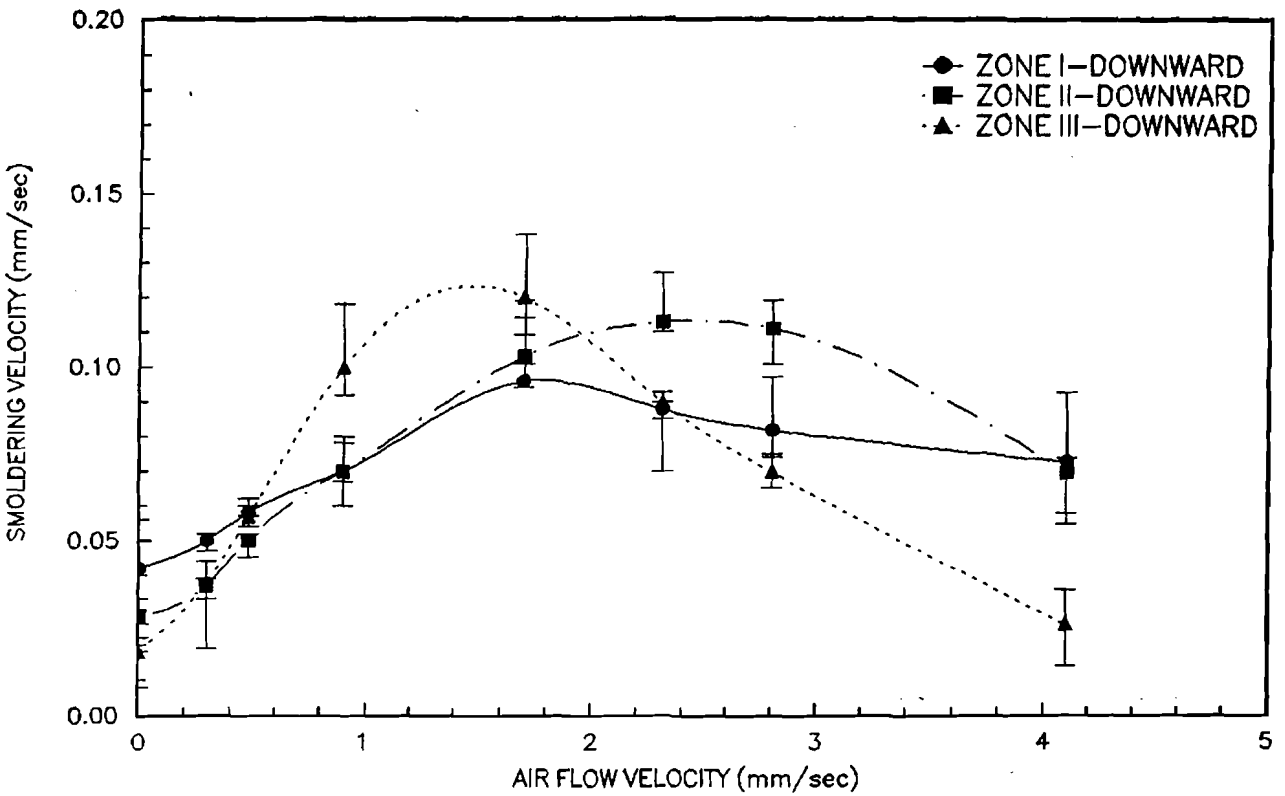

Figure 3.4 - Dependence of the downward propagating smolder velocity on the opposed air flow rate in the three identified regions of the polyurethane foam sample. The smolder velocities are averaged values in each region.

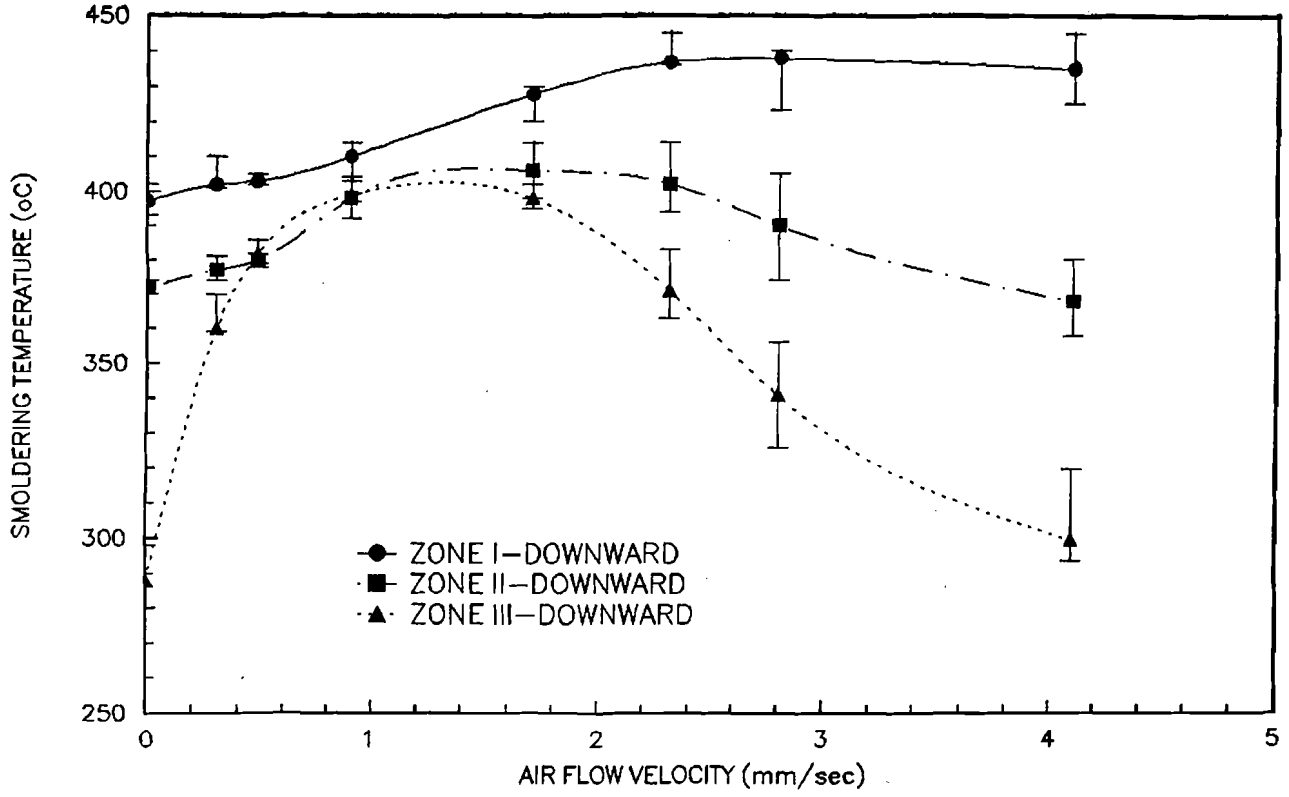

Figure 3.5 - Dependence of the downward propagating maximum smolder reaction temperature on the opposed air flow rate in the three identified regions of the polyurethane foam sample. The smolder temperatures are averaged values in each region.

is for downward smolder with an opposed flow velocity of 2.8 mm/sec. It is seen that the smolder velocity increases as the initial temperature is increased, as it could be expected. What it is more interesting, however, is that the initial temperature can also affect the characteristics of the smolder reaction itself. In this case, for example, at the standard temperature of 20°C, the smolder reaction weakens and tends to extinction in zone III as it approaches the sample end. At 110°C, however, the extinction regime has basically disappeared, and at 140°C the trend is reversed, and an enhancement of the smolder propagation velocity takes place as the smolder reaction approaches the sample end.

3.3.2 Upward Burning

The objective of these experiments is to further determine the effect of buoyancy on the smolder process. In upward propagation, buoyancy induces an upward flow of the hot post-combustion gases that opposes the downward moving forced air flow. while in downward smolder both the buoyant and forced flows would flow in the same direction. Thus, the buoyancy effect on the smolder process should appear through the differences between the downward and upward smolder characteristics. These differences should decrease as the forced air velocity is increased and becomes significantly larger than the buoyant induced flow velocity. The apparatus and experimental procedure for the upward smolder experiments are the same as those of the above described downward experiments, except that the apparatus is positioned upside down.

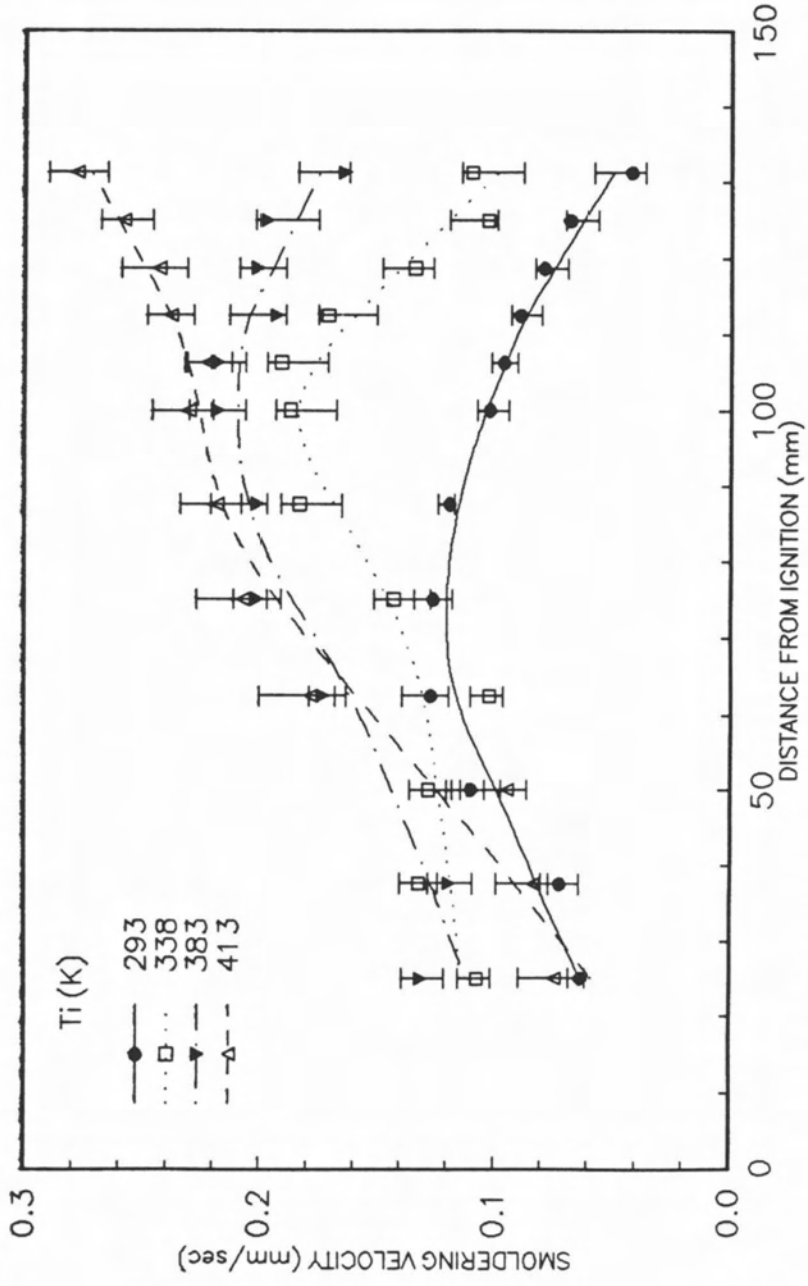

Figure 3.6 - Variation of the smolder velocity along the polyurethane foam sample for downward propagation in an opposed air flow, for several representative initial temperatures (forced flow velocity of 1.7 mm/sec. and 150 mm sample length).

The variation of the upward smoldering propagation velocity through the foam sample length is presented in figure 3.7, and of the smolder reaction temperature in figure 3.8, for a few representative opposed air flow velocities. Here also three zones with particular smolder characteristics can be identified. The extent of the zones and the smolder characteristics in each zone are similar to those observed in downward smoldering, although there are some noticeable differences. As in downward smolder, region I occupies the first 60 mm of the sample, and is influenced by the heat transferred from the igniter. In this region the smolder velocity and temperature increase with the air velocity due to the increased supply of oxidizer to the reaction zone. Region II (middle of the sample) is narrower and less defined, with smolder velocities that at some air velocities change throughout the region. Another notable difference is that smolder occurs at larger air velocities than in downward propagation. In region III the end effects are more marked with strong variations of the smolder velocity in some cases.

The variation of the averaged upward smolder velocity with the opposed forced air flow rate in each zone is presented in figure 3.9, and the averaged maximum smolder temperature in figure 3.10. It is seen that the effect of the forced air flow on the upward smolder velocity is similar to that of the downward smoldering (figure 3.4) with the smolder velocity first increasing and then decreasing as the air velocity is increased. The air velocity at which the smolder velocity reaches a maximum is, however, higher than in downward smolder. Comparison of figures 3.5 and 3.10, shows less differences in the smolder

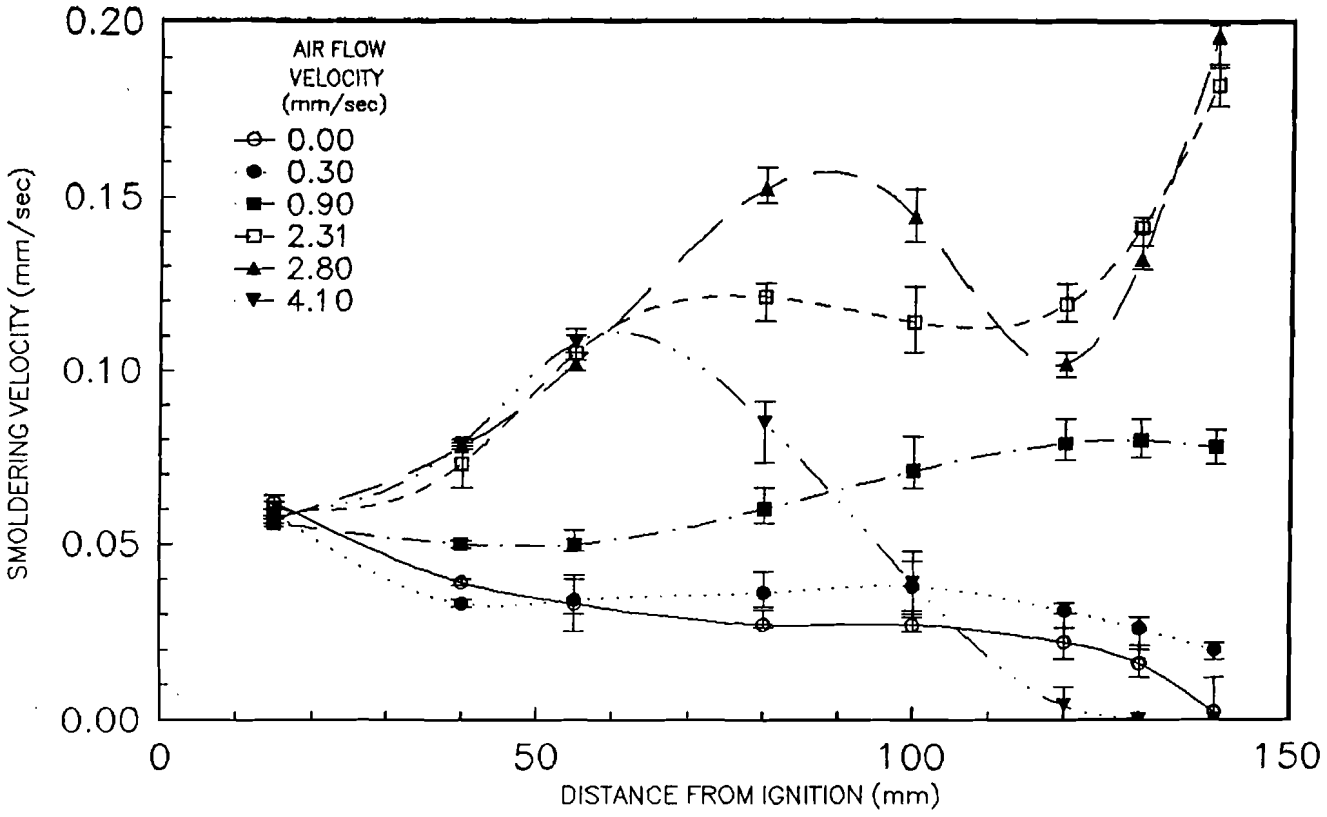

Figure 3.7 - Variation of the smolder velocity along the polyurethane foam sample for upward propagation in an opposed air flow, for several representative air flow rates. Extinction is observed for no flow and air flow velocity of 4.10 mm/sec.

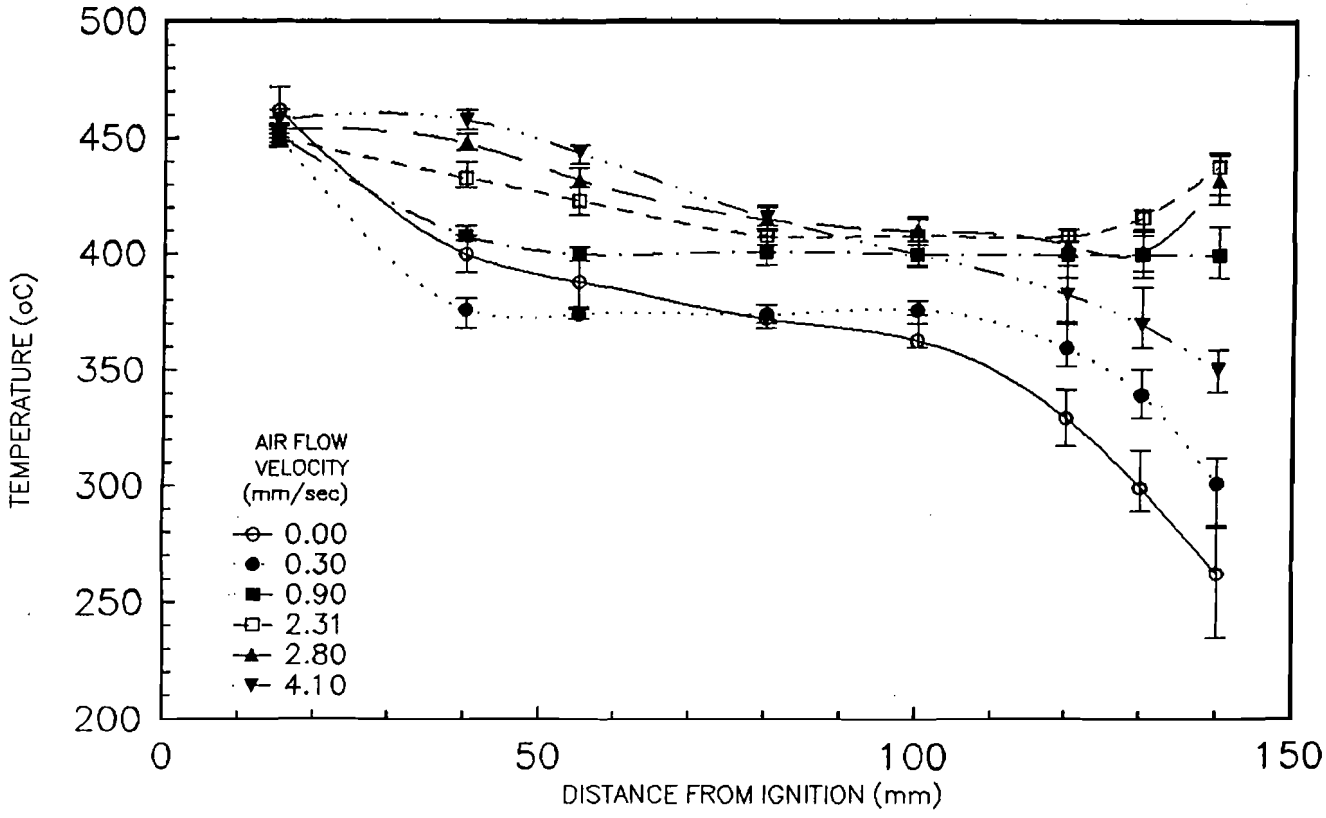

Figure 3.8 - Variation of the maximum smolder reaction temperature along the polyurethane foam sample for upward propagation in an opposed air flow, for several representative air flow rates. Extinction is observed for no flow and air flow velocity of 4.10 mm/sec.

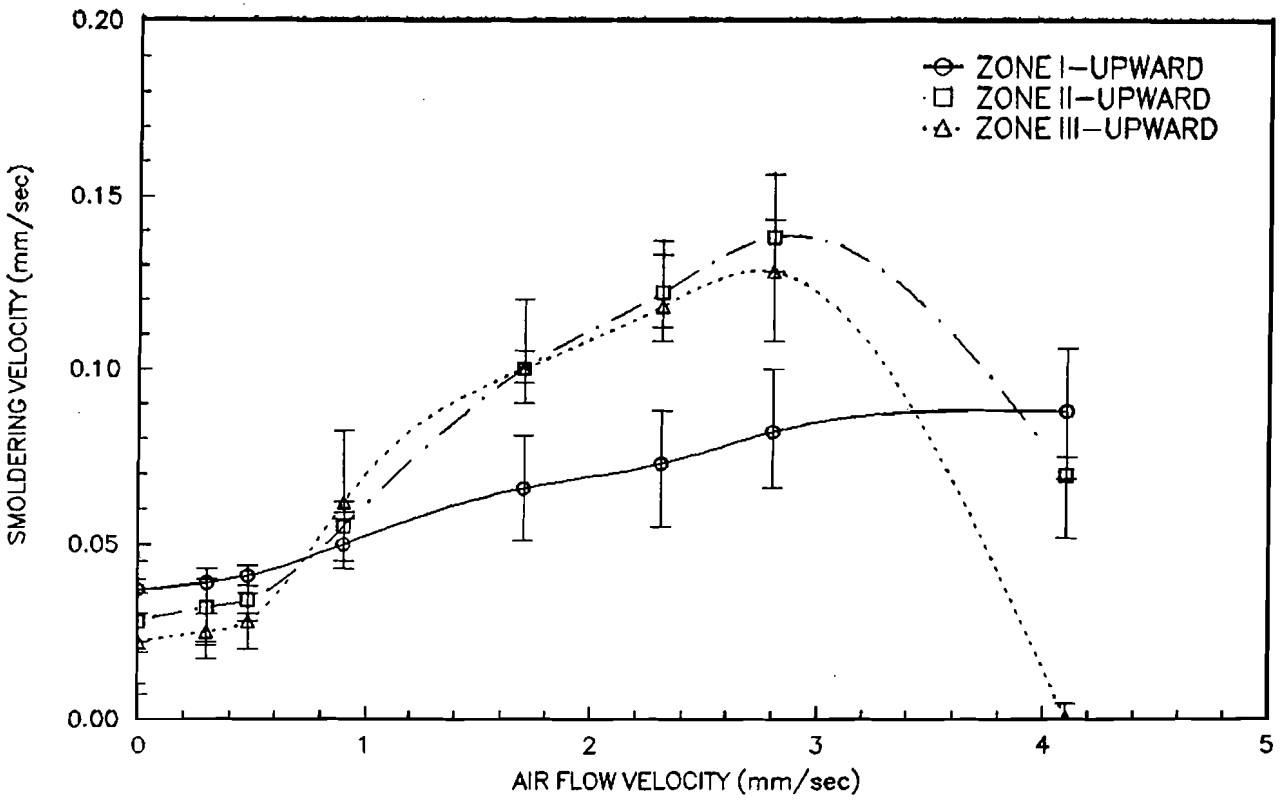

Figure 3.9 - Dependence of the upward propagating smolder velocity on the opposed air flow rate in the three identified regions of the polyurethane foam sample. The smolder velocities are averaged values in each region.

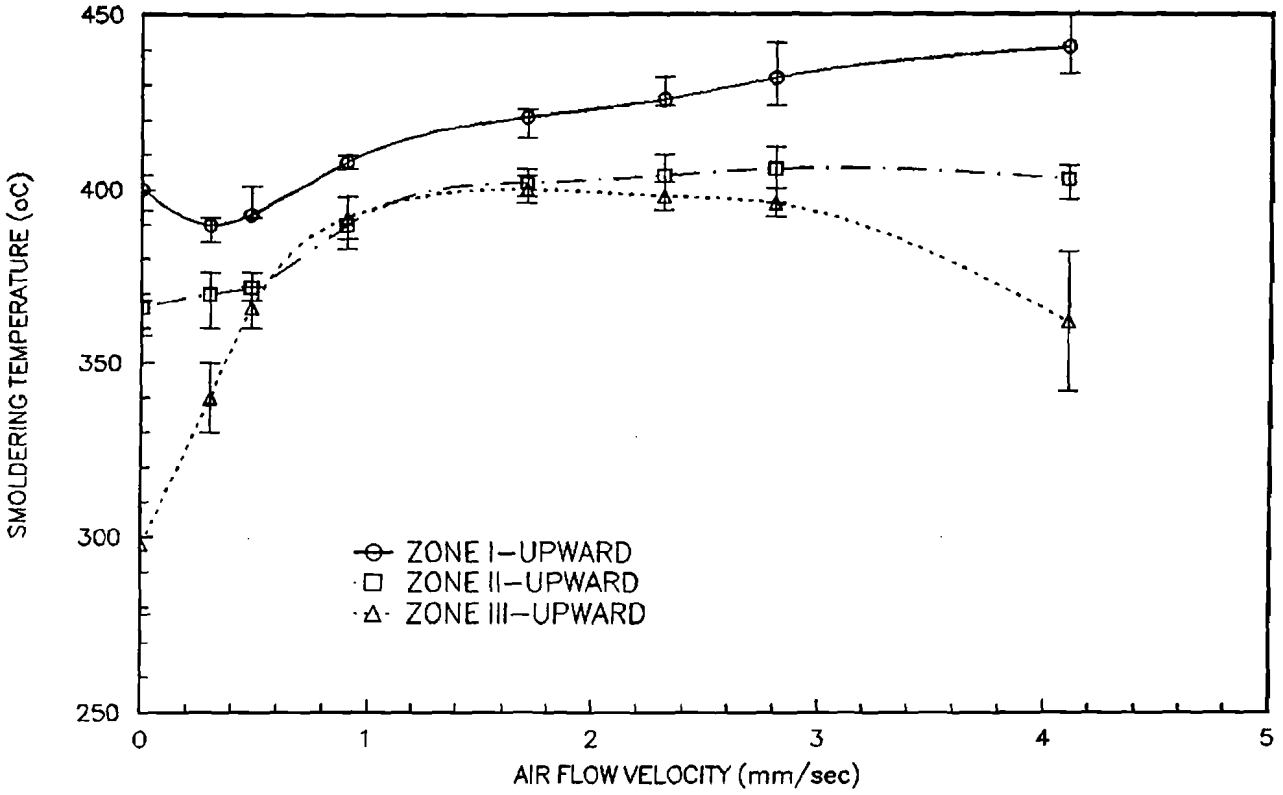

Figure 3.10 - Dependence of the upward propagating maximum smolder reaction temperature on the opposed air flow rate in the three identified regions of the polyurethane foam sample. The smolder temperatures are averaged values in each region.

temperatures, although it should be taken into account that the data are averaged values, and since small changes in temperature result in large changes in the smolder velocity, the average values may not be too representative of the process in certain cases.

3.4 Smoldering Model

The theoretical model of opposed flow smolder developed by Dosanjh et. al.[5,7] is used in this work to correlate the above reported data. To facilitate the understanding and discussion of the correlation, a brief description of the model is given here.

In opposed smoldering, with frame of reference anchored at the reaction zone, the fuel and oxidizer enter the reaction zone in the same direction (figure 3.11). Since smoldering is generally oxygen limited, the heat released by the smolder reaction can be expressed in terms of the mass flux of oxidizer at the reaction zone. This heat is transported by conduction and radiation upstream of the reaction zone, and sustains the propagation of the smolder front. It should be noted that the fuels of interest in smolder are very porous, and consequently conduction is a relatively poor mode of heat transfer [12]. Thus radiation heat transfer is important despite the relatively small temperatures encountered in smoldering combustion.

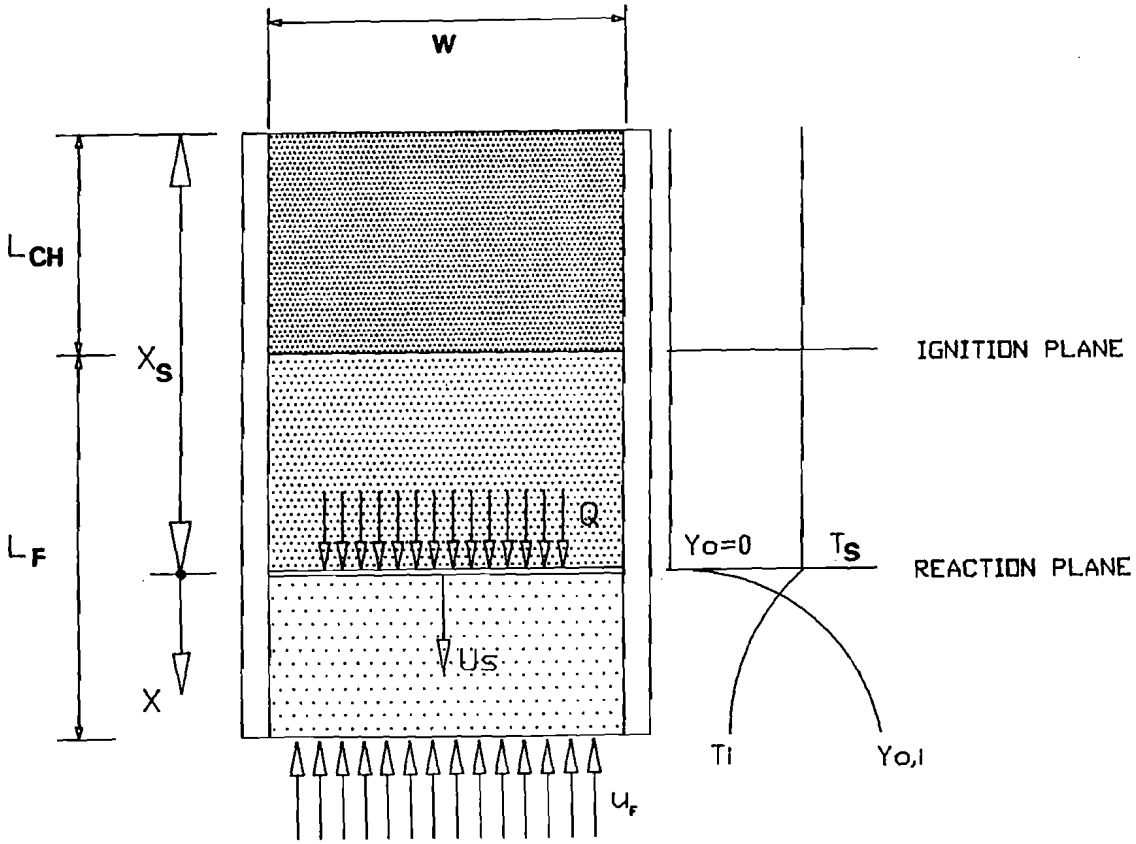

Figure 3.11 - Schematic of one dimensional smoldering combustion viewed in a frame of reference moving with the smolder wave.

In the model of Dosanjh et al.[5,7] smoldering is modeled as a finite rate, one-step reaction, of the form

$$\nu_F[\text{FOAM}]+\nu_O O_2 \rightarrow \nu_{CH}[\text{CHAR}]+\nu_{gp}[\text{GaseousProducts}]+Q\nu_O M_O \quad (3.1)$$

Smoldering is assumed to be one-dimensional and steady in a frame of reference fixed to the smolder wave. The gas and solid are presumed to be in local thermal equilibrium [5], and the solid phase is considered continuous with a constant void volume fraction. Energy transport due to concentration gradients, energy dissipated by viscosity, work done by the body forces, and the kinetic energy of the gas phase are ignored. Furthermore, since smoldering velocities are much smaller than flow velocities, flow velocities can be taken as known quantities at each location in the sample, x_S.

With the above assumptions, and neglecting heat losses to the environment, the one dimensional form of the energy conservation equation becomes

$$(\dot{m}_F'' Cp_F+\dot{m}_{AIR}'' Cp_A)\frac{dT}{dx}=(\lambda_{eff}+\lambda_{rad})\frac{d^2T}{dx^2}+Q\frac{d\dot{m}_O''}{dx} \quad (3.2)$$

where the mass fluxes of fuel and oxidizer entering the reaction zone are given by,

$$\dot{m}_F''=(1-\phi)\rho_F U_S$$

$$\dot{m}_A''=\rho_A u_g$$

$$\dot{m}_O''=Y_O\dot{m}_A''-\phi\rho_A D\frac{\partial Y_O}{\partial x}$$

λ_{eff} is an effective thermal conductivity of the form

Radiation is incorporated in the analysis using a diffusion approximation with an

$$\lambda_{eff}=\phi\lambda_A+(1-\phi)\lambda_F$$

equivalent thermal conductivity given by

$$\lambda_{rad}=\frac{16\sigma d_p T^3}{3}$$

The boundary conditions for the above equation are

$$\text{at} \quad x=x_S \qquad \frac{\partial T}{\partial x}=0$$

$$T=T_S$$

$$\dot{m}_O''=0$$

$$\text{at} \quad x\to\infty \qquad \frac{\partial T}{\partial x}=0$$

$$T=T_i$$

$$\dot{m}_O''=\dot{m}_{O,i}''$$

Integrating with respect to x from x_S to ∞, the following expression is obtained for the smolder propagation velocity

$$U_S=\frac{\rho_A[QY_{O,i}-Cp_A(T_S-T_i)]}{\rho_F Cp_F(1-\phi)(T_S-T_i)}\,u_g \qquad (3.3)$$

The analysis of Dosanjh et al.[7] also provides an expression for the smolder temperature T_S. However, the asymptotic analysis leading to that expression imposes a number of restrictive conditions that are often not applicable to the experiments. For this reason, in this work the value of the smolder reaction temperature is obtained from the experimental data of figures 3.3 and 3.8. The heat of combustion Q, is not well determined for smoldering combustion [1]. In this work it will be selected such the correlation of the data with the above equation is

optimized. As it will be shown later, the resulting value for the heat of combustion agrees well with that previously reported in other works [1,2,4,5,7]. Finally, the oxidizer velocity u_g, is known if there is only a forced flow of oxidizer. However, the forced flow velocities at which smolder can progress through the foam are so small (figure 3.2), that under normal gravity conditions, buoyancy induced flows can become important as a means of oxidizer transport to the reaction zone. Thus, the potential generation of buoyant flows inside the foam requires the treatment of the flow through the foam as a mixed, forced and free, flow problem. This is done in the following section.

3.5 Flow Induced Through the Polyurethane Foam

The onset of buoyant flows inside a porous media depends strongly on the permeability of the material [3]. The polyurethane foam used in the present experiments has a relatively low permeability in spite of the high void fraction, and no buoyant flows are expected to be generated inside the foam unless a chimney type, natural draft, is induced by the hot post-combustion gases. However, the char left behind by the propagating smolder reaction is quite permeable, and buoyant recirculation flows can be easily generated downstream from the smolder front. The permeability of the char depends on the strength of the smolder reaction, because more of the fuel is consumed when the reaction is vigorous, and on the char structure itself. This is reflected in the measured dependence of the char permeability on the forced flow velocity for downward smolder

that is presented in figure 3.12. Since increasing the forced velocity enhances the smolder reaction (figures 3.2 and 3.3), the char permeability also increases. The increase however its not linear because at small flow rates the char keeps its structure [3], but as the smolder reaction strengthen the filaments that form the micro-structure of the foam break down [5], thus resulting in a sudden increase in the permeability as it is seen in figure 3.12.

The recirculating flow in the char region are induced by the natural convection boundary layer that is generated at the tests section walls by the difference in the wall and char/post-combustion gases temperatures. A schematic of these recirculating flow is shown in figure 3.13. In downward smolder, fresh air flows downward along the cold walls of the char region toward the reaction zone where it encounters the unburned foam that since it has a much smaller permeability prevents the air from flowing through. Instead, the air turns around at the reaction zone and moves upward along the duct centerline together with the gases being forced through the foam by forced convection. From the point of view of the smolder reaction, the net result is the added flux of air that tends to enhance the reaction since is oxygen limited, but also tends to cool it off. If forced flow of air is in the range that the smolder reaction is strong, the addition of the free flow

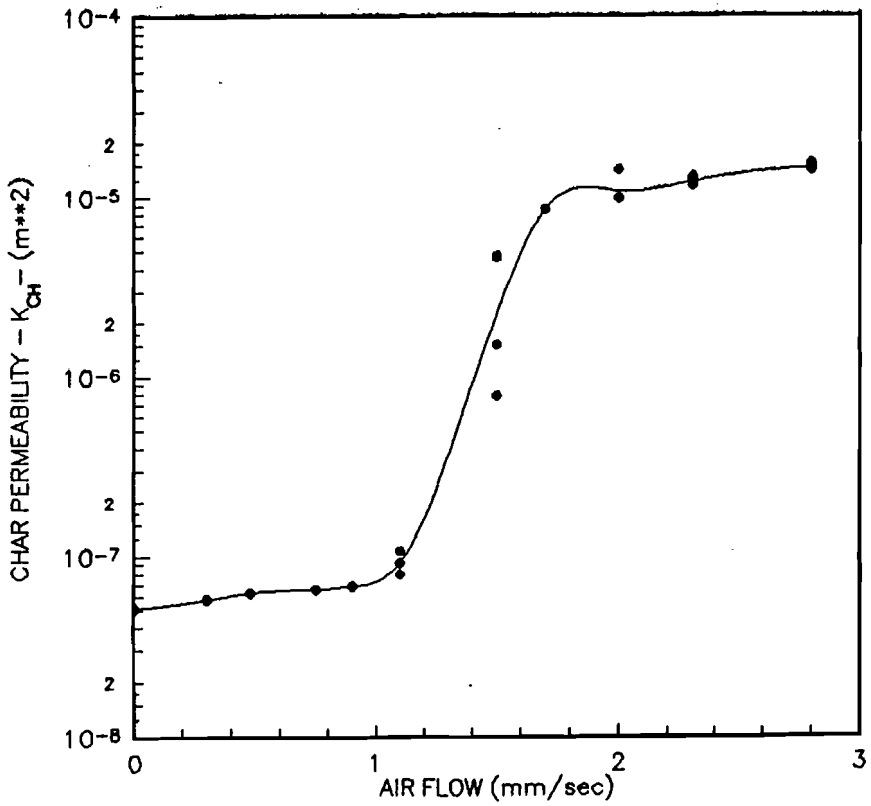

Figure 3.12 - Variation of the average permeability of the char left after smoldering at different flow rates. The values are obtained by measuring the pressure drop of a completely burnt sample for different air flow velocities.

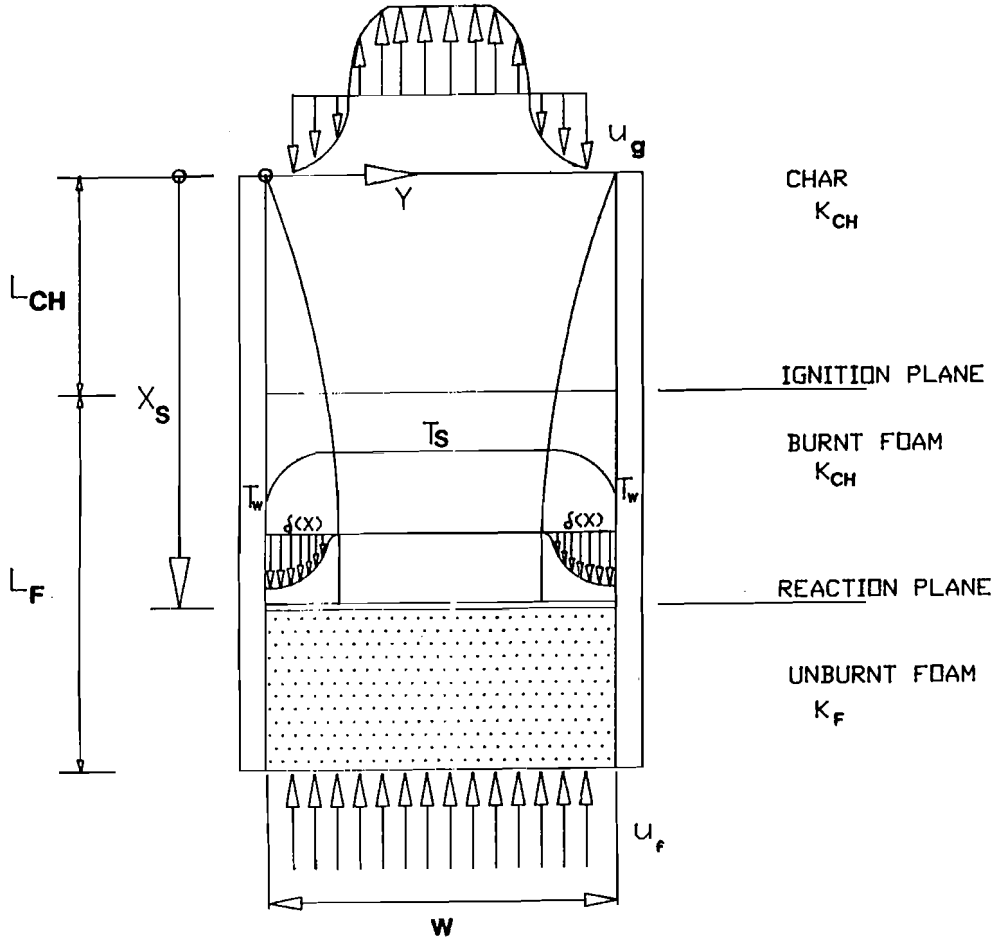

Figure 3.13 - Schematic of the mixed flow occurring inside the sample. For upward burning the diagram has to be rotated 180°; for downward burning forced and boundary layer flow add at the sample centerline (aiding flow) for upward burning they oppose (opposing flow).

will result in the enhancement of the reaction. However, if it is in a range where the reaction is already weak, the cooling effect becomes dominant and the reaction will tend to extinction. In upward smolder, the direction of the recirculating flow is reversed, but the net result is the same.

Few works have been conducted on the mixed, free and forced, flow in a porous media. The analysis developed here is based on the works of Burns et.al.[57], Bejan [14], Lai et. al. [63], Hadim and Govindarajan [65] and Nield and Bejan [55]. In natural convection, an asymptotic solution for buoyantly induced flows in vertical ducts has been developed by Burns et. al. [57]. For the mixed flow problem other considerations have to be taken on account. In the char, the recirculating flow moves from top to bottom near the walls and from bottom to top near the sample centerline; therefore, for downward burning, forced and buoyantly induced flows add at the centerline (aiding flows), while for upward burning, the flows oppose at the centerline region (opposing flows). A numerical analysis of the problem [63] shows that for aiding flows the mixed flow solution is valid for values of the Ra/Pe smaller than 50, for values greater than 50 the solution resembles more the pure natural convection solution. For downward smolder (aiding flow) and for the present experimental conditions it is found that for flow rates smaller than 1 mm/sec, the Ra/Pe is larger than 50. Thus, the natural convection solution prevails for air velocities smaller than 1 mm/sec, and the mixed convection solution for greater air velocities. For upward smolder (opposing flows), the mixed flow solution is found to give a more accurate description of the problem for values

of Ra/Pe smaller than 500, which covers the whole range of flows used in the present experiments. Below, a summary is given of the mixed and natural convection flow analyses used in this work to derive the air velocity to be imputed in equation 3.3.

3.5.1 Mixed Convection Conditions

In the analysis it is assumed that the convective fluid and the porous medium are everywhere in thermodynamically equilibrium [5], that there is no phase change in the solid, and that the properties of the fluid and the porous medium are homogeneous and isotropic. With the governing equations of mass, momentum and energy, and applying Darcy's Law together with the Boussinesq approximation, the following expression is obtained for the flow averaged velocity along the center region of the foam [13,55,63]. A more detail development is presented in chapter 2.

$$u_b = \frac{2\delta}{W}\left(\frac{Gr_K}{Re_K}\right)u_f \qquad (3.4)$$

with

$$\delta = x\, Ra_x^{-0.5}$$

$$Re_K = \frac{\rho_A u_f K_{CH}^{0.5}}{\mu}$$

and

$$Gr_K = \frac{K_{CH}^{1.5} g \rho_A^2 \beta (T_W - T_S)}{\mu^2}$$

3.5.2 Natural Convection Boundary Layer Solution

The natural convection problem has been studied extensively [14,55,56,57]. Particularly relevant for the present work is the analysis of Burns et. al.[57] for buoyantly induced flows in vertical ducts with different temperature walls. Burns et al.[57] gives an asymptotical solution to the problem of the form

$$u_b(y) = -\frac{\alpha Ra_x}{W}\left(\frac{4y}{W} - 1\right)$$

The sample centerline gives the same boundary conditions as a hot wall, therefore, application of that analysis to the present problem gives the following expression for the averaged flow velocity at the char centerline

$$u_b = \frac{\alpha Ra_x}{4W} \qquad (3.5)$$

with

$$Ra_x = \frac{K_{CH} g \rho_A \beta (T_W - T_S) x}{\alpha \mu}$$

3.5.3 Diffusion of Oxidizer into the Reaction Zone

Another possible transport mechanism of oxidizer to the reaction zone is by diffusion from the external environment through the char. From the governing species conservation equation, the following characteristic diffusion length is deduced

$$\delta_D = \frac{D}{u_f + u_b + \phi U_S}$$

For the present experimental conditions it can be shown that this characteristic length is much smaller than the characteristic length of the problem, and that consequently diffusion can be neglected as a transport mechanism in this problem when compared to the forced and natural convection flows. A more detailed explanation is developed in chapter 2.

3.5.4 Overall oxidizer transport to the reaction zone

From the above analysis, and in a frame of reference anchored at the reaction zone, it is deduced that the overall transport of oxidizer to the reaction zone is given by an overall velocity that includes the forced flow velocity, u_f, as given by the test condition; the buoyant velocity ,u_b, as deduced from either of the above mixed or natural convection flow analyses, and the smolder velocity times the void fraction, to account for the oxidizer that is contained in the foam pores and that

enters the reaction zone as it progresses through the sample. Thus, this velocity is given by

$$u_g = u_f + u_b + \phi U_s \qquad (3.6)$$

which is then used in equation 3.3 to correlate the smolder velocity experimental data.

3.6 Data Correlation

In this section, equation 3.3 for the smolder velocity together with equation 3.6 for the oxidizer velocity, are used to correlate the opposed smolder velocity data obtained in the present experiments. The values of the fuel and oxidizer properties used in the equation are given in table 2-1. The results of the correlation of the smolder velocity data of figure 3.2 is presented in figure 3.14. It is seen that the model predicts very well the smolder velocity data except when the smolder process is weak and approaching extinction, that is at very low, or very high, flow velocities and near the sample end. This is understandable since the model assumes fast chemistry, and that the energy released by the reaction is sufficient to heat up the fuel to its smolder temperature. Thus, if the flux of oxidizer is not large enough to ensure a strong reaction (low flow velocities), or the convective cooling losses are too large (High flow velocities, end of the sample), then it is expected that the model cannot predict correctly the experimental measurements. This is further verified from the correlation of the smolder velocity data of figure 3.6, at a forced flow velocity of 2.8 mm/sec and at different initial temperatures, which is presented in figure 3.15. It is seen that the model does not correlate the data well at low

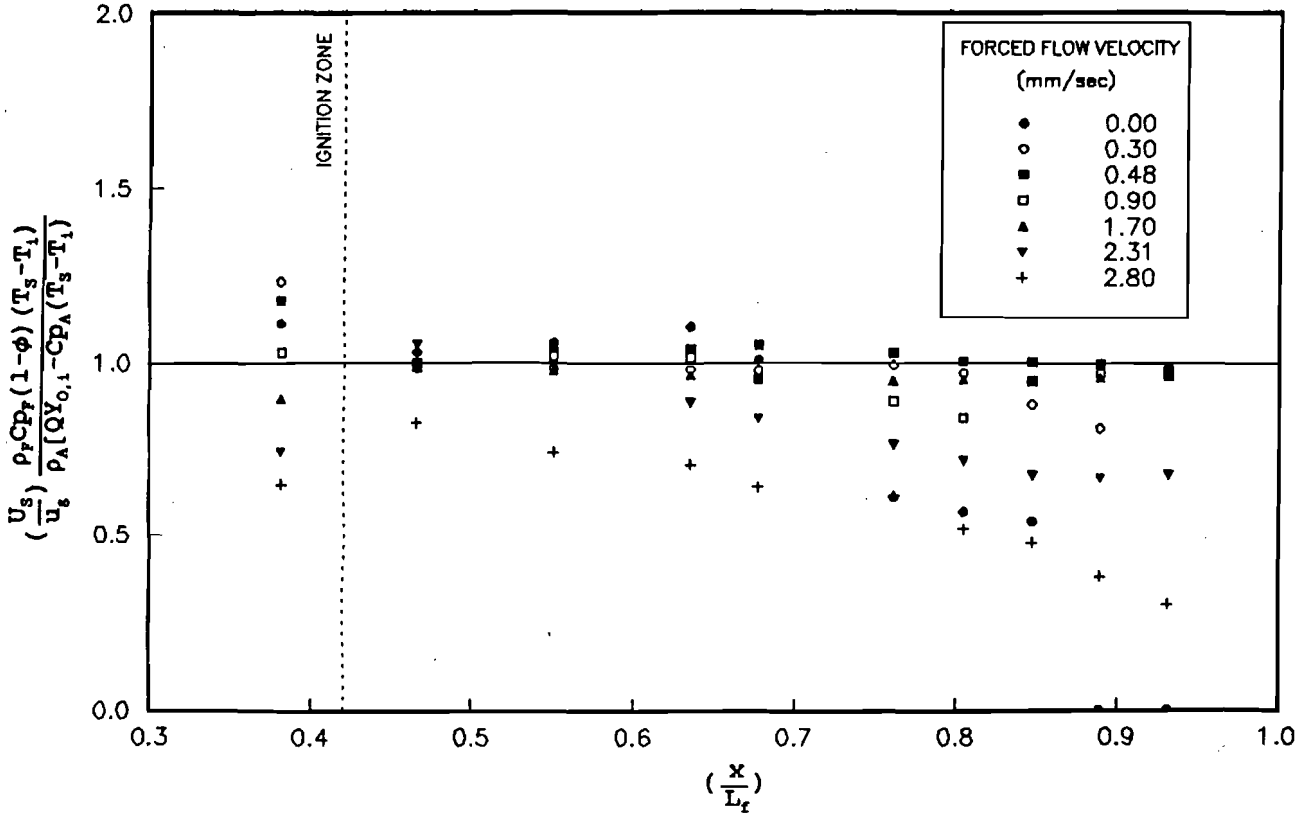

Figure 3.14 - Correlation between experimental and theoretical smoldering propagation velocities for different forced flow velocities. The experiments were conducted in downward burning configuration and all samples were 150 mm long.

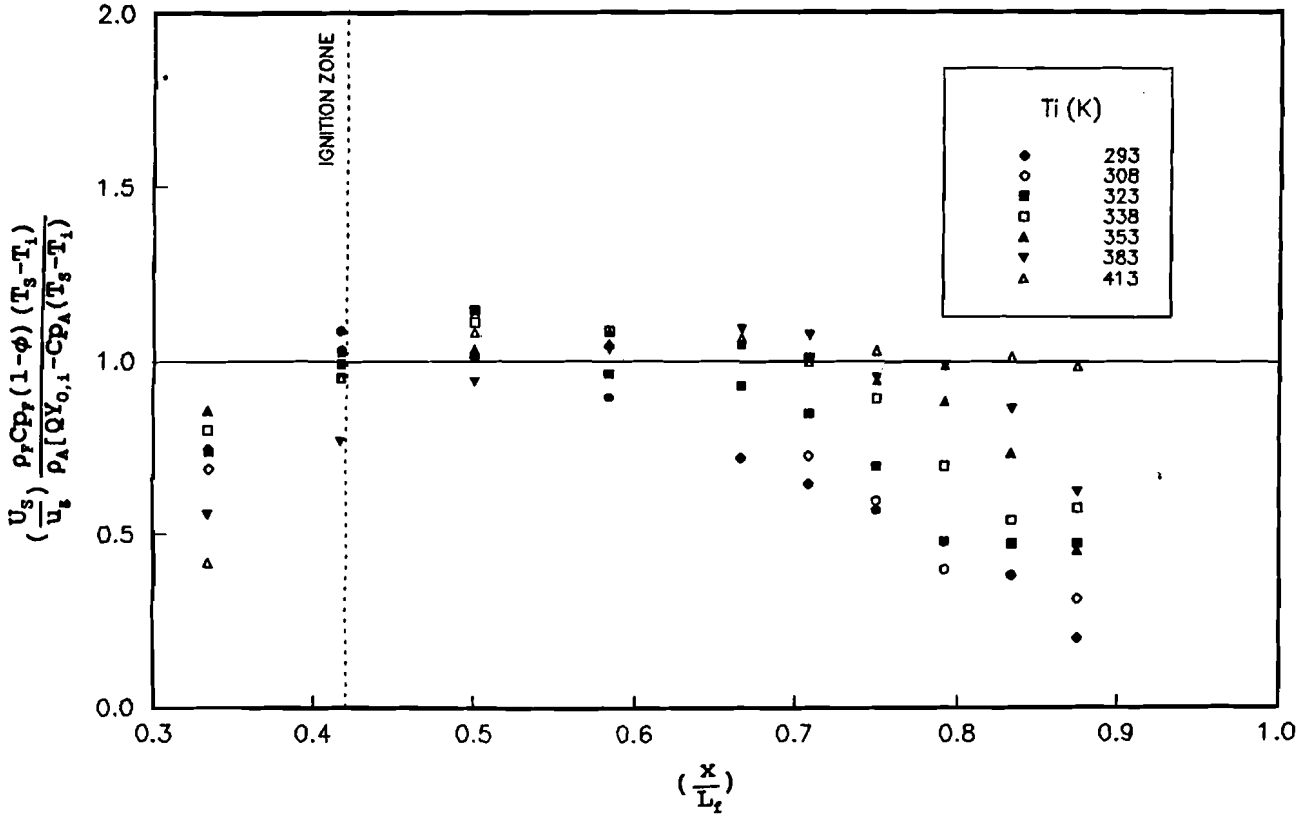

Figure 3.15 - Correlation between experimental and theoretical smoldering propagation velocities for different initial temperatures of foam and air. The experiments were conducted in downward burning configuration and all samples were 150 mm long.

initial temperatures, when the smolder velocity decreases along the fuel sample tending toward extinction. However, as the initial foam temperature is increased and the smolder process becomes more vigorous because less energy is needed to heat up the foam, the model predicts increasingly better the experimental measurements.

For this reason, when correlating with the model all of the different data obtained in the present experiments we have excluded those conditions of flow velocity and sample location where the smolder process was clearly not self-sustained and moving toward extinction. The resulting correlation of the data is presented in figure 3.16, where data from downward and upward smoldering, and for different sample lengths and initial temperatures are correlated in terms of equation 3.6. It is seen that the model predict very well all the different data, verifying that when the smolder process is vigorous and self-sustained it is controlled primarily by the transport of oxidizer to the reaction zone and the transfer of energy form the reaction zone to the virgin fuel ahead. However, when the smolder process is weak and approaching extinction, the model fails to predict the experiments, indicating that it will be necessary to include in the model the chemical kinetics of the solder reaction in order for it to describe adequately the actual smolder process.

3.7 Discussion of the Results

The above results point out to a smolder process that is controlled by the

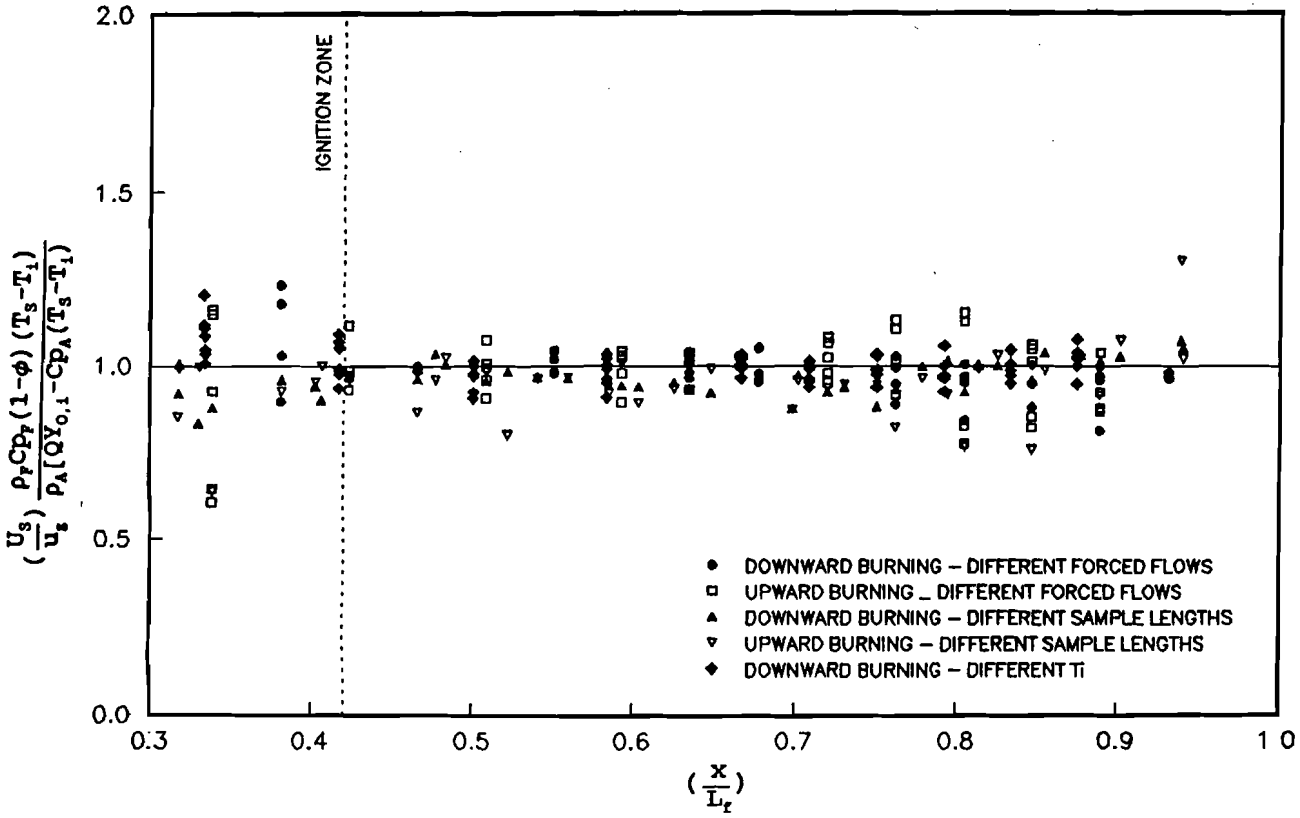

Figure 3.16 - Correlation between experimental and theoretical smoldering propagation velocities for different velocities (upward and downward burning), different lengths (forced air velocity of 1.70 mm/sec, upward and downward burning, sample lengths 150, 175, 200 and 300 mm), different initial temperatures (forced air velocity of 0.48 mm/sec, initial temperatures, 293, 308, 323, 338, 353, 383, 413 K). All extinguishing experiments have been eliminated.

competition between the supply of oxidizer to the reaction zone and the loss of heat from the reaction zone. The presence of two smolder controlling mechanisms, chemical kinetics and heat losses, has been suggested before by Ohlemiller and co-workers [1] from their observations of the effect of oxygen concentration and pressure on the smolder of polyurethane foam. To understand how these two controlling mechanisms affect the characteristics of the smolder process in the present results, it is convenient to analyze the raw smolder data and the model correlations presented above.

3.7.1 Downward Smoldering

Analyzing first zone II, which as indicated above is the most representative of forced flow self sustained smolder. The temperature data of figure 3.3 shows that for zero and low air flow velocities (< 0.5 mm/sec) the reaction zone temperature is low, indicating the presence of a weak smolder reaction. This is most likely due to the low supply of oxidizer to the reaction zone. The weak reaction also results in a small smolder propagation velocity, and in a poor prediction of the data by the model. It is interesting to note that the smolder reaction propagates even at zero flow rate, which indicates that the oxygen contained in the foam pores and transported by recirculation is enough to sustain the smolder reaction, although weakly. As the air flow velocity is increased, the smolder reaction temperature and velocity first increase, reach a maximum (at approximately 2.5 mm/sec), and then start to decrease. The initial increase in the smolder temperature and velocity is

due to the increased supply of oxidizer to the reaction zone which enhances the chemical reaction and consequently the heat production. This regime is the one predicted better by equation 3.6. The larger amount of heat generated by the smolder reaction compensates for the larger convective heat losses caused by the larger air flow rate. As the air velocity is increased further, the heat generated at the reaction and the convective heat losses eventually balance each other and the smolder reaction reaches a maximum in temperature and velocity. If the air flow rate is increased even further the heat losses overcome the heat generation and the smolder temperature and velocity start to decrease. For air flow rates larger than 2.8 mm/sec, the heat losses dominate and cause the weakening and final extinction of the smolder reaction. Here again the model starts to fail since the energy generation cannot overcome the heat losses, and the chemistry of the smolder reaction becomes of increased importance.

The above discussed controlling mechanisms also apply to the other two zones, although the external effects modify somewhat the balance between them. In zone I the fuel is preheated by the igniter which helps the establishment of the reaction, and results in elevated fuel temperatures as it is seen in figure 3.3. However, since as explained above the forced air is not initially on, the amount of air available to the reaction is small and consequently the reaction is weak and propagates slowly initially, as seen in figure 3.2. Once the air flow is turned on, and sufficient oxygen is made available to the reaction, the smolder reaction becomes vigorous with high propagation velocities and temperatures, although the latter are

reduced from the cooling

effect of the flowing air. As the smolder reaction moves further away from the zone of igniter influence, the convective cooling of the air flow becomes dominant over the increased oxygen supply and the reaction temperature and velocity start to decrease until the reaction stabilizes itself in zone II, or extinguishes.

In zone III, the sample's end is close enough, and the unburnt fuel length and its drag resistance are small enough to permit the generation of buoyant flows through the remaining char as explained above. Furthermore, the air velocities generated by the buoyant flow can be similar or even larger than those of the forced flow, and consequently can play an important role in the smolder process. As it is seen in figure 3.2, the onset of buoyant currents affects the characteristics of the ongoing smolder reaction by either enhancing the reaction or by weakening it, depending on whether the added supply of air is dominant over the convective cooling, which in turn depends on whether the ongoing reaction is already strong or not. For example, at low flow velocities the reaction is already weak, and the as heat losses to the environment increase at the end of the sample the reaction weakens even further reducing the smolder temperature (figure 3.3), and the propagation velocity (figure 3.2). Under these conditions the model is not capable of predicting the experimental data. At intermediate air flow velocities, the smolder is strong enough to benefit from the increase in air supply caused by the buoyant flows, an the smolder temperature and velocity increases. This regime is well predicted by the model. At large flow velocities the buoyant flows are too small to

affect the already decaying smolder reaction.

3.7.2 Upward Burning

The quantitative differences between the smolder in the upward and downward configurations are worth discussing. In upward smoldering the buoyantly generated flow tends to flow upwards against the downward forced flow, and consequently a recirculation flow must be generated at low forced flow velocities. These recirculating flows can have a dual effect. In one hand they can produce a region of low velocity, but with a large air supply, where the flow turns around that will favor the propagation of the smolder reaction. This type of effect is more likely to occur in region II, and could explain the observation that smolder occurs at higher air velocities. The upward recirculating air can also flow past the reaction zone, heating up as it flows past the elevated temperature char and preheating the virgin fuel ahead of the smolder zone as it flows down after turning, which would result in larger smolder velocities . However, these upwardly moving gases also contain combustion products that can reduce the supply of oxidizer to the reaction zone and cause the weakening of the smolder reaction. Depending on which effect is dominant, the buoyant flow could deter or enhance the progress of the smolder reaction. The former seems to be what takes place in the zone between regions II and III, and the latter at the end of the sample. The smolder temperature variation along the sample appears to confirm this view of the process.

3.8 Conclusion

The present experiments on the effect of an opposed forced flow of oxidizer on a smoldering reaction propagating downward and upward through a high void fraction porous fuel have helped to identify the controlling mechanisms of opposed smoldering, and to determine the potential importance of buoyancy on the process. They have also helped verifying the potential predictive capabilities of the theoretical models presently available of smolder combustion. Particularly interesting is the verification that the competition between oxygen supply and heat losses determines, in conjunction with the state of the reaction, the fate of the smolder reaction. The reaction presents an intensity maximum at relatively low air velocities (2 to 3 mm/sec). At lower and larger air velocities the smolder reaction is weak due to either lack of oxidizer or excessive heat losses.

The range of air velocities that produce the stronger smoldering reactions are surprisingly small in comparison to those in other combustion phenomena, which confirms that the smolder reaction is weak and very sensitive to the balance between heat losses and oxygen supply. These observations indicate that buoyancy can have a significant role in the smolder process since buoyantly generated air currents, even if they are slow, can easily influence weak smolder reactions. Buoyantly induced flow is an oxidizer transport mechanism, and its magnitude depends on the permeability of the char, since the char permeability increases with the reaction rate, the magnitude of the buoyant flow increases too; resulting in an increase in oxidizer supply to the reaction. The magnitudes of buoyant and forced

flow are comparable for all ranges of air forced velocities studied. The limit for this flow was determined by extinction.

Upward and downward smolder only show significant differences for air forced flow velocities smaller than 1 mm/sec, for this velocity range the difference between aiding flow (downward burning) and opposing flow (upward burning) inside the char affected the characteristics of the smolder reaction.

Smoldering in the opposed configuration is a steady premixed like combustion process. The mechanism controlling its propagation is heat transport from the reaction to the virgin fuel, and since the heat released by the reaction is proportional to the oxygen reaching the reaction, smoldering propagation velocities and total average air velocities are linearly proportional. This is valid for strong self-sustained reactions. This model does not apply for weak reactions leading to extinction (flow rates smaller than 0.5 mm/sec and larger than 2.5 mm/sec) where considerations dealing with the chemistry of the problem need to be taken.

Chapter 4
FORWARD FORCED FLOW SMOLDER

4.1 Introduction

An experimental study is carried out of the effect on the propagation velocity of a smolder reaction of oxidizer forced to flow in the same direction of smolder propagation. The experiments are carried with a high void fraction polyurethane foam as fuel and air as oxidizer, in a geometry that approximately produces a one-dimensional smolder propagation. Measurements are performed of the smolder propagation velocity and smolder reaction temperature as a function of the flow velocity, location in the sample and direction of propagation (downward and upward). Very few fundamental studies of forward smoldering exist in the literature. Qualitative descriptions of the process are given by Ohlemiller [1], Ohlemiller and Rogers [3] and Summerfield and Messina [2]. Ohlemiller and Lucca [29] performed a series of forward smoldering experiments using powder cellulose as fuel and changed the air flow rate, their experiments were all in upward burning configuration. Here polyurethane foam is used as fuel, and the effect of buoyancy is determined by comparing the smolder parameters in downward and upward propagation. This type of smoldering is also referred to as counter-current smoldering because if the reaction front is considered as stationary the fuel and oxidizer reach the reaction zone in opposite directions. In downward smoldering the gravitational acceleration is in the same direction as that of smolder propagation, and for upward smoldering in opposite direction. Therefore when the upward and

downward experiments are compared, the difference between the two can be attributed to gravity. The smolder parameters that are compared in this work are the propagation velocity and reaction temperature.

Forced forward smolder incorporates an important new parameter, pyrolysis. For small flow rates, smolder propagation and flow velocities are of similar magnitude, therefore, post-combustion products are not carried into the foam, diluting the oxidizer content inside the pores. No evidence of pyrolysis is observed. As the air flow velocity increases a pyrolysis front appears ahead of the oxidation front, for a certain range of velocities both pyrolysis and oxidation propagation velocities are very similar. For large flow rates an oxidation front is no longer clear.

The smolder velocity data are correlated in terms of a non-dimensional smolder velocity derived from a theoretical model of the process previously developed. The analysis of the results confirm that the smolder process is controlled by the competition between the supply of oxidizer to the reaction zone and the loss of heat from the reaction zone. Forward smoldering shows a clear effect of gravity for flows smaller than approximately 2.0 mm/sec. For opposed flow, previously described experiments, chapter 3, showed that increasing the flow velocity strengthens the smolder reaction resulting in larger velocities and temperatures, but for flows over 2.5 mm/sec convective cooling to the air becomes dominant leading to extinction. For this configuration the air flow is forced through the hot char, therefore, when it reaches the reaction zone its temperature is that of the reaction, so convective cooling does not play as significant a role as in opposed smolder,

instead, the forced flow carries the reaction heat to the virgin fuel resulting in temperatures and velocities increasing monotonically with the flow rate. The effect of the buoyantly induced recirculations in the char is again observed for large flow rates where smolder would not transition to flaming in downward burning (buoyantly induced convective currents oppose the forced flow) instead transition to flaming will occur in upward burning (buoyantly induced convective currents act in the same direction of the forced flow). Comparison between downward and upward smoldering corroborates the above observations.

4.2 Description of the Experiment and Experimental Hardware

A schematic diagram of the experimental installation is shown in figure 4.1. The porous fuel is contained in a 300 mm long vertical duct with a 150 mm side square cross section. The duct walls are made of insulating 10 mm thick Fiberfax sheet mounted on an aluminum frame and covered by aluminum foil to prevent diffusion through the walls. The oxidizer gas flows to the test section through a diffuser fitted at one end of the duct, after being metered with a Tyland type FC280S controlled mass flow meter. Controlling the mass flow rate is important in this experiments because the pressure losses through the porous material decrease with time as the smolder reaction propagates, and conventional flow meters would not prevent the resulting increase in flow rate. The fuel ignition is accomplished with an electrically heated igniter placed in close contact with the foam. The igniter consists of a Nichrome wire placed in between two, 5 mm thick, porous ceramic honeycomb

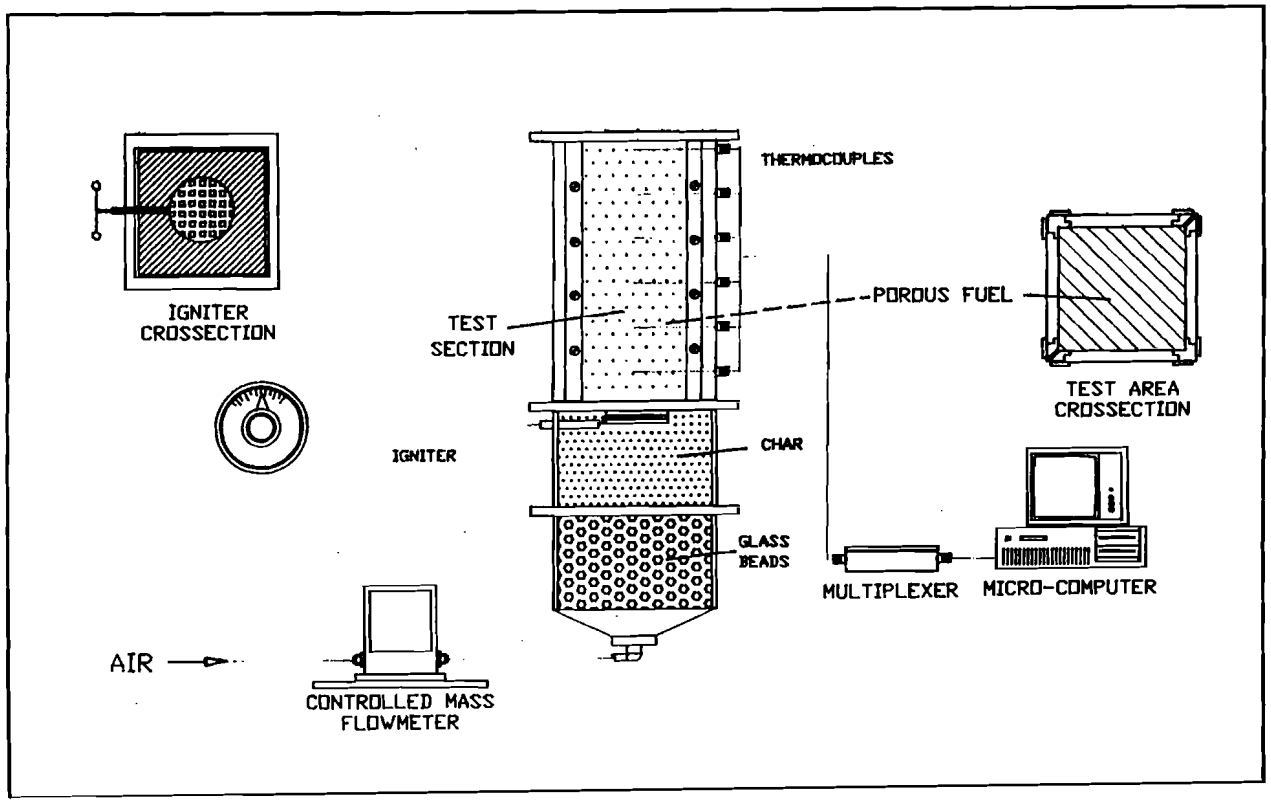

Figure 4.1 - Schematic of experimental apparatus. Air flows from the controlled mass flow meter through the igniter section into the test section.

plates that provide rigidity to the igniter and heating uniformity. To insulate the ignition zone and simulate an ongoing smolder process, a layer of char from an already smoldered foam is placed at the other side of the igniter, the cold forced flow moving through the char keeps the char insulation cold preventing it from igniting and altering the process. For the forward smoldering experiments the section containing the igniter and the char is placed at the diffuser exit upstream from the section containing the virgin foam.

The foam ignition is accomplished by bringing the temperature of the igniter up to approximately 500 °C. For these specific experiments the power needed was of approximately 1.7 KW/m^2 during a period of 900 sec. Most of the energy is used, however, to heat up the igniter ceramic plates to the temperature mentioned above. Since the air flows through the igniter before reaching the fuel, the air flow is turned off, during the heating period, to avoid extending the igniter influence to a larger fraction of the virgin material, and to standardize the ignition process, that, if performed with the air flow on, will depend on the flow rate. The heating period is selected to ensure the self-supported propagation of the smolder reaction. Once the ignition heating period is completed, the igniter current is turned off and the flow of air is turned on, initiating the flow assisted smolder process.

The rate of smolder propagation is obtained from the temperature histories of eight Chromel-Alumel thermocouples 0.8 mm in diameter that are embedded at predetermined positions in the porous fuel with their junction placed in the fuel centerline. The smolder velocity is calculated from the time lapse of the reaction

zone arrival to two consecutive thermocouples, and the known distance between the thermocouples. Although the arrival of the reaction zone is characterized by a maximum in the temperature profile, under most experimental conditions this maximum is not sharply defined. The location of the pyrolysis front is defined by the intersection of the tangent to the temperature curve at the inflexion point and a horizontal line at a temperature near to the pyrolysis temperature (300 °C in this work). The location of the oxidation front is defined by the intersection of a horizontal line at a temperature near to the maximum temperature (380 °C in this work) and a tangent to the temperature curve drawn after the pyrolysis front has passed the thermocouple and the temperature has started to increase again.

All the experiments are conducted with 150 mm side cubes of an open cell, unretarded, white polyurethane foam, with a 26.5 Kg/m^3 density and 0.975 void fraction. The foam sample width was selected to reduce the effect of the cold walls on the smoldering reaction thus helping to obtain one dimensional smolder propagation in a region of at least 50 mm in diameter from the sample centerline. The length is enough to permit the observation of self propagating smolder without the influence of the igniter and end effects. House compressed air is used as oxidizer. For the downward experiments the igniter and char are placed on top of the foam sample and the air flow is introduced through the igniter. For the upward experiments the apparatus is simply rotated 180 degrees. The characteristics of the smolder process are determined from the propagation velocity and temperature traces.

4.3 Experimental Results

The data obtained from these experiments is the temperature traces of the above mentioned 8 thermocouples; from these temperature traces it can be observed that the reaction characteristics vary depending on the magnitude of the forced air flow and the location of the reaction with respect to the ignition plane. For a more clear presentation of the results, the different regimes that the reaction undergoes as the forced air flow is increased will be introduced from characteristic temperature histories; smoldering and pyrolysis propagation velocities along with maximum temperatures as a function of the distance from ignition will then be used to introduce different zones along the sample where the reaction has different characteristics. Downward and upward burning will be treated separately.

To describe the characteristics of the smolder reaction as it propagates away from the ignition plane the analysis of the data is done by dividing the foam sample in three different zones. An initial zone (I) of length dependant on the flow rate, but that is never more than 50 mm away from the igniter, where the smolder process is affected by the heat from the igniter. A second zone (II) covering approximately the central 60 mm of the sample, where the smolder process is self sustained and relatively free from end effects. A third zone (III) at the end of the sample where smolder is affected by the ambient air and by the small size of the virgin fuel left for smoldering. The extent and characteristics of the smolder reaction at each zone depend on the air flow rate. Since during the period of ignition there is no forced air flow through the foam this region is not representative of the type of smoldering

studied here, therefore the data from the first 35 mm of the sample is not presented. Also since the velocities are obtained from the temperature histories of two thermocouples and assigned to the midpoint between the two, the corresponding figures for smoldering velocities do not show data points for the first 50 mm.

The smoldering in zone II is the most representative of a forced flow, forward smoldering, at least from the point of view of modeling, since external effects are limited. The smoldering in the other zones, however, are also interesting because they provide additional information about the process, and describe situations that may occur in practice. The smoldering in zone I is representative of a situation where smoldering is supported by an external heat source. As it will be explained later, the smolder in zone III is of particular interest from the point of view of buoyant effects on smoldering. In this zone the length of the virgin fuel, and consequently its drag resistance, are small enough to permit the generation of buoyant flows through the virgin foam and remaining char.

4.3.1 Downward Burning

Experiments in the downward burning configuration were conducted for the following forced flow velocities; 0.00, 0.30, 0.90, 1.70, 2.80, 4.10, 5.30, 7.80 and 14.10 mm/sec. and were repeated, on average, five times for each forced flow velocity. The temperature traces of figures 4.2, 4.3, 4.4 and 4.5 are each representative of one different characteristic regime, each trace represents the temperature history at a specific location along the sample as recorded by a thermocouple; the distance

between thermocouples is known but is not necessarily the same between different consecutive thermocouples. To avoid unnecessary crowding of the figures all eight thermocouples are not presented unless considered necessary. For very low flow rates (0.00 and 0.30 mm/sec), the maximum temperature is observed to remain almost constant as the reaction propagates through the sample (figure 4.2). No significant preheating of the fuel can be observed from the temperature traces and a weak reaction propagating upwards is initiated as the smoldering reaction reaches the end of the sample. In general the characteristics of this regime are very similar to what was described in chapter 3 for opposed smoldering it is important to note that the maximum temperatures for these experiments are approximately 10 to 20°C lower than the maximum temperatures of opposed forced flow experiments conducted with equal air flow velocities. As the forced flow velocity increases the reaction weakens and extinction is observed for several experiments conducted with forced flow velocities of 0.30, 0.90 and 1.70 mm/sec, figure 4.3 shows that as the air flow is started at 900 sec. the temperatures immediately start to decay and extinction follows. For higher flow rates the extinction regime disappears and a strong reaction follows. Figure 4.4 is a characteristic example of this regime, the pyrolysis front is followed by an oxidation front and both propagate at very similar velocities. The pyrolysis front is characterized by a constant temperature (approximately 320°C) and its location is clearly determined by a period of time where the temperature remains almost constant, due to the endothermic nature of the pyrolysis reaction. The oxidation front is characterized by a decaying maximum temperature, from

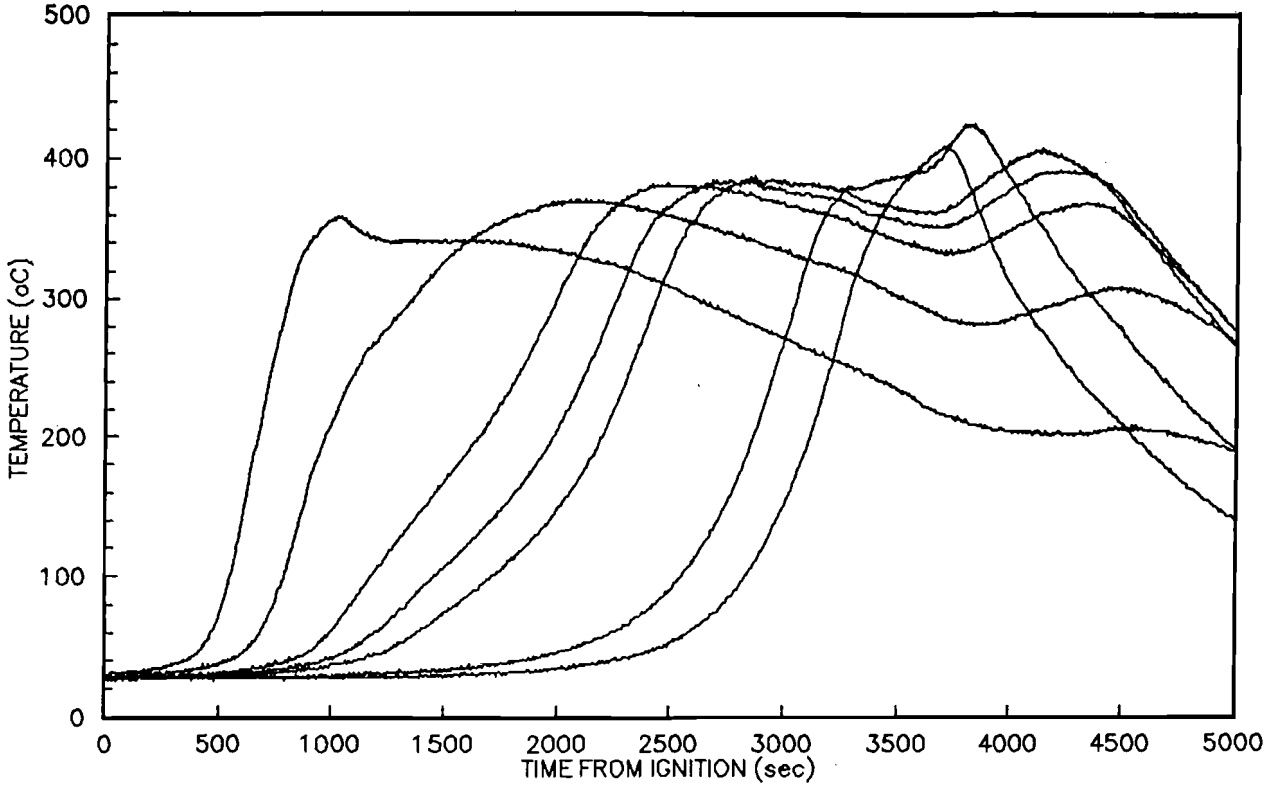

Figure 4.2 - Temperature histories for seven thermocouples, downward forward smoldering (flow rate 0.30 mm/sec). No evidence of pyrolysis can be extracted from this temperature histories. Thermocouples are not necessarily placed at a constant distance from each other.

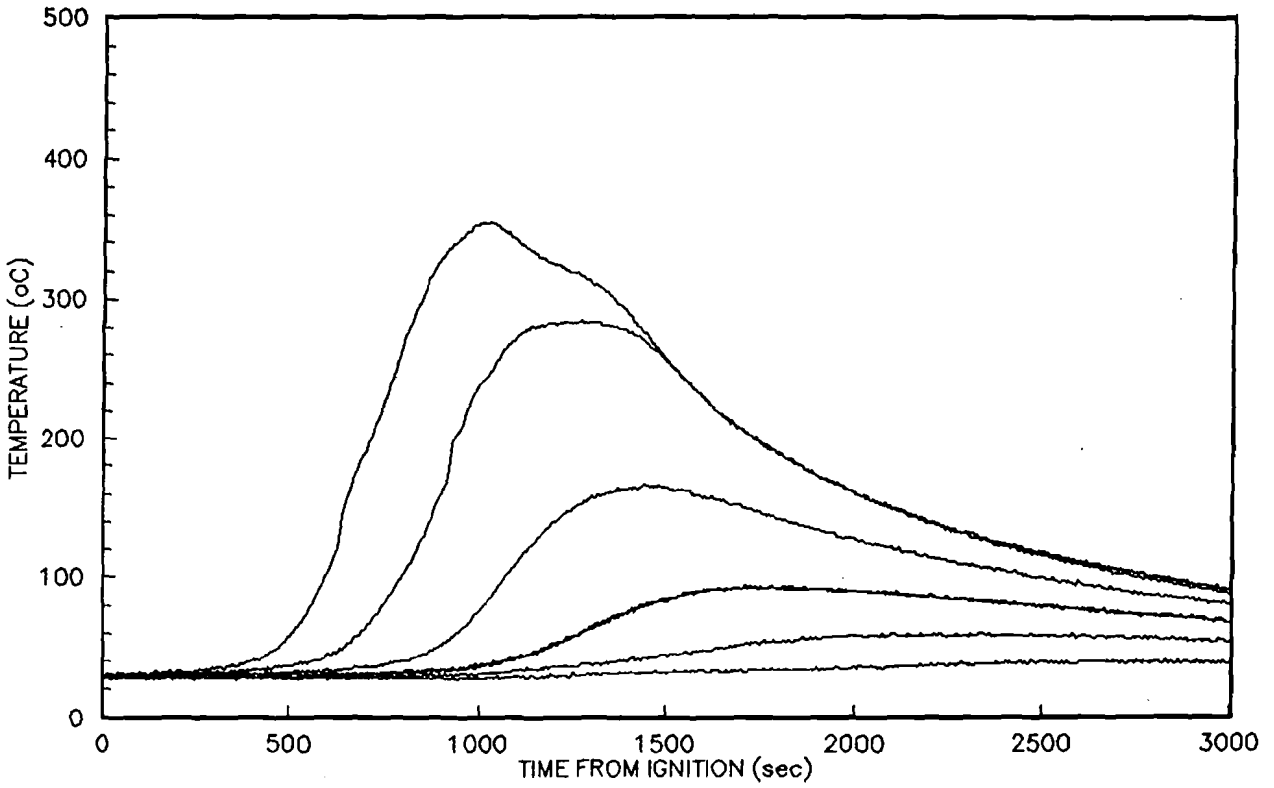

Figure 4.3 - Temperature histories for six thermocouples, downward forward smoldering (flow rate 0.90 mm/sec). Extinction occurs immediately after ignition is completed. Thermocouples are not necessarily placed at a constant distance from each other.

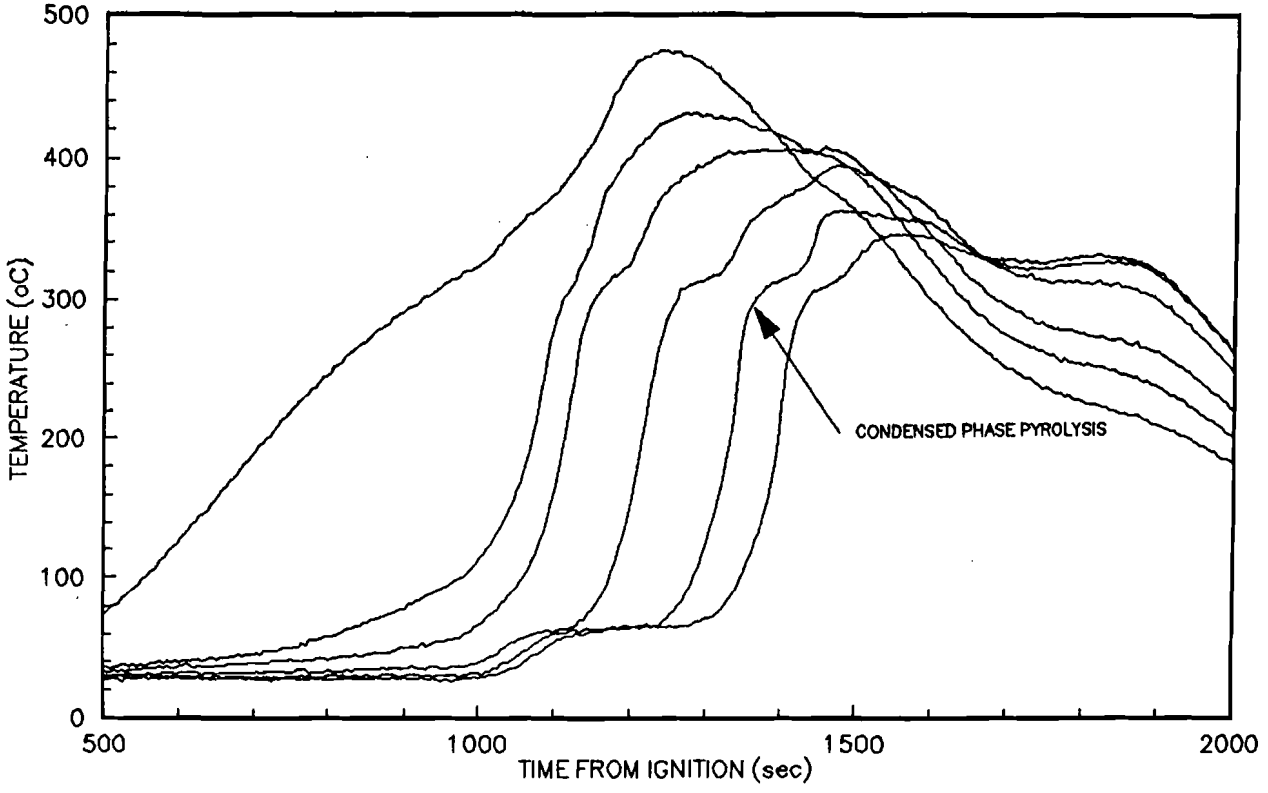

Figure 4.4 - Temperature histories for six thermocouples, downward forward smoldering (flow rate 2.80 mm/sec). Thermocouples are not necessarily placed at a constant distance from each other. Clear evidence of pyrolysis appears in this figure, pyrolysis and oxidation fronts propagate at approximately equal velocities.

temperatures as high as 460°C, near to the ignition plane, to approximately 350°C, at the end of the sample. Characteristic smoldering temperatures for polyurethane foam have been observed by several authors [1,3,15] to be approximately 360-380°C. Significant preheating of the foam ahead of the pyrolysis front can be observed from figure 4.4. For air flow velocities larger than 6 mm/sec the propagation velocity of the oxidation front is much faster than the pyrolysis propagation velocity, thus, the oxidation front approaches the pyrolysis front and the two distinctive fronts are replaced by one single front, as observed from figure 4.5. Maximum temperatures are approximately 450°C, decaying towards the end of the sample; these values are significantly higher than characteristic smolder temperatures for polyurethane foam [1,3,15].

The variation of the downward smolder propagation velocity and of the maximum smolder reaction temperature through the sample length are presented in figures 4.6, 4.7 and 4.8 respectively, for several representative opposed air flow velocities. Tests conducted at other flow velocities are not presented to avoid crowding of the figure. The data is the average from five tests, and the error bars describe the maximum deviations from the mean. The results of figures 4.6, 4.7 and 4.8 are better analyzed if the processes involved in each zone are treated separately. Although the boundaries between the different zones cannot be clearly determined, the following trends are identified from the measurements. Since the smoldering in zone II is the most representative of a forced flow we will begin by describing this zone. With no flow the smolder velocities for this zone remains almost constant

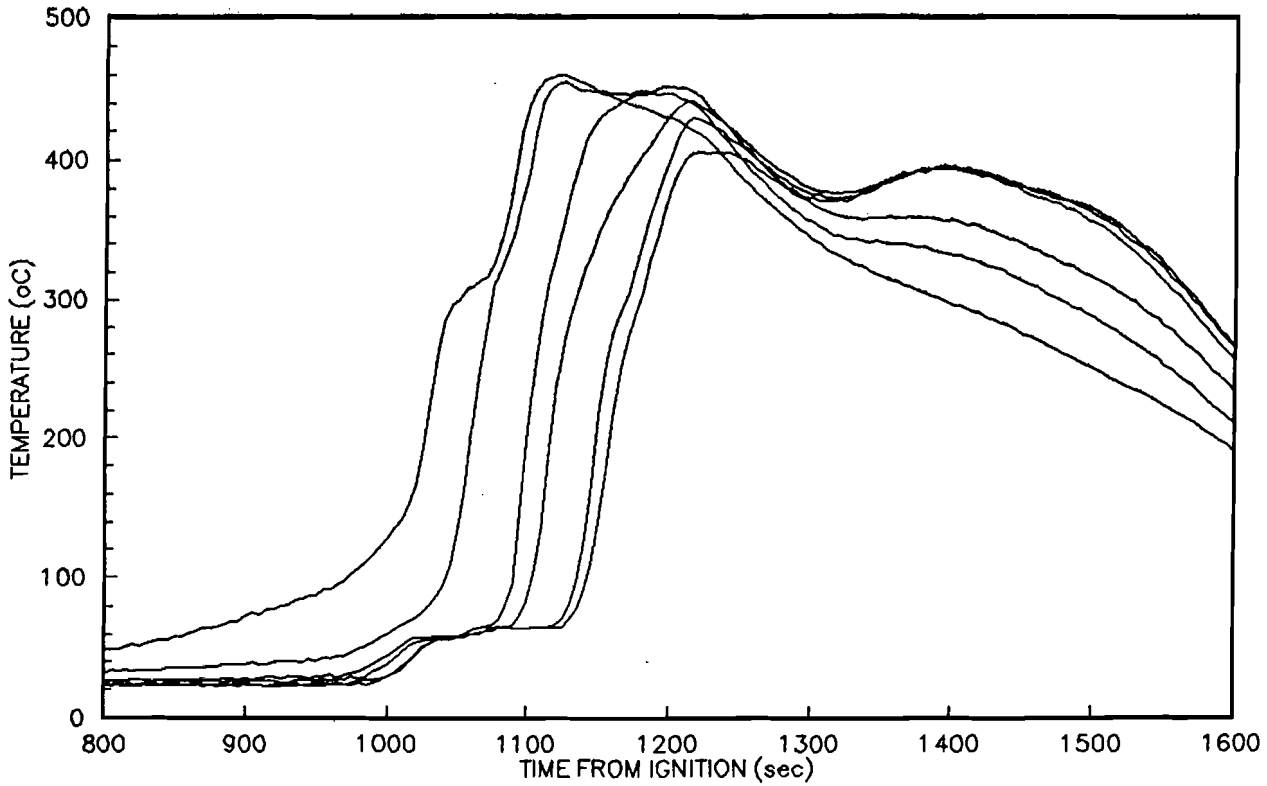

Figure 4.5 - Temperature histories for six thermocouples, downward forward smoldering (flow rate 7.80 mm/sec). Thermocouples are not necessarily placed at a constant distance from each other. The oxidation front approaches the pyrolysis front until one single front is observed.

decaying in the last 30 mm of the sample. When the air flow is increased to 0.3 mm/sec extinction is observed very early in the sample, a further increase in the flow velocity, 0.9 mm/sec, shows again a slowly propagating reaction that reaches extinction in the last 30 mm of the sample, data for these air flow velocities is not presented in figure 4.6. For higher flow velocities the smolder velocity increases monotonically with the flow velocity (figure 4.9). Smolder velocities as the reaction propagates through the sample are not constant for flow velocities greater than 1.70 mm/sec instead it is observed that the smolder velocities increase towards the end of the sample. Propagation velocities of the pyrolysis front for air flow velocities between 1.70 and 7.80 mm/sec are equal to the smoldering velocities, for air flow velocities of 7.80 and 14.10 mm/sec smoldering propagates faster than pyrolysis until they both form a single front, as shown in figures 4.5 and 4.7.

The smolder reaction temperatures follow a different trend; for no flow temperature remains almost constant and below 400°C along all zone II. For the cases where extinction occurs (0.30 mm/sec) it can be observed that the temperature drops down along the fuel sample until the reaction finally extinguishes. As the flow velocity is increased above values of 1.70 mm/sec the maximum reaction temperatures keeps increasing as the air flow velocity is increased (figure 4.8). The temperatures for a given flow rate shows that the reaction temperatures decay through zone II.

The same mechanisms described for zone II basically apply for zone I. In zone I the heat from the igniter represents an extra source of heat and introduces a

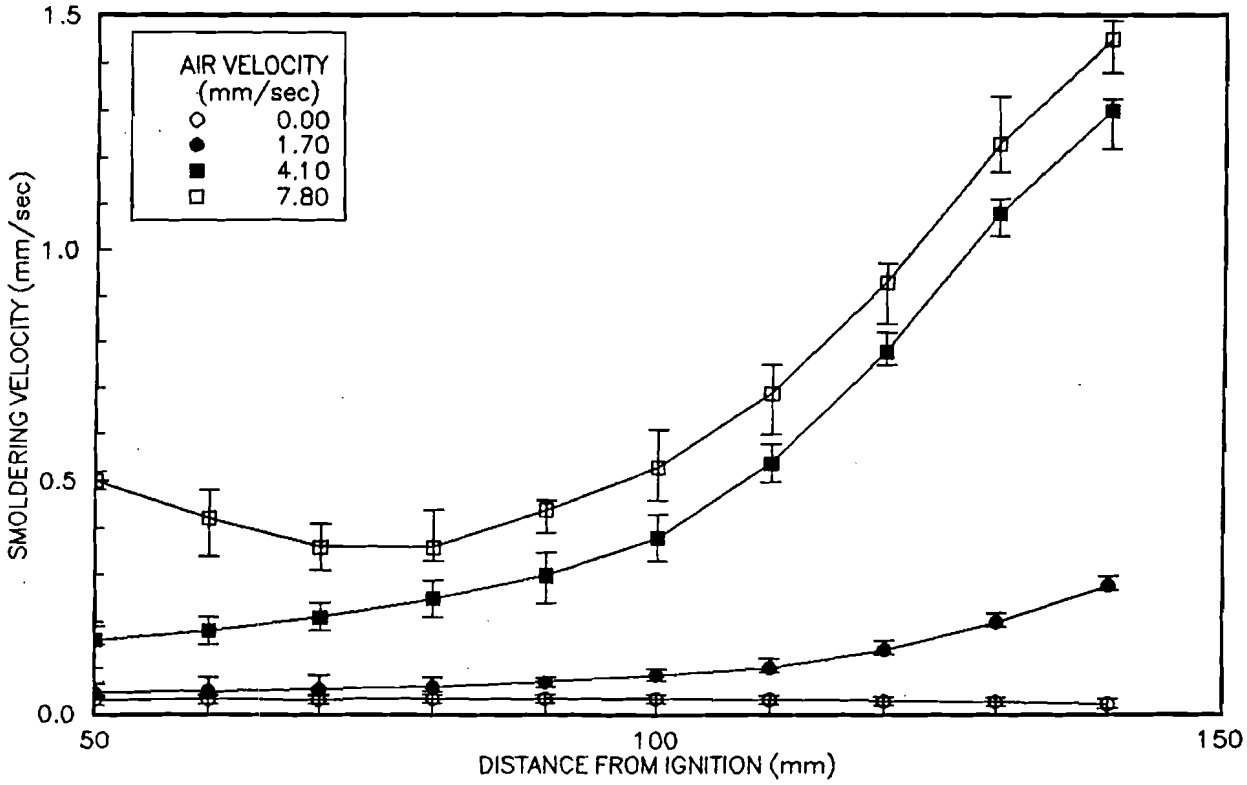

Figure 4.6 - Variation of the smolder propagation velocity along the foam sample for forward downward smolder. Experiments were conducted at several other flow rates but were not included to avoid crowding the figure.

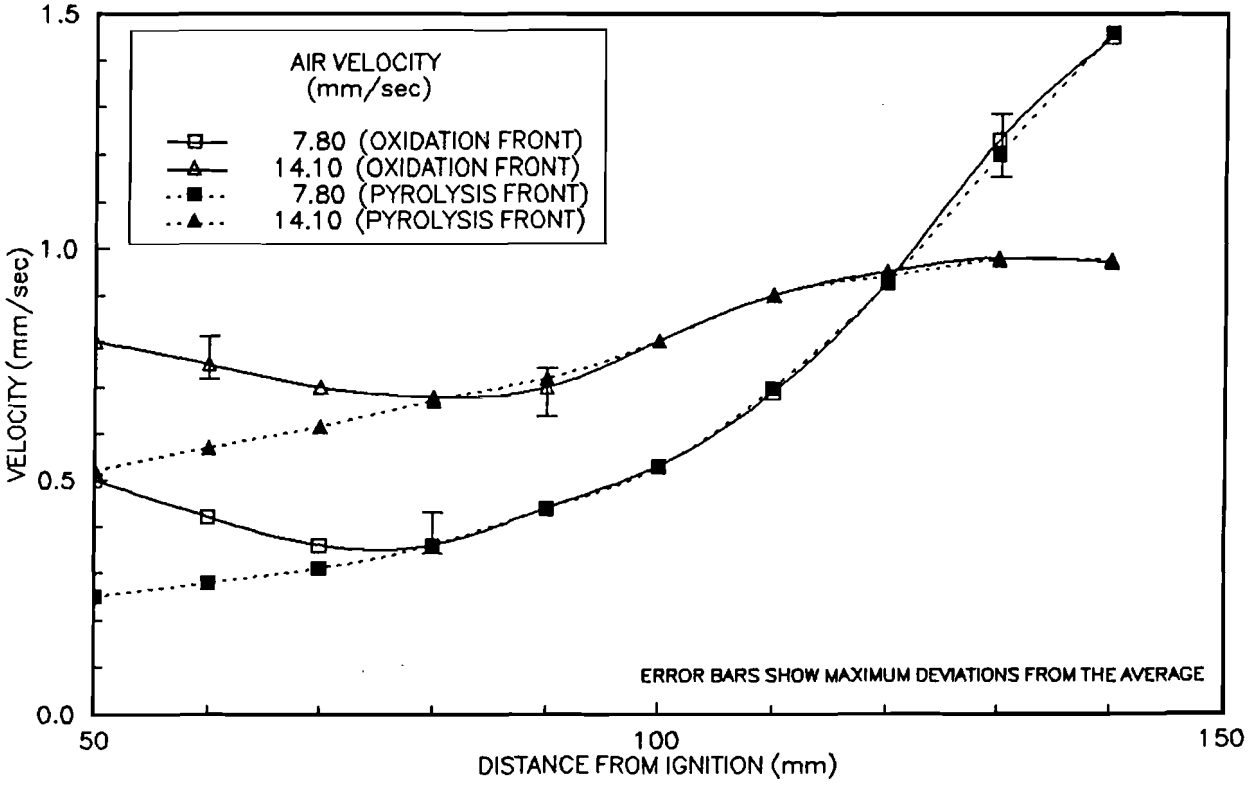

Figure 4.7 - Comparison between the pyrolysis and oxidation propagation velocities along the foam sample for forward downward smolder. For all other flow rates both velocities were almost equal.

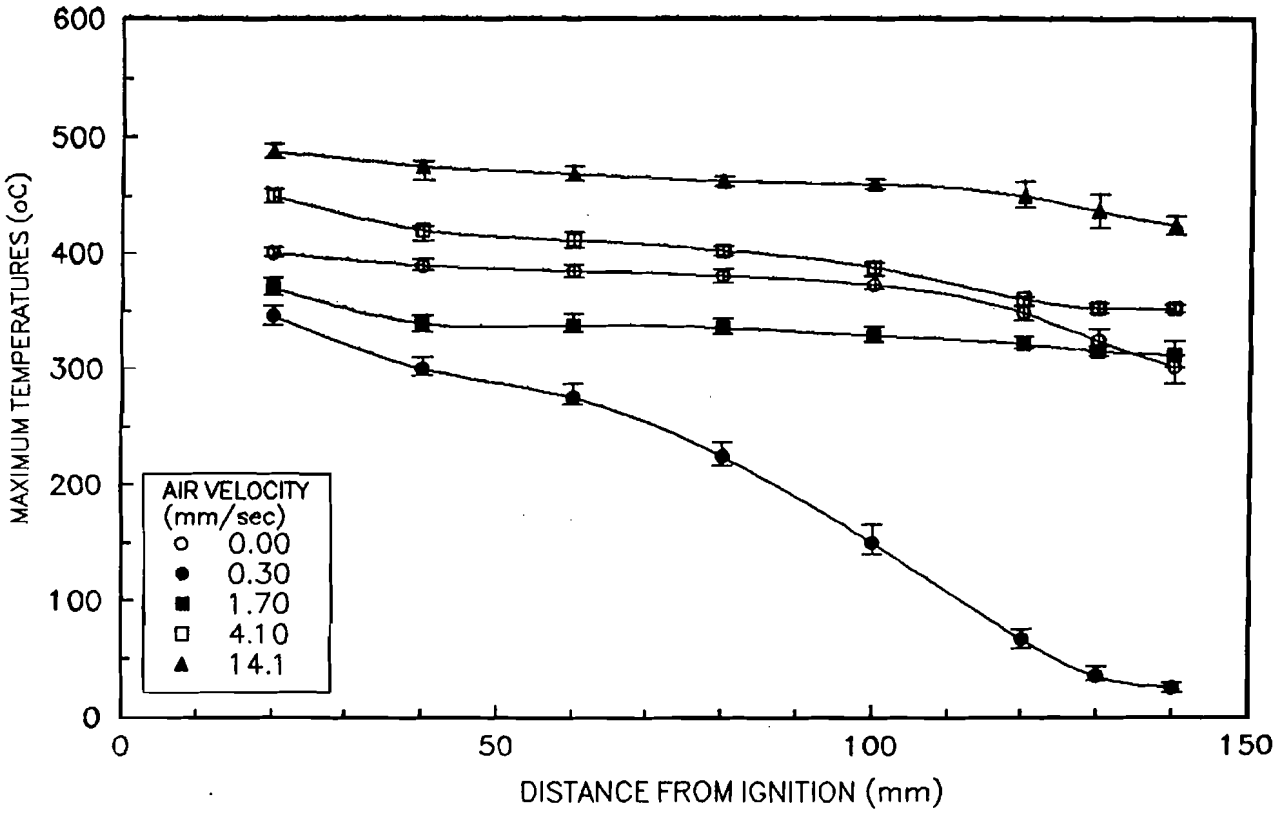

Figure 4.8 - Variation of the smolder reaction maximum temperature along the foam sample for forward downward smolder. Experiments conducted with 0.30 mm/sec air flow velocity extinguished.

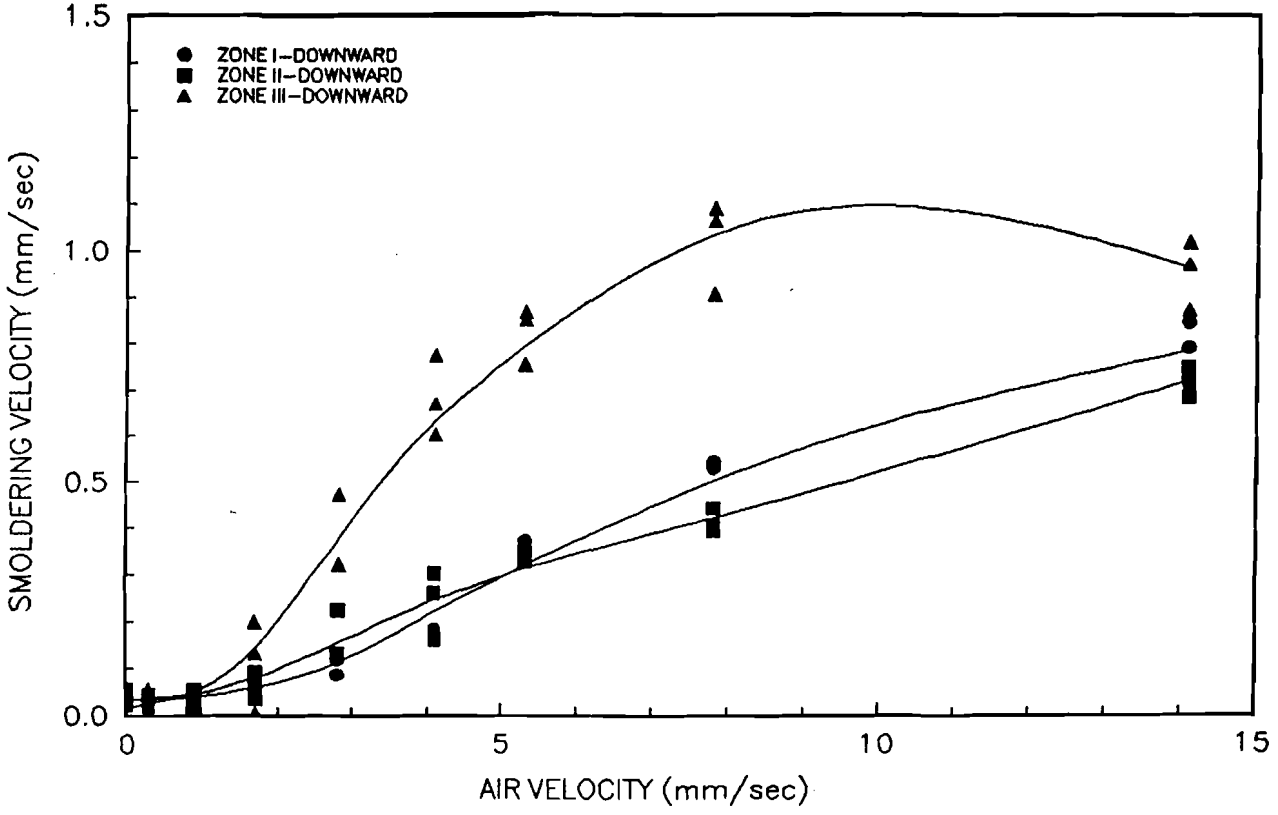

Figure 4.9 - Dependance on the forward air flow rate of the downward smolder velocity at three different sample zones. The values in this figure are averages of smolder propagation velocities at different locations within each zone.

transient period where the process transitions from the no flow ignition heating regime to the forced flow described above. The high propagation velocities of the oxidation front, observed in the first 70 mm of the sample, for air flow velocities of 7.80 and 14.10 mm/sec can be considered as part of this transient period (figure 4.7). As smoldering propagates into zone III the trends observed in figure 4.6, 4.7 and 4.8 for zone II are magnified. From figure 4.6 it can be seen that for all flow rates the smolder velocities increase strongly as the smolder front reaches the end of the sample. The process at this stage becomes extremely complicated, for flows smaller than 10 mm/sec smoldering velocity increases monotonically (figures 4.6 and 4.7) and reaction temperatures decrease (figures 4.8) as the reaction moves into zone III. For flows greater that 10 mm/sec, figure 4.7 shows a significant change in the way smoldering velocities increase as they enter zone III, even though observation shows that the reaction is getting stronger the smolder velocity increase turns weaker. Transition to flaming was not observed for these range of flow rates for downward burning.

The effect of the forced air flow velocity on the smolder propagation velocity is presented in figure 4.9, for the three zones indicated above. An expansion of the data at low air velocities is presented in figure 4.10. The smolder velocities are obtained from the results in figure 4.6 and 4.7 and are averaged values of the smolder velocities at each zone. From figure 4.10 it is seen that in zones I and II the smolder velocity has a minimum at a flow velocities between 0.4 and 1.2 mm/sec, and increases monotonically with the flow velocity for larger flow rates. Zone III

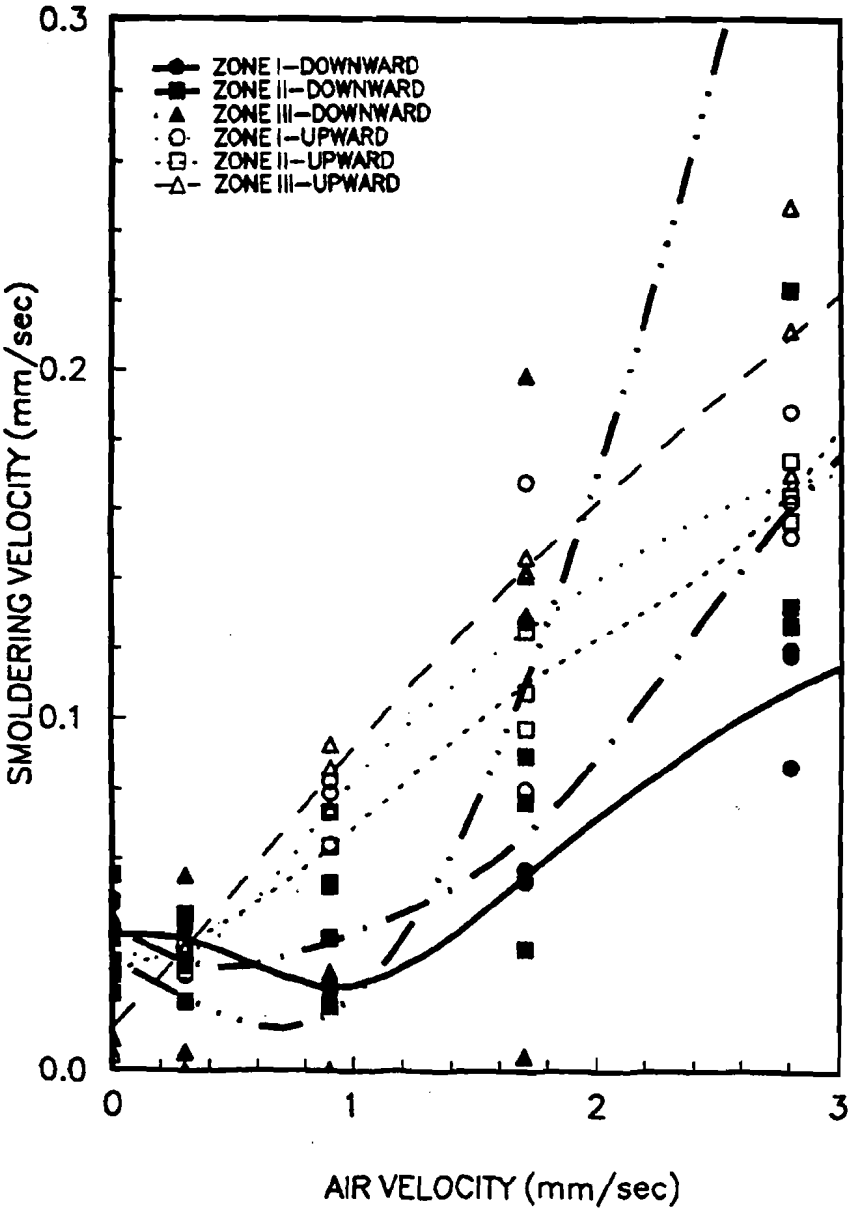

Figure 4.10 - Dependence on the forward air flow rate of the downward smolder velocity at three different sample zones (detail).

shows a minimum between 0.4 and 1.2 mm/sec and a maximum at approximately 7 mm/sec (figure 4.9). After the extinction regime, temperatures increase with the flow rate for all three zones (figure 4.11).

4.3.2 Upward Burning

Experiments in the upward burning configuration were conducted for the following forced flow velocities; 0.00, 0.30, 0.90, 1.70, 2.80, 4.10, 5.30, 7.80 and 14.10 mm/sec. and were repeated, on average, five times for each forced flow velocity. The temperature traces of figures 4.12, 4.13, 4.14, 4.15, 4.16 and 4.17 are each representative of one different characteristic regime, each trace represents the temperature history at a specific location along the sample as recorded by a thermocouple; the distance between thermocouples is known but is not necessarily the same between different consecutive thermocouples. To avoid unnecessary crowding of the figures all eight thermocouples are not presented unless considered necessary. For very low flow rates (0.00 and 0.30 mm/sec), the maximum temperature is observed to remain almost constant as the reaction propagates through the sample (figure 4.12 and 4.13). Significant preheating of the foam ahead of the pyrolysis front can be observed from the temperature traces. As in downward burning, the general characteristics of this regime are very similar to what was described in chapter 3 for opposed smoldering. As the forced flow velocity increases the reaction becomes stronger, higher maximum temperatures are observed. For 0.90 mm/sec, figure 4.14 shows a pyrolysis front appearing ahead of the smolder

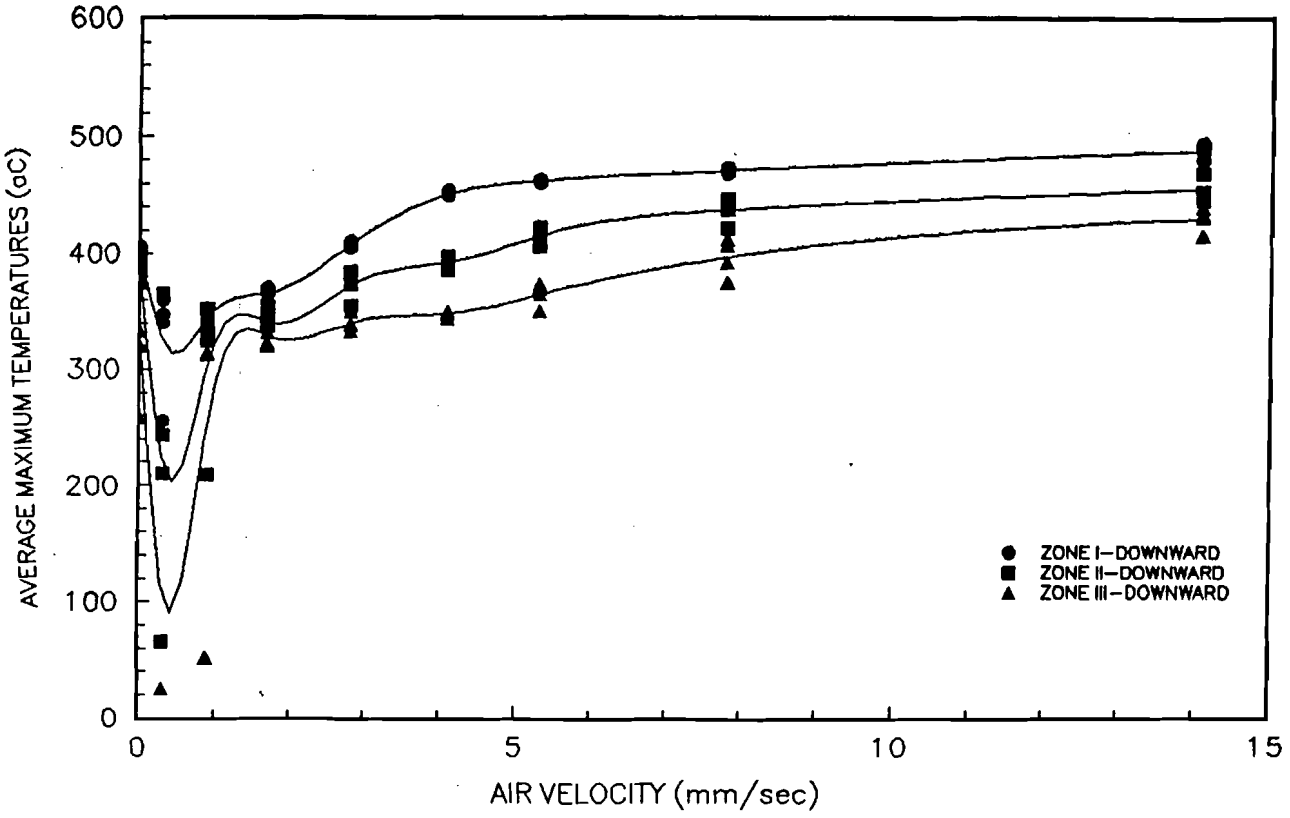

Figure 4.11 - Dependence on the forward air flow velocity of the maximum reaction temperature at three sample zones for downward smolder.The values in this figure are averages of maximum temperatures at different locations within each zone.

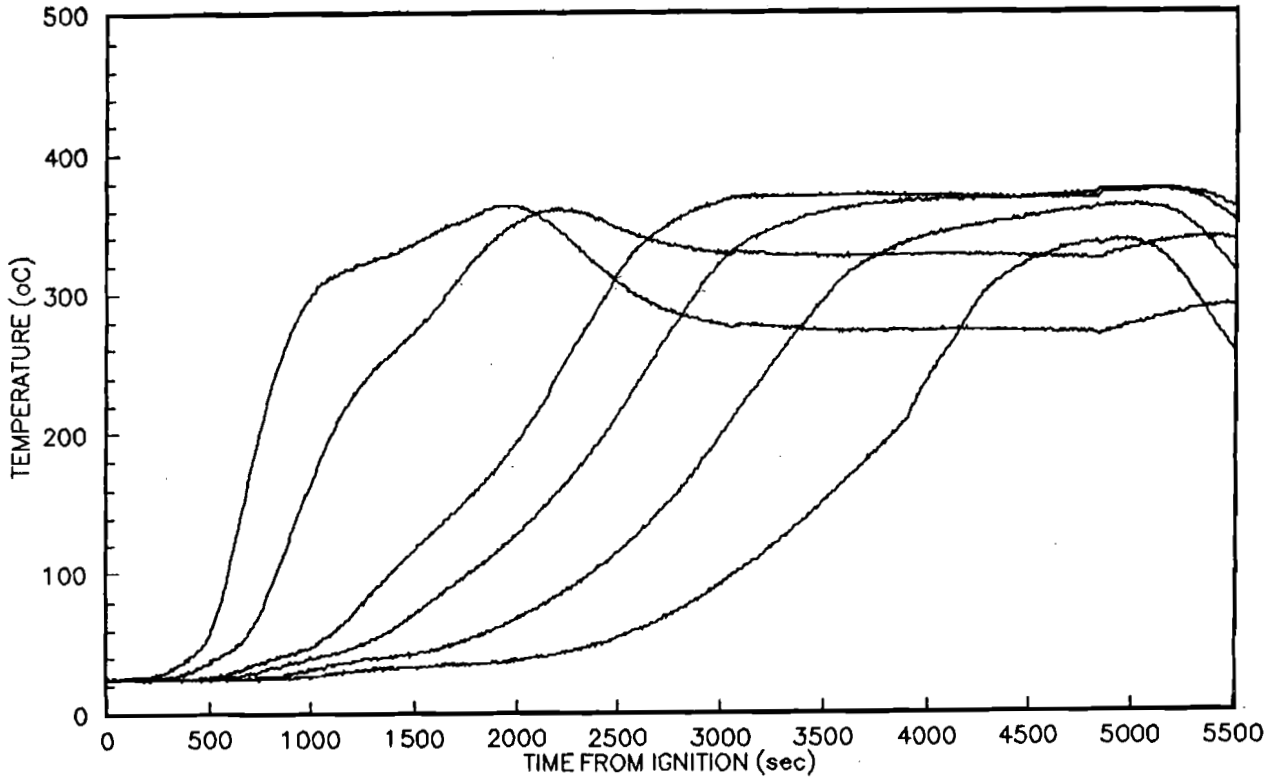

Figure 4.12 - Temperature histories for six thermocouples, upward forward smoldering (flow rate 0.00 mm/sec). No evidence of pyrolysis can be extracted from this temperature histories. Thermocouples are not necessarily placed at a constant distance from each other.

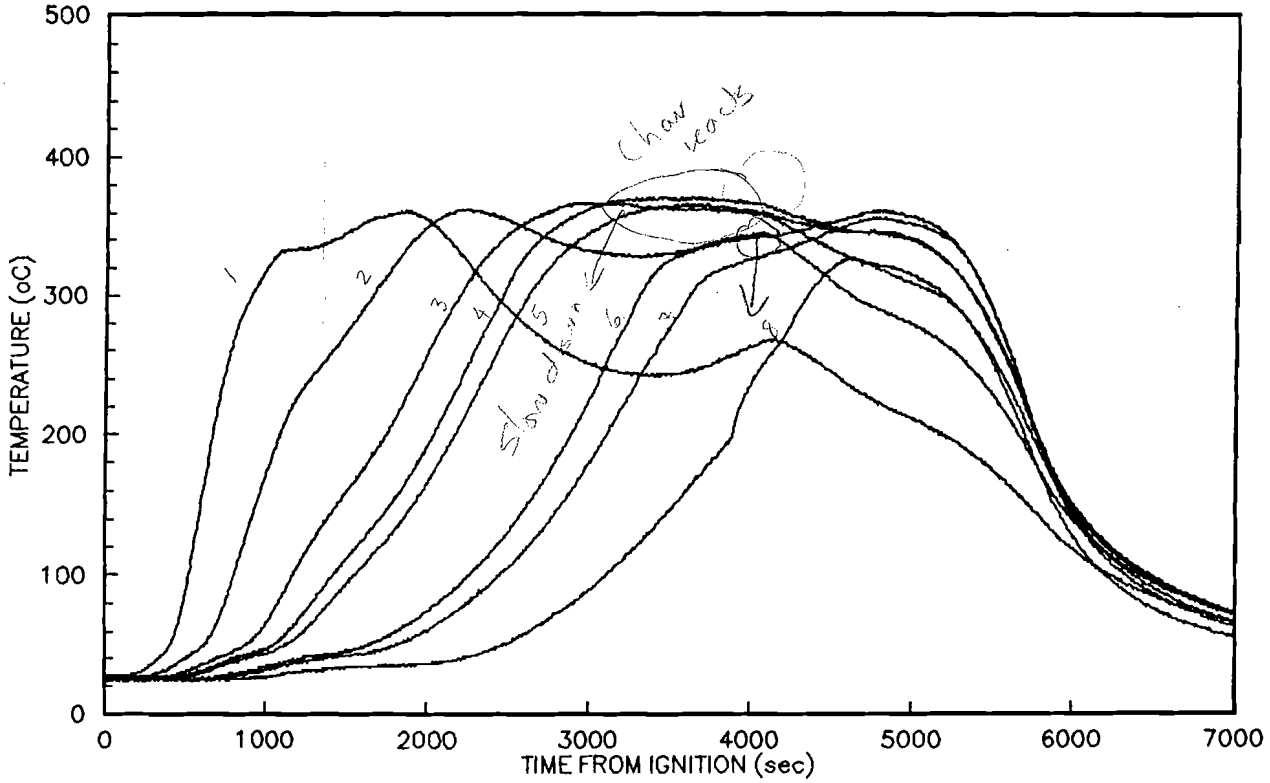

Figure 4.13 - Temperature histories for eight thermocouples, upward forward smoldering (flow rate 0.00 mm/sec). No evidence of pyrolysis can be extracted from this temperature histories. Thermocouples are not necessarily placed at a constant distance from each other.

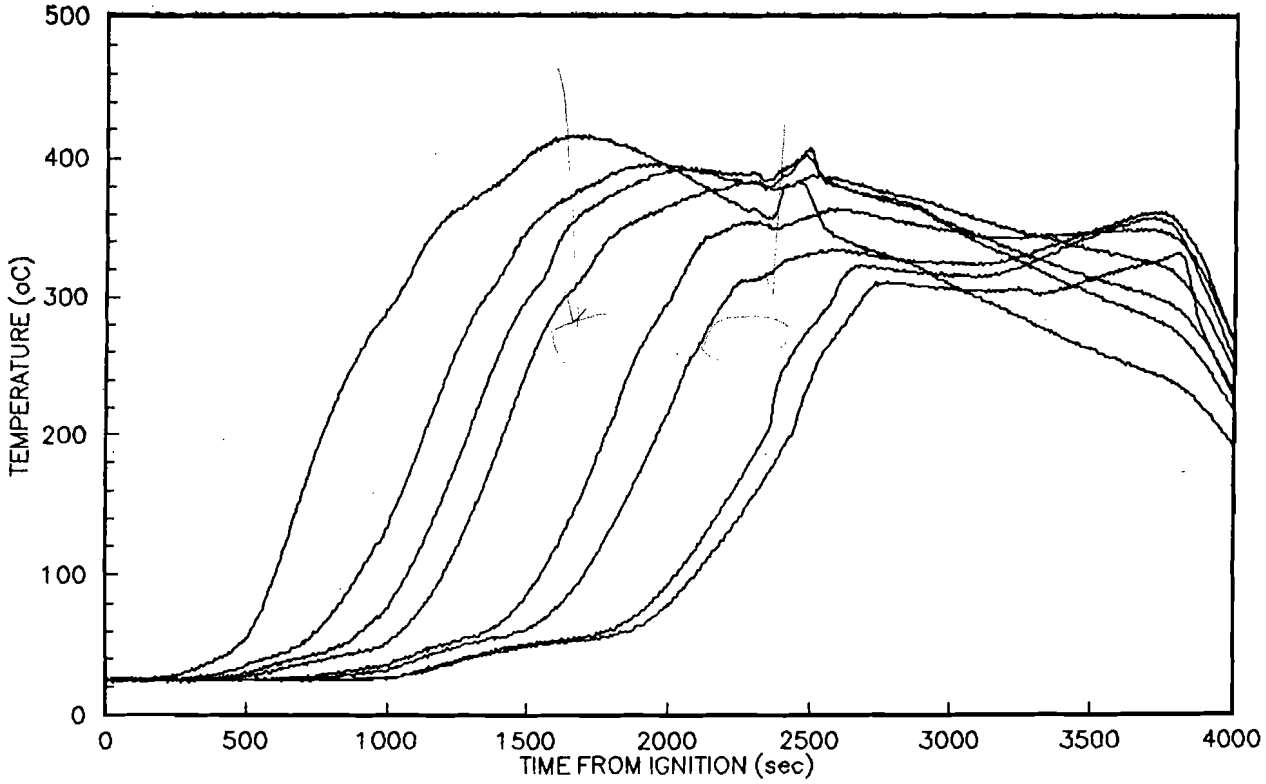

Figure 4.14 - Temperature histories for eight thermocouples, upward forward smoldering (flow rate 0.90 mm/sec). Thermocouples are not necessarily placed at a constant distance from each other. Foam pyrolysis follows strong oxidation of the char (2,500 sec).

front for the first four thermocouples, maximum temperatures for this thermocouples are still characteristic smolder temperatures. A significant increase in temperature in the char 2500 sec. after ignition is observed, the thermocouples that are ahead of the reaction zone show a decrease in the maximum temperatures (thermocouples 5 and 6) until thermocouples 7 and 8 stabilize at temperatures characteristic of condensed phase pyrolysis. After 3500 sec from ignition, the last three thermocouples undergo weak oxidation. This temperature traces show a transition process between a one step smoldering reaction and a two step pyrolysis-smoldering reaction. For higher flow rates the transition regime disappears and a strong reaction follows. Figure 4.15 is a characteristic example of this regime, the pyrolysis front is followed by an oxidation front and both propagate at very similar velocities. The pyrolysis front is characterized by a constant temperature (approximately 320°C) and its location is clearly determined by a period of time where the temperature remains almost constant, due to the endothermic nature of the pyrolysis reaction. The oxidation front is characterized by a decaying maximum temperature, from temperatures as high as 460°C, near to the ignition plane, to approximately 350°C , at the end of the sample. For air flow velocities larger than 6 mm/sec pyrolysis and oxidation fronts propagate at similar velocities throughout the sample, as the reaction reaches the end of the sample the oxidation front starts to propagate faster than the pyrolysis front followed by strong oxidation reactions occurring in the opposite direction (figure 4.16), at this point an oxidation front is hard to determine. For forced flow velocities of 14.10 mm/sec. (figure 4.17) a clear pyrolysis front

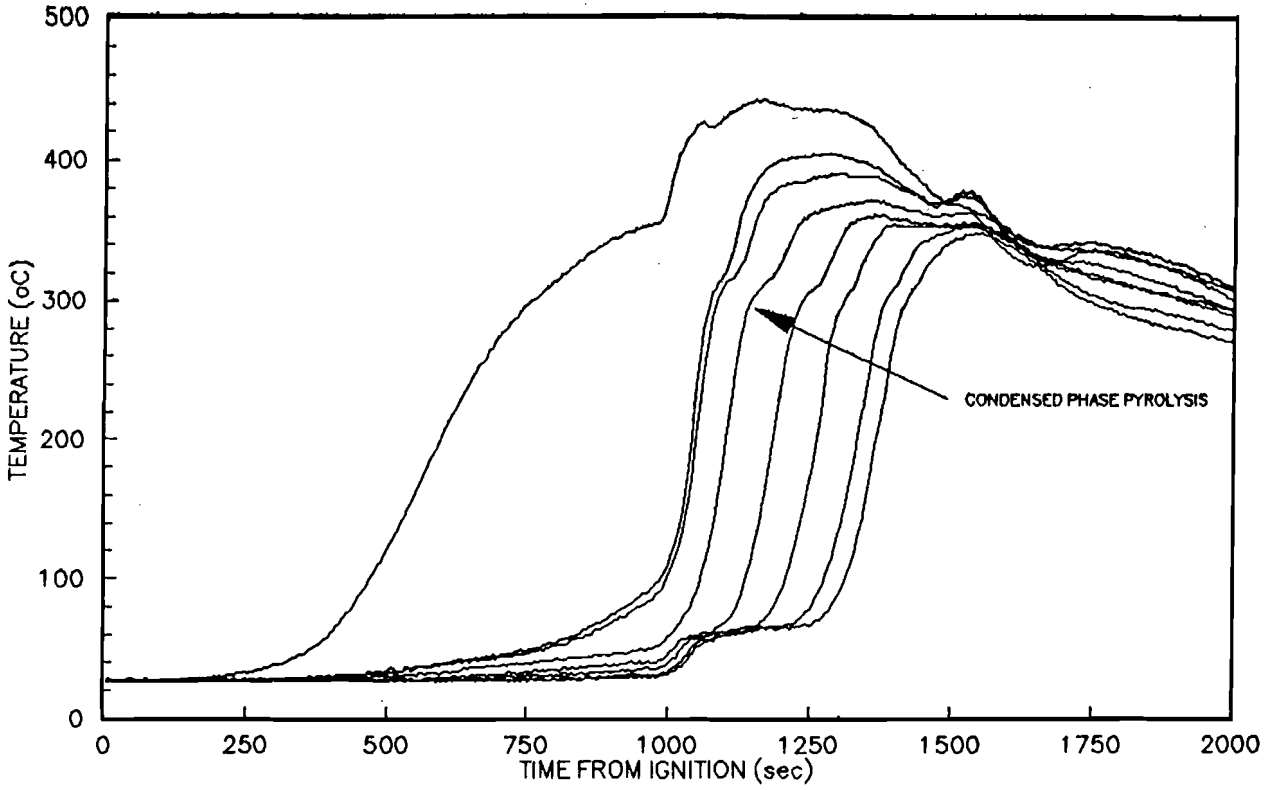

Figure 4.15 - Temperature histories for eight thermocouples, upward forward smoldering (flow rate 2.80 mm/sec). Thermocouples are not necessarily placed at a constant distance from each other. Clear evidence of pyrolysis appears in this figure, pyrolysis and oxidation fronts propagate at approximately equal velocities.

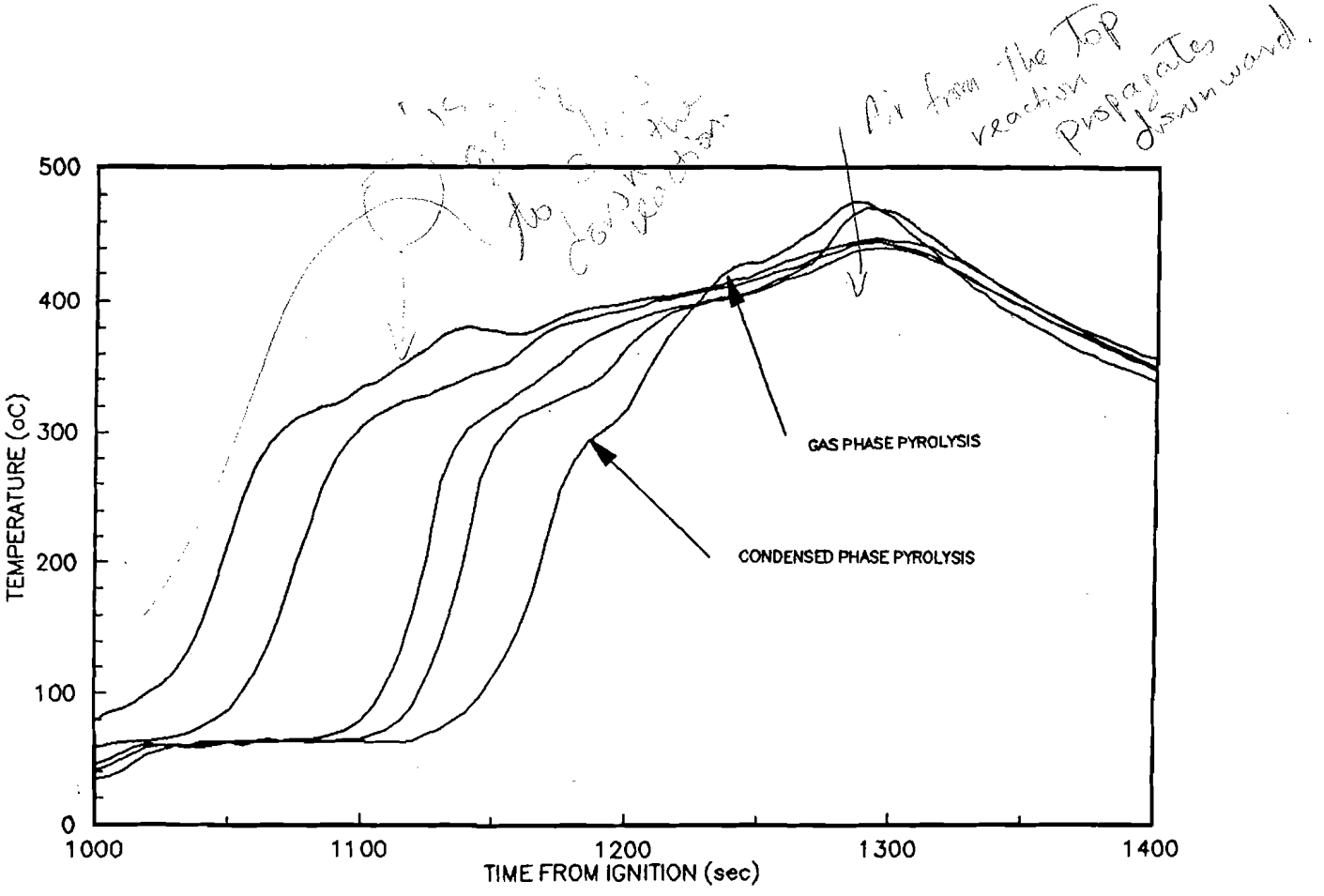

Figure 4.16 - Temperature histories for five thermocouples, upward forward smoldering (flow rate 7.80 mm/sec). Thermocouples are not necessarily placed at a constant distance from each other. The oxidation front velocity increases with respect to the pyrolysis propagation velocity as the reaction reaches the end of the sample.

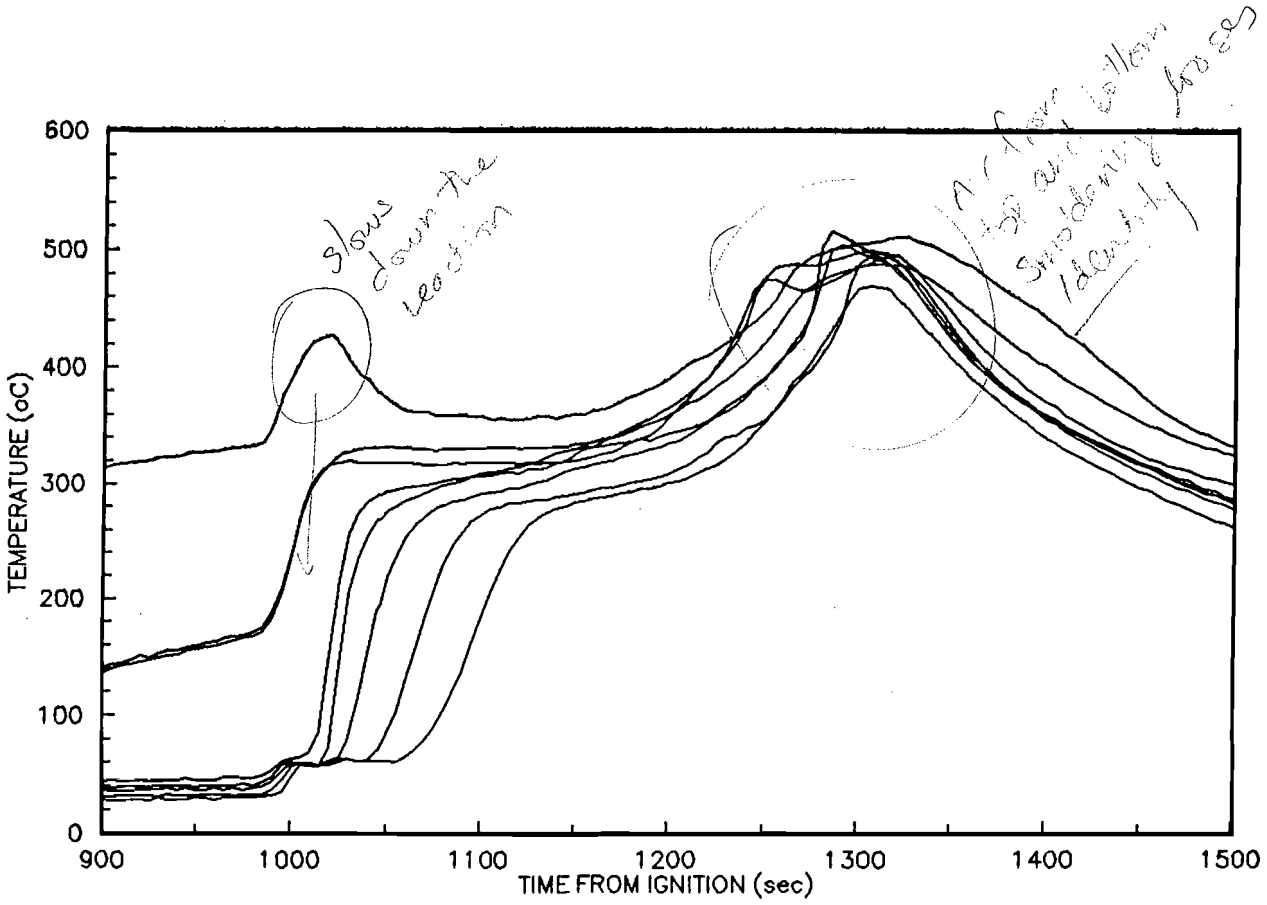

Figure 4.17 - Temperature histories for eight thermocouples, upward forward smoldering (flow rate 7.80 mm/sec). Thermocouples are not necessarily placed at a constant distance from each other. Simultaneous oxidation of the char occurs after the pyrolysis front has propagated through the whole sample.

propagates through the sample, oxidation occurs almost simultaneously throughout the char and no clear oxidation front can be identified, transition to flaming followed in most cases. Maximum temperatures are approximately 460-500°C, these values are significantly higher than characteristic smolder temperatures for polyurethane foam [1,3,15].

The variation of the upward smoldering propagation velocity along the foam sample length is presented in figure 4.18. Here also the three zones indicated above are used to describe the data. Zone II has almost constant velocities for small flow rates and the velocities in zone III increase as the smoldering front reaches the end of the sample. Smoldering and pyrolysis velocities have similar values for air flow velocities smaller than 7 mm/sec, for larger forced flow velocities smoldering velocities become larger than pyrolysis propagation velocities as both reactions move towards the end of the sample (figure 4.19). Pyrolysis propagation velocities show a weaker increase towards the end of the sample as the oxidation front becomes faster, for air flow velocities of 14.10 mm/sec, where simultaneous oxidation of the char is observed, pyrolysis velocities increase slower than for lower air flow velocities. In figure 4.20 it can be observed that for small flow velocities temperatures are constant through zones I and II and that as the flow velocity is increased temperatures are highest in zone I and decay through zones II and III for flow rates larger than approximately 1.5 mm/sec. Temperatures cease to decay towards the end of the sample for air velocities larger than 4 mm/sec, temperatures from then on are higher in zones I and III and remain almost constant through zone II.

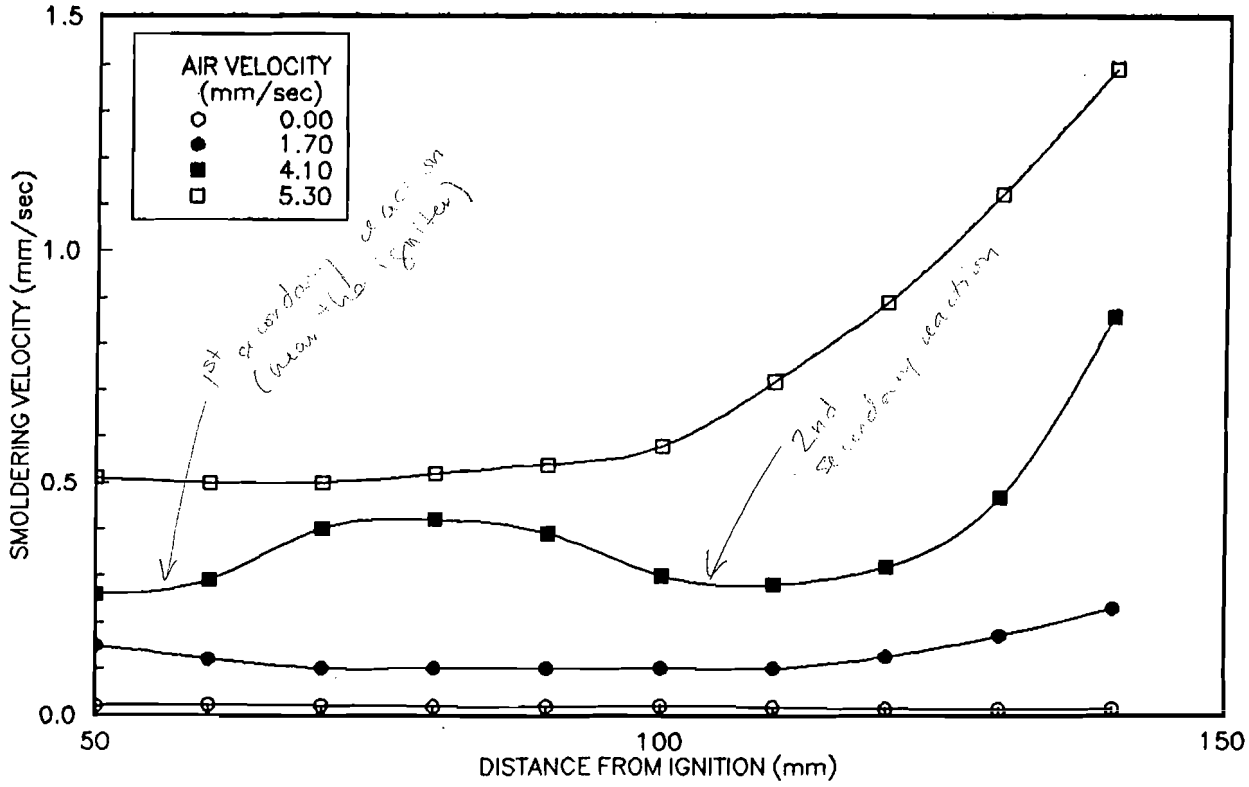

Figure 4.18 - Variation of the smolder propagation velocity along the foam sample for forward upward smolder. Experiments were conducted at several other flow rates but were not included to avoid crowding the figure.

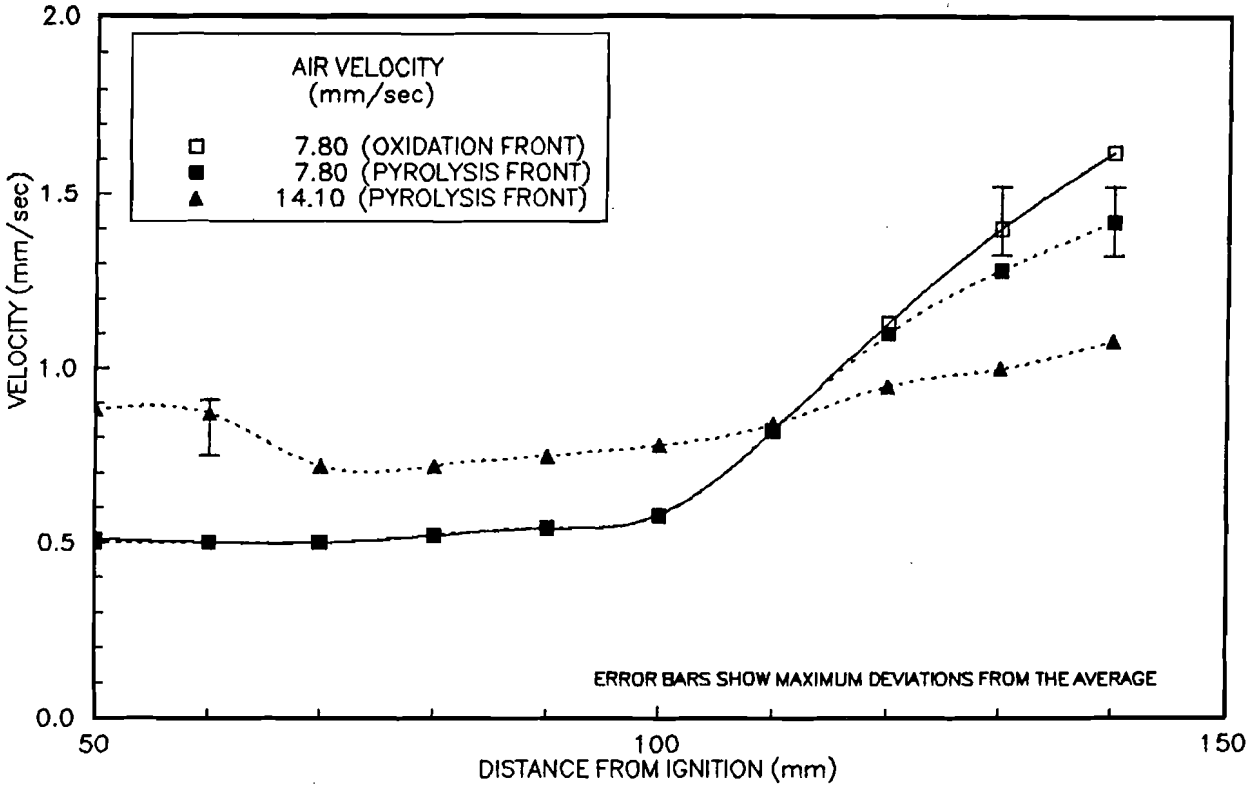

Figure 4.19 - Comparison between the pyrolysis and oxidation propagation velocities along the foam sample for forward upward smolder. For all other flow rates both velocities were almost equal.

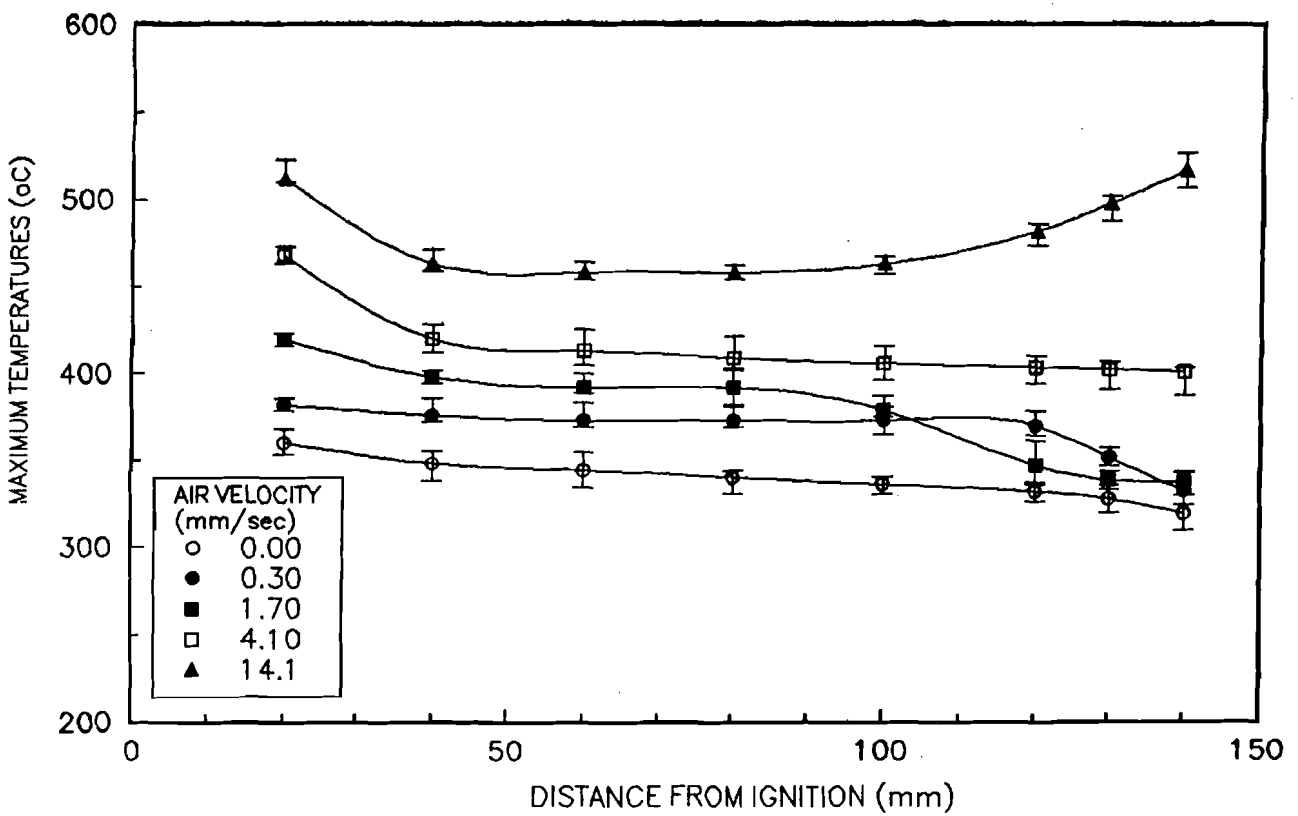

Figure 4.20 - Variation of the smolder reaction maximum temperature along the foam sample for forward upward smolder. Experiments propagated self-sustained for all air flow velocities.

The variation of the upward smolder velocity with the forced air flow rate is presented in figure 4.21 (a detail for low flow rates is presented in figure 4.10). From these figures it can be observed that for upward burning, velocities increase monotonically with flow rate and the initial region of extinction present in downward smolder does not appear. The variation of the maximum smoldering temperature is presented in figure 4.22, upward burning shows a monotonically increasing temperature. It has to be made clear that the values plotted in figures 4.10,4.21 and 4.22 are average values for the entire zone, therefore, even though they give extra insight on the process they might be misleading in the details of the problem.

4.4 Smoldering Model

The experimental results show that there is no single regime that describes the smoldering process for the entire range of forced flow velocities. Although several transition regimes have been observed three main regimes will be used to attempt a correlation of the experimental data. The theoretical model of forward flow smolder developed by Johnson et al.[51] is used in this work to correlate the above reported data for flow rates below 1.5 mm/sec, this model is a solution for forward propagation of an exothermic reaction in the absence of pyrolysis as a heat sink. A substantial simplification of assuming pyrolysis and smoldering propagation velocities to be equal is made for flow velocities greater than 1.5 mm/sec and smaller than 5 mm/sec. All the energy released by the oxidation reaction is used to heat the fuel to the pyrolysis temperature and to pyrolyze it. A schematic of this configuration is

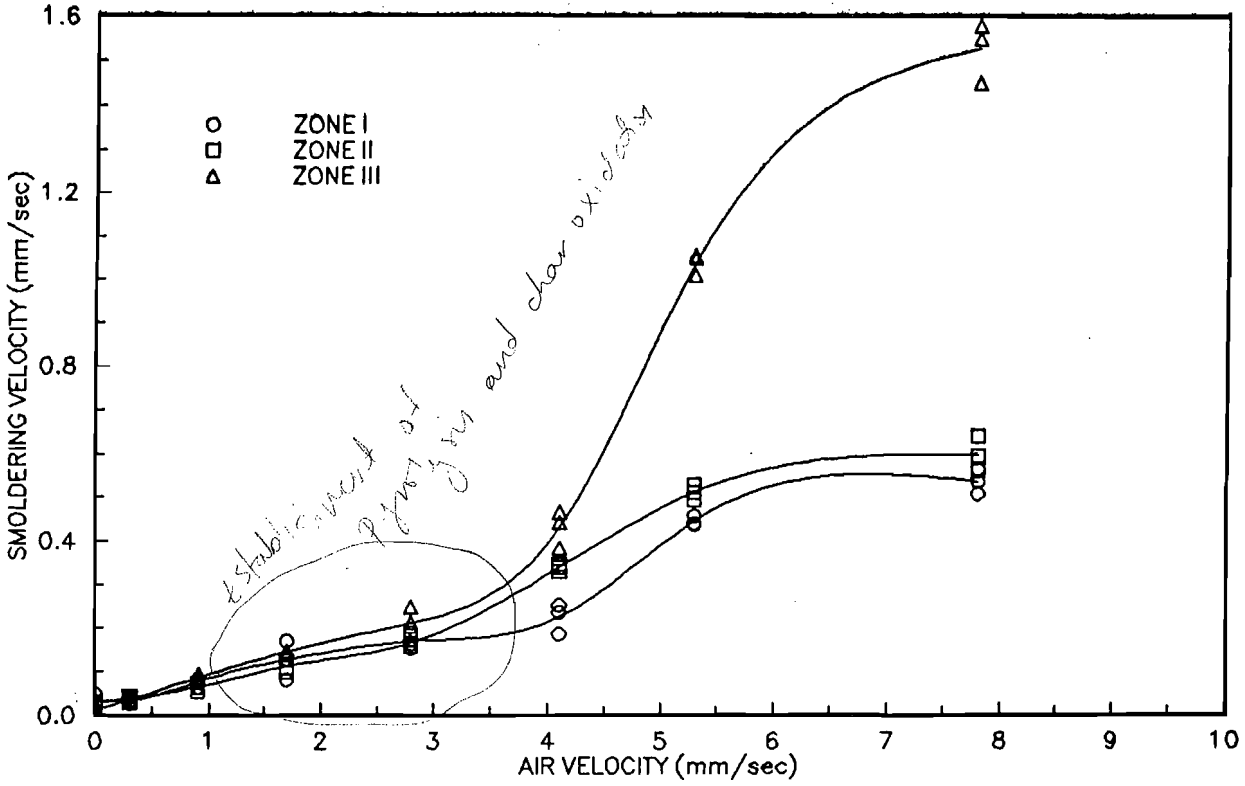

Figure 4.21 - Dependance on the forward air flow rate of the upward smolder velocity at three different sample zones. The values in this figure are averages of smolder propagation velocities at different locations within each zone.

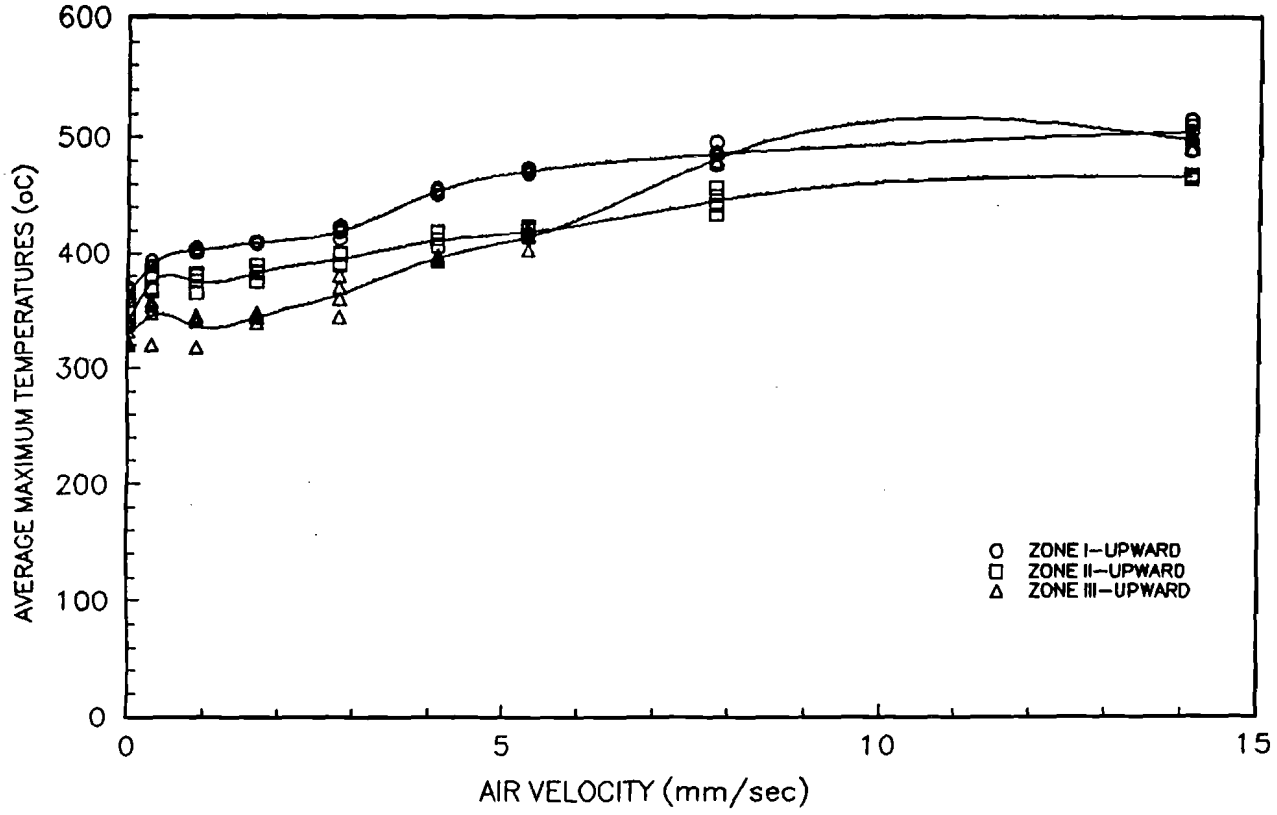

Figure 4.22 - Dependence on the forward air flow velocity of the maximum reaction temperature at three sample zones for upward smolder. The values in this figure are averages of maximum temperatures at different locations within each zone.

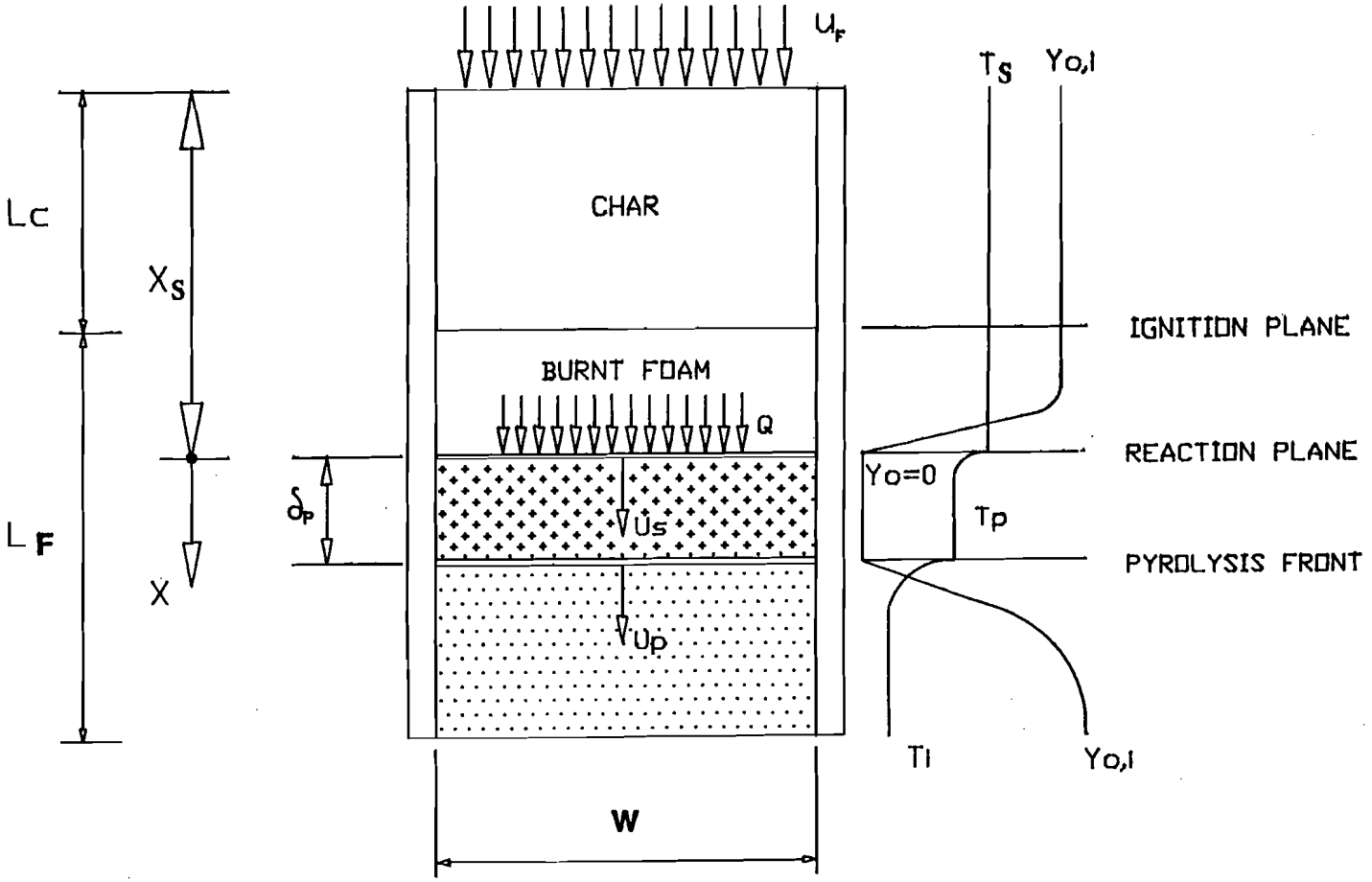

Figure 4.23 - Schematic of the char oxidation/condensed phase pyrolysis reaction from a frame of reference anchored with the oxidation front.

shown in figure 4.23. For air flow velocities greater than 5 mm/sec the assumption of equal pyrolysis and smoldering propagation velocities is no longer valid, therefore this model is not suitable. A theoretical model of forward flow smolder with no residual ash was developed by Dosanjh et. al.[5,8], this model assumes that all the char is consumed in before the oxidation front moves forward and that pyrolysis front propagates much faster than the oxidation front. Pyrolysis propagation velocities are in general equal or smaller than the propagation velocity of the oxidation front therefore this model is not suitable for this regime, furthermore, the oxidation front is not well determined, therefore, a correlation of the experimental results with any of the previously described models was considered inadequate for this air flow velocity range. To facilitate the understanding and discussion of the correlations, a brief description of the models is given here.

In forward smoldering, with frame of reference anchored at the oxidation zone, the fuel and oxidizer enter the reaction zone in the opposite direction. Since smoldering is generally oxygen limited, the heat released by the smolder reaction can be expressed in terms of the mass flux of oxidizer at the reaction zone. This heat is transported by conduction and radiation downstream of the reaction zone, and sustains the propagation of the smolder front, for flows below 1.5 mm/sec and the pyrolysis and smolder fronts for flows above that value. It should be noted that the fuels of interest in smolder are very porous, and consequently conduction is a relatively poor mode of heat transfer [12]. Thus radiation heat transfer is important despite the relatively small temperatures encountered in smoldering combustion.

In the model of Dosanjh et al.[5,8] opposed smoldering is modeled as a finite rate, one-step reaction, of the form

$$\nu_F[\mathrm{FOAM}] + \nu_O O_2 \rightarrow \nu_{CH}[\mathrm{CHAR}] + \nu_{gp}[\mathrm{GaseousProducts}] + Q\nu_O M_O \qquad (4.1)$$

This reaction seems to be the one that describes best the process for flow velocities smaller than 1.5 mm/sec. For forward smoldering Dosanjh [5,8] proposes a two step reaction of the form

$$\begin{gathered} \nu_F[\mathrm{FOAM}] + Q_p \nu_F M_F \rightarrow \nu_{CH}[\mathrm{CHAR}] + \nu_{gp1}[\mathrm{GASPRODUCTS}] \\ \nu_{CH}[\mathrm{CHAR}] + \nu_O O_2 \rightarrow \nu_{gp2}[\mathrm{GASPRODUCTS}] + Q\nu_O M_O \end{gathered} \qquad (4.2)$$

This reaction will be used for flow velocities above 1.5 mm/sec. The stoichiometries for these reactions are obtained from Summerfield and Messina [2].

Smoldering is assumed to be one-dimensional and steady in a frame of reference fixed to the smolder wave (figure 4.23). The gas and solid are presumed to be in local thermal equilibrium , and the solid phase is considered continuous with a constant void volume fraction. Energy transport due to concentration gradients, energy dissipated by viscosity, work done by the body forces, and the kinetic energy of the gas phase are ignored. It is assumed that the pyrolysis reaction occurs at a constant temperature [5,8]. Furthermore, since smoldering velocities are much smaller than flow velocities, flow velocities can be taken as known quantities at each location in the sample, x_S.

With the above assumptions, and neglecting heat losses to the environment, the one dimensional form of the energy conservation equation becomes

$$(\dot{m}_F'' Cp_F + \dot{m}_A'' Cp_A)\frac{dT}{dx} = (\lambda_{eff} + \lambda_{rad})\frac{d^2T}{dx^2} + Q\frac{d\dot{m}_O''}{dx} \qquad (4.3)$$

where the mass fluxes of fuel and oxidizer entering the reaction zone are given by,

$$\dot{m}_F'' = (1-\phi)\,\rho_F U_S$$

$$\dot{m}_A'' = \rho_A (u_g - U_S) + \rho_A \phi U_S$$

$$\dot{m}_O'' = Y_O \dot{m}_A'' - \phi \rho_A D \frac{\partial Y_O}{\partial x}$$

λ_{eff} is an effective thermal conductivity of the form

$$\lambda_{eff} = \phi\lambda_A + (1-\phi)\,\lambda_F$$

Radiation is incorporated in the analysis using a diffusion approximation with an equivalent thermal conductivity given by

$$\lambda_{rad} = \frac{16\sigma d_p T^3}{3}$$

The boundary conditions for the above equation are

$$\text{at} \quad x=x_s \qquad \frac{\partial T}{\partial x}=0$$

$$T=T_s$$

$$\dot{m}_O''=0$$

$$\text{at} \quad x=x \qquad \frac{\partial T}{\partial x}=0$$

$$T=T_i$$

$$\dot{m}_O''=\dot{m}_{O,i}''$$

Integrating with respect to x from x_s to ∞ , the following expressions are obtained for the smolder propagation velocity

$$U_S=\frac{\rho_A Q Y_{O,i}}{[\rho_A Cp_A \phi+\rho_F Cp_F(1-\phi)](T_S-T_i)+(1-\phi)Q\rho_A Y_{O,i}}u_g \qquad (4.4)$$

$$\text{for} \quad 0\le u_g \le 1.5\text{mm/sec}$$

$$U_S=\frac{\rho_A Q Y_{O,i} u_g}{[\rho_A Cp_A \phi+\rho_F Cp_F(1-\phi)](T_S-T_i)+[Q_p\rho_F+Q\rho_A Y_{O,i}](1-\phi)} \qquad (4.5)$$

$$\text{for} \quad 1.5\text{mm/sec}\le u_g \le 5.0\text{mm/sec}$$

The analysis of Dosanjh et al.[5,8] also provides an expression for the smolder temperature T_S. However, the asymptotic analysis leading to that expression imposes a number of restrictive conditions that are often not applicable to the experiments. For this reason, in this work the value of the smolder reaction

temperature is obtained from the experimental data of figures 4.8 and 4.20. For these experiments the initial temperature varies with time, therefore the value of the initial temperature is obtained from the temperature histories. The heat of combustion Q is the same as for all previous chapters. Finally, the oxidizer velocity u_g, is the forced flow of oxidizer plus the contribution from the air in the foam pores. Significant buoyantly induced flows can only occur in the char, therefore, from figure 4.1 it can be observed that the virgin foam from one side and the controlled mass flow meter from the other prevent any addition of air to the reaction zone, other than the forced flow. However, the data from figure 4.10 and transition to flaming only occurring in upward burning provide enough evidence that under normal gravity conditions, buoyancy induced flows are important as a means of oxidizer transport to the reaction zone. Thus, the potential generation of buoyant flows inside the char requires the treatment of the flow through the foam as a mixed, forced and free, flow problem. This is done in the following section.

4.5 Flow Induced Through the Polyurethane Foam

The onset of buoyant flows inside a porous media depends strongly on the permeability of the material [14]. The polyurethane foam used in the present experiments has a relatively low permeability in spite of the high void fraction, and no buoyant flows are expected to be generated inside the foam unless a chimney type, natural draft, is induced by the hot post-combustion gases. However, the char left behind by the propagating smolder reaction is quite permeable, and buoyant

recirculation flows can be easily generated up-stream from the smolder front. The permeability of the char depends on the strength of the smolder reaction, because more of the fuel is consumed when the reaction is vigorous, and on the char structure itself. This is reflected in the measured dependence of the char permeability on the forced flow velocity for downward smolder that is presented in figure 4.24. Since increasing the forced velocity enhances the smolder reaction (figures 4.6 and 4.18), the char permeability also increases. The increase however its not linear because at small flow rates the char keeps its structure [3], but as the smolder reaction strengthen the filaments that form the micro-structure of the foam break down [5,8], thus resulting in a sudden increase in the permeability as it is seen in figure 4.24. The recirculating flow in the char region is induced by the natural convection boundary layer that is generated at the tests section walls by the difference in the wall and char/post-combustion gases temperatures. A schematic of these recirculating flow is shown in figure 4.25. In downward smolder, cold air flows downward along the cold walls of the char region toward the reaction zone where it encounters the unburned foam that since it has a much smaller permeability prevents the air from flowing through. Instead, the air turns around at the reaction zone and moves upward along the duct centerline opposing the gases being forced through the duct by forced convection, therefore, air is being pushed towards the walls decreasing the total flow near the sample centerline (opposing flow). For upward burning the cold air moves down the walls and upward along the duct centerline in the same direction of the forced flow, therefore, flow is being

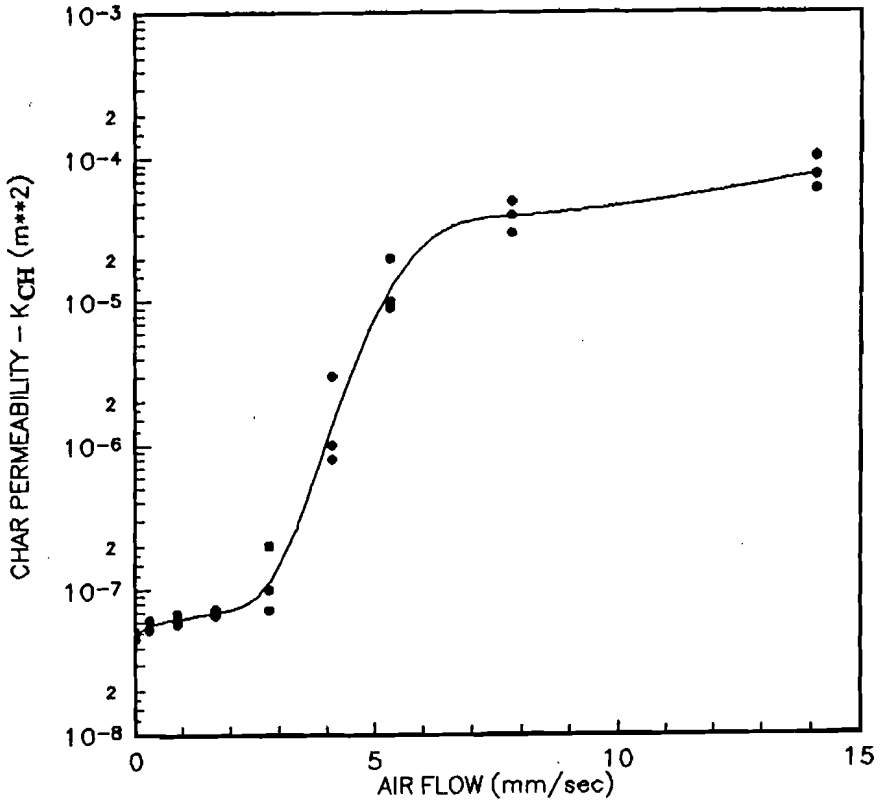

Figure 4.24 - Variation of the average char permeability with the air flow velocity.

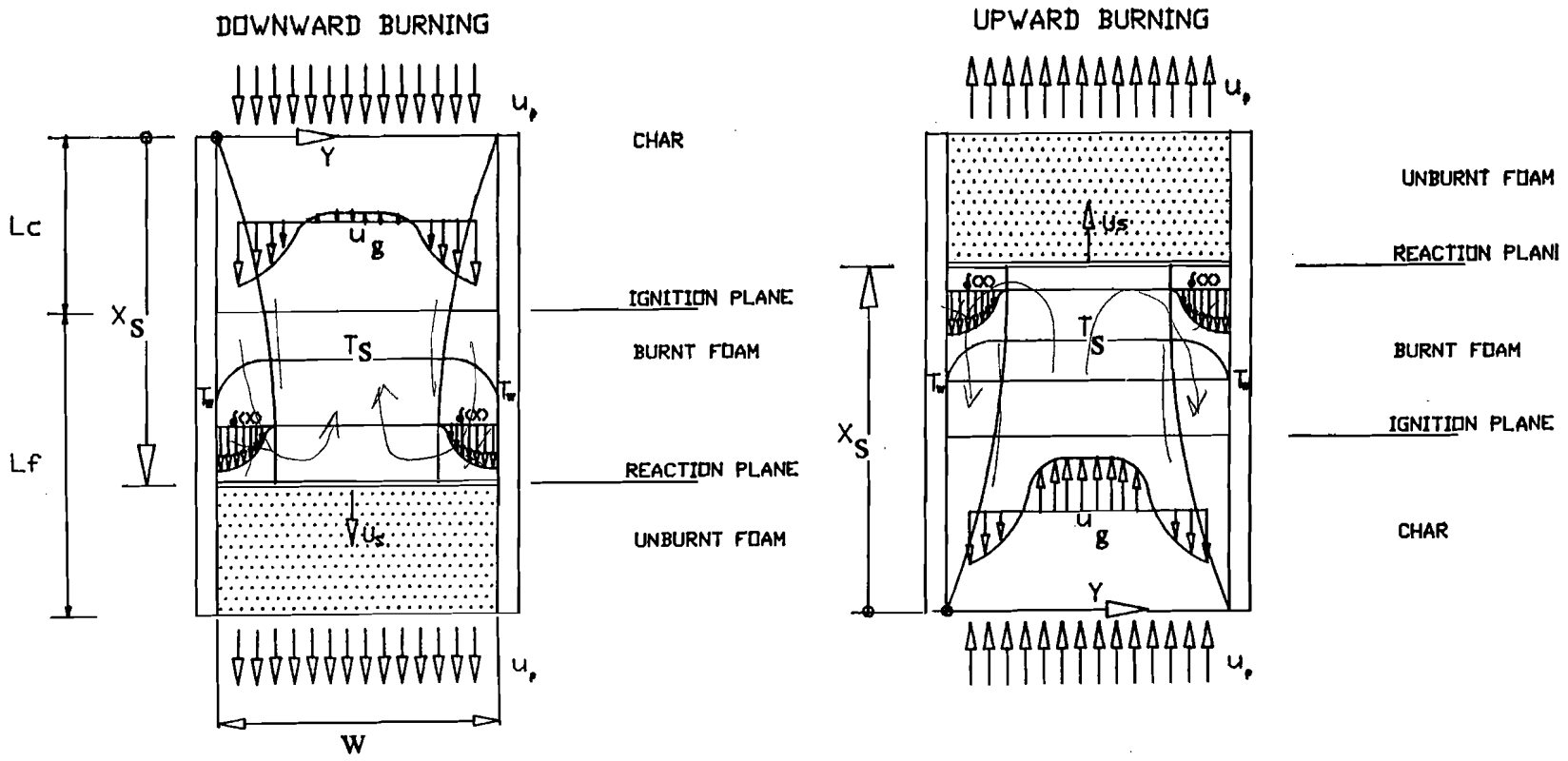

Figure 4.25 - Schematic of the flow field inside foam and char during a forward smoldering reaction for upward (aiding flow) and downward burning (opposing flow) configurations.

forced through the sample centerline and away from the walls (aiding flow).

Few works have been conducted on the mixed, free and forced, flow in a porous media. The analysis developed here is based on the works of Burns et.al. [57], Bejan [14], Lai et al. [63], Hadim and Govindarajan [64] and Nield and Bejan [55]. In natural convection, an asymptotic solution for buoyantly induced flows in vertical ducts has been developed by Burns et. al. [57]. For the mixed flow problem, in the char, for upward burning, forced and buoyantly induced flows add at the centerline (aiding flows), while for downward burning, the flows oppose at the centerline region (opposing flows). A numerical analysis of the problem [63] shows that for aiding flows the mixed flow solution is valid for values of the Ra/Pe smaller than 50, for values greater than 50 the solution resembles more the pure natural convection solution. For downward smolder (aiding flow) and for the present experimental conditions it is found that for flow rates smaller than 1 mm/sec, the Ra/Pe is larger than 50. Thus, the natural convection solution prevails for air velocities smaller than 1 mm/sec, and the mixed convection solution for greater air velocities. For upward smolder (opposing flows), the mixed flow solution is found to give a more accurate description of the problem for values of Ra/Pe smaller than 500, which covers the whole range of flows used in the present experiments. Below, a summary is given of the mixed and natural convection flow analyses used in this work to derive the air velocity to be imputed in equations 4.4 and 4.5.

4.5.1 Mixed Convection Conditions

In the analysis it is assumed that the convective fluid and the porous medium are everywhere in thermodynamically equilibrium, that there is no phase change in the solid, and that the properties of the fluid and the porous medium are homogeneous and isotropic. With the governing equations of mass, momentum and energy, and applying Darcy's Law together with the Boussinesq approximation, the following expression is obtained for the flow averaged velocity along the center region of the foam [13,55]

$$u_b = \frac{2\delta}{W}\left(\frac{Gr_K}{Re_k}\right) u_f \qquad (4.6)$$

with

$$\delta = x\, Ra_x^{-0.5}$$

$$Re_K = \frac{\rho_A u_f K_{CH}^{0.5}}{\mu}$$

and $$Gr_K = \frac{K_{CH}^{1.5} g \rho_A^2 \beta (T_W - T_S)}{\mu^2}$$

4.5.2 Natural Convection Boundary Layer Solution

The natural convection problem has been studied extensively [14,55,56,57]. Particularly relevant for the present work is the analysis of Burns et. al. [57] for buoyantly induced flows in vertical ducts with different temperature walls. Application of that analysis to the present problem gives the following expression

for the averaged flow velocity at the char centerline

$$u_b = \frac{\alpha Ra_x}{4W} \qquad (4.7)$$

with

$$Ra_x = \frac{K_{CH} g \rho_A \beta (T_W - T_S) x}{\alpha \mu}$$

4.5.3 Diffusion of Oxidizer into the Reaction Zone

Another possible transport mechanism of oxidizer to the reaction zone is by diffusion from the external environment through the char. From the governing species conservation equation, the following characteristic diffusion length is deduced

$$\delta_D = \frac{D}{u_f + u_b + \phi U_S}$$

For the present experimental conditions it can be shown that this characteristic length is much smaller than the characteristic length of the problem, and that consequently diffusion can be neglected as a transport mechanism in this problem when compared to the forced and natural convection flows.

4.5.4 Overall oxidizer transport to the reaction zone

From the above analysis, and in a frame of reference anchored at the

reaction zone, it is deduced that the overall transport of oxidizer to the reaction zone is given by an overall velocity that includes the forced flow velocity, u_f, as given by the test condition and the smolder velocity times the void fraction, to account for the oxidizer that is contained in the foam pores and that enters the reaction zone as it progresses through the sample. Thus, this velocity is given by

$$u_s = u_f + \phi U_s \qquad (4.8)$$

which is then used in equations 4.4 and 4.5 to correlate the smolder velocity experimental data.

4.6 Data Correlation

In this section, equations 4.4 and 4.5 for the smolder velocity together with the forced air velocity, are used to correlate the forward smolder velocity data obtained in the present experiments. The values of the fuel and oxidizer properties used in the equation are given in table 2-1. The results of the correlation of the smolder velocity data of figure 4.6 and 4.18 is presented in figure 4.26 for air flow velocities lower than 1.5 mm/sec and in figure 4.27 for air flow velocities higher than 1.5 mm/sec and lower than 5 mm/sec.

From figure 4.26 it can be observed that equation 4.4 predicts well the smoldering velocity. The oxygen concentration used is that to obtain the best agreement between theory and experiments. For equation 4.4, $Y_{O,i}=0.188$ which is lower than the oxygen mass fraction of air, this is understandable, since the fresh air moves through the hot char before reaching the reaction zone; even though weak,

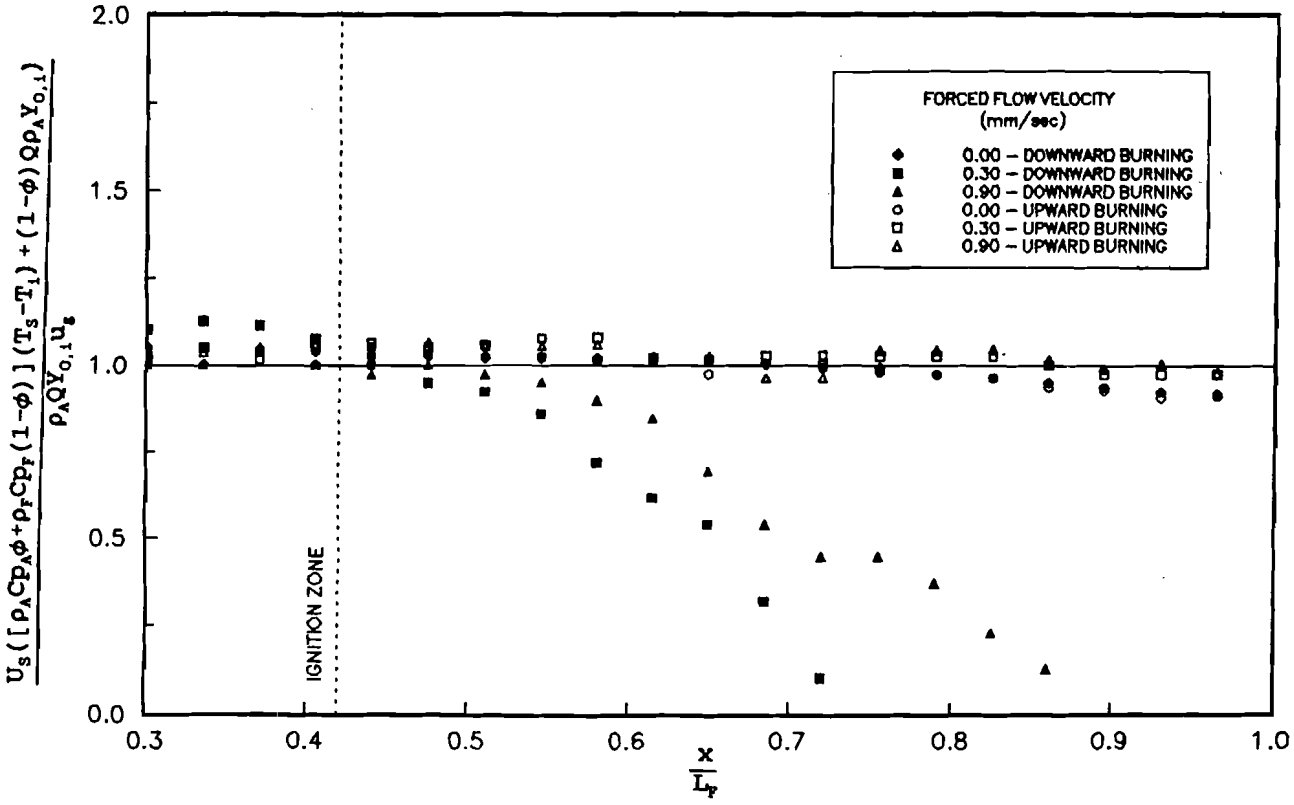

Figure 4.26 - Correlation of experimental and theoretically predicted smoldering propagation velocities for different air flow velocities at different locations in the sample. Air flow velocities smaller than 1.5 mm/sec. Experiments conducted for forced flows of 0.30 and 0.90 mm/sec in downward burning configuration extinguished.

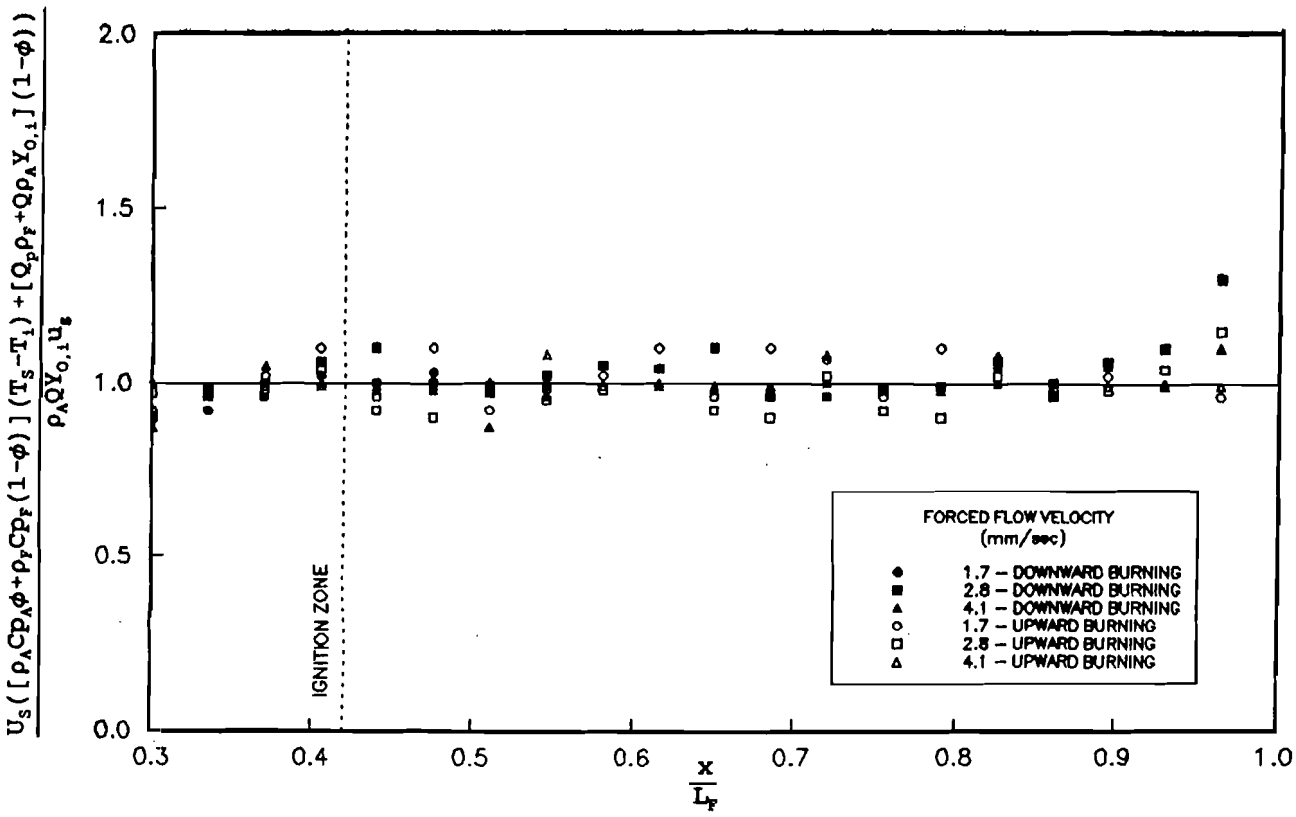

Figure 4.27 - Correlation of experimental and theoretically predicted smoldering propagation velocities for different air flow velocities at different locations in the sample. Air flow velocities greater than 1.5 mm/sec and smaller than 5.0 mm/sec.

the air is expected to react with the char diminishing the oxygen concentration of the gases reaching the reaction. Analysis of the composition of the gases reaching the reaction zone could corroborate this assumption, unfortunately all attempts were unsuccessful because the tars resulting from the reaction tend to clog the sampling lines. As mentioned above for flow velocities of 0.30 and 0.90 mm/sec downward burning experiments extinguished, and under extinguishment conditions the model does not predict very well the results, since the model assumes fast chemistry and that the energy released by the reaction is sufficient to heat up the fuel to its smolder temperature, if the flux of oxidizer is not large enough to ensure a strong reaction then it is expected that the model cannot predict correctly the experimental measurements. For flow velocities between 1.5 and 5 mm/sec (figure 4.27) it is seen that the model predicts very well all the different data, verifying that when the smolder process is vigorous and self-sustained it is controlled primarily by the transport of oxidizer to the reaction zone and the transfer of energy form the reaction zone to the virgin fuel ahead. For this flow velocities, the char oxidation reaction consumes most of the fuel therefore oxygen depletion by the reaction between the incoming air and the char left upstream of the oxidation reaction is not significant.

4.7 Discussion of the Results

The above results point out to a smolder process of very different characteristics for different flow velocities, from a weak smoldering reaction in the

virgin foam, for low flow rates; to a steady condensed phase pyrolysis supported by an oxidative reaction of the char, for intermediate flow rates, to a very strong oxidation of the char, that almost completely consumes all the fuel, supporting a condensed phase pyrolysis that eventually will lead to a gas phase pyrolysis that could result in transition to flaming, for high flow rates.

Forward smoldering combustion is an oxygen starved process [1], therefore for low flow velocities, the process is weak and the competition between the two controlling mechanisms, chemical kinetics and heat transfer [1] is important. In smoldering the heat transfer from the smoldering reaction to the adjacent material, and the oxygen supply to the reaction zone are the two main mechanisms that control the smolder reaction characteristics [1,4,53]. In the forward flow configuration heat is being carried away from the reaction zone towards the virgin foam by the flow after passing through the char. As a consequence the heat transferred to the virgin fuel is enhanced as the flow rate is increased, which favors the propagation of the smolder reaction. The oxidizer transport effect of the forced flow is two fold; increasing the flow rate increases the oxygen supply to the reaction zone, on the other hand the products of combustion are carried into the virgin foam mixing with the oxidizer inside the pores generating a zone of low oxygen concentration that in the presence of enough heat will undergo a pyrolysis reaction. Furthermore, the oxidizer is reaching the reaction zone through the char which while preheating the air may also cause oxygen depletion due to char oxidation. The fresh oxidizer moving through the char will encounter hot char that will be readily oxidized

depleting the oxygen, and due to heat transport from the reaction zone to the virgin fuel; by conduction, radiation and convection of the hot post-combustion gases, will generate, for certain cases, a pyrolysis front ahead of the oxidative reaction. The final characteristics of the smolder reaction in a given case depend on the relative importance of each one of these effects.

For forward smoldering no simple argument can describe the process for all flow rates. For very small flow rates smoldering propagates through the virgin fuel leaving a weakly reacting char behind that does not entirely deplete the oxidizer incoming with the forced flow, and does not produce enough energy to sustain pyrolytic decomposition of the foam. The flow field established by the combination between buoyantly induced boundary layer flow and forced flow is very significant. A favorable distribution of the flow field (upward burning) will result in self-sustained smoldering, and an unfavorable distribution will result in extinction (downward burning). From the point of view of the smolder reaction, for these flow rates, in downward burning, buoyant recirculations and forced flow almost cancel out near the centerline of the sample (figures 4.25 and 4.28), driving the oxidizer towards the walls, which are more susceptible to heat losses to the environment, slowing down the chemistry leading to extinction, instead in upward burning the post-combustion gases are being pushed through the reaction near the sample centerline pre-heating the virgin fuel and resulting in an enhancement of the reaction.

As the flow rate is increased the char behind the smoldering front undergoes a stronger oxidation reaction depleting the oxidizer from the forced flow and

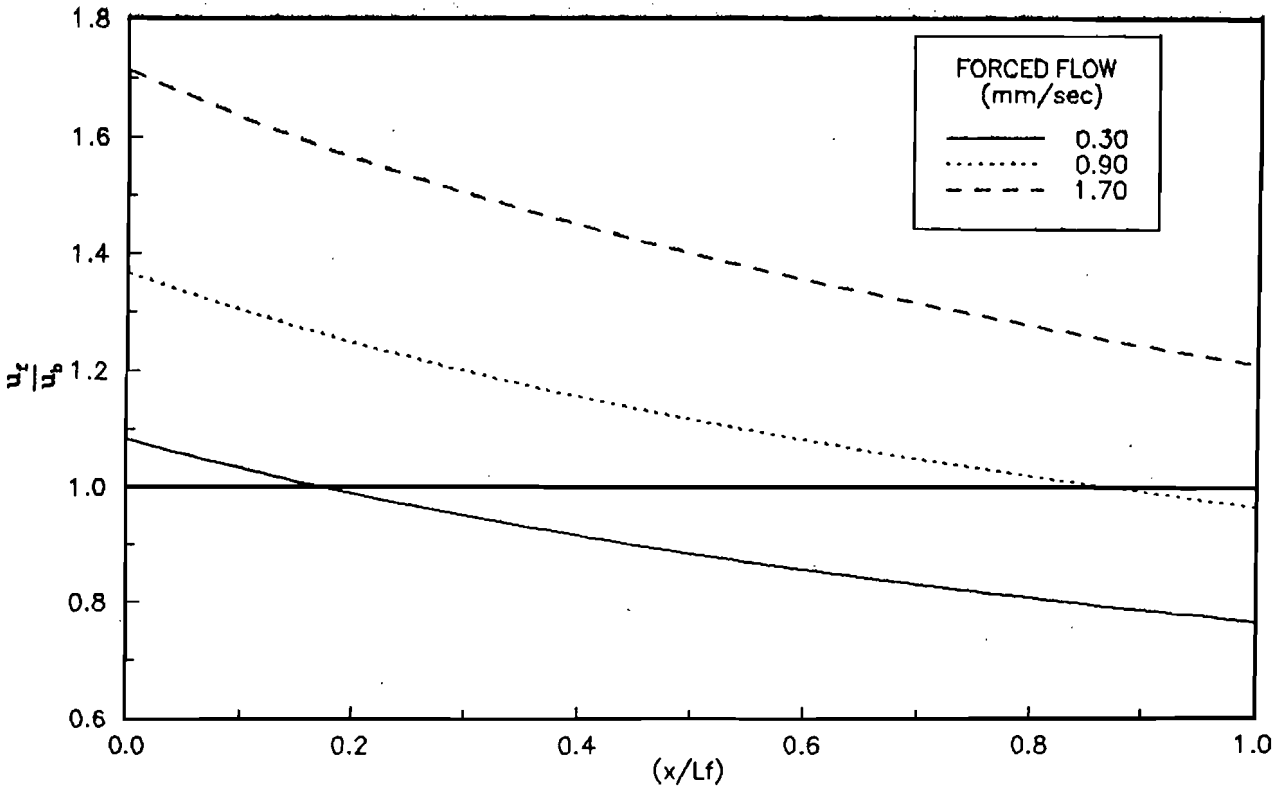

Figure 4.28 - Variation of the forced flow/buoyantly induced average flow ratio for different forced flow velocities and locations in the sample. The forced flow and average flow induced by the boundary layer are of the same order for these small flow rates.

producing enough heat to change the pathway of the reaction from smoldering to condensed phase pyrolysis [1,3,4]. Chemical decomposition of polyurethane foam can choose two possible pathways, an oxidative charring reaction (smoldering) or a non-oxidative tarring reaction (condensed phase pyrolysis), for the latter to occur oxygen concentrations have to be low and since pyrolysis is endothermic, heat has to be provided for the reaction to propagate. Oxidation of the char is characterized by strong energy release, therefore temperatures are higher than those obtained during the smoldering of the virgin foam. The enhancement of this char oxidation results in a strong heat release and the depletion of the oxidizer reaching the virgin fuel, therefore smoldering dies and is substituted by condensed phase pyrolysis supported by char oxidation. All the energy provided by the oxidation of the char is used to pyrolyse the foam, therefore a region of no temperature increase is observed. The exact pyrolysis temperature is not well known, but there is extensive literature that coincide in placing it in a range between 300 to 320°C [1,3,4,5,8], similar values can be observed in figures 4.4, 4.14, 4.15 and 4.16. Pyrolysis propagation velocity and the char oxidation velocity are approximately equal. For this range of flow rates a significant amount of char is still left behind the oxidation front, which acts as insulation for the reaction allowing the assumption that all the heat generated by the oxidation of the char is transferred to the pyrolysis front. As the reaction propagates through the sample the temperature of the foam ahead increases, therefore the energy needed to increase the temperature to the pyrolysis velocity decreases resulting in an increase of both pyrolysis and char oxidation propagation velocities.

At this stage the reaction is very strong, therefore the importance of the buoyantly induced recirculation currents decreases and figure 4.9 and 4.21 show almost no difference for this air flow velocity range. The recirculating flow does not provide any extra oxidizer, to the reaction, thus, its significance decreases as the reaction strengthens, but the magnitude of this recirculation flow never decreases in importance with respect to the forced flow, since the permeability of the char increases with the flow rate (Figure 4.24).

The importance of buoyancy is seen again at very high flow rates, near the end of the sample, where buoyantly induced flows can bring fresh oxidizer from the outside resulting in transition to flaming only for the upward burning case. The temperatures inside the foam are high enough to sustain gas phase pyrolysis, therefore the restrictive factor for transition to flaming is lack of oxidizer, so the structure of the flow becomes of extreme importance. Thus, for very large flow rates (above 7.8 mm/sec) downward and upward burning behave differently. For downward burning, an increase in the air supply to the oxidation reaction occurring in the char results in an increase in the propagation velocity of the oxidation front, the oxidation front approaches the pyrolysis front until only one front can be identified. When the air flow is started after ignition is completed, the oxidation front accelerates until it approaches the pyrolysis front. For air flow velocities smaller than 7.8 mm/sec the oxidative reaction propagates leaving residual char behind, for flow rates larger than 7.8 mm/sec, the oxidative reaction seems to alter its stoichiometry to burn all the fuel available. Thus, for flow velocities smaller than

7.8 mm/sec heat transfer is the controlling mechanism, the reaction propagates as fast as the fuel temperature can be increased to the reaction temperature, for higher flow rates, total fuel consumption is the controlling parameter, therefore, the reaction will propagate as soon as enough oxidizer has reached the reaction zone to burn entirely the fuel available, the result of this change is a slower increase in the propagation velocity of both oxidation and pyrolysis fronts. For upward burning the whole sample undergoes pyrolysis before oxidation occurs, an initial oxidative reaction near the igniter provides enough heat to sustain pyrolysis through the sample, pyrolysis propagation velocities therefore do not increase as strongly for flow rates larger than 7.8 mm/sec. Reverse oxidation reactions in zone III are a result of oxidizer reaching the reaction from the outside. For downward burning buoyant flows and forced flow tend to cancel near the sample centerline, resulting in a minor increase in the oxygen supply to the reaction; for upward burning forced and buoyant flows add near the sample centerline, resulting in a mayor increase in oxygen supply to the reaction leading to transition to flaming.

4.8 Conclusion

By studying the effect of a forced flow of oxidizer on smoldering reaction propagating downward and upward through a high void fraction porous fuel, the present work has helped to identify the controlling mechanisms of forward smoldering combustion, and to determine the potential importance of buoyancy on the process. Particularly interesting is the verification that in this type of smoldering,

the competition between oxygen supply and heat transport determines, in conjunction with the initial state of the reaction, the fate of the smolder reaction. Heat transport mechanisms are always favorable in this type of smoldering, but even under this favorable conditions lack of oxidizer can lead to weak reactions and even to extinction.

Chemistry is a significant parameter in forward smoldering; parameters of the problem such as oxidizer availability determine the pathway of the chemical reaction. High energy supply and low oxygen concentrations favor condensed phase pyrolysis; high oxygen supply favors oxidation. A pyrolysis front is evident for forced air flow velocities larger than 1.5 mm/sec. For forced air flow velocities smaller than 1.5 mm/sec there is no evidence in the thermocouple histories of such a reaction.

The post-combustion products transport heat from the reaction to the fuel , therefore heat accumulates in the foam as the reaction propagates through the sample, resulting in an unsteady reaction that under the appropriate conditions might lead to transition to flaming, which could be observed only in upward burning for forced air flow velocities greater than 14 mm/sec.

The role of buoyancy in this process is unclear but its influence extends to all forced air flow velocities studied, the range was limited by transition to flaming. Buoyant flow does not bring any extra oxidizer to the reaction for this configuration, therefore, the influence of buoyancy on the reaction have to be attributed to the changes that buoyant flow impose in the forced flow field moving through the char. For low forced air flow velocities the reaction extinguishes only in the downward

burning configuration. The different characteristics of the flow field in the char for downward (opposing flow) and upward burning (aiding flow) determine the fate of the reaction for this low flow rates. As the forced air flow velocity increases the reaction strength increases, and although the relative magnitude of the buoyantly induced flow with respect to the forced flow does not decrease its influence on the reaction disappears. For flow rates higher than 14 mm/sec transition to flaming only occurs in upward burning, therefore, for this forced air flow velocity range, enough oxidizer can only reach the reaction when buoyant and forced flow aid.

The coupling between oxidizer transport, permeability changes, buoyancy, reaction pathway and heat transfer mechanisms not allow for a good quantitative correlation of the experimental data.

Chapter 5
VARIABLE GRAVITY NATURAL CONVECTION EXPERIMENTS

5.1 Introduction

An experimental study is conducted to determine the effect of gravity changes on the smolder characteristics of flexible polyurethane foam, smoldering in natural convection. Gravity, and consequently buoyancy, is expected to affect smoldering because it induces convective transport of mass and heat, to and from the reaction zone. The overall objective of the work is to provide information about the potential onset of a smolder-initiated fire in a space-based facility. Experiments are conducted in an aircraft following a parabolic trajectory (KC-135A (NASA 930) and Learjet Model 25) that provides up to 25 sec of low gravity for the KC-135A and 20 sec for the Learjet Model 25, with a pull-up and pull-out of approximate 2 g's per parabola. Although the variable gravity periods are too short to study smolder propagation, they allow the observations of trends in the smolder reaction temperature aiding understanding how gravity affects smoldering. Measurements are performed, during a series of parabolas, of the temperature histories of the polyurethane foam at several locations along the fuel sample, both for upward and downward propagation. The measurements show that gravity plays a significant role in the competition between the supply of oxidizer to, and the transfer of heat to and from the reaction zone. It is found that within the reaction zone, the supply of oxidizer is dominant in downward smolder, and that the smolder temperature decreases at low gravity for lack of oxidizer. Away from the reaction zone there is a temperature increase at low

gravity because of the reduction in buoyantly induced convective cooling. The opposite is observed at high gravity. Similar mechanisms are observed in upward smoldering, although here high gravity results not only in an increase in the smoldering temperature but also an increase in the temperature of the fuel ahead of the reaction. This is either, because of the increase in the flow of hot post-combustion gases ahead of the reaction zone, the extra heat generated by secondary reactions occurring in the char, or the reduction in convective cooling.

Considerable amount of work has been conducted to date on smoldering; reviews on the subject can be found in the works of Ohlemiller [1] and Drysdale [70]. Not much attention has been given, however, to the effect of buoyancy on the process. Dosanjh et. al.[5,6] and Newhall et. al.[23], studied the effect of buoyancy on downward smoldering of cellulose by varying the ambient pressure. The former found that the smolder reaction propagation velocity and temperature increase with the air flow rate, thus confirming that smoldering is an oxygen limited process [1]. Newhall, et al. [23] confirmed the dependence of the smolder velocity on the oxidizer flow rate, showing buoyancy plays a role in cellulose smolder at low flow velocities. The preceding chapters deal with a series of experiments conducted under normal gravity conditions, where the effect of buoyantly induced flows in smoldering of polyurethane foam is studied. The analysis developed for the buoyantly induced flow for natural convection is included in this chapter to link the effect of gravity to oxidizer supply to the reaction. Cantwell [49] conducted preliminary studies of the effect of gravity changes on the smolder characteristics of

polyurethane foam, near the ignition source, and close to the ambient air fuel interface. Their experiments were conducted in a 2.2 second drop tower and in a KC-135 aircraft following a parabolic trajectory. The present work extends the above study investigating the effect of gravity changes on the natural convection smoldering of polyurethane foam as it propagates in a quasi one-dimensional fashion, downward and upward through the sample. By conducting a larger number of experiments, and analyzing the smolder process at different regions within the fuel sample, more conclusive and informative results are obtained of the role of gravity on smolder combustion.

5.2 Description of the Experiment and Experimental Hardware

A schematic diagram of the experimental package flown on the KC-135 and Learjet aircrafts is shown in figure 5.1. The combustion chamber is made of steel, 435 mm high and with a 300 mm side square cross section, with one of the side walls fitted with a Lexan window for optical access. The porous fuel is tightly fitted in an open-ended 300 mm long vertical duct with a 150 mm side square cross section. The duct walls are made of insulating 10 mm thick Fiberfax sheet covered with aluminum tape to prevent diffusion through the walls. The fuel sample is 150 mm long and occupies one half of the duct, the igniter and a 150 mm insulating char section occupies the other duct's half; ignition is performed as explained in previous chapters. The char is the solid residue of a previously smoldered foam and is separated from the foam by a stainless steel mesh to prevent re-ignition of the char.

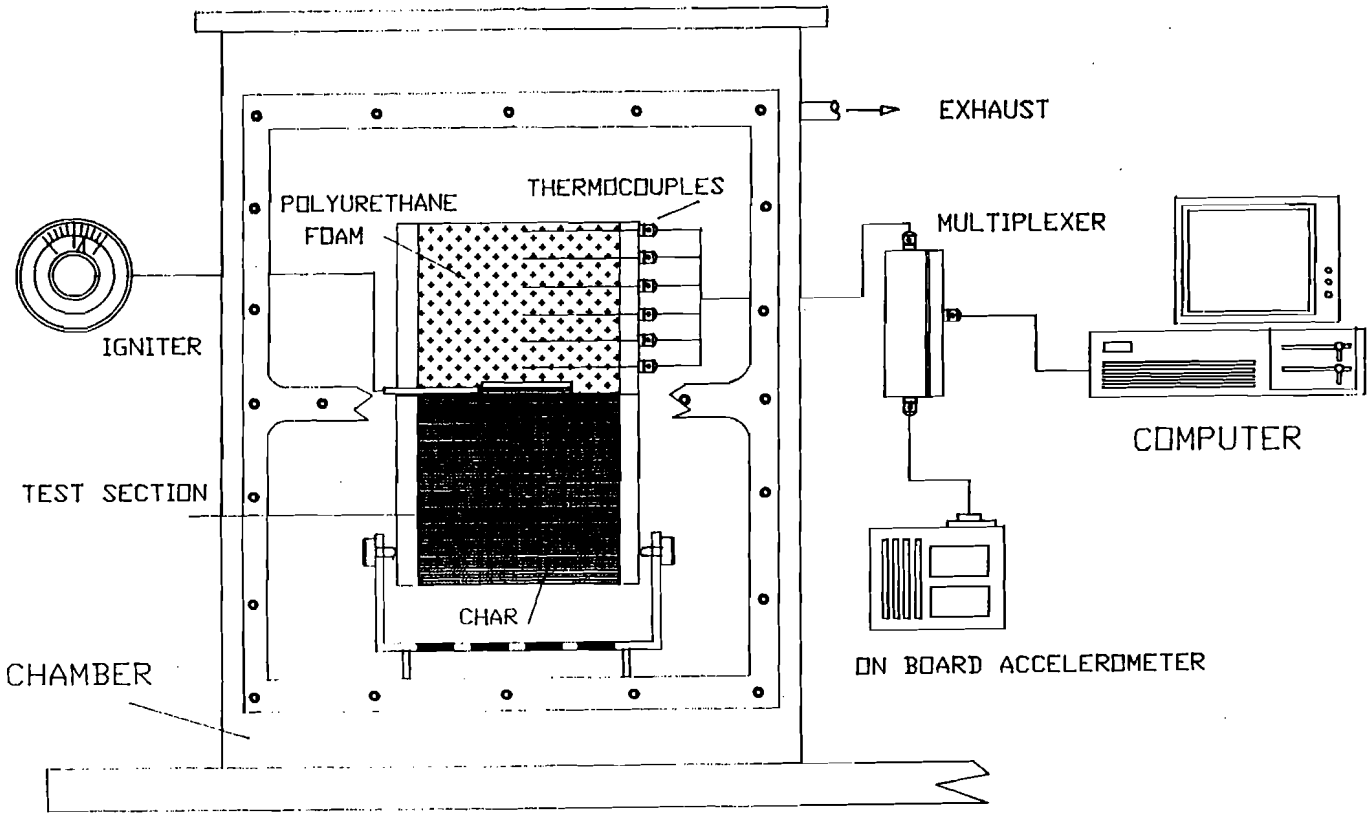

Figure 5.1 - Schematic of experimental apparatus. A similar test section to the one used for ground experiments was placed in a sealed chamber. The on-board accelerometer was connected to the thermocouple multiplexer to record acceleration readings in real time.

The foam sample width and length are selected to ensure a region of one dimensional smolder propagation free of end effects. All the tests in this work are conducted with open cell, unretarded, white polyurethane foam, with a 26.5 kg/m^3 density and 0.975 void fraction.

Experiments are started approximately 15 minutes before the parabolas start to avoid the effects of the variable gravity on ignition, and the igniter power is left on during the whole length of the experiment (the length of the igniter affected region was determined in chapter 2 on similar experiments). Only one sample is ignited per flight and generally smolders for the whole period that the maneuvers are performed.

Temperature histories along the foam sample are measured with six Chromel-Alumel thermocouples 0.8 mm in diameter embedded at fixed locations in the foam. These temperature histories are used to analyze the effect of gravity changes on the smolder process. However, they are not considered to be the actual foam temperature since it is impossible to determine whether the thermocouples are measuring the foam or the air temperature, or a combination of both. The rate of smolder propagation could also be obtained from the temperature histories of consecutive thermocouples, however the smolder velocities are too small to be measured during the time of each parabola.

The experimental chamber had an flow inlet and an exhaust which enable air to circulate in the chamber in an attempt to keep the chambers atmosphere clean of combustion products. Experiments were conducted without recirculating the air in

the chamber and with very small air flow (12.5 cm^3/s). The flow was only kept in the period between parabolas and was external to the foam; no flow was allowed during zero and 2-g periods. The air flow did not have any observable effect in the temperature histories. the pressure inside the chamber was kept constant.

A first group of experiments were conducted aboard a KC-135A, NASA 930 aircraft, which flies a parabolic trajectory to produce periods of low gravity lasting about 25 sec, with typical accelerations of approximately +/-0.2 m/sec^2. Each parabolic trajectory is initiated and terminated with a pull-up and pull-out of 1.8 to 2.0 g's. These trajectories are flown consecutively, typically in groups of 10, with a total of 30 to 40 parabolas per flight. The acceleration is measured by an accelerometer attached to the airframe. A second group of experiments were conducted aboard a Learjet, Model 25, which flies a parabolic trajectory to produce periods of low gravity lasting about 20 sec, with typical accelerations of approximately +/-0.04 m/sec^2. The pull-up and pull-out were requested to match the characteristics of the KC-135A parabolas. The Learjet performs a maximum of 6 prabolas per flight and the maneuvers are conducted at specified times during the smoldering process, enabling a closer look of the behavior of smoldering as it propagates through the sample.

The chamber was designed by Elizabeth Cantwell [49] and built at NASA Lewis Research Center.

5.3 Experimental Results

All experiments were conducted under natural convection conditions, for downward and upward smoldering propagation. In downward smoldering experiments, the foam is ignited at the top of the sample and the smolder reaction propagates downward through the sample. In the presence of gravity the smolder propagation is expected to be of the opposed type [1] with the air being naturally induced upward through the virgin foam towards the reaction zone, and the products through the char toward the top. In upward smoldering the foam is ignited at the bottom and the reaction propagates upward. Thus, with gravity the smolder propagation is expected to be in this case of the forward type, with air flow induced upward through the char towards the reaction zone, and the products through the virgin foam towards the top. Comparison and individual study of both smolder configurations should provide information of the effects of buoyancy on smolder.

5.3.1 Downward Smoldering

Two typical downward smolder temperature histories at normal gravity and during a parabolic flight, at three locations along the foam sample, are presented in figure 5.2 as a function of the time from ignition. As the smolder reaction approaches the thermocouple location, the temperature increases due to the streamwise heat transfer from the reaction zone to the fuel ahead. Significant heat transfer occurs by conduction, radiation [12], as well as convection. The convective heat transfer depends on the flow direction, which in the downward smolder case has a

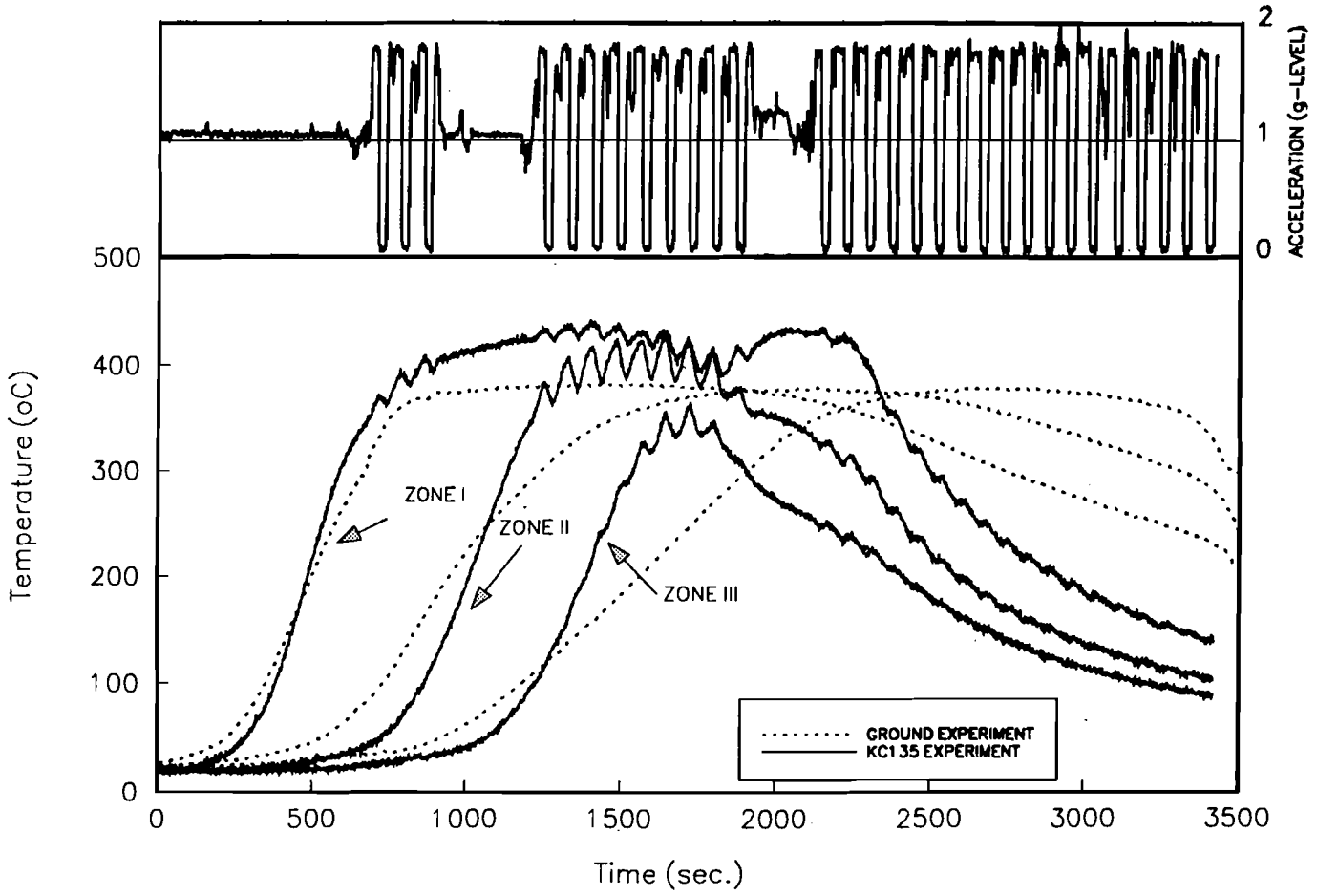

Figure 5.2 · Temperature histories for downward burning natural convection experiments. The three thermocouples in the above figure are located at 15, 70 and 105 mm from the igniter, and correspond each to one characteristic zone of the process. This particular experiment was conducted on board of the KC-135A plane.

cooling effect, as the buoyantly induced flow moves in the opposite direction to that of smolder propagation, and in upward smolder the opposite effect. Once the smolder reaction reaches the thermocouple, the temperature levels off and becomes relatively constant due to a balance between the exothermic surface smolder reaction, the endothermic decomposition of the fuel, and the heating of the adjacent gas and solid material. After the reaction has passed the thermocouple location, the temperature recorded is that of the char, which decays due to heat losses to the wall and the environment. Some of these heat losses are due to convective currents that are generated by the combination of the hot post-combustion gases and the extremely high permeability of the char.

The three thermocouples whose temperatures are presented in figure 5.2 are located at 15, 70 and 105 mm from the igniter, and their temperature profiles are representative of three regions within the sample that have specific characteristics (chapter 2). An initial zone, zone I, near the igniter, approximately 50 mm long, where the smolder reaction is strongly influenced by the heat transferred from the igniter. A second zone, zone II, 50 mm long in the middle of the sample where the smolder process is relatively free from end effects. An end zone (III) 50 mm long, where there is a significant influence from the external environment on the smolder. The gravity variation is superimposed in the figure to facilitate the data interpretation.

Analysis of the measured temperature histories indicates that the effect on the temperature profile of the gravity changes occurring during the parabolic flight

depends on the location of the thermocouple within the sample, and in relation to the reaction zone. Thus results will be presented separately according to zone and location relative to the reaction front.

Presentation of the results begins with zone II, since the smolder in this zone is the most representative of a self-propagating smolder. Representative periods of the temperature history, covering at least two parabolas, are presented in figures 5.3, 5.4 and 5.5, these correspond to a thermocouple located 70 mm away from the igniter. These show the virgin foam ahead of the smolder reaction, in the reaction zone, and in the char behind the reaction, respectively. An acceleration trace for the same period is overlaid in the figures to facilitate the interpretation of the results. The noise in the data is believed due to RF noise on the aircraft. From the temperature profiles of figure 5.3, it is observed that in the virgin foam ahead from the reaction, where the temperature gradient is positive due to heating from the reaction, the temperature gradients are larger during low gravity than during high gravity. In the reaction zone (figure 5.4), where the temperature is fairly uniform, the temperature decreases sharply during low gravity and increases during high gravity. Finally, from the temperature profile of figure 5.5, corresponding to the char region, which has an overall negative gradient due to heat losses to the environment, a gradient reversal can be seen in the low gravity and a steepening of the negative gradient in high gravity.

Further information about the effect of gravity on the downward smoldering controlling mechanisms can be obtained from the temperature histories in zones I

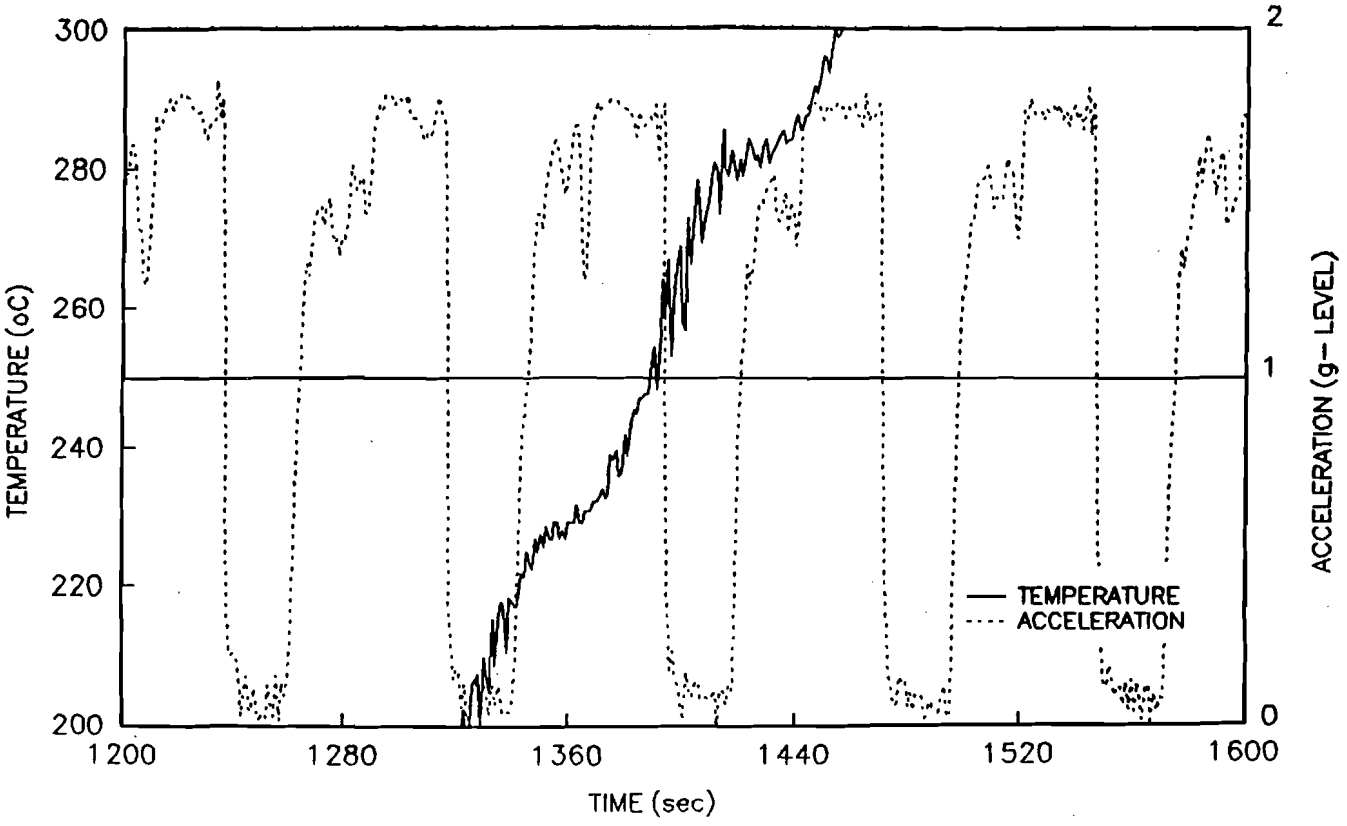

Figure 5.3 - Temperature history detail for downward burning experiment for a zone II thermocouple (70 mm from the ignition plane) before the reaction front has reached the thermocouple (unburnt foam). This particular experiment was conducted on board of the KC-135A plane.

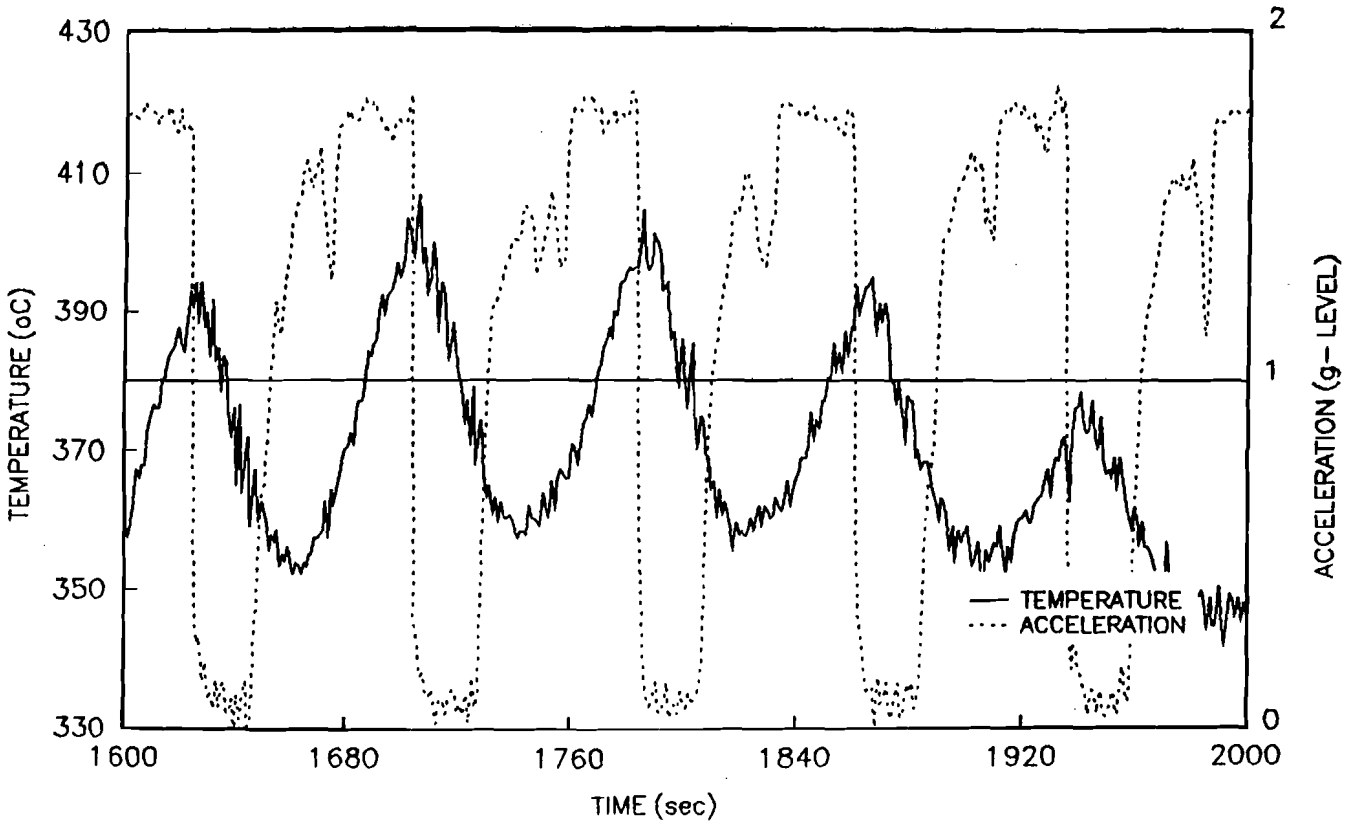

Figure 5.4 - Temperature history detail for a downward burning experiment for a zone II thermocouple (70 mm from the ignition plane) when the reaction front has reached the region close to the thermocouple (reaction zone). This particular experiment was conducted on board of the KC-135A plane.

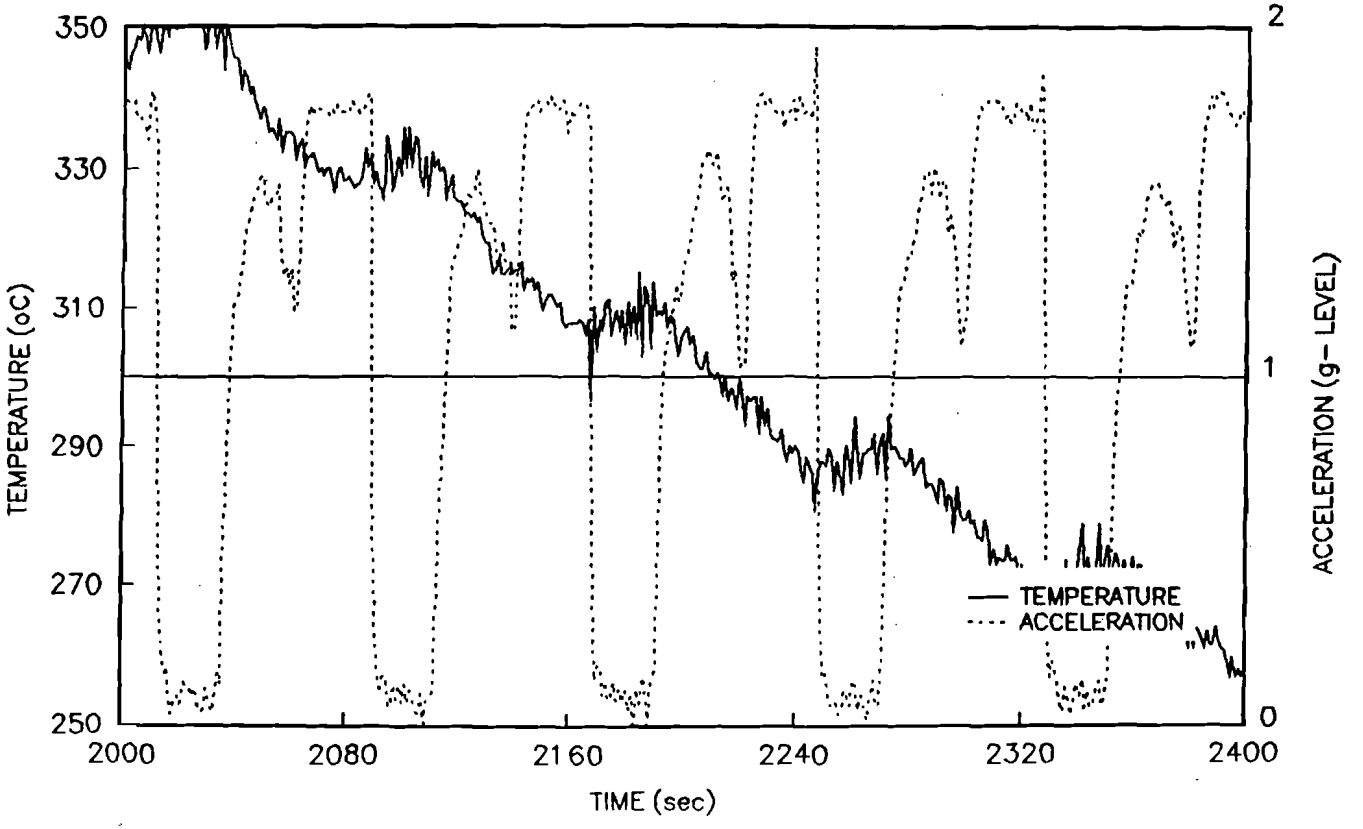

Figure 5.5 - Temperature history detail for a downward burning experiment for a zone II thermocouple (70 mm from the ignition plane) when the reaction front has passed the region close to the thermocouple (burnt foam). This particular experiment was conducted on board of the KC-135A plane.

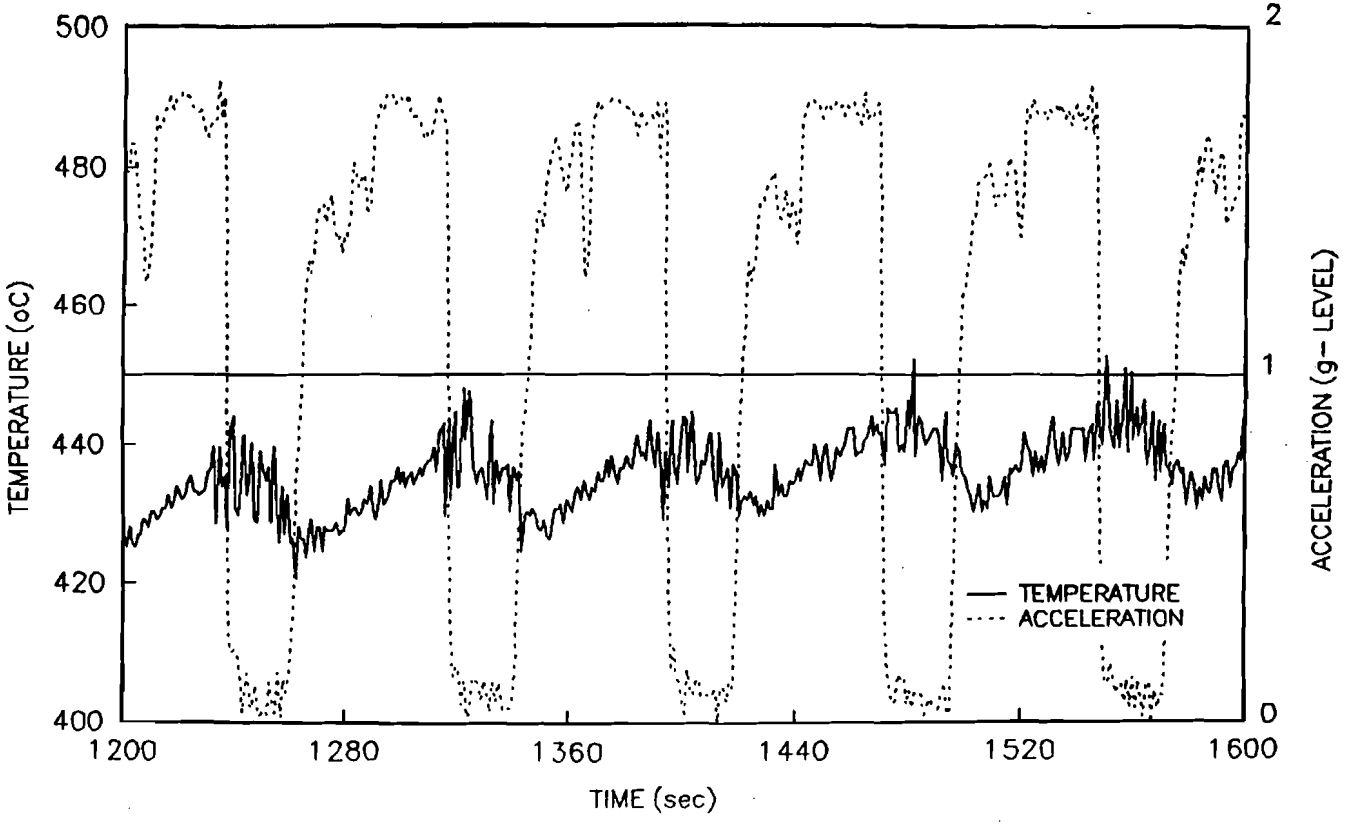

Figure 5.6 - Temperature history detail for a downward burning experiment for a zone I thermocouple (15 mm from the ignition plane) when the reaction front has reached the region close to the thermocouple (reaction zone). This particular experiment was conducted on board of the KC-135A plane.

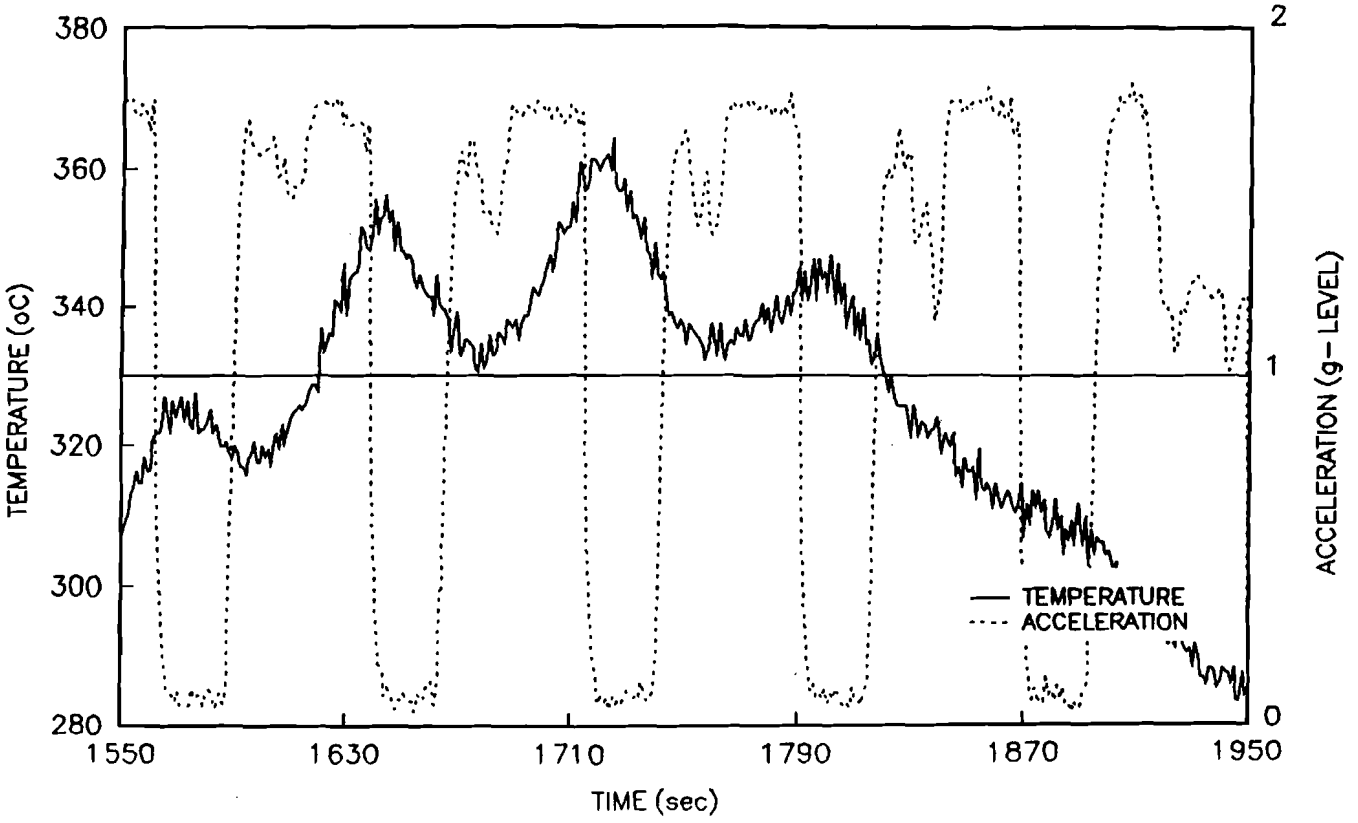

Figure 5.7 - Temperature history detail for a downward burning experiment for a zone III thermocouple (105 mm from the ignition plane) when the reaction front has reached the region close to the thermocouple (reaction zone). This particular experiment was conducted on board of the KC-135A plane. This temperature history enters an extinction regime after approximately 1750 sec. as can be observed from the change in temperature increase gradients for the high gravity period.

and III, these are presented in figures 5.6 and 5.7 respectively. The temperature history of figure 5.6 is obtained from a thermocouple located 15 mm from the igniter while the reaction is passing. The effect of the gravity change on the reaction temperature in this zone follows the same trend as observed in zone II. However, the quantitative effect is weaker, with a temperature drop in the low gravity period of approximately 15°C versus the 50°C observed in zone II. The temperature history of the smolder reaction as it passes by a zone III thermocouple is given in figure 5.7, here the proximity to the end of the sample results in the weakening of the reaction. The characteristics of the temperature histories in the virgin material and char in zones I and III are similar to those in zone II, except for quantitative differences as those indicated above. Thus, they will not be presented here for brevity of presentation.

The variable gravity cycles resulted in an overall weakening of the reaction which lead to extinction in the KC-135 experiments, as shown in Figure 5.7. In the Learjet experiments it was possible to space the 6 parabolas, allowing the reaction to recover, thus, preventing extinction and enabling a closer study of zone III. These experiments showed identical trends to the KC-135A experiments; in the reaction zone temperatures decreased in the low gravity periods and increase in the high gravity period, but extinction was avoided. For thermocouples in the reaction zone, maximum and minimum temperatures are measured for each cycle and the difference is plotted as a function of distance from ignition (figure 5.8). The temperature difference increased as the reaction moved away from the ignition plane. As

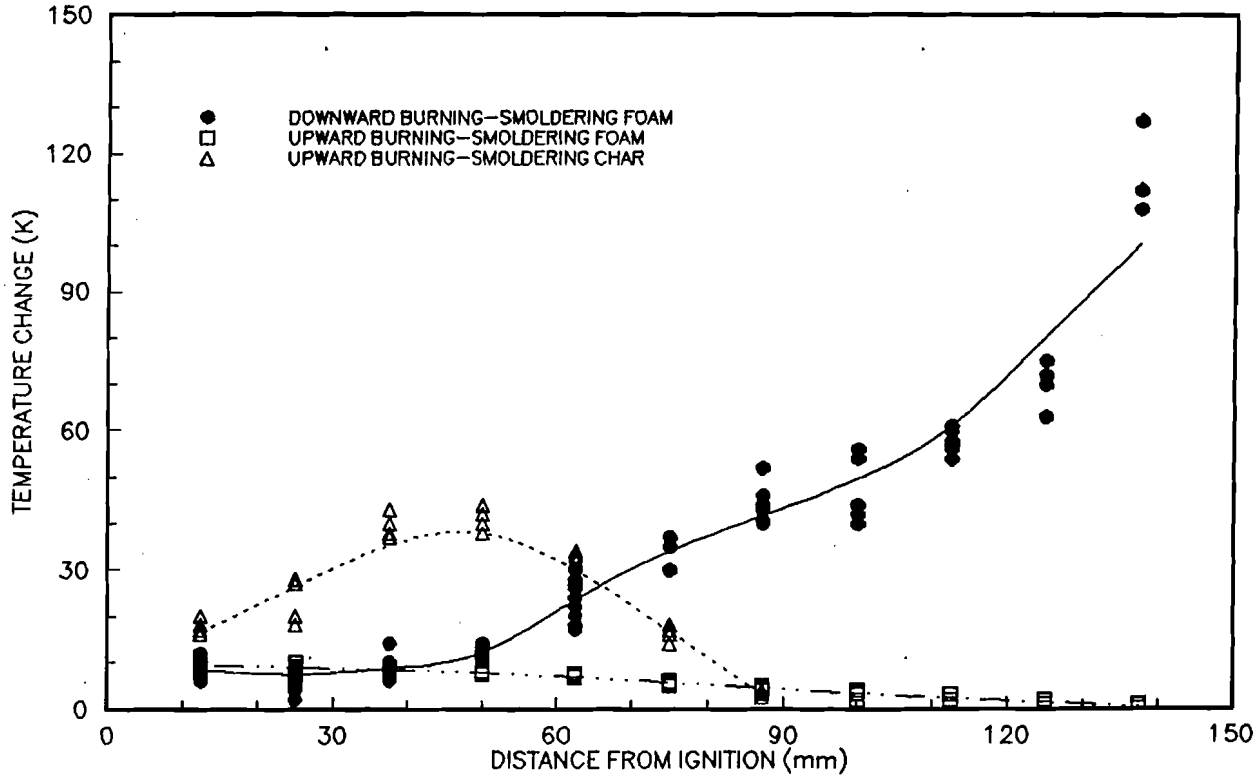

Figure 5.8 - Variation of the temperature drop through a low gravity period for a thermocouple in the reaction zone along the foam sample, for both upward and downward burning. The magnitudes are obtained by subtracting maximum and minimum temperatures during a low gravity period. This figure shows data from experiments conducted on board of KC-135A and Learjet planes.

previously observed in figure 5.6, near the igniter (zone I) the temperature difference between the maximum and minimum temperatures during a cycle is approximately 15°C increasing to approximately 40°C for a thermocouple 70 mm away from the ignition plane, and continues to increase to values over 100°C near the end of the sample. Even though these temperature have no physical meaning they provide a comparative idea of the influence of buoyancy at different locations in the sample. If extinction occurs the temperature difference will decrease, as observed in figure 5.7. Only data from experiments where extinction did not occur is presented in figure 5.8.

5.3.2 Upward Smoldering

A characteristic example of the temperature histories for upward smoldering at different locations along the foam sample is presented in figure 5.9. The three thermocouples whose temperatures are presented in figure 5.9 are located at 15, 70 and 105 mm from the igniter, and their temperature profiles are representative of the same three regions previously mentioned for downward burning. In this case, it can be observed, that the smolder reaction weakens and its temperature decreases as it propagates upward through the sample. Temperatures within the char remain high (approximately 450°C), values which are higher than characteristic smolder temperatures, approximatelly 380°C [3,10,11,15], and more representative of char oxidation temperatures. No significant cooling of the char can be observed from figure 5.9. This results from the effect of periodic gravity changes on the smolder

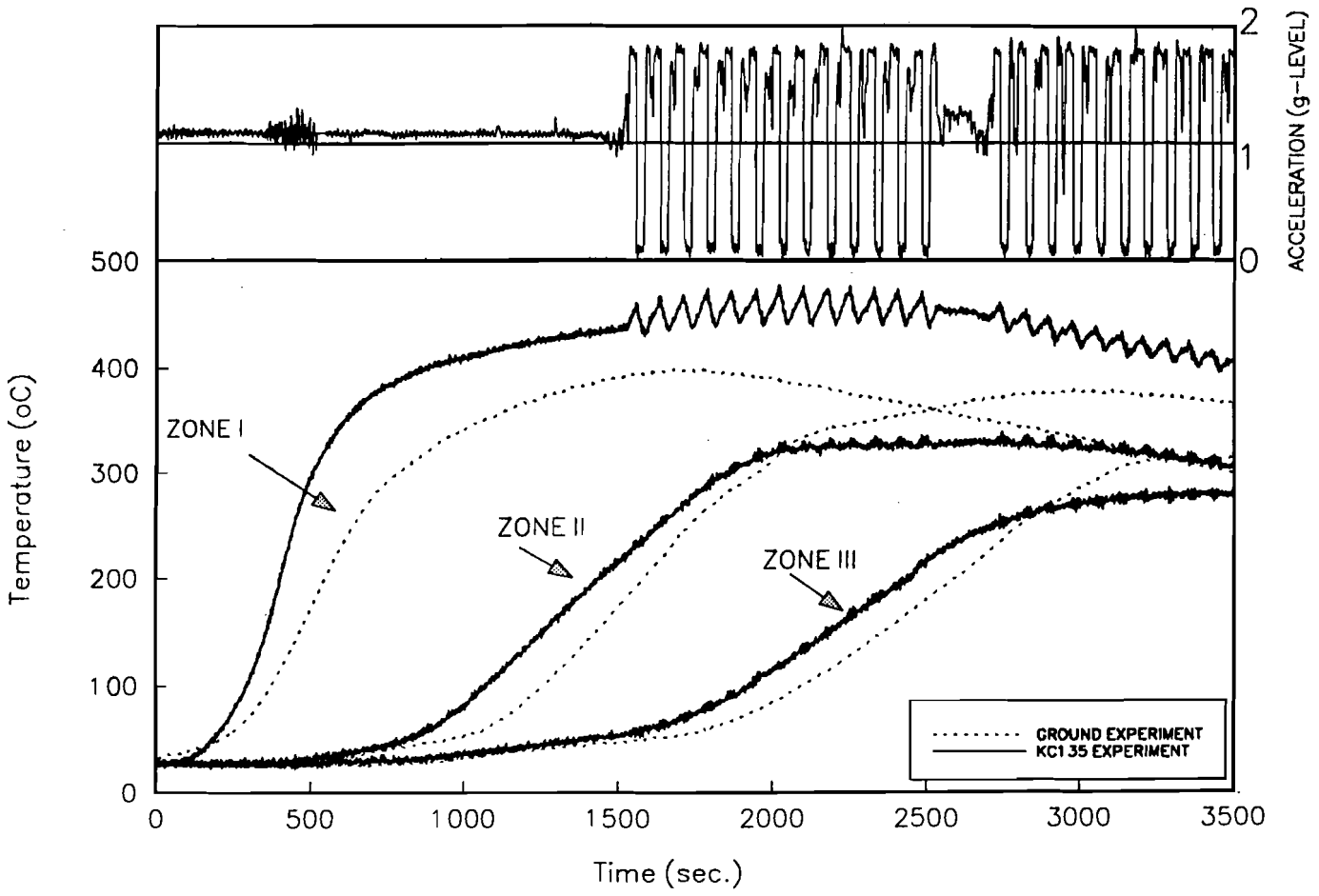

Figure 5.9 - Temperature histories for upward burning natural convection experiments. The three thermocouples in the above figure are located at 15, 70 and 105 mm from the igniter, and correspond each to one characteristic zone of the process. This particular experiment was conducted on board of the KC-135A plane.

reaction, since similar experiments conducted at normal gravity did not show these patterns (figure 5.9). Analysis of the temperature profile from the first thermocouple (zone I) shows that within the reaction zone the effect of gravity is similar to that observed in downward smolder, with the temperature increasing in the high gravity periods and decreasing in low gravity. The magnitude of the temperature fluctuations is, however, smaller than in downward smolder (figures 5.9 and 5.10).

For the experiments performed in the Learjet, fewer and more spaced variable gravity cycles were conducted, therefore a strong reaction could be obtained deeper into the sample. Maximum temperatures also decayed as the reaction moved away from the ignition plane. For upward smoldering, air comes through the char towards the reaction, therefore strong oxidative reactions occurring in the char were observed, since most of the oxidizer is depleted in the char, the foam undergoes a pyrolysis reaction [1,9] sustained by the heat released from the oxidation of the char. High gravity enhances char oxidation reactions, showing an increase in the temperature of the char, the temperatures in the pyrolysis region also increased in the high gravity periods, presumably due to the greater heat release from the oxidative reaction and enhanced convective heat transfer. The consequence of multiple variable gravity cycles was the weakening of the reaction, as it propagated upward along the sample, that eventually lead to extinction in all KC-135A and Learjet experiments. Thermocouples placed more than 70 mm away from ignition show temperatures characteristic of pyrolysis [1,9]. The temperature traces of figures 5.9 and 5.10 are

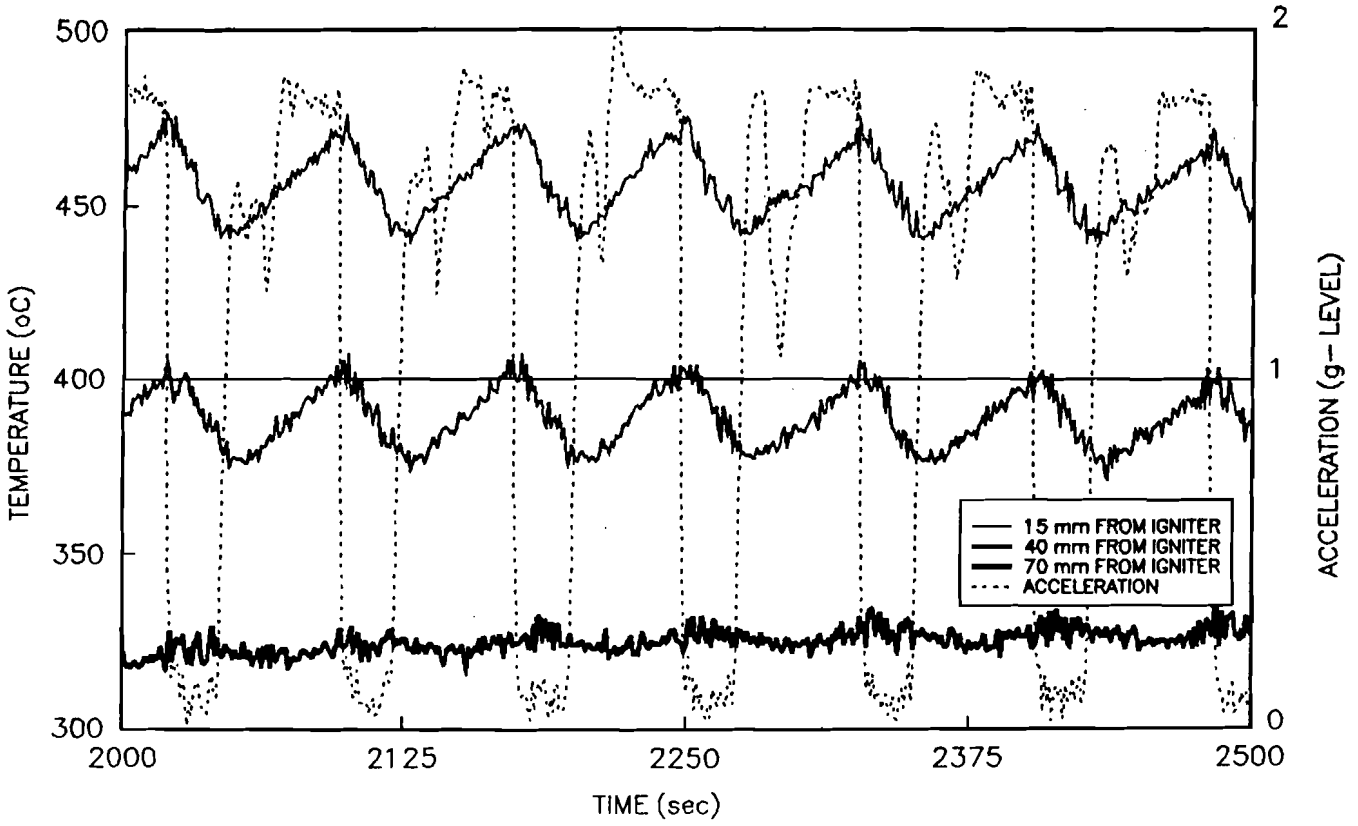

Figure 5.10 - Temperature history detail for an upward burning experiment for thermocouples placed in zones I and II when the reaction front has reached the region close to the thermocouples. This particular experiment was conducted on board of the KC-135A plane.

typical examples of this scenario.

The difference between maximum and minimum temperatures for each variable gravity cycle in both the pyrolysis region and char oxidation reaction is presented in figure 5.8. It can be observed that the temperature difference decays in the pyrolysis region as the reaction propagates upwards. The temperature difference in the char increases as the reaction moves away from the ignition plane, reaches a maximum and then decays leading to extinction.

For comparison purposes, figure 5.11 shows a cross-section of a downward burning sample and figure 5.12 an upward burning sample after the experiment has been completed. For downward burning smoldering the reaction propagates almost to the end of the sample and the char left behind keeps the structure of the unburnt foam, no evidence of pyrolyzed foam can be observed. For upward burning smoldering, the reaction extinguished approximately 50 mm before reaching the end of the sample, the part of the foam that is left unburnt shows evidence of pyrolysis, the foam has been decolorated and has changed its structure. The filaments that are characteristic of polyurethane foam have disappeared in the pyrolyzed foam. For upward burning smoldering almost no char is left behind the pyrolysis front, random holes cover almost entirely the region behind the pyrolysis reaction.

5.4 Discussion of the Results

The above results suggest a smolder process that is controlled by the competition between the supply of oxidizer to the reaction zone and the loss of heat

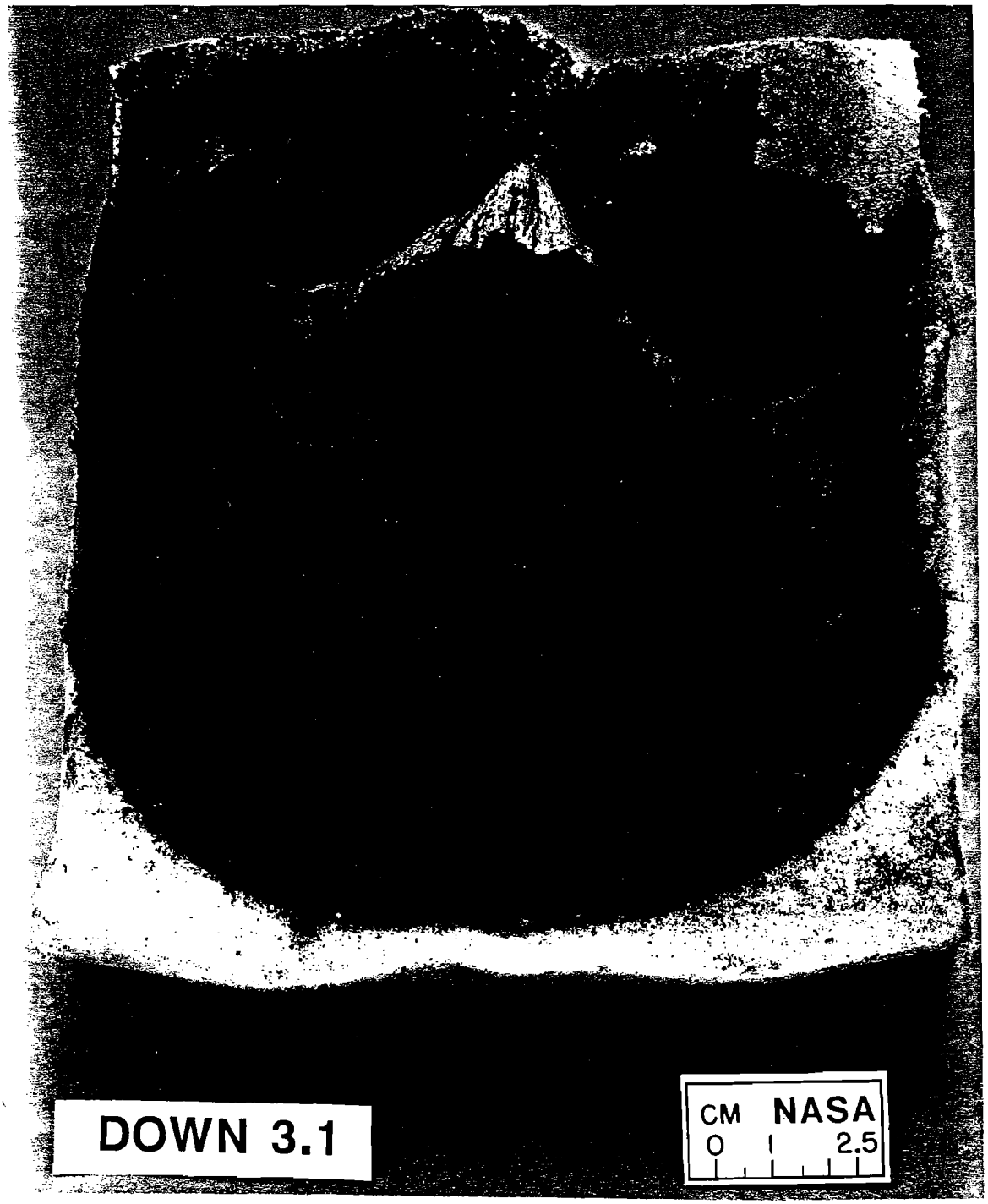

Figure 5.11 - Photograph showing a sample cross-section after a downward burning experiment has been conducted. For downward burning, smoldering propagates from top to bottom leaving an almost homogeneous char behind.

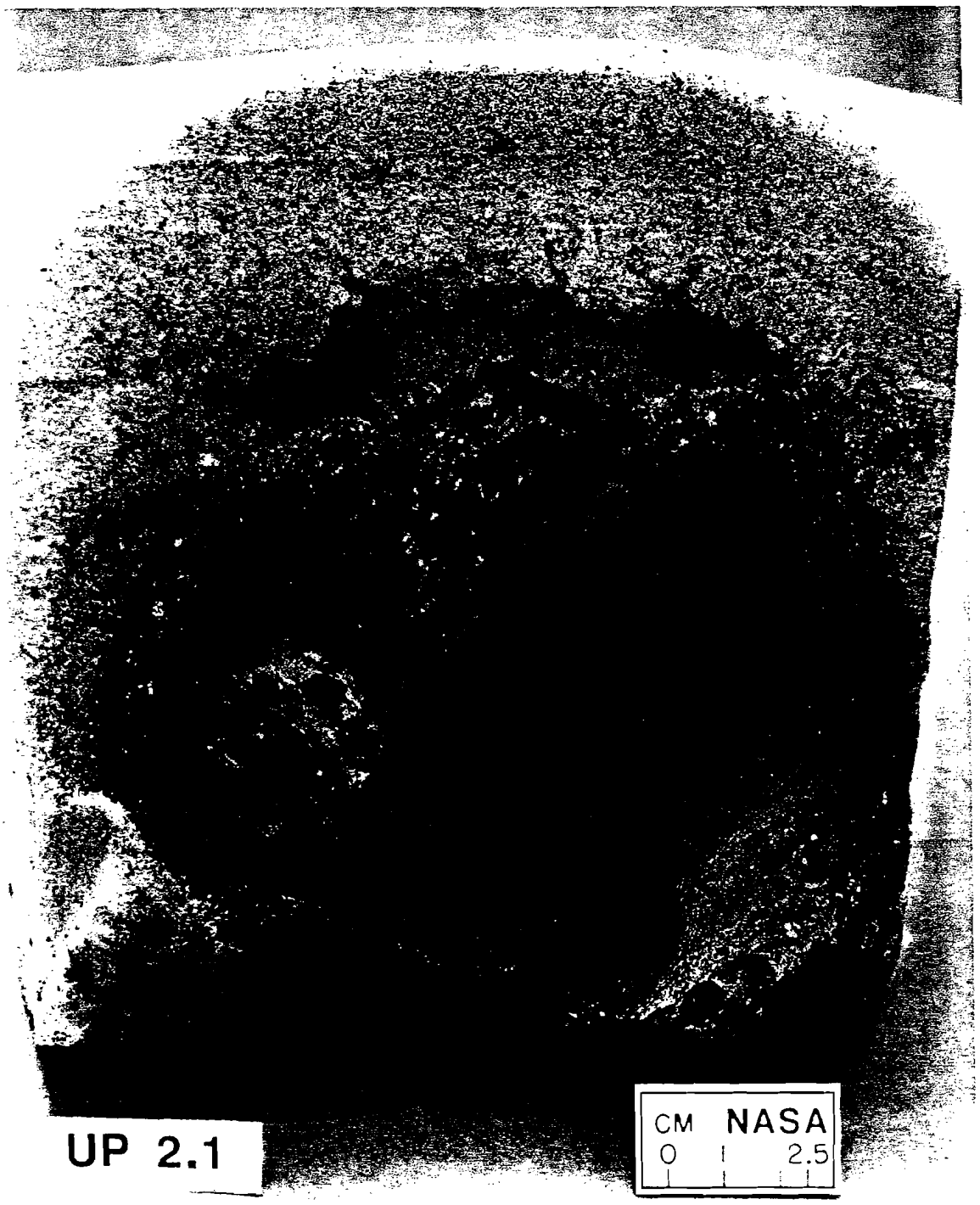

Figure 5.12 - Photograph showing a sample cross-section after an upward burning experiment has been conducted. For upward burning regions of complete char consumption can be observed as well as a region where pyrolysis has occurred.

from the reaction zone. The presence of two smolder controlling mechanisms, chemical kinetics and heat losses, has been previously suggested [1]. In the virgin material the temperature is determined by the heat transferred from the reaction zone by conduction, radiation [12] and convected by the buoyantly induced air flow. In low gravity the buoyant flow is largely suppressed, in high gravity the opposite effect takes place. For downward burning convective heat transfer from the reaction to the virgin fuel is adverse, thus the trends observed in figure 5.3, an increase in the slope of the temperature traces for low gravity periods and a decrease for high gravity periods. For upward burning convective heat transfer from the reaction zone to the virgin fuel is favorable, therefore temperatures increase during high gravity periods and decrease during low gravity periods as can be observed from figure 5.9.

Within the reaction zone, the temperature is determined primarily by the balance between the heat generated by the smolder reaction, and the heat transported away from the reaction. The former is strongly dependent on the supply of oxidizer [1,5,6,7,8], and on the reaction rate which in turn depends on the heat losses through the solid temperature. Buoyancy affects the transport of both oxidizer and heat to and from the reaction zone. At low gravity, diffusion is the only mechanism of oxidizer transport to the reaction zone, and since diffusion is slow and the reaction is oxygen limited, the reaction and heat generation rates are reduced. If the reduction in the convective losses does not compensate for the reduction in heat generation, the smolder reaction temperature decreases during low gravity, as observed in figure 5.4, for downward burning and figure 5.10 for upward burning.

At high gravity the increase in the oxygen supply becomes dominant and the smolder temperature increases. A competition between an oxidative smoldering reaction and pyrolysis has been mentioned before [1,9], for upward burning, during high gravity periods, char oxidation is strongu, depleting the oxidizer reaching the smoldering reaction, this along with the large heat release, from the reacting char, favors the pyrolysis chemical pathway [1,3,9]. During periods of low gravity the oxidative reaction of the char weakens and is unable to sustain the endothermic pyrolysis reaction with the consequent decay of the temperature in both the oxidation and pyrolysis regions. Pyrolysis inhibits smolder [1,3,9] therefore the natural consequence of the variable gravity cycles is extinction.

The char is very porous and because of this and potentially uneven temperature distribution, buoyantly induced flows are easily established within the char region. For downward burning experiments these flows tend to cool the char and cause the decrease in temperature observed in figures 5.2 and 5.5. Also, a very weak smolder reaction that steadily decays is possible as the temperature decreases. In low gravity, buoyant cooling is suppressed, and the heat generated by this weak reaction, together with the heat transferred from the reaction zone causes the temperature to increase. In the high gravity period, convective cooling becomes dominant and the temperature decreases (figure 5.5). As explained before, for upward burning, oxidizer reaches the reaction zone through the char where strong oxidative reactions are established, therefore the char never cools down and temperatures increase during high gravity periods (enhanced oxidyzer supply) and

decrease during low gravity periods (diminished oxidyzer supply) as shown in figure 5.9, this continues until oxidation of the char is almost complete, figure 5.12 shows that there is almost no char left behind the pyrolysis zone.

It was previously mentioned that the effect of the variable gravity cycles on the reaction changes as the reaction propagates deeper into the sample (figure 5.8). Since oxygen supply to the reaction zone and convective cooling are the controlling mechanisms for the smoldering reaction, an analysis of the variation of the air flow velocity as the reaction propagates deeper into the sample is necessary. The following flow analysis is extracted from chapter 2. An air flow pattern is established through the foam by two effects that will be superposed, natural draft through a duct (u_D) and boundary layer flow (u_b) induced by a gradient of temperature in the y direction (figure 5.13). In the mathematical formulation of the problem it will be assumed that (i) the convective fluid and the porous medium are everywhere in thermodynamical equilibrium, (ii) there is no phase change in the solid, (iii) properties of the fluid and the porous medium are homogeneous and isotropic, and (iv) the Boussinesq approximation is invoked. The results of this analysis are as follows

$$u_D = \frac{(\rho_H - \rho_C)\ g\ x}{\frac{\mu}{K_F}\left((L_F + L_{CH} - x) + \left(\frac{K_F}{K_{CH}}\right)\left(\frac{\phi_F}{\phi_{CH}}\right)^{\frac{2}{3}}\left(\frac{n_H}{n_C}\right)\left(\frac{T_S}{T_i}\right)\ x\right)} \qquad (5.1)$$

$$u_b = \frac{2\delta}{W}\left(\frac{Gr_K}{Re_K}\right) u_D \qquad (5.2)$$

n_H and n_C are obtained from Summerfield and Mesina [2]

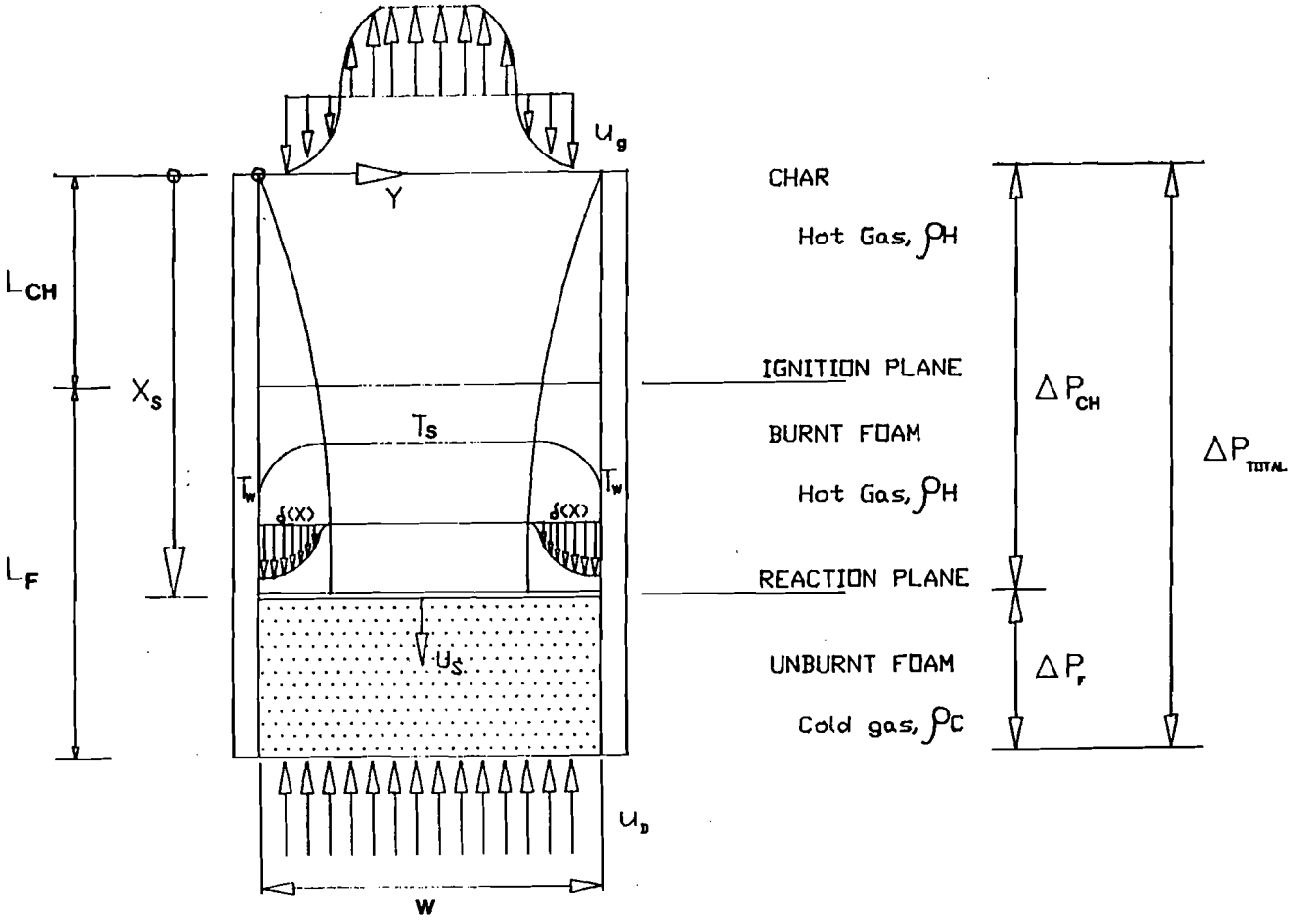

Figure 5.13–Schematic of the flow field induced by buoyancy, for downward burning. For upward burning the diagram has to be rotated 180°, the resultant flow in the char is the same. Both in downward and upward burning recirculation flow adds to the natural draft flow in the core of the sample (aiding flow).

where

$$Re_K = \frac{\rho_A u_D K_{CH}^{0.5}}{\mu}$$

and $$Gr_K = \frac{K_{CH}^{1.5} g \rho_A^2 \beta (T_W - T_S)}{\mu^2}$$

so

$$u_g = u_D + u_b + \phi_F U_S \qquad (5.3)$$

Figure 5.14 shows the value of u_g for different locations in the sample, for gravitational accelerations of 1 and 2 g's. For both cases diffusion is neglected. For the value of U_S several authors give a characteristic smolder velocity of 0.1 mm/sec [1,3,5,6,7,8,9].

For zero gravity

$$u_g = \phi_F U_S + D\frac{Y_{O,i}}{\delta_D} \qquad (5.4)$$

where $$\delta_D = \sqrt{\frac{DL_F}{U_S}}$$

the total flow is of the order of 0.1 mm/sec, much smaller than the buoyantly generated flow, for both 2 and 1 g levels.

The results of these calculations show an increasing air flow velocity as the reaction propagates deeper into the sample, during periods where buoyancy is significant (figure 5.14); constant total air flow velocities of much smaller magnitude

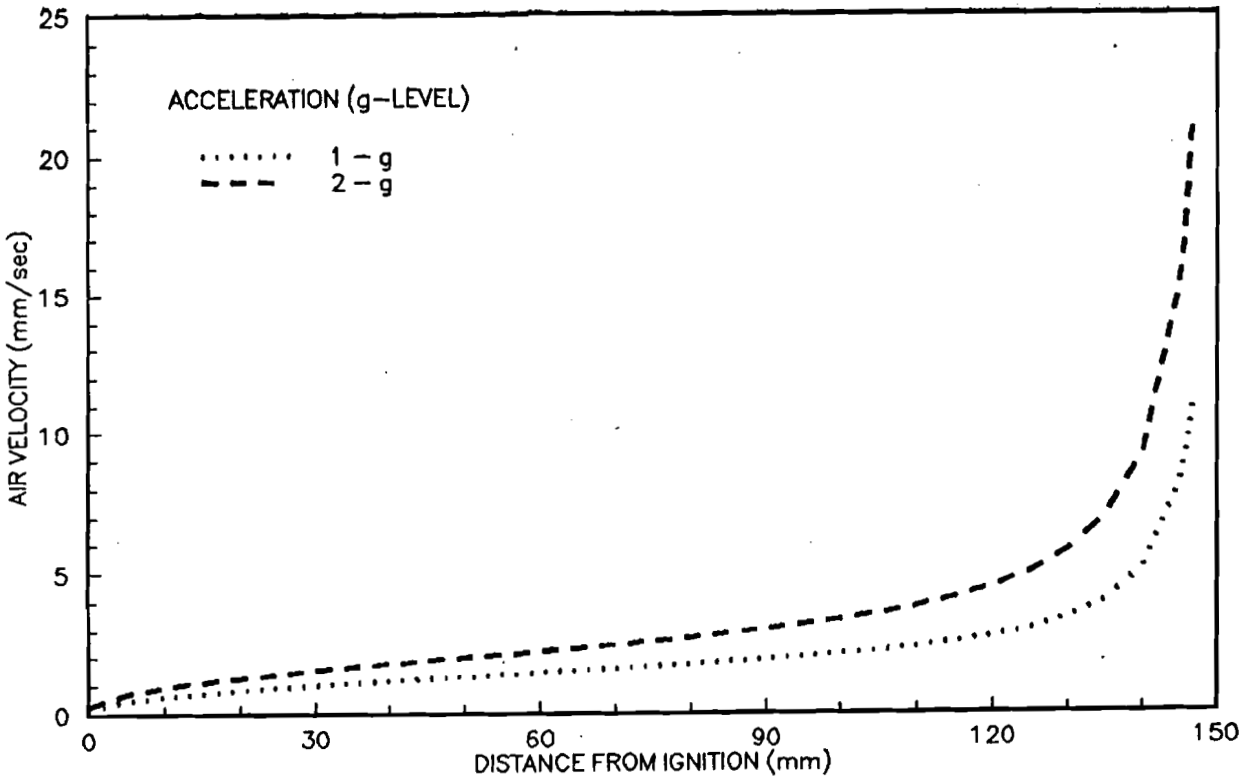

Figure 5.14- Variation of the total air flow velocity as a function of the distance from ignition. Calculations for different g-levels are presented. The magnitude of the air flow velocity is the same for both downward and upward burning.

are calculated for periods where buoyancy is negligible. For downward burning smolder, comparison of figures 5.8 and 5.14 confirm the above statement that convective oxygen transport to the reaction zone and heat transfer from the reaction zone are the competing mechanisms that control smolder. If the smolder reaction is strong, oxidizer supply is the controlling mechanism therefore as the magnitude of the buoyantly induced flow increases its effect on the reaction temperature increases, showing greater temperature differences during the variable gravity cycles (figure 5.8). For weaker smolder reactions heat losses play a more significant role, enhanced oxidizer transport to the reaction during high gravity periods does not compensate for greater heat losses, thus, extinction results (figure 5.7). For the experiments performed in the KC-135, the large number of consecutive variable gravity cycles resulted in a weaker reaction that extinguished as it propagated towards the end of the sample, where the effect of buoyancy was greater. The effect on the temperature traces of changes in the magnitude of oxidyzer reaching the reaction zone is larger than changes in heat transfer characteristics, therefore, oxidizer transport controlled reactions (figure 5.4) show larger temperature differences, during a variable gravity cycle, than heat transport controlled reactions (figure 5.7).

For upward burning smolder, the effect of buoyancy on the oxidative reaction occurring in the char is enhanced as the reaction propagates away from the ignition plane, strong char oxidation consumes most of the char (figure 5.12); due to lack of fuel the reaction in the char weakens (figure 5.9) and thus the effect of buoyancy on the temperature decays. Since the pyrolysis reaction is supported by the heat

released from the oxidative reaction in the char, as the reaction weakens less heat is being transported to the pyrolysis front and therefore the temperature difference during each variable gravity cycle is less significant; thermocouples placed more than 90 mm away from the ignition plane show almost no change during the variable gravity cycles (figure 5.8). This is more evident for experiments performed on board of the KC-135 where the large number of parabolas lead to extinction earlier, and thermocouples 70 mm away from the igniter already showed no change during the variable gravity cycles (figure 5.10). The magnitude of the flow calculated above is not very accurate for upward burning experiments since the permeability of the char varies after each variable gravity cycle and the structure of the pyrolyzed foam obstructs the flow of air [3,9].

5.5 Conclusion

The present study has helped to identify the controlling mechanisms of free convection smolder, and to determine the potential influence of gravity on the process. Particularly interesting is the determination that the competition between oxygen supply and heat transfer that determines the characteristics of the smolder reaction, is altered by the changes in gravity levels. Within the reaction zone, the reduction in oxygen supply in low gravity is dominant, and the reaction weakens. Away from the reaction zone, the reduction in convective cooling at low gravity tends to increase the material temperature.

The present experiments, although providing a phenomenological view of the

smolder characteristics in a variable gravity environment, cannot determine the final fate of the reaction in a micro-gravity environment. However it is possible to infer some of the events that may occur in micro-gravity smolder. Under self-smolder conditions, smolder will probably be maintained because the oxygen contained in the foam pores is enough to sustain smolder, although at significantly low smolder propagation velocities and temperatures; it also could extinguish as a result of oxygen dilution by the combustion products. Under external heating, or within the char, the insulating conditions that micro-gravity provide may result in an enhancement of the smolder reaction, and its possible transition to flaming.

Chapter 6
CONCLUSIONS

6.1. Summary of Results

A systematic experimental study has been carried out to investigate the controlling mechanisms of smoldering combustion. The primary interest has been focused on the effect of buoyancy on the smolder propagation velocities. The experiments are conducted in natural convection and forced flow, both opposed and forward; in downward and upward burning configurations. Polyurethane foam is used as fuel because it maintains its structure after burning, thus allowing experiments in upward and downward configurations. An array of thermocouples is placed in the sample centerline to obtain temperature histories from which the smoldering propagation velocity is calculated. Smolder propagation velocities and maximum temperatures are measured as functions of the distance from ignition, forced flow velocity and direction of propagation. From the experimental data the following main results are obtained:

Natural Convection Smoldering

(1) Downward burning smolder behaves in an opposed flow manner. The controlling propagation mechanism is heat transport from the reaction to the virgin fuel. Since smoldering is oxygen limited the reaction rate and thus, the

heat release, is directly proportional to the oxidizer supply to the reaction zone. Therefore smolder propagation velocities are directly proportional to the total average oxidizer velocity.

(2) Upward burning smolder behaves in a forward flow manner. It is an unsteady reaction where exothermic oxidation competes with endothermic pyrolysis. For self-sustained smolder the heat released by the oxidation front has to provide sufficient heat to support the pyrolysis reaction ahead of it. Heat transport from the reaction to the fuel is still the controlling propagation mechanism.

(3) Buoyancy is present as an oxidizer transport mechanism, either as flow induced by natural draft or natural boundary layer flow. The significant difference between the permeability of char and foam is an important parameter in the establishment of buoyantly induced flow.

(4) $\frac{u_g}{U_s} \approx 30$, thus, heat is being convected from the reaction zone by the buoyantly induced flow. This shows no effect for downward burning. For upward burning, convective heat transfer increases the fuel temperature, resulting in an acceleration of the reaction front that will lead to transition to flaming for samples longer than 200 mm.

Opposed Flow

(1) Smoldering propagation velocities are controlled by a sensitive competition between oxidizer supply to the reaction and heat losses. If

$$\frac{U_S \rho_F Cp_F (1-\phi)(T_S-T_i)}{\rho_A [QY_{O,i} - Cp_A (T_S-T_i) u_g + \dot{q}_i''(x)} \geq 1$$

the reaction is strong, heat losses are not a relevant parameter of the problem and smolder propagation velocities increase linearly with the total average air velocity. If

$$\frac{U_S \rho_F Cp_F (1-\phi)(T_S-T_i)}{\rho_A [QY_{O,i} - Cp_A (T_S-T_i) u_g + \dot{q}_i''(x)} < 1$$

the reaction is weak, heat losses will determine the fate of the reaction. Propagation velocities are no longer linearly proportional to total air flow velocities and chemical kinetics become an important parameter in the problem.

(2) Opposed smolder is a steady reaction where the controlling propagation mechanism is heat transport from the reaction to the virgin fuel.

(3) Buoyancy is present as an oxidizer transport mechanism.

(4) Smolder can propagate for $0 \text{ mm/sec} \leq u_f \leq 4 \text{ mm/sec}$

(5) For the entire forced flow velocity range for which smolder can propagate the magnitude of the flow induced by the horizontal temperature gradient is

comparable to the forced flow, $0.1 \leq \frac{u_b}{u_f} \leq 10$, since the magnitude of the buoyantly induced flow is proportional to the permeability of the char which increases with the reaction rate.

(6) Buoyantly induced flow changes the flow field in the char, aiding flow for downward burning, opposing flow for upward burning; quantitative evidence of this difference is significant only for forced air flow velocities smaller than 1 mm/sec.

Forward Smoldering

(1) Chemistry is a significant parameter in forward smoldering. High energy supply and low oxygen concentrations favor condensed phase pyrolysis; high oxygen supply favors oxidation. Strong oxidation can support a pyrolysis front ahead of the oxidation front, and thus self-sustained smolder can occur. A weak reaction can not provide enough heat to support a pyrolysis front, therefore extinction will follow.

(2) Forced flow and oxygen from the foam pores are the only oxidizer source for the reaction.

(3) Buoyantly induced flow changes the flow field in the char but does not provide any extra oxidizer to the reaction zone. For downward burning boundary layer flow opposes the forced flow in the core of the sample (opposing flow), the opposite occurs for upward burning (aiding flow).

(4) The flow field is buoyantly dominated for forced flow velocities smaller than

1 mm/sec. The char permeability increases with the reaction rate and thus the magnitude of the boundary layer flow. Buoyantly induced flows become significant again for forced flow velocities over 10 mm/sec.

(5) Transition to flaming occurs only for forced air flow velocities larger than 14 mm/sec and only in an upward burning configuration (aiding flow).

(6) Extinction occurs only for forced air flow velocities smaller than 1 mm/sec and only in a downward burning configuration (opposing flow).

Micro-Gravity Smoldering

(1) Micro-gravity eliminates convective heat losses from the reaction and convective oxidizer transport to the reaction. For a self-sustained smolder reaction elimination of convective oxidizer transport to the reaction seems to be the dominant parameter, therefore, under micro-gravity conditions smolder strength decreases.

(2) The final fate of a smolder reaction propagating in a micro-gravity environment can not be determined in ground-based low gravity facilities, since smoldering time scales represent an unsolvable problem.

6.2 Limitations of this Work

Time scales impose an unsolvable problem for smoldering experiments designed to understand the effect of gravity on the process, and performed in ground-based facilities. For the experiments described in Chapters 2, 3 and 4 it is observed

that absolute opposed or forward forced flow smoldering could not be obtained. The presence of buoyantly induced recirculation flow in the char alters the forced flow structure. For certain cases the influence of buoyantly induced flow can be accounted for (downward natural convection smolder, opposed forced flow smolder) but it is always an important factor in the problem. For other cases (upward natural convection smolder, forward forced flow smolder) its effect can be observed but not accurately quantified. The importance of an increase in the permeability of the char, that allows the existence of recirculating flow, is an inherent characteristic of the process. It can not be quantified because it is coupled with an increase of the buoyantly induced flow. Experiments performed in ground-based low gravity facilities, KC135A and Learjet, give maximum times at low gravity which are of the order of 30 sec (KC-135A) that period of time that allows observation of trends. The history of the reaction is also an important element in the propagation characteristics as described in chapter 5. Consecutive maneuvers with high and low gravity periods lead to extinction in most upward burning experiments and some downward burning experiments. The only possible way to overcome these limitations is conducting space-based experiments.

6.3 Future Work

Given the potential impact of comparisons of the present study with theoretical prediction for smoldering propagation velocities and smolder characteristics, and the important practical applications such as fire safety in both

normal and micro-gravity environments, it is important to extend this work to the other aspects of the problem. This work includes a preliminary assessment of the process of transition to flaming. Experiments in a two dimensional configuration with an open interface to allow for optical access and thus, the possibility of using non-intrusive diagnostics seem to provide the best approach to the transition problem. A more systematic study on ignition and extinction, both theoretical and experimental, is important since this remains a largely unaddressed issue.

Clear evidence of the effect of buoyancy on smoldering combustion has been presented in this work, quantitative information on the scale of its influence is necessary. For this purpose a small scale experiment was designed based on the results previously described. The hardware was built at NASA Lewis Research Center and flew in the US Micro-gravity Laboratory mission. The smoldering combustion in micro-gravity experiment hardware consisted of four modules. Each module contains an instrumented fuel sample (6 thermocouples), with an embedded igniter and an internal fan for convection. A single module was used for each test; a total of four tests were conducted during the mission. The objective of this experiment was to investigate the ignition and propagation of smoldering combustion in micro-gravity, in both quiescent and convective environments. The principal test variables were the igniter geometry and the convective environment. Through the use of an axial igniter and a plate igniter, both radial and axial smolder propagation were investigated. For each igniter geometry a test was conducted with a quiescent environment and with a low velocity flow. Due to the restrictions imposed by NASA,

mainly from a fire safety perspective and space availability, the size of the fuel is very small, and therefore the information that can be obtained is limited. Further experiments have been planned to fly on board of a Space Shuttle in 1995; the conceptual design of these experiments has already been completed. These experiments are of size and characteristics similar to the ones described through this work.

The results of this work show that the effect of buoyancy extends to large ranges of forced air flow rates, contrary to what could be expected. Transition to flaming and extinction limit the air flow rates for this experiments, but by changing the oxygen concentration of the forced flow the working ranges could be extended. The chemistry of the problem is still unsolved, a one step chemical reaction seems to be sufficient to model strongly propagating opposed smolder. For forward smolder, weakly propagating smolder and extinction, no existing model for the chemistry seems to be adequate.

REFERENCES

1. Ohlemiller, T.J.,(1986) "Modeling of Smoldering Combustion Propagation," Progress in Energy and Combustion Science,**11**, 277-310, 1986.

2. Summerfield, M. and Mesina, N.,"Smoldering Combustion in Porous Fuels, Progress in Astronautics and Aeronautics,**73**, 129-194, 1981.

3. Ohlemiller, T.J. and Rogers, F.E., "A Survey of Several Factors Influencing Smoldering Combustion in Flexible and Rigid Polymer Foams," Journal of Fire and Flammability,**9**, 489-509, 1978.

4. Ohlemiller, T.J., Bellan, J. and Rogers, F.E.,"A Model of Smoldering Combustion Applied to Flexible Polyurethane Foams, Combustion and Flame,**36**, 197-215, 1979.

5. Dosanjh, S.S.,"Smoldering Combustion Analyses", Phd. Thesis. University of California, Berkeley, 1986.

6. Dosanjh, S.S., Peterson, J., Fernandez-Pello, A.C. and Pagni, P.J.,"Buoyancy Effects on Smoldering Combustion," Acta Astronautica,**13**, No. 11/22, 689-696, 1987.

7. Dosanjh,S.S., Pagni, P.J. and Fernandez-Pello, A.C.,"Forced Cocurrent Smoldering Combustion", Combustion and Flame, **68**, 131-142, 1987.

8. Dosanjh,S.S. and Pagni, P.J.,"Forced Countercurrent Smoldering Combustion,"Proceedings of the 1987 ASME-JSME Thermal Engineering Joint Conference, P.J. Marto and I. Tanasawa, eds.,1, 165-173, 1987.

9. Ohlemiller, T.J. and Lucca, D.A.,"An Experimental Comparison of Forward and Reverse Combustion," Combustion and Flame,**54**, 131-147, 1983.

10. Rogers,F.E.,Ohlemiller,T.J.,Kurtz,A. and Summerfield,M., "Studies of the Smoldering Combustion of Flexible Polyurethane Cushioning Materials," Journal of Fire and Flammability, **9**, pp.5-13, 1978.

11. Rogers,F.E. and Ohlemiller,T.J.,"Smolder Characteristics of Polyurethane Foams," Journal of Fire and Flammability, **11**, pp.32-44, 1980.

12. Kansa, E.J.,Perlee, H.E. and Chaiken, R.F.,"Mathematical Model of Wood Pyrolysis Including Internal Forced Convection," Combustion and Flame, **29**, 311-324, 1977.

13. Darcy, H.,"Les Fontaines Publiques de la Ville de Dijon", Victor Dalmont, Paris, 1856.

14. Bejan A.,"Convection Heat Transfer", John Wiley and Sons.,New York, 1984.

15. Rogers, F.E. and Ohlemiller, T.J.,"Studies of the Smoldering Combustion of Flexible Polyurethane Cushioning Materials," Journal of Fire and Flammability,**9**, 5-13, 1978.

16. McCarter,r.J.,"Smoldering Combustion of Cotton and Rayon," Journal of Consumer product Flammability, **4**, pp.346-358, 1977.

17. Rogers,F.E. and Ohlemiller,T.J.,"Cellulosic Insulation Material: I. Overall Degradation Kinetics and Reaction Heats," Combustion Science and Technology, **24**, pp.129-137, 1980.

18. McCarter,R,J.,"Smoldering Combustion of Wood Fibers: Cause and Prevention," Journal of Fire and Flammability, **9**, pp.119-126, 1978.

19. Day,M. and Wiles,D.M.,"Combustibility of Loose Fiber Fill Cellulose Insulation: The Role of Borax and Boric Acid," Journal of Thermal Insulation, **2**, pp.30-39, 1978.

20. Palmer,K.N.,"Smouldering Combustion in Dusts and Fibrous Materials," Combustion and Flame, **1**, pp.14-17, 1957.

21. Orzel,R.A.,Womble,S.E.,Ahmed,F. and Brasted,H.S.,"Flexible Polyurethane Foam: A Literature Review of Thermal Decomposition Products and Toxicity," Journal of the American College of Toxicology, **8**, 6, pp.1139-1175, 1989.

22. Paabo,M. and Levin,B.,"A Review of the Literature on the Gaseous Products and Toxicity Generated from Pyrolysis and Combustion of Rigid Polyurethane Foams," Fire and Materials, **11**, pp.1-29, 1987.

23. Newhall, J., Fernandez-Pello, A.C., and Pagni, P.J., "Experimental Observations of the Effect of Pressure and Buoyancy on Cellulose Co-Current Smoldering, Journal of Fire Materials, **14**,145-150, 1989.

24. Gann,R.G. and Cheng,I.T.,"Flow Study of Smoldering Charcoal Combustion," American Chemical Society, 172nd National Meeting, Division of Organic Coatings and Plastics, report N°20, 1976.

25. Beshty,B.S., "A mathematical Model for the Combustion of a Porous Carbon Particle," Combustion and Flame, 32, pp.295-311, 1978.

26. Stephens,D.R., Pasternak,A. and Maimoni,A.,"The LLL In Situ Coal gasification Program," UCRL-75990. Lawrence Livermore Laboratory, University of California, Livermore, CA, 1974.

27. Donaldson,D.T., Yeadon,D.A. and Harper,R.J.,"Smoldering Phenomenon Associated with Cotton," Textile research Journal, 53, pp.160-164, 1983.

28. Damant,G.,"Smoldering Characteristics of Fabrics used as Upholstered Furniture Coverings," Journal of Fire and Flammability/Consumer Product Flammability, 2, 5, 1975.

29. Moussa, N.A., Toong, T.Y. and Garris, C.A., "Mechanisms of Smoldering of Cellulosic Materials," Sixteenth Symposium (International) on Combustion, The Combustion Institute, pp.1447-1457, 1976.

30. Kinbara, T., Endo H. and Sega,S.,"Downward Propagation of Smoldering Through Solid Materials," Eleventh Symposium (International) on Combustion, The Combustion Institute, pp.525-531, 1967.

31. McCarter,R.J.,"Smoldering Combustion of Polyurethane Foam," Journal of Consumer Product Flammability, 3, pp.128-140, 1976.

32. Muramatsu,M.,Umemura,S. and Okado,T.,"Mathematical Model of Evaporation-Pyrolysis Processes Inside a Naturally Smoldering Cigarette," Combustion and Flame, 36, pp.245-262, 1979.

33. Baker,R.R.,"Combustion and Thermal Decomposition Inside a Burning Cigarette," Combustion and Flame, 30, pp.21-32, 1977.

34. Summerfield,M.,Ohlemiller,T.J. and Sandusky,H.W.,"A Thermophysical Mathematical Model of Steady-Draw Smoking and Prediction of Overall Cigarette Behavior," Combustion and Flame, 33, pp.263-279, 1978.

35. Cohen,L. and Luft,N.W.,"Combustion of Dust Layers in Still Air," Fuel, 34,pp.154-163, 1954.

36. Chen,Y., Kauffman,C.W., Sichel,M., Fangrat,J. and Guo,Y.,"The Transition from Smoldering to Glowing to Flaming Combustion," Chemistry and Physics Processes in Combustion, 68, pp.1-68, 1990.

37. Winslow,A.M.,"Numerical Model of Coal Gasification in a Packed," Sixteenth Symposium (International) on Combustion, The Combustion Institute, pp.503-514, 1976.

38. Kotowski,M. and Gunn,R.,"Theoretical Aspects of Reverse Combustion in Underground Gasification of Coal," USDOE Laramie Research Center Report LERC/RI 76/4, Laramie, Wyoming, 1976.

39. Sato,K. and Sega,S., "Effect of Convection on Smoldering Spread," Japanese Association of Fire Science and Engineering, 1984.

40. Sato,K.,Hasegawa,T.,Shiono,M. and Sega,S.,"A Study on the Characteristics of Smolder Spread," Japanese Association of Fire Science and Engineering, 1988.

41. Gugan,K.,"Natural Smoulder in Cigarettes", Combustion and Flame, 10, pp.161-164, 1966.

42. Williams,F.A.,"Mechanisms of Flame Spread," Sixteenth Symposium (International) on Combustion, The Combustion Institute, pp.1281, 1976.

43. Williams,F.A.,"Combustion Theory," Second Edition, The Benjamin/Cummings Publishing Company, Inc.,Menlo Park, California, 1985.

44. Glassman,I.,"Combustion," Second Edition, Academic Press, Inc.,New York, 1987.

45. Kanury,M.,"Introduction to Combustion Phenomena," Gordon and Breach Science Publishers, Inc., New York, 1975.

46. Shafizadeh,F.,and Bradbury,A.G.W.,"Smoldering Combustion of Cellulosic Materials," Journal of Thermal Insulation, 2, pp.141-152, 1979.

47. Ortiz-Molina,M.G., Toong,T.Y., Moussa,N.A. and Tesero,G.C.,"Smoldering Combustion of Flexible Polyurethane Foams and its Transition to Flaming or Extinguishment," Seventh Symposium (International) on Combustion, The Combustion Institute, pp.1191-1200, 1979.

48. Leisch,S.O.,Kauffman,C.W. and Sichel,M.,"Smoldering Combustion in Horizontal Dust Layers," Twentieth Symposium (International) on Combustion, The Combustion Institute, pp.1601-1610, 1984.

49. Cantwell,E.R.,"Buoyancy and Heat Loss Effects in Near Interface Smoldering Combustion," PhD. Thesis, University of California, Berkeley, California, 1992.

50. Williams,F.A.,"Urban and Wildland Fire Phenomenology," Progress in Energy and Combustion Science, **8**, pp.317-354, 1982.

51. Johnson,B.M.,Froment,G.F. and Watson,C.C.,"Temperature Profiles in Packed Beds of Catalyst During Regeneration," Chemical Engineering Science, **17**, pp.835-848, 1962.

52. Kailasanath,K. and Zinn,B.T.,"Theoretical Investigation of the Smoldering Combustion of Porous Solids," Proceedings of the Fluids Engineering Conference, pp.81-86, 1981.

53. Ohlemiller, T.J.,"Smoldering Combustion Propagation Through a Permeable Horizontal Fuel Layer," Combustion and Flame,**81**, 341-354, 1990.

54. Sato,K. and Sega,S.,"Effects of Oxidizing Agent Flow on Combustion Spread of Cellulosic Material," Annual Meeting of the Japanese Assoc. of Fire Science and Engineering, pp.92-102, 1987.

55. Nield, D.A. and Bejan A.,"Convection in Porous Media," Springer-Verlag, New York, 1992.

56. Horton, C.W. and Rogers, F.T.,"Convection Currents in a Porous Medium," Journal of Applied Physics, **16**, 367-370, 1945.

57. Burns, P.J.,Chow,L.C. and Tien, C.L.,"Convection in a Vertical Slot Filled with Porous Insulation," International Journal of Heat and Mass Transfer, **20**, 919-926,1977.

58. Chan,B.K.C.,Ivey,C.M. and Barry,J.M.,"Natural Convection in Enclosed Porous Media with Rectangular Boundaries," Journal of Heat Transfer, pp.21-27, 1970.

59. Gebhart,B. and Pera,L.,"The Nature of Vertical Natural Convection Flows Resulting from the Combined Buoyancy Effects of Thermal and Mass Diffusion," International Journal of Heat and Mass Transfer, **14**, pp.2025-2050, 1971.

60. Weber,J.E.,"The Boundary-Layer Regime for Convection in a Vertical Porous Layer," International Journal of Heat and Mass Transfer, **18**, pp.569-573, 1975.

61. Yen,Y-C.,"Effects of Density Inversion on Free and Convective Heat Transfer in Porous Layer Heated from Below," International Journal of Heat and Mass Transfer, **17**, pp.1349-1356, 1974.

62. Elder,J.W.,"Steady Free Convection in a Porous Medium Heated from Below," Journal of Fluid Mechanics, **27**, part 1, pp.29-48, 1967.

63. Lai,F.C.,Prasad,V. and Kulacki,F.A.,"Mixed Convection in Saturated Porous Media," Convective Heat and Mass Transfer in Porous Media, Kluwer Academic, Dordrecht, pp.225-287, 1991.

64. Lai, F.C., Prasad, V. and Kulacki, F.A.,"Aiding and Opposing Mixed Convection in a Vertical Porous Layer with a Finite Wall Heat Source," International Journal of Heat and Mass Transfer, **31**, 5, 1049-1061, 1988.

65. Hadim, A. and Govindarajan, S.,"Development of Laminar Mixed Convection in a Vertical Porous Channel," ASME, Heat Transfer Division, **105**, 145-153, 1988.

66. Combarnous,M.A. and Bia,P.,"Combined free and Forced Convection in Porous Media," Transactions of the American Society of Petroleum Engineers, **251**, pp.399-405, 1971.

67. Cheng,P.,"Combined Free and Forced Convection Flow About Inclined Surfaces in Porous Media," International Journal of Heat and Mass Transfer, **20**, pp.807-814,1977.

68. Ozisik,M.N.,"Heat Conduction," John Wiley and Sons,New York, 1980.

69. Incropera,F.P. and De Witt,D.P.,"Fundamentals of Heat and Mass Transfer," John Wiley and Sons, 3rd Edition, New York, 1990.

70. Drysdale, D.,"An Introduction to Fire Dynamics," p.265, John Wiley and Sons, New York, 1987.